


Abstracts of Presentations at the International Conference on Basic and Clinical Multimodal Imaging (BaCI), a Joint Conference of the International Society for Neuroimaging in Psychiatry (ISNIP), the International Society for Functional Source Imaging (ISFSI), the International Society for Bioelectromagnetism (ISBEM), the International Society for Brain Electromagnetic Topography (ISBET), and the EEG and Clinical Neuroscience Society (ECNS), in Geneva, Switzerland, September 5-8, 2013

Clinical EEG and Neuroscience
201X, Vol XX(X) 1–121
© EEG and Clinical Neuroscience
Society (ECNS) 2013
Reprints and permissions:
sagepub.com/journalsPermissions.nav
DOI: 10.1177/1550059413507209
eeg.sagepub.com


Keynote Lectures

The Functional Implications of Intrinsic Brain Activity

B.J. He¹

¹National Institutes of Health, Bethesda, MD, USA

The brain is not a silent, complex input/output system waiting to be driven by external stimuli; instead, it is a closed, self-referential system operating on its own with sensory information modulating rather than determining its activity. In this talk, I will outline several related lines of research substantiating this view. First, it is now well established that intrinsic brain activity is organized within multiple functional brain systems, and that the integrity of this organization is compromised in various neurological and psychiatric disorders. Second, recent studies have characterized the rich temporal dynamics of intrinsic brain activity, which has important behavioral implications. Third, we recently demonstrated that intrinsic brain activity interacts significantly with task-evoked brain activity. Instead of a linear summation of ongoing noise and stereotypical task-evoked activity, these results strongly favor the view of the brain as an active nonlinear dynamical system, whose trajectory embodies active information processing in a task context.

Estimating True Functional Connectivity From EEG and MEG Data

G. Nolte¹

¹Department of Neurophysiology and Pathophysiolog, UKE, Hamburg, Germany

The poor spatial resolution of electroencephalography (EEG) and magnetoencephalography (MEG) data analysis constitutes

a major confounder when trying to interpret statistical dependencies between time series as signatures of dynamical dependencies between different groups of neurons. Several methods exist to solve this problem of “artifacts of volume conduction” by exploiting different time scales of neuronal communications and propagation of electromagnetic fields. In this talk I will address two aspects of these approaches: (a) local versus remote interactions and (b) nonlinear measures to estimate functional connectivity free of artifacts of volume conduction. The focus will be on methods which will be illustrated for schizophrenic patients and controls under resting state condition.

While one is mostly interested in long-range interactions, methods that do not properly address the mixing problem trivially misinterpret blurred source estimates as local interactions. Corrections for this, either by exploiting time delays or by analyzing differences between conditions, seem to yield the desired results: only remote interactions remain. Such methods are biased toward long-range interactions while it is in fact short-range interactions that dominate observable brain connectivity. The cause of this misinterpretation can be traced to an eventually inappropriate model. It will be argued that it is not reasonable to model distributed sources with a fixed orientation for each location even though this is true for true source distributions.

Most methods that are rigorously robust to artifacts of volume are linear or quasi-linear. A theoretical framework to generalize such methods to arbitrary nonlinear phenomena is still missing. It will be demonstrated that the problem is much more difficult than it seems and a solution will not be presented in this talk. Instead, only one step in this direction is taken by constructing measures robust to artifacts of volume conduction from third-order moments, that is, cross-bispectral densities, allowing analysis of, for example, couplings between

alpha and beta rhythms as true interactions. Even though non-linear phenomena are much weaker than linear ones they eventually give rise to much deeper insight into the dynamics of the interacting brain.

Hemodynamic and Electromagnetic Correlates of Cognitive Function in Brain Aging and Dementia

K. Nagata¹, D. Takano¹, T. Yamazaki¹, Y. Fujimaki¹, T. Maeda¹, and Y. Satoh¹

¹Department of Neurology, Research Institute for Brain and Blood Vessels, Akita, Japan

Since Paul Broca reported a case of motor aphasia in which the responsible cortical lesion was identified in the left inferior frontal lobe in 1861, the brain–behavior relationship has been argued from both the localization theory and holism concerning the cognitive function. Although the holistic interpretation of the brain–behavior relationship is supported by the facts of functional recovery from the severe brain injuries, the localization theory has been validated by the identification of cortical structures that subserve cognitive functions in previous reports based on the postmortem studies as well as morphological neuroimaging such as X-ray computed tomography (CT) and magnetic resonance imaging (MRI). With the advent of modern functional neuroimaging such as positron emission tomography (PET), functional MRI, and magnetoencephalography (MEG), hemodynamic and electrophysiological brain activation studies refined the framework of the localization theory down to the temporal correlation and functional connectivity. Hemodynamic brain activation utilizing a mirror-tracing paradigm elucidated a transfer of brain regions during the motor learning process that can be interpreted as a shift from the central executive network to the default mode network. Using our new software, correlation imaging plots (CIPs), cerebral blood flow (CBF) data from the single photon emission computed tomography (SPECT) were compared with the neuropsychological and behavioral parameters from the neuropsychological batteries statistically in the 3-dimensional axis, and the results were projected to the surface-rendered anatomical images in patients with mild cognitive impairment (MCI), those with Alzheimer's disease (AD), and normal volunteers. Among the functional neuroimaging modalities, the relationship between the hemodynamic and electrophysiological parameters was compared statistically in patients with ischemic stroke and normal volunteers. Slow wave components, including delta and theta bands, correlated negatively with CBF and cortical oxygen metabolism, whereas alpha background activity correlated positively throughout the course of stroke, although the degree of correlation was much stronger in stroke patients rather than in normal controls.

Imaging Hippocampal Dysfunction in Psychotic Disorders

S. Heckers¹

¹Department of Psychiatry, Vanderbilt University, Nashville, TN, USA

The hippocampal formation has attracted considerable interest as a neural substrate for psychotic disorders. Initial neuroimaging studies focused on hippocampal volume and shape, but more recent studies have explored hippocampal blood flow and blood volume as an index of hippocampal activity.

The lecture will review the current literature, highlight several methodological challenges, and articulate a strategy for future studies. It is likely that imaging hippocampal structure and function will contribute greatly to a better understanding of psychotic disorders, which may serve as a guide for the study of other psychiatric disorders.

TMS: Neural Mechanisms and Clinical Applications

M.S. George¹

¹Medical University of South Carolina, Charleston, SC, USA

In 1985, Dr Tony Barker and colleagues developed a transcranial magnetic stimulation (TMS) machine that was powerful enough to stimulate the spine, and therefore also the brain.¹ Since then, researchers and more recently clinicians have used TMS to poke, prod, excite, inhibit, and treat the brain (>9000 references, Pubmed, since May 2013). TMS is a relatively unique tool in that *it can both be used to investigate* cortical excitability or neuronal plasticity, confirm or reject brain–behavior relationships suggested by conventional noninterventional imaging studies like fMRI, *or serve as a potential treatment*. In 1993, I and others wondered if TMS' ability to interact with brain circuits noninvasively might be used to “reset” and treat depression, in a manner analogous to what is produced by electroconvulsive therapy (ECT), but without causing a seizure.^{2–6} In the intervening 20 years, daily left prefrontal rTMS has developed into a clinically useful depression treatment for those patients who have not responded to medications. In the United States alone, more than 12 000 patients have been treated with TMS since the Food and Drug Administration approval in 2008. (Data supplied May, 2013 by Neuronetics, Inc.)

This talk will focus on what is known about how TMS interacts with the brain to cause changes. In addition to discussing work in animals and in human motor system studies, this talk will rely heavily on data learned by combining TMS with brain imaging. In 1998, Dr Daryl Bohning here at the Medical University of South Carolina showed that one could safely stimulate with TMS inside an MRI scanner while concurrently

scanning.⁷ This technically complex form of multimodal imaging is now available at many imaging centers and has shown that conventional TMS stimulates through cortical “windows” and their connected brain regions at a scale very close to normal brain activity (eg, volitional movement).⁸ Current work involves advanced image guided stimulation building on within-individual functional maps.⁹ Some groups are now developing multichannel TMS systems that are designed to stimulate different brain regions simultaneously but independently with varying frequencies, opening up remarkable possibilities for exciting certain circuits and, at the same time, inhibiting others.

Transcranial magnetic stimulation is thus a powerful research tool, especially when combined with neuroimaging. It has now shown clinical utility as a treatment in one disease, major depression, with active research in many more.

References

1. Barker AT, Jalinous R, Freeston IL Non-invasive magnetic stimulation of the human motor cortex. *Lancet*. 1985;1:1106-1107.
2. George MS, Wassermann EM, Williams WA, et al. Daily repetitive Transcranial Magnetic Stimulation (rTMS) improves mood in depression. *Neuroreport*. 1995;6:1853-1856.
3. George MS, Post RM, Ketter TA, Kimbrell TA. Neural mechanisms of mood disorders. In: Rush AJ, ed. *Current Review of Mood Disorders*. Philadelphia, PA: Current Medicine; 1995:1.
4. George MS, Wassermann EM. Rapid-rate transcranial magnetic stimulation (rTMS) and ECT. *Convuls Ther*. 1994;10:251-254.
5. George MS, Ketter TA, Post RM. Prefrontal cortex dysfunction in clinical depression. *Depression*. 1994;2:59-72.
6. George MS. An introduction to the emerging neuroanatomy of depression. *Psychiatr Ann*. 1994;24:635-636.
7. Bohning DE, Shastri A, Nahas Z, et al. Echoplanar BOLD fMRI of brain activation induced by concurrent transcranial magnetic stimulation (TMS). *Invest Radiol*. 1998;33:336-340.
8. Bohning DE, Shastri A, McConnell K, et al. A combined TMS/fMRI study of intensity-dependent TMS over motor cortex. *Biol Psychiatry*. 1999;45:385-394.
9. Hanlon CA, Jones EM, Li X, Hartwell KJ, Brady KT, George MS Individual variability in the locus of prefrontal craving for nicotine: implications for brain stimulation studies and treatments. *Drug Alcohol Depend*. 2012;125:239-243.

Multimodal Imaging of Alpha Rhythms: From Local Field Potentials, EEG/MEG, fMRI, to BCI

F. Lopes da Silva¹

¹Centre of Neuroscience, Swammerdam Institute for Life Sciences, University of Amsterdam, Amsterdam, Netherlands.

There are several kinds of brain rhythmic activities within the alpha frequency range that have different distributions in the cortex (visual cortex, sensorimotor cortex [mu rhythm], auditory

cortex [tau rhythm]) and functional connotations. A well-established feature of the visual alpha is that its neuronal generators at the level of local field potentials (LFPs) constitute cortical dipolar fields centered on layer V-IV.^{1,2} In addition, recent findings in monkey^{3,4} showed that alpha rhythms occurring in deep layers are associated with gamma-band activity in superficial cortical layers, and that alpha and gamma power are anti-correlated, displaying different dynamics in space and time associated with attention.⁵

Dipolar source localization based on scalp distributions of alpha and mu rhythmic activities reveals complementary information obtained from EEG and MEG recordings⁶; simultaneous recordings of EEG and fMRI puts in evidence typical correlations between alpha power modulation and BOLD signals, characteristic of the resting state.^{7,8}

Both in the visual and in the sensorimotor modalities alpha/mu power⁹ and phase¹⁰ can modulate sensory perception demonstrating that alpha rhythms constitute oscillations of brain excitability expressed in “attention systems,” such that the threshold of sensory detection fluctuates over time along with the power and phase of these ongoing rhythmic activities. These findings support the notion that ongoing rhythmic oscillations within the alpha frequency range modulate attention and perception, and appear to operate as “traffic controllers” of the flow of neural information in thalamocortical systems. Thus it is not appropriate to say that alpha activity corresponds to an “idling state”; it rather corresponds to an active “gating” process that may be operational in controlling the focus of attention. This latter feature is particularly evident with respect to the phenomenon of event-related “(de)synchronization” of the sensorimotor mu rhythm, with characteristic spatial and dynamic properties¹¹ associated with the intention to make, or to imagine, a movement. Furthermore, in this way it is possible to generate specific brain signals at will, with a high degree of accuracy,¹² that can be transformed into electrical messages acting on the environment by means of brain-computer interfaces (BCIs).

References

1. Lopes da Silva FH, Storm van Leeuwen W. The cortical source of the alpha rhythm. *Neurosci Lett*. 1977;6:237-241.
2. Bollimunta A, Chen Y, Schroeder CE, Ding M. Neuronal mechanisms of cortical alpha oscillations in awake-behaving macaques. *J Neurosci*. 2008;28:9976-9988.
3. Spaak E, Bonnefond M, Maier A, Leopold DA, Jensen O. Layer-specific entrainment of gamma-band neural activity by the alpha rhythm in monkey visual cortex. *Curr Biol*. 2012;22:2313-2318.
4. Srinivasan R, Thorpe S, Nunez PL. Top-down influences on local networks: basic theory with experimental implications. *Front Comput Neurosci*. 2013;7:29.
5. Buffalo EA, Fries P, Landman R, Buschman TJ, Desimone R. Laminar differences in gamma and alpha coherence in the ventral stream. *Proc Natl Acad Sci U S A*. 2011;108:11262-11267.

6. Manshanden I, De Munck JC, Simon NR, Lopes da Silva FH. Source localization of MEG sleep spindles and the relation to sources of alpha band rhythms. *Clin Neurophysiol.* 2002;113:1937-1947.
7. de Munck JC, Gonçalves SI, Mammoliti R, Heethaar RM, Lopes da Silva FH. Interactions between different EEG frequency bands and their effect on alpha-fMRI correlations. *Neuroimage.* 2009;47:69-76.
8. de Munck JC, Gonçalves SI, Huijboom L, et al. The hemodynamic response of the alpha rhythm: an EEG/fMRI study. *Neuroimage.* 2007;35:1142-1151.
9. Hanslmayr S, Aslan A, Staudigl T, Klimesch, W. Prestimulus oscillations predict visual perception performance between and within subjects. *Neuroimage.* 2007;37:1465-1473.
10. Busch NA, Dubois J, VanRullen R. The phase of ongoing EEG oscillations predicts visual perception. *J Neurosci.* 2009;29:7869-7876.
11. Pfurtscheller G, Lopes da Silva FH. Event-related EEG/MEG synchronization and desynchronization: basic principles. *Clin Neurophysiol.* 1999;110:1842-1857.
12. Pfurtscheller G, Scherer R, Müller-Putz GR, Lopes da Silva FH. Short-lived brain state after cued motor imagery in naive subjects. *Eur J Neurosci.* 2008;28:1419-1426.

Symposia

S01_1. Artifacts in EEG/fMRI: Challenges and Opportunities

J.C. de Munck¹, P.J. Van Houdt^{1,2}, R.M. Verdaasdonk¹, and P. Ossenblok²

¹VU University Medical Center, Amsterdam, Netherlands

²Kempenhaghe, Heeze, Netherlands

Co-registered EEG/fMRI provides an independent way of pre-surgical evaluation of patients with epilepsy that are candidates for surgery. Furthermore, the analysis of co-registered EEG/fMRI data provides fundamental insight into the precise physiological meaning of both fMRI and EEG data. Routine application of EEG/fMRI data to the localization of epileptic foci is hampered by large artifacts in the EEG, caused by scanner gradients and heart beat effects. Conversely, the gel used to connect electrodes to the skin causes small artifacts on the MRI scan. We present a method to exploit these artifacts to determine electrode positions.

When the EEG sampling frequency and EEG low-pass filtering are sufficient in relation to MR gradient switching, gradient artifacts can be reduced using a shifting averaging algorithm. When this is not the case, the gradient artifacts repeat themselves at time intervals that depend on the remainder between the fMRI repetition time and the closest multiple of the EEG acquisition time. These repetitions are hard to predict and we propose to estimate them using clustering and selective averaging. The elimination of cardioballistic artifacts

by template averaging is hampered by their finite duration causing overlap of subsequent artifacts. We model the precise timings of these overlaps in a sparse matrix and disentangle artifacts with a least squares procedure.¹

The novelties introduced here provide a substantial improvement of the quality of the EEG signal. In several EEG/fMRI data sets that would otherwise have been discarded because of insufficient quality, the improvements allowed reliable annotation of interictal spikes despite the large BCG-artifacts in the uncorrected data.

All electrodes artifacts visualized simultaneously in a single view, using a “pancake view” of the scalp. Electrodes are determined with a simple mouse click for each electrode. Electrode labels are attached to the electrode positions by fitting a template grid of the electrode cap in which the labels are known. The correspondence problem between template and sample electrodes is solved by minimizing a cost function over rotations, shifts and scalings of the template grid. The crucial step here is to use the solution of the so-called Hungarian algorithm as a cost function, which makes it possible to identify the electrode artifacts in arbitrary order.

In our implementation of this method, the whole procedure can be performed within 15 minutes, including import of MRI, surface reconstruction and transformation, electrode identification, and fitting to template. The method is robust in the sense that an electrode template created for one subject can be used without identification errors for another subject for whom the same EEG cap was used.²

References

1. de Munck JC, Houdt PJ, van Wegen E, Gonçalves SI, Ossenblok PP. Novel artefact removal algorithms for co-registered EEG/fMRI based on selective averaging and subtraction. *Neuroimage.* 2012;64:407-415.
2. de Munck JC, Houdt PJ, Verdaasdonk RM, Ossenblok PP. A semi-automatic method to determine electrode positions and labels from gel artifacts in EEG/fMRI-studies. *Neuroimage.* 2012;59:399-403.

S01_2. Moving Simultaneous EEG–fMRI to Higher Field Strengths: The Advantages and Disadvantages

K. Mullinger¹ and R. Bowtell¹

¹SPMMRC, School of Physics and Astronomy, University of Nottingham, University Park, Nottingham, UK

Performing functional magnetic resonance imaging (fMRI) at ultra-high field strength (7 T) is highly desirable due to the increased contrast-to-noise ratio of fMRI signals. Ultra-high field fMRI is particularly useful when studying trial-by-trial variability in brain responses. Since simultaneous EEG–fMRI is valuable when studying unpredictable brain responses,

ultra-high field fMRI with simultaneous EEG could provide new insights in brain function.

However, the pulse and motion artifacts present in EEG data collected simultaneously with fMRI scale with static-field strength. Therefore the EEG data quality reduces as MR field strength increases. These differences in signal-to-noise with MR field strength present difficult trade-offs between data collected from the 2 modalities simultaneously. To reduce the compromises that are needed, improved methods to reduce and remove the pulse and motion artefact from EEG data are needed. However, the pulse artifact is poorly understood and highly variable with time, making it difficult to fully correct with current techniques. We have shown through modeling and experimental work that the main source of the pulse artifact is head rotation caused by pulsatile blood flow, suggesting that this may be reduced at source.^{1,2} Head motion artifacts are also problematic as they are unpredictable. Our work has shown the danger of residual EEG motion artifacts in creating correlations with fMRI responses in neurologically plausible brain regions at 3 T,³ a problem that is only exacerbated at higher field strength. However, within the limitations of the current methodology simultaneous EEG–fMRI can still prove very useful in the interrogation of neurovascular coupling.

References

1. Yan WX, Mullinger KJ, Geirsdottir GB, Bowtell R. Physical modeling of pulse artefact sources in simultaneous EEG/fMRI. *Hum Brain Mapp.* 2010;31:604–620.
2. Mullinger KJ, Havenhand J, Bowtell R. Identifying the sources of the pulse artefact in the EEG recordings made inside an MR scanner. *Neuroimage.* 2013;71:75–83.
3. Jansen M, White TP, Mullinger KJ, et al. Motion-related artefacts in EEG predict neuronally plausible patterns of activation in fMRI data. *Neuroimage.* 2012;59:261–270.

S01_3. Investigating Thalamocortical Networks With EEG–fMRI

A.P. Bagshaw¹

¹School of Psychology, University of Birmingham, Edgbaston, Birmingham, UK.

The human brain operates as a series of structurally and functionally interconnected networks, whose activity must be temporally coordinated with millisecond precision if the system as a whole is to perform successfully. How this is accomplished remains unknown, although several lines of evidence, ranging from animal models, slice preparations, and network modeling approaches, suggest that thalamocortical (TC) and corticothalamic (CT) recurrent loops play a pivotal role in coordinating distributed cortical activity. TC networks underlie most basic and higher cognitive functions, as well as being implicated in a

number of neurological and neuropsychiatric disorders, with generalized epilepsy being perhaps the most obvious example. We use EEG–fMRI to investigate networks defined by TC-generated electrophysiological oscillations that occur during wakefulness, sleep and in patients with generalised epilepsy (occipital alpha rhythm, sleep spindles, K-complexes, and generalized spike and wave discharges). Each of these oscillations has been investigated extensively with in vitro and invasive in vivo electrophysiological methods, and this prior characterization of network topology and directionality motivates their use as model brain networks. We apply connectivity measures and graph theoretical tools for complex network analysis, as well as using diffusion tensor imaging (DTI) to investigate underlying structural connectivity and its relationship to functional connectivity.

S02_1. Discovering Oscillatory EEG Interactions After Electroconvulsive Therapy (ECT) Interventions in Patients With Severe Depression

D. Keeser^{1,2}, S. Karch¹, F. Segmiller¹, I. Hantschk¹, A. Berman², F. Padberg¹, and O. Pogarell¹

¹Department of Psychiatry and Psychotherapy, Ludwig-Maximilians University, Munich, Germany

²Institute of Clinical Radiology, Ludwig-Maximilians University, Munich, Germany

Background. Electroconvulsive therapy (ECT) is one of the most effective treatment options for patients with major depression. The mechanisms of action are not fully understood. To further investigate the neurobiological mechanisms of ECT, techniques are needed to noninvasively measure brain function before and following ECT sessions and during the course of ECT series. Electroencephalography (EEG) offers the opportunity to noninvasively investigate changes of brain electric activity before and after ECT. **Methods.** We investigated EEG data of 20 patients with severe depression (ICD 10 diagnoses F31.x, F32.x, F33.x) eligible for ECT and who underwent a series of right unilateral ECT. The mean age of the patients was 51.3 ± 10.7 years. The subjects underwent 13 ± 3.8 ECT sessions. EEG recordings were done 16.8 ± 6.3 days before ECT and 6.2 ± 6 days after completion of the ECT series. Spectrotemporal dynamics were analyzed in sensor and source space (sLORETA) to validate neurophysiologic changes pre- to post-ECT treatment. Delta (δ), theta (θ), alpha (α), beta (β), gamma (γ) power, and sLORETA analyses were calculated from artifact-free EEG epochs. **Results.** Post-pre ECT treatment comparisons revealed significant increased δ and θ power in frontal sensor EEG electrodes. The sLORETA analysis indicates the sources of slow-wave current density increases at inferior frontal, superior

frontal, insular, and temporal cortices. Statistical nonparametric mapping showed increased δ activity (1–6.5 Hz) in the middle frontal gyrus ($x, y, z = 35, 35, -10$; BA 47) compared with pre-treatment baseline EEG ($P < .01$). The comparison also revealed δ current density increases in the inferior frontal gyrus ($x, y, z = 35, 30, -15$; BA 11; $P < .01$). ECT also affected activity in the δ current density at the insular cortex ($x, y, z = 30, 25, 0$; BA 13; $P < .05$) and the superior temporal gyrus ($x, y, z = 45, 25, 20$; BA 38, $P < .05$). **Conclusion.** The main finding of the present study was a change in brain electric activity in the low δ frequency band in frontal brain regions. The frontal cortex is a key anatomical region in depression and alterations of neuronal activity in this region is a common finding in neurophysiological and neuroimaging studies. Changes in low frequency power, directly linked to ECT, might be a neurophysiological correlate of the mechanisms of action of ECT.

S02_2. Real-Time fMRI for Training of Brain Functional Connectivity

F. Scharnowski^{1,2}

¹University of Geneva, Geneva, Switzerland

²Swiss Institute of Technology, Lausanne, Switzerland

Neurofeedback based on real-time fMRI is an emerging technique that can be used to train voluntary control of brain activity. Such brain training has been shown to lead to behavioral effects that are specific to the functional role of the targeted brain area. Recent studies even demonstrated therapeutic effects in specific patient populations. However, real-time fMRI-based neurofeedback so far was limited to training localized brain activity within a region of interest. Here, we overcome this limitation by presenting near real-time dynamic causal modeling in order to provide neurofeedback information based on connectivity between brain areas rather than activity within a brain area. Using a visual-spatial attention paradigm, we show that such a connectivity feedback signal can be used to train voluntary control over functional brain networks. Because most mental functions and most neurological disorders are associated with network activity rather than with activity within a single brain region, this novel method is an important methodological innovation in order to more specifically target such brain networks.

S02_3. Craving-Related Brain Responses and Real-Time fMRI in Patients With Substance Use Disorder

S. Karch¹, S. Hümmer¹, D. Keeser^{1,2}, M. Paolini², V. Kirsch³, G. Koller¹, B. Rauchmann², M. Kupka², J. Blautzik², and O. Pogarell¹

¹Department of Psychiatry and Psychotherapy, Ludwig-Maximilians University, Munich, Germany;

²Institute of Clinical Radiology, Ludwig-Maximilians University, Munich, Germany

³Department of Neurology, Ludwig-Maximilians University, Munich, Germany

Craving, the intense desire for the substance, is one of the most important aspects of substance use disorder. Functional brain imaging studies demonstrated that craving is associated with increased BOLD responses in several brain areas, including the anterior cingulate cortex (ACC) and adjacent medial-frontal areas that demonstrated to be important for attention and motivation, the orbitofrontal cortex (OFC) that seems to be relevant for the cognitive evaluation processes, the dorsolateral prefrontal cortex, and the striatum. The close relationship between craving and relapse rates demonstrates the importance of craving during the therapeutic process.

The aim of the present project was the voluntary modulation of craving-associated neuronal responses in patients with alcohol use disorder using real-time neurofeedback with functional magnetic resonance imaging (fMRI). It is assumed that neurofeedback offers the possibility to influence BOLD responses with the aid of learning processes (eg, operant conditioning) and to provoke changes of behaviour. In the present study, neurofeedback training has been offered as an add-on to a standard therapeutic treatment in a ward specialized for addiction disorders. In addition, the influence of neurofeedback to craving for alcohol will be presented. Perspectively, real-time neurofeedback may offer the opportunity of a neurophysiology-based therapeutic treatment strategy that probably can be integrated in the psychotherapeutic context.

S02_4. Decoupling of EEG Driving Frequencies and fMRI Resting State Networks in Schizophrenia Spectrum Disorders

N. Razavi¹, K. Jann^{1,2}, T. Koenig¹, M. Kottlow¹, M. Hauf³, W. Strik¹, and T. Dierks¹

¹Department of Psychiatric Neurophysiology, University Hospital of Psychiatry, University of Bern, Bern, Switzerland

²Ahmanson-Lovelace Brain Mapping Center, Department of Neurology, University of California, Los Angeles, CA, USA

³Institute of Diagnostic and Interventional Neuroradiology, Inselspital, University of Bern, Bern, Switzerland

Multimodal resting state EEG/fMRI studies in healthy controls propose that a correct coupling between neural oscillations (EEG) and resting state network (fMRI) activity is necessary to organize cognitive processes optimally. A dysfunctional coupling may thus have an impact on cognitive performance during internal and external stimulus processing. Schizophrenia spectrum disorders exhibit enormously disabling symptoms during the resting state and it has already been demonstrated that the patients present aberrant resting state networks, as well as changed frequency spectra distributions. Using simultaneous, high-resolution resting state EEG/fMRI, we could identify that the coupling between resting state networks and related EEG frequencies in patients with schizophrenia spectrum disorders was significantly shifted toward lower frequencies compared with the healthy control group. The finding of an aberrant driving of fMRI resting state networks in schizophrenia spectrum disorders offers one possible neurophysiological explanation of how the diverse symptoms might arise (ie, thought disorders, hallucinations).

S03_1. EEG–fMRI in Focal and Generalized Epilepsy: Negative BOLD Responses in the Default Mode Network and Other Regions

J. Gotman¹

¹Montreal Neurological Institute, Montréal, Québec, Canada

In the context of epileptic discharges seen in the scalp EEG, most BOLD responses are positive, reflecting the expected intense neuronal activity occurring during the epileptic discharges. Negative BOLD responses have been observed however and they have been more difficult to explain. Negative BOLD responses can be divided in 3 main categories:

- BOLD responses in regions of the default mode network (DMN) have been observed principally during generalized spike-wave discharges but also during some focal epileptic discharges occurring in different brain regions. The mechanisms by which epileptic discharges affect the DMN remain unknown, but it is hypothesized that its deactivation may result in a decreased level of attention during epileptic discharges.
- Apparent negative responses that are actually the undershoot of an earlier positive response, in situations when the primary positive response occurs seconds earlier than expected.
- Genuine negative BOLD responses occurring as a primary response in the epileptic focus. These seem to occur primarily, but not exclusively, when the EEG discharge includes a prominent slow wave component or in the presence of a burst of spike and slow waves. The negative response may result from the fact that the epileptic discharge is in such cases primarily an inhibitory phenomenon.

Negative BOLD responses must therefore be considered in this complex context and each should be analyzed. It is possible that there are also different types of positive BOLD responses.

S03_3. Clinical Contribution and Added Value of EEG–fMRI in Presurgical Assessment

S. Vulliemoz¹

¹EEG and Epilepsy, Neurology, University Hospital and Functional Brain Mapping Lab, Faculty of Medicine, Geneva, Switzerland

In patients suffering from medically intractable epilepsy, the surgical resection of the epileptic focus can provide seizure freedom or significant improvement in the majority of well-selected cases. To reach this goal, the presurgical workup involves multimodal functional imaging sometimes involving invasive EEG for estimating the epileptogenic zone to be removed. Simultaneous EEG and functional MRI (EEG–fMRI) is increasingly used for mapping focal epileptic activity, as a complement to more widely used techniques. Initial studies

showed promising localizing results but limited specificity due to multifocal EEG–fMRI findings and limited sensitivity due to the frequent absence of epileptiform activity on the EEG recorded inside the MRI scanner.

This talk will present clinical studies validating EEG–fMRI results, most of them with gold standard current validation for brain imaging techniques, that is, concordance with intracranial EEG and/or resection volume with postoperative outcome. The benefits and limitations of interictal versus ictal scalp EEG–fMRI and of simultaneous intracranial EEG–fMRI imaging will be discussed. More precisely, this talk will review how EEG–fMRI can contribute to clinical decision making in presurgical evaluations, what additional useful information it carries and how its results can help predict postoperative seizure outcome. Several methodological advances for increasing sensitivity and specificity will be highlighted, using advanced EEG analysis to markedly improve EEG-informed fMRI analysis and its clinical reliability. Notably, EEG topography and electric source imaging can improve the selection of relevant haemodynamic changes and localize the pathological brain activity in the absence of visible epileptic activity.

S03_4. Localization of Epileptogenic Brain From High-Density Scalp EEG and fMRI

Y. Lu¹, H. Zhang¹, L. Yang¹, G. Worrell², and B. He^{1,3}

¹Department of Biomedical Engineering, University of Minnesota, Minneapolis, MN, USA

²Department of Neurology, Mayo Clinic, Rochester, MN, USA

³Institute for Engineering in Medicine, University of Minnesota, Minneapolis, MN, USA

In this presentation, we will review 2 novel imaging approaches based on high-density electroencephalography (EEG) recordings and functional MRI (fMRI). Scalp EEG has been established as an important component of the presurgical evaluation for epilepsy surgery. However, its ability to localize seizure onset zones (SOZs) is significantly restricted by its low spatial resolution and indirect correlation with underlying brain activities. In the EEG source imaging approach, we have developed a dynamic seizure imaging (DSI) technique to image the dynamic changes of ictal rhythmic discharges that evolve through time, space, and frequency.^{1,2} In addition, we have developed a high frequency (HF) activity source imaging technique to localize and image epileptogenic zones from scalp recorded EEG.³ Our work demonstrates the possibility to directly image seizure sources from noninvasive scalp EEG; and the feasibility of imaging and localizing epileptic sources from scalp-recorded HF EEG. The methods were rigorously evaluated in a group of partial epilepsy patients and the imaging results were concordant with the clinical diagnosis as compared with the surgical resection outcome and intracranial recording of the patients. Functional MRI measures the hemodynamic response of brain, and is a powerful tool for noninvasively imaging the brain activation with high spatial resolution. The application of fMRI in epilepsy includes mapping eloquent

cortex, studying brain networks, and localizing abnormal brain regions. We will review our recent study about data-driven resting state fMRI analysis in partial epilepsy patients. Our results suggest the localization value of fMRI in the presurgical planning of medically intractable epilepsy patients.⁴

Acknowledgments

This work was supported by NIH EB006433, EB007920, NSF CBET-0933067, and a grant from the Minnesota Partnership for Biotechnology and Medical Genomics.

References

1. Yang L, Wilke C, Brinkmann B, Worrell GA, He B. Dynamic imaging of ictal oscillations using non-invasive high-resolution EEG. *Neuroimage*. 2011;56:1908-1917.
2. Lu Y, Yang L, Worrell GA, Brinkmann B, Nelson C, He B. Dynamic imaging of seizure activity in pediatric epilepsy patients. *Clin Neurophysiol*. 2012;123:2122-2129.
3. Lu Y, Worrell GA, Zhang C, et al. Submitted for publication.
4. Zhang H, Lu Y, Brinkmann B, Worrell GA, He B. Submitted for publication.

S04_2. Neuroimaging of Symptoms and Endophenotypic Brain Dysfunctions: Future Psychopathophysiology?

O. Gruber¹

¹Department of Psychiatry and Psychotherapy, University Medical Center, Göttingen, Germany

Diagnosis and classification of schizophrenia and other major psychoses is mainly based on the clinical phenotype, that is, on psychopathological symptoms observed in the patients. Many doubts have been raised whether such diagnoses represent “natural disease entities” (Kraepelin) in the sense of disorders with common pathogenesis and pathological substrates. Because schizophrenic and affective disorders are highly heritable, that is, there is clear evidence for genetic factors in their etiology, investigation of endophenotypic brain dysfunctions is an alternative approach for research into the pathophysiology and the pathogenesis of these mental disorders. Modern functional neuroimaging methods have been used to investigate the neural correlates of psychopathological symptoms. Findings of these studies have in part been confirmed by meta-analyses. On the other hand, neuroimaging investigations of healthy first-degree relatives of patients with schizophrenic and affective disorders permit to assess brain dysfunctions that may represent potential endophenotypes and that may foster research into the genetic etiology of these disorders. This talk will focus on multifunctional MRI studies in healthy first-degree relatives of patients with schizophrenia or bipolar disorder. In these studies, endophenotypic brain dysfunctions in schizophrenia have been identified in terms of a hyperresponsivity of a saliency/evaluation network (eg, of the nucleus accumbens) to reward stimuli. In first-degree relatives of patients with bipolar

affective disorder endophenotypic brain dysfunctions could be found particularly in the right middle frontal gyrus showing hyperactivation during verbal working memory performance. Genome-wide association studies for these endophenotypic neuroimaging markers are currently underway. The endophenotypic approach in functional neuroimaging may help to identify genes involved in the pathogenesis of schizophrenic and affective disorders and may provide important information for the development of valid animal models for further research. This line of research may provide more direct insight into pathophysiological brain processes and may pave the way for future diagnostic systems in psychiatry.

S04_3. Cognitive Symptoms in Mood Disorder: A Dimensional Approach

C. Piguet^{1,2}

¹Laboratory for Neurology and Imaging of Cognition, Neuroscience Department, Faculty of Medicine, Geneva, Switzerland

²Mood Disorder Program, Service des Spécialités Psychiatriques, Département de Santé Mental et Psychiatrie, Geneva University Hospital, Switzerland

Current research emphasizes the need for studies less based on diagnostic criteria (cf. actual debate around *DSM-5* release) and more on trait characteristic of psychiatric disorders as proposed by the Research Domain Criteria project, for example. In the context of studying thoughts disorders such as rumination, crowded thoughts, and racing thoughts, we assessed cognitive dimensions in mood disorder patients in a dimensional fashion.

Cognitive flexibility/inhibition and word association patterns were investigated through functional magnetic resonance imaging among 32 mood disorders patients, in different mood states, and healthy matched controls. Participants performed a task-switching task (measuring both switching and inhibition), and a free word association task (measuring both associative patterns and inhibition).

We found that mood disorder patients in general present increased switch cost, and need greater activation of the fronto-parieto-cingulate networks to achieve a demanding task. They also show a deficit in production during automatic word association, concomitant with less activation in regions implicated in the initiation of language and word access. Mood disorder patients show a deficit to inhibit automatic response in word association, associated with less recruitment of right prefrontal cortex (PFC) areas implicated in inhibition. Even in this cognitive task, mood disorder patients fail to downregulate subgenual anterior cingulate as revealed specifically when they must inhibit a previous mental set. For word associations, patients showed enhanced activity of areas involved in (autobiographical) memory and self-referential processing (parahippocampal gyrus [PHG], ventral medial prefrontal cortex [VMPFC])—especially for emotional stimuli. Finally, the tendency to ruminate, across different tasks and different

conditions, is associated with activation in medial temporal lobe and especially the PHG.

Taken together, this dimensional approach allows concluding that mood disorder patients present probably persistent hyperactivation of self-related regions, either with regard to automatic-interoceptive monitoring associated with subgenual anterior cingulate cortex (sgACC), or to autobiographical processing associated with entorhinal cortex/PHG. We also showed that mood disorder patients present some degree of impaired cognitive control, which might further be dampened by this self-related bias.

S03_5. Neurobiology of Psychiatric

Symptomatology: From Origin to Treatment of Auditory Verbal Hallucinations

D. Hubl¹, Ph Homan¹, J. Kindler¹, and T. Dierks¹

¹Department of Psychiatric Neurophysiology, University Hospital of Psychiatry, University of Bern, Bern, Switzerland

One of the most intriguing phenomena in psychopathology is auditory verbal hallucination (AVH). With the advent of the computerized neuroimaging techniques we have the potentiality to investigate brain processes directly in those who experience hallucinations. The results of resting perfusion and functional imaging studies have implied that AVH are associated with altered neuronal activity in cerebral areas that are responsible for language production and perception. This seems to be pronounced in the dominant hemisphere, but with sometimes unexpected lateralities most probably due to compensatory mechanisms. The current literature suggests that in addition to primary and secondary sensory cortices, dysfunctions in prefrontal premotor, cingulate, subcortical, and cerebellar regions contribute to AVH.

However, in schizophrenia, therapy of AVH comprises a critical domain. The 1-month prevalence of these hallucinations exceeds 70% and, in 25% to 30% of patients, these perceptions are resistant to medication, resulting in functional disability and a low quality of life. The development of new therapeutic strategies additional to the standard of pharmacological antipsychotic treatment is urgent. Noninvasive brain stimulation expands the therapeutic regimens. Transcranial magnetic stimulation (TMS) and transcranial direct current stimulation (tDCS) have been recently shown to be potential and safe methods to relieve the hallucinatory burden in those, who did not respond to conventional approaches. In about 50% of pharmacoresistant patients, AVH could be significantly diminished or cured.

With our TMS and tDCS treatment study we further improved the understanding of the neurobiological mechanisms responsible for basic hallucinatory mechanisms as well as responsiveness to the brain stimulation treatment approaches. Brain perfusion measurements before and after successful TMS treatment indicated significant reduced brain activity as

measured by regional cerebral blood flow in the auditory cortex and Broca's areas, 2 of the main players in the generation of AVH. Regarding the identification of responders we demonstrated an involvement of the language system in the generation of AVH. Especially the superior temporal lobe, including primary auditory cortex and its connections, was identified as a region involved in the generation, modulation and therapy of AVH. First results indicate that an increased spontaneous neuronal activity in this region may be marker for response to TMS therapy.

S05_1. Cardiac Source Imaging: Realistic Conductor Model Versus Simplified Conductor Model

K. Kim¹

¹Center for Brain and Cognition Measurement, Korea Research Institute of Standards and Science, Daejeon, Republic of Korea

In spite of its usefulness, it is not easy to find a magnetocardiography (MCG) system in the clinical field. One of the reasons is that the interpretation of the analyzed results is not intuitive enough to medical doctors compared with the results of other competing diagnostic imaging modalities such as echocardiogram, multidetector computed tomography (CT), magnetic resonance imaging (MRI), positron emission tomography (PET), single-photon emission computed tomography (SPECT), and so on. After developing many kinds of inverse problem-solving techniques for the source localization and visualization, cardiologists have been interested in the practical usage of MCG.

However, what is the most effective localization method for the clinical diagnosis in the practical sense? The question excited a controversy: One opinion is that the realistic source localization with a realistic heart conductor model can provide more accurate diagnostic results while the other opinion insists that source localization with a simplified conductor model is more concise, fast and enough to obtain the pathological information.

In this talk, I will discuss the issue on the practical source localization and visualization in the real-world clinical field. Technically, the source imaging process from multichannel SQUID measurements is to find an underdetermined solution and the quality and information of the result depends on the constraints from the conductor model and regularization. A localized conduction anomaly like a reentry of atrial fibrillation can be well-visualized with a realistic conductor model obtained by CT or MRI. However, a pathological malfunction of myocardial ischemia can be efficiently visualized by a simplified conductor model. One interesting point in use of the simplified model is that we should be careful not to use too strong regularization. General diagnostics are based on an angular deviation of the main source current vector. The eigen-components implying the pathological anomaly tend to be regarded as noise components and to be ignored during the

regularization process. Here, I stress the importance of the ignored components for the clinical ischemia diagnosis.

S05_2. Cardiac Excitation Currents Reflected in the MCG: Diagnostic Opportunities

U. Steinhoff¹

¹Physikalisch-Technische Bundesanstalt, Berlin, Germany

Magneticcardiography (MCG), the noninvasive measurement of the magnetic field of the heart, provides another view on cardiac excitation. The magnetic field of the heart is associated with the intra- and extracellular current flow during cardiac excitation. Due to the complicated anisotropic and inhomogeneous conductivity of cardiac and body tissue, the MCG surface pattern cannot be related one by one to the surface potential distribution as it is measured by the electrocardiography (ECG). This finding is based on numerical simulations and simultaneous measurements of MCG and ECG. Thus the careful analysis of MCG data allows getting insight into structural information on cardiac tissue that is different from ECG. Current MCG technology is limited by the spatial separation between cardiac sources and extracorporeal sensors. As the intrinsic noise level of the sensors is known, the number of truly independent parameters of the electrophysiological current distribution that are resolvable from instantaneous MCG data can be estimated; it turns out to be considerably less than the number of channels in a multichannel MCG system. A quantification of structural properties of MCG maps or map sequences avoids the need for detailed current reconstruction, but still contains useful information for diagnostic purposes. Thus, by changing the final goal from current reconstruction to identification of pathologic cardiac conditions, MCG might be a valuable tool in cardiac diagnostics. Recent developments in room temperature-operated optical magnetometers open a path for considerable reduction of experimental effort in MCG, one of the main barriers of its clinical application in the past.

S05_4. Fetal Magnetocardiography: An Effective and Practical Tool for Fetal Cardiology

R. Wakai¹

¹University of Wisconsin–Madison, Madison, WI, USA

Fetal magnetocardiography (fMCG) is a relatively new technique that has shown impressive clinical promise and is likely to be a prime beneficiary of a recent breakthrough in magnetometer technology. In this presentation, I will review the efficacy of fMCG for evaluation of fetal heart rate and rhythm, based on our study of more than 400 fetuses with fetal arrhythmia, congenital heart disease, and other high-risk conditions. These diseases are rare, but are associated with high morbidity and mortality. While ultrasound can also detect abnormal fetal heart rate and rhythm, it is indirect and

imprecise compared with electrophysiological techniques, such as electrocardiography (ECG) and MCG. In most situations, ECG and MCG are similar in quality; however, the fetus is a notable exception. The fECG is strongly attenuated by the poor conductivity of the fetal skin and vernix caseosa, whereas the fMCG is relatively unaffected. Over the past decade, we and other groups have shown that the use of fMCG can lead to improvements in the diagnosis and understanding of the major forms of fetal arrhythmia, such as supraventricular tachycardia and atrioventricular (AV) block. Fetal MCG is also able to detect abnormal repolarization, such as QT prolongation and T-wave alternans in fetal long QT syndrome (LQTS), which cannot be diagnosed at all with ultrasound. We have evidence that fetal LQTS is more prevalent and amenable to therapy in utero than is generally believed.

Due to its susceptibility to magnetic interference, fMCG usually cannot be combined with ultrasound and other techniques; however, we have recently used battery-powered ultrasound scanners to record fMCG simultaneously with 2D and pulsed Doppler ultrasound. While fMCG and ultrasound are concordant the vast majority of times, we have observed that for some arrhythmias, such as blocked atrial bigeminy, the mechanical rhythm does not accurately reflect the magnetic rhythm. This implies that ultrasound can give misleading results in some circumstances.

The use of fMCG has been limited by the high cost of SQUID magnetometer technology; however, a breakthrough in atomic magnetometers is likely to change this situation. My physics collaborators and I have recently have made high-quality fMCG recordings using an atomic magnetometer. We believe it will be possible to manufacture a complete fMCG system, including a magnetic shield, for less than \$100 000 in the near future.

S06_1. Electrical Neuroimaging in Psychiatry: Methodological Challenges and Clinical Applications

T. Koenig¹, M. Kottlow^{1,2}, and L. Melie-García³

¹Department of Psychiatric Neurophysiology, University Hospital of Psychiatry, University of Bern, Bern, Switzerland

²Institute of Pharmacology and Toxicology, University of Zurich, Zurich, Switzerland

³Neuroinformatics Department, Cuban Neuroscience Center, Havana, Cuba

Psychiatric diagnoses are rarely based on pathognomic biomarkers, and the description of psychiatric symptoms as for example thought disorders, hallucinations, or affective problems is typically such that multiple and broadly distributed brain regions may be involved in producing those symptoms. For neurobiological research, the psychopathological assessment of psychiatric patients thus tends to yield rather broad and unspecific a-priori hypotheses. At the same time, electrophysiological measurements such as EEG and event-related potentials (ERPs) are well tolerated by psychiatric patients and tend to be very sensitive to changes in cognitive state and

functioning. EEG and ERP data yields a wealth of data that represents rapidly changing patterns of widespread, but well-structured neural activity that can yield important cues to the neurobiological understanding of the psychopathology. However, in the absence of precise a priori hypotheses, the selection of EEG or ERP features to associate with a diagnosis or a symptom remains a difficult, but nonetheless decisive part of most studies in the domain of psychiatry, and includes (a) the risk of false negative results if inappropriate features were selected or results were overcorrected for multiple testing on irrelevant features or (b) false positives if too many features have been tested and an insufficient correction for multiple tests was applied.

In this context, the authors will present a series of custom-tailored ERP statistical methods that reduce the need for a priori hypotheses without inflating the risk of type 1 errors. These methods consider the multichannel brain electric field as the basic analysis unit, and use randomization tests to assess whether an independent variable is associated with a consistent change in field configuration during some time period.^{1,2} As a consequence, a rigorous statistical evidence for the significance of an effect can be obtained before it is known where and when this effect is supposed to occur precisely. Given the evidence for a topographic effect, further, more in-depth analyses such as statistical parametric mapping in sensor and source space can be applied for a precise delineation and functional interpretation of the effect.

We expect that the application of such methods facilitates the assessment electrophysiological indices of psychopathological brain processes and helps improve the consistency and reliability of research in this domain.

References

1. Strik WK, Fallgatter AJ, Brandeis D, Pascual-Marqui RD. Three-dimensional tomography of event-related potentials during response inhibition: evidence for phasic frontal lobe activation. *Electroencephalogr Clin Neurophysiol*. 1998;108:406-413.
2. Koenig T, Kottlow M, Stein M, Melie-García L. Ragu: a free tool for the analysis of EEG and MEG event-related scalp field data using global randomization statistics. *Comput Intell Neurosci*. 2011;2011:938925.

S06_2. ERP Topography and Tomography in Schizophrenia: Translational Aspects

A. Mucci¹, U. Volpe¹, A. Prinster², M. Salvatore³, and S. Galderisi¹

¹Department of Psychiatry, University of Naples SUN, Naples, Italy

²Biostructure and Bioimaging Institute, National Research Council, Naples, Italy

³Department of Biomorphological and Functional Studies, University of Naples "Federico II", Naples, Italy

The identification of biomarkers has been the focus of recent research to further the current understanding of the neurobiology of schizophrenia and develop novel treatment targets for this disorder. Several event-related potentials (ERPs), including

early and late components (P50, MMN, N100, and P300) abnormalities were proposed as candidate biomarkers, as they are independent of the disorder stage and patients' treatment. However, even for one of the most robust of these biomarkers, the P300 amplitude reduction, topographic and tomographic findings have been inconclusive, as most of the research findings in schizophrenia. Discrepancies in research findings are related to the heterogeneity of the disorder and studies adopting dimensional or/and categorical approaches to reduce schizophrenia heterogeneity are needed to foster the translation of research findings into clinical applications. The presentation will focus on recent ERP and fMRI findings from a study adopting a categorical approach to investigate neurobiological correlates of negative symptoms in patients with schizophrenia. Functional MRI results showed that only patients with deficit schizophrenia (DS), a subtype characterized by primary and enduring negative symptoms, did not activate the dorsal caudate, and showed abnormalities of an early ERP microstate (MS), during reward anticipation. For the same MS, sLORETA demonstrated current source density reduction in bilateral posterior occipitotemporal regions, posterior cingulate, and left frontal and parietal areas in DS patients.

According to our ERP findings, topographic and tomographic abnormalities are present in the early processing stages in the DS subgroup. During these early stages, a fine attentional modulation of sensory processing is carried out to enhance processing of salient stimuli. In the light of fMRI findings, we concluded that a failure to activate the caudate during reward anticipation might impede the activation of an attentional network thus preventing the enhancement of value anticipating cues processing. Specific cognitive training targeting attentional modulation and pharmacological or nonpharmacological interventions enhancing dorsal caudate activation should be designed and studied in patients with DS.

S06_3. The Challenges and Promise of Electrical Neuroimaging in Psychiatry

D.E.J. Linden¹

¹MRC Centre for Neuropsychiatric Genetics and Genomics and National Centre for Mental Health, Cardiff University, Cardiff, UK

The techniques of electrophysiological neuroimaging (electroencephalography [EEG] and magnetoencephalography [MEG]) have particular attraction for the study of the biological mechanisms of mental disorders. Through their high temporal resolution they have the capacity to capture changes in information processing in these disorders; they can probe altered activity of brain networks and their fine-grained temporal/oscillatory structure, which are at the core of many neural models of mental disorders¹; and finally they have unique translational potential because homologous measures can be obtained across species and model systems. EEG and event-related potential (ERP) signatures of neural information processing are also amongst the most promising endophenotypes of mental disorders. I will review the evidence for some key EEG and ERP components as biomarkers and endophenotypes of mental disorders, with a focus on the schizophrenia spectrum.^{2,3}

References

1. Linden D. *The Biology of Psychological Disorders*. Basingstoke, England: Palgrave Macmillan; 2012.
2. Haenschel C, Linden D. Exploring intermediate phenotypes with EEG: working memory dysfunction in schizophrenia. *Behav Brain Res*. 2011;216:481-495.
3. Linden D. Towards a functional neuroanatomy of symptoms and cognitive deficits of schizophrenia. In: Ritsner MS, ed. *The Handbook of Neuropsychiatric Biomarkers, Endophenotypes and Genes: Vol. 2: Neuroanatomical and Neuroimaging Endophenotypes and Biomarkers*. New York, NY: Springer; 2009:55-66.

S06_4. Electrical and Multimodal Neuroimaging in ADHD: Translational Aspects

D. Brandeis^{1,2,3,4}

¹Department of Child & Adolescent Psychiatry, University of Zurich, Zurich, Switzerland

²Central Institute of Mental Health Mannheim, Medical Faculty Mannheim/Heidelberg University, Mannheim, Germany

³Neuroscience Center Zurich, University of Zurich and ETH Zurich, Zurich, Switzerland

⁴Center for Integrative Human Physiology (ZIHP), University of Zurich, Zurich, Switzerland

Introduction. Attention deficit/hyperactivity disorder (ADHD) is a highly prevalent and persistent neurodevelopmental disorder. Despite its heterogeneity, electroencephalographic/event-related potential (EEG/ERP) and hemodynamic (functional magnetic resonance imaging [fMRI]) neuroimaging have revealed consistent deficits of state regulation, inhibition, and motivation in ADHD. Translational neuroimaging draws on these results for diagnostics or subtyping, and learning self-regulation of core brain dysfunctions through neurofeedback. Still, neuroimaging markers may not be sufficiently diagnostic, and the sizeable clinical effects of EEG-neurofeedback treatment in ADHD are partly confounded by expectancy¹ and other unspecific factors.² Neurofeedback using activity from specific dysfunctional regions, like the anterior cingulate cortex (ACC) affected in ADHD, represents a new approach to increase specificity. **Methods.** An initial translational study examined the diagnostic utility of topographic EEG markers for ADHD.³ Next, tomographic EEG neurofeedback (tNF³) using frequency (theta and beta bands), and slow cortical potentials (SCP) protocols for bidirectional regulation of ACC brain activity, was observed in 12 ADHD children. The ACC activity across training and rest phases was computed using sLORETA (low-resolution electromagnetic tomography) of the 30-channel EEG. **Results.** Topographic EEG spectra reliably indicated developmental lag but were not diagnostic for ADHD. Reduction of ADHD symptoms and movement-related artifacts were obtained after tNF. Control over ACC activity was learned only in a simple SCP condition, but ACC frequency distribution at rest normalized over the course of tNF training. **Discussion.** Clinical improvements support

bidirectional self-regulation approaches in ADHD, but the improvements after ACC tNF occurred without substantial learning of ACC control, despite stabilisation of ACC activity. Future translational studies should promote learning of control, use multimodal approaches to improve specificity of diagnostic and treatment, and clarify brain mechanisms underlying nonspecific contribution to NF.

Acknowledgments

Project funded by grants from the EU COST B26, SBF, and Health Department, Canton of Zurich.

References

1. Sonuga-Barke EJ, Brandeis D, Cortese S, et al; European ADHD Guidelines Group. Nonpharmacological interventions for ADHD: systematic review and meta-analyses of randomized controlled trials of dietary and psychological treatments. *Am J Psychiatr*. 2013;170:275-289.
2. Drechsler R, Straub M, Doehner M, Heinrich H, Steinhausen HC, Brandeis D. Controlled evaluation of a neurofeedback training of slow cortical potentials in children with attention deficit/hyperactivity disorder (ADHD). *Behav Brain Funct*. 2007;3:35.
3. Liechti MD, Valko L, Müller UC, et al. Diagnostic value of resting electroencephalogram in attention-deficit/hyperactivity disorder across the lifespan. *Brain Topogr*. 2013;26:135-151.
4. Liechti MD, Maurizio S, Heinrich H, et al. First clinical trial of tomographic neurofeedback in attention-deficit/hyperactivity disorder: evaluation of voluntary cortical control. *Clin Neurophysiol*. 2012;123:1989-2005.

S07_I. Mechanisms and Functional Significance of Excitability Oscillations in Neuronal Ensembles

C.E. Schroeder¹

¹Nathan Kline Institute, Department of Psychiatry, Columbia University College of Physicians and Surgeons, New York, NY, USA.

Neuronal oscillations reflecting synchronous, rhythmic fluctuation of neuron ensembles between high and low excitability states, dominate ambient activity in the sensory pathways. Because excitability determines the probability that neurons will respond to input, a top-down process like attention can use oscillations as “instruments” to amplify or suppress the brain’s representation of external events. That is, by tuning the frequency and phase of its rhythms to those of behaviorally-relevant event streams, the brain can use its rhythms to parse event streams and to select or gate-out inputs. To do this, the brain orchestrates a complex interplay of “modulatory” inputs (regulating physiological context) with “driving” inputs (bearing information content). I will discuss findings from parallel experiments in humans and non-human primates that describe the operation of this parsing and selection mechanism. I will also discuss key implications and questions raised by these findings.

S07_2. Oscillatory Phase: A Signature and Mechanism for Sensory Encoding?

C. Kayser¹ and S. Panzeri¹

¹Institute of Neuroscience and Psychology, University of Glasgow, Glasgow, UK

Oscillations are pervasive in encephalographic (electroencephalography/magnetoencephalography [EEG/MEG]) signals and are considered an important marker or even a causal mechanism for cognitive processes and sensory representations. While the relation between oscillation amplitude (power) and sensory-cognitive variables has been extensively studied, recent work revealed that the dynamic oscillatory signature (phase patterns) can carry information about such processes to a degree greater than the amplitude. To elucidate the direct neural correlates of these, we study the stimulus selectivity of neural firing rates and of EEG oscillations generated by these, both in visual and auditory domains. In one study we studied the encoding of natural sounds in human EEG and intracortical field potentials and single neurons in macaque auditory cortex. We found that stimulus selective firing patterns imprint on the phase rather than the amplitude of slow oscillations and that stimuli that can be discriminated by firing rates can also be discriminated by oscillatory phase patterns but not by oscillation amplitude. This directly suggests a neural basis for stimulus selective EEG phase patterns. In a second study we are investigating whether and how neural encoding varies during the cycles of slow (theta, alpha) oscillations. Estimates of single-neuron input-output filters suggest variations in encoding quality and latency during individual cycles, providing first views into the oscillatory duty-cycles of sensory encoding. All in all this suggests not only correlative but also clear mechanistic roles of cortical oscillations in sensory perception.

S07_3. Alpha Oscillations, Alertness, and Attention

A. Kleinschmidt¹

¹Department of Clinical Neurosciences, University Hospital of Geneva, Geneva, Switzerland

Oscillations near 10 Hz are the single most salient property in population activity of the human brain. Accordingly, they have been called the “alpha” rhythm. Traditionally these oscillations have been taken to indicate cortical idling but recent research has assigned them a more active role. What exactly is this role? Locally, alpha oscillations result in a rhythmic inhibition of neural activity but how this relates to active processing and behavioral benefit is still far from clear.

Some contributions to the understanding of alpha oscillations have emerged from multimodal approaches and in particular from simultaneous recordings of ongoing brain activity by EEG and fMRI. This avenue has proven interesting because the observation which neuroanatomical structures

show activity changes that correlate with alpha oscillations can also inform hypotheses about the function of alpha oscillations. At least 3 so-called resting-state networks seem to correlate in their activity with fluctuations in different features of alpha oscillations. Based on such findings we have proposed the “windshield wiper” model according to which the functional role of alpha oscillations is to cyclically clear accumulated cortical information. As a consequence, alpha activity can bias cortical processing in favor of strong and recent signals. We postulate that this is a suitable mechanism for a low-level attentional function, that of tonic alertness. Moreover, we have shown a direct functional consequence of rhythmic inhibition on cortical processing, namely that responses evoked by brief sensory stimuli are modulated by the phase of the alpha cycle during which stimulation occurs. Strong evoked responses despite high ongoing alpha activity hence presumably require sustained and/or salient sensory input. Conversely, whenever priors permit the deployment of selective attention, this leads to the disabling of alpha activity in specific channels that are likely to convey the attended information. Whether alpha activity facilitates or impedes behavioral performance will hence depend on the neural sites where it manifests and the cognitive context within which it occurs, thus reconciling apparent discrepancies in the literature.

S07_4. Full Brain Modeling

P. Ritter^{1,2}

¹Max Planck Institute for Cognitive and Brain Sciences, Leipzig, Germany

²Charité, University Medicine, Berlin, Germany

My presentation points out how experimental and theoretical studies complement each other to understand the dynamic processes that drive brain oscillatory activity and their functional implications. I will set a particular focus on full brain models that are equipped with individual anatomical skeletons. By fitting them to multimodal functional data such as EEG and fMRI these models become the virtual brains of individual persons. On this basis, we explore mechanisms that lead to the emergence of brain state transitions, plasticity, and information processing and the intersubject variability therein.

S08_3. Neural Correlates of Hypokinesia in Schizophrenia

S. Walther¹

¹University Hospital of Psychiatry, University of Bern, Bern, Switzerland

Schizophrenia patients display less physical activity compared to the general population. However, the neurobiology of hypokinesia in schizophrenia remains unclear. Associations with anhedonia (negative symptoms) or bradykinesia (parkinsonism)

are suspected. Here, we aimed at investigating neurobiological correlates of hypokinesia in schizophrenia patients.

Schizophrenia patients and controls were scanned using a 3 T MRI scanner assessing resting perfusion (arterial spin labeling), and diffusion tensor imaging with 42 diffusion gradients. In all participants, continuous wrist actigraphy was performed for 24 hours in order to measure motor activity. The study on resting perfusion included 11 patients and 14 matched controls, the diffusion tensor imaging (DTI) study included 21 patients and 24 controls. The DTI data were analyzed using a whole brain analysis of fractional anisotropy and additionally in a probabilistic fiber tracking approach.

Resting perfusion in schizophrenia correlated with motor activity in bilateral prefrontal areas in patients, while in controls correlations were exclusively in the ventral anterior nucleus of the thalamus. In both groups, whole brain white matter integrity correlated with motor activity in various frontal regions and the corticospinal tract. The group difference, however, was the inverse correlation of integrity and activity underneath the right supplemental motor area in patients. Structural connectivity between cortical and subcortical motor areas differed between groups. Furthermore, motor activity was related to connectivity of cortico-subcortical loops in controls but not in schizophrenia. Instead, motor activity was related to connectivity in cortico-cortical motor loops in schizophrenia but not in controls.

Interindividual differences in brain structure and perfusion are associated with variations of a behavioral marker such as motor activity. In controls, the association of cortical and subcortical structures of the motor system was found to be involved in motor control. In schizophrenia, the cortico-subcortical motor loops seem to be affected. Hence, hypokinesia in schizophrenia may result from defective motor loop function. The results argue for an important role of the motor system in schizophrenia pathology.

S09_1. Skull Defects Influence MEG Source Reconstruction

J. Haueisen^{1,2}, S. Lau^{1,2,3,4}, L. Flemming², H. Sonntag⁵, and B. Maess⁵

¹Institute of Biomedical Engineering and Informatics, Ilmenau University of Technology, Ilmenau, Germany

²Biomagnetic Center, Department of Neurology, University Hospital Jena, Jena, Germany;

³NeuroEngineering Lab, Department of Electrical and Electronic Engineering, University of Melbourne, Melbourne, Victoria, Australia

⁴Department of Medicine, St. Vincent's Hospital, University of Melbourne, Fitzroy, Victoria, Australia

⁵Max Planck Institute for Human Cognitive and Brain Sciences, Leipzig, Germany

Skull conductivity inhomogeneities include naturally occurring large conductivity variations such as fontanels in infants or the spongy bone structure embedded in the compact bone.

Artificial skull inhomogeneities comprise, for example, surgical holes or sutures. During the modeling process, artificial skull inhomogeneities might be introduced due to erroneous segmentation or meshing. Skull conductivity inhomogeneities are known to influence electroencephalography (EEG) signals and consequently EEG source reconstruction. However, they are thought to have no or minor influence on magnetoencephalography (MEG) signals and MEG source reconstruction. In this talk, the influence of skull conductivity inhomogeneities caused by surgical holes and modeling errors on the MEG forward and inverse problem will be assessed.

We implanted an artificial current dipole in the brain of rabbits and measured simultaneously electric surface potentials (64 channels) and magnetic fields (16 channels). One or two skull defects (holes) were introduced in a surgical procedure. The electric potential amplitudes changed up to a factor of 10 and the magnetic field amplitudes up to 20%, when comparing the data measured over intact skull and skull with one or two holes.

We constructed individual finite element method (FEM) models for the rabbits, including gray and white matter, cerebrospinal fluid (CSF), intracranial blood vessels, compact and spongy bone, skull defects, ocular humour and lens, and body. The computed magnetic field and electric potential differences based on models with and without skull defects confirmed the experimental results. Artificial skull inhomogeneities (a number of small holes) introduced due to erroneous segmentation and meshing resulted on average in 20% amplitude change of the magnetic field; however, in worst cases up to 200%.

We conclude that skull conductivity inhomogeneities have a nonnegligible effect on the MEG forward and inverse problem. Especially when source positions are expected to be in the vicinity of the conductivity inhomogeneity and when a large difference with respect to the skull conductivity is indicated, the modeling approach should take the inhomogeneities into account.

Acknowledgment

BMBF3IPT605A, DFG Ha 2899/14-1.

S09_2. Skull Modeling Using FEM

T.R. Knösche¹, B. Lanfer², M. Dannhauer³, and C.H. Wolters²

¹Max Planck Institute for Human Cognitive and Brain Sciences, Leipzig, Germany

²Institute for Biomagnetism and Biosignalanalysis, University of Münster, Münster, Germany

³Scientific Computing and Imaging Institute, University of Utah, Salt Lake City, UT, USA

The conductivity properties of the human skull have great influence on the way electrical brain activity expresses as EEG

features on the head surface. Its proper modeling is therefore of paramount importance for EEG source modeling. Here, we investigate the relative accuracy of different skull modeling approaches and quantify the effects of common errors and simplifications.

We used computer simulations to investigate finite element models [FEMs]¹ of the human skull in EEG source analysis. In the first part, we present a systematic investigation on the accuracy of different ways to account for the layered skull structure. We investigated local models, where each skull location was modeled differently, and global models, where the skull was assumed to be homogeneous, both using isotropic as well as anisotropic conductivity assumptions. We determined errors both in the forward calculation and the reconstructed dipole position.²

In the second part, we investigate the effect of a number of common errors and limitations in skull modeling, using both forward and inverse simulations. Test models included erroneous skull holes, local errors in skull thickness, modeling cavities as compact bone, downward extension of the volume conductor and simplifying the inferior skull and the inferior skull and scalp as layers of constant thickness.³

Our results show that accounting for the local variations over the skull surface is important, while assuming anisotropic skull conductivity has little influence. Furthermore, it was found, that large skull geometry inaccuracies close to the source space led to considerable errors more than 20 mm for extended regions of the source space. Local defects, for example, erroneous skull holes, caused nonnegligible errors only in the vicinity of the defect.

In terms of the general method to model the skull, we recommend that if compact and spongy bone can be identified with sufficient accuracy, one should model these explicitly by assigning each voxel to one of the two conductivities. Otherwise, one should model the skull as either homogeneous and isotropic, but with considerably higher skull conductivity than the usual 42 mS/m, or as homogeneous and anisotropic, but with higher radial conductivity than the usual 42 mS/m and a considerably lower radial:tangential conductivity ratio than the usual 1:10. Furthermore, we derived detailed guidelines for modeling the skull geometry in individual volume conductor models.

References

1. Wolters CH, Grasedyck L, Hackbusch W. Efficient computation of lead field bases and influence matrix for the FEM-based EEG and MEG inverse problem. Part I. Complexity considerations. *Inverse Problems*. 2004;20:1099-1116.
2. Dannhauer M, Lanfer B, Wolters CH, Knösche TR. Modeling of the human skull in EEG source analysis. *Hum Brain Mapp*. 2011;32:1383-1399.
3. Lanfer B, Scherg M, Dannhauer M, Knösche TR, Burger M, Wolters CH. Influences of skull segmentation inaccuracies on EEG source analysis. *Neuroimage*. 2012;62:418-431.

S09_3. Modeling the Skull Fine-Structure With Boundary Element Method

M. Stenroos^{1,2} and J. Hauelsen³

¹Aalto University, BECS, Aalto, Finland

²MRC Cognition and Brain Sciences Unit, Cambridge, UK

³Ilmenau University of Technology, Ilmenau, Germany

In neuroelectromagnetic source imaging, the conductivity profile of the head needs to be modeled. In this forward model, the poorly conducting skull plays a large role; errors and simplifications in the skull model may be detrimental to source localization. In experimental EEG and combined MEG + EEG use, the head model typically contains 3 homogeneous compartments (brain, skull, and scalp). The skull, however, contains regions of compact and spongy bone that have different conductivities. This fine-structure has previously been modelled with the finite element method (FEM). In this study, we show that accurate skull modelling is feasible with the boundary element method (BEM) as well.

An anatomical head model was built using the Curry software and T1-weighted MR images of a volunteer. The inner and outer boundaries of the skull and scalp were segmented using standard procedures, and the 4 regions of spongiosa were segmented manually. Three- and 4-compartment boundary element models were built using the linear Galerkin BEM formulated with the isolated source approach (LGISA)¹ at various mesh densities, and the skull conductivity of the 3-shell models was optimized. The most dense model (37 074 vertices) was used as the reference. Forward solutions of cortically constrained sources were then compared across models using relative error (RE) and relative difference (RDM) metrics.

The results showed that all 4-compartment models performed considerably better than the best 3-shell model; the mean REs and RDMs of these models were <2% and 6.9% and <1.1% and 4.9%, respectively. When only the regions affected by the spongiosa were compared, the corresponding REs were <2.2% and 10.1% and the RDMs <1.3% and 6.6%. The RDMs are similar to those obtained using the FEM by Dannhauer et al.² The use of our most coarse spongiosa mesh (1707 vertices) increased the RE for some occipital and anterolateral sources by a couple of percents. A similar increase of error was obtained with a very coarse inner skull mesh (938 vertices). A good balance between the accuracy and computational cost was found with a model comprising a total of 9671 vertices; the mean RE of this model was 0.8%. Such a model can be built in a standard workstation in less than 1 hour.

The results of this study show that the skull fine-structure can be modeled with the LGISA BEM without using especially fine meshes. The challenges of BEM skull modeling are thus in segmentation, meshing, and estimating the conductivities, not in numerical computation.

References

1. Stenroos M, Sarvas J. Bioelectromagnetic forward problem: isolated source approach revisited. *Phys Med Biol.* 2012;57:3517-3535.
2. Dannhauer M, Lanfer B, Wolters CH, Knösche TR. Modeling of the human skull in EEG source analysis. *Hum Brain Mapp.* 2011;32:1383-1399.

S09_4. Influence of Volume Conduction on EEG and MEG Source Analysis and Brain Stimulation

C. Wolters¹, Ü. Aydin¹, B. Lanfer^{1,2}, S. Lew³, F. Lucka^{1,4}, L. Ruthotto⁵, J. Vorwerk¹, and S. Wagner¹

¹Institute for Biomagnetism and Biosignalanalysis, University of Münster, Münster, Germany

²BESA GmbH, Gräfelfing, Germany

³Athinoula A. Martinos Center for Biomedical Imaging, Massachusetts General Hospital, Charlestown, MA, USA

⁴Institute for Applied Mathematics, University of Münster, Münster, Germany

⁵Department of Earth, Ocean and Atmospheric Sciences, University of British Columbia, Vancouver, Canada.

We present fast and accurate realistic modeling approaches for the forward problem in electroencephalography (EEG) and magnetoencephalography (MEG) source analysis and for simulation of transcranial direct current stimulation (tDCS) and transcranial magnetic stimulation (TMS).

We start with the presentation of a new pipeline for the construction of a 6-compartment (skin, skull compacta, skull spongiosa, cerebrospinal fluid [CSF], brain gray and white matter) individually calibrated (with regard to skull conductivity) anisotropic (with regard to brain tissue) finite element (FE) head volume conductor model. Head compartments are modeled individually: With regard to geometry we use a combination of T1- and T2-weighted magnetic resonance images (MRI). Skull conductivity is estimated from simultaneously measured somatosensory evoked potential and field data. Brain tissue conductivity anisotropy is modeled using diffusion-weighted MRI. First, a diffeomorphic MR susceptibility artifact correction method is used that allows accurate determination of diffusion tensor images (DTI).¹ In a second step, using an effective medium approach, the artifact-corrected DTI will then be transformed into conductivity tensor images that are embedded in the FE head model.²⁻⁴

We validate the numerical accuracy of different FE approaches in multicompartment sphere models in comparison with state-of-the-art boundary element approaches and put these numerical errors in relation with the modeling error when ignoring the CSF.⁵ Using Helmholtz's reciprocity, we show that this also serves as a validation for tDCS simulation.⁴ Transfer matrix approaches and algebraic-multigrid preconditioned conjugate gradient solver methods speed up FE computation⁵ in a way that even very high resolution FE models can easily be used in inverse EEG and MEG source analysis scenarios^{2,6} or in complex tDCS/TMS simulations.⁴

Finally, we present volume conduction effects in adult⁷ and in infant (skull fontanel and suture modeling⁸) EEG and MEG source analysis investigations, in combined EEG/MEG/MRI presurgical epilepsy diagnosis^{2,6} and in the simulation of tDCS⁴ and TMS.³

Acknowledgments

This research has been supported by the German Research Foundation (DFG) through projects WO1425/2-1, 3-1.

References

1. Ruthotto L, Kugel H, Olesch J, et al. Diffeomorphic susceptibility artifact correction of diffusion-weighted magnetic resonance images. *Phys Med Biol.* 2012;57:5715-5731.
2. Aydin Ü, Vorwerk J, Küpper P. 2013. Submitted for publication.
3. Janssen A, Rampersad S, Lucka F, et al. The influence of sulcus width on simulated electric fields induced by transcranial magnetic stimulation. *Phys Med Biol.* 2013;58:4881-4896.
4. Wagner S, Rampersad S, Aydin Ü, et al. 2013. In revision.
5. Vorwerk J, Clerc M, Burger M, Wolters CH. Comparison of boundary element and finite element approaches to the EEG forward problem. *Biomed Tech (Berl).* 2012;57:795-798.
6. Rullmann M, Anwender A, Dannhauer M, Warfield SK, Duffy FH, Wolters CH. EEG source analysis of epileptiform activity using a 1 mm anisotropic hexahedra finite element head model. *Neuroimage.* 2009;44:399-410.
7. Wolters CH, Anwender A, Tricoche X, Weinstein D, Koch MA, MacLeod RS. Influence of tissue conductivity anisotropy on EEG/MEG field and return current computation in a realistic head model: a simulation and visualization study using high-resolution finite element modeling. *Neuroimage.* 2006;30:813-826.
8. Lew S, Sliva DD, Choe MS, et al. Effects of sutures and fontanels on MEG and EEG source analysis in a realistic infant head model. *Neuroimage.* 2013;76:282-293.

S09_5. Whole Head Model of Spontaneous Brain Activity

C. Ramon^{1,2}

¹Department of Electrical Engineering, University of Washington, Seattle, WA, USA

²Department of Bioengineering, Reykjavik University, Reykjavik, Iceland

Our objective was to model scalp EEGs due to the spontaneous brain activity. We used a 3-D finite element method (FEM) model of an adult male subject constructed from 192 segmented axial MR slices with 256×256 pixel resolutions. The FEM voxel resolution was $1 \times 1 \times 1$ mm. Majority of the tissues were identified that included scalp, fat, muscle, dura layer, cerebrospinal fluid (CSF), cerebellum, gray and white matter, and hard and soft skull bone. The background electrical activity of the whole cortex was represented by 120 000 dipoles and of the cerebellum by 24 000 dipoles. Each dipole in a cortical voxel was oriented normal to the local gray and white matter boundary and it represented the averaged electrical activity of

approximately 10 000 neurons. The dipole intensity distribution was in the range of 0.0 to 0.4 mA meter with a uniform random distribution. Spontaneous brain activity was modelled as a Gaussian i.i.d. random process. Its $1/f$ slope of the temporal power spectral densities (PSDt) was matched with the PSDt computed from the measured 256-channel scalp EEG data of the subject. Iterative optimization techniques were used for this. In addition, thalamocortical oscillations in the theta (3–7 Hz) band were superimposed on the spontaneous brain activity by use of a neural mass model. Spatiotemporal effects of the inclusion of dura layer on EEG simulations were also examined. Two models were used. In the reference model the dura layer was included, while in the other model, it was replaced with CSF. The electrical conductivities of various tissues were obtained from the literature. Using an adaptive FEM solver the potential and flux distributions in the whole head model were computed. Spatiotemporal contour plots of potentials on the scalp surface (EEG) were made. The PSDt exhibited a $1/f$ slope with broad peak in the theta band, which was above the slope of $1/f^2$. Inclusion of the dura layer significantly reduced the amplitude of the simulated EEGs, PSDt and also the spatial power spectral densities (PSDs). There were broad peaks in the PSDs plot, which possibly are related to gyri and sulci structures. These results suggest that it is feasible to simulate spatiotemporal characteristics of scalp EEGs with a whole head model that included a detailed structure of the cortical electrical activity. We also found that the inclusion of the dura layer is essential for an accurate simulation of scalp EEGs.

S10_I. Clinical Studies and Neuroimage Analysis of Brain–Computer Interface for Stroke Rehabilitation

C. Guan¹, K.K. Ang¹, S.G. Chua², W.K. Kuah², K.S. Phua¹, E. Chew³, H. Zhou⁴, K.H. Chuang⁵, B.T. Ang⁶, C. Wang¹, H. Zhang¹, H. Yang¹, Z.Y. Chin¹, H. Yu¹, and Y. Pan¹

¹Institute for Infocomm Research, Singapore

²Tan Tock Seng Hospital, Singapore

³National University Hospital, Singapore

⁴Duke-NUS Graduate Medical School, Singapore

⁵Singapore Biomedical Imaging Consortium, Singapore

⁶National Neuroscience Institute, Singapore

Recently, brain–computer interface (BCI) technology has been actively investigated to provide a new alternative way of rehabilitation to help stroke survivors restore motor function by inducing activity-dependent brain plasticity. Worldwide, stroke is one of the leading causes of severe disabilities. About one third of stroke survivors need various forms of rehabilitation. Among these, upper limb weakness and loss of hand function are among the most devastating types of disabilities. Limitations in current physiotherapy and occupational therapy techniques include (a) difficulties in rehabilitation for the severely paralyzed arm and hand, which are often treated with passive modalities; (b) difficulties in achieving intensive rehabilitation

and high repetitions in those with moderate to severe upper extremity paralysis; (c) problems in motivating and sustaining patient interest in repetitive exercises; and (d) therapy is often perceived to be boring due to lack of immediate biofeedback.

The hypothesis of using BCI for stroke rehabilitation is built on the following basis: (a) motor imagery activates primary motor cortex, premotor cortex, and possibly some other parts of the brain that are responsible for motor control, therefore rehabilitation using motor imagery can lead to motor recovery; (b) BCI provides a contingent feedback for stroke patients, which helps reinforce the neural pathway of motor control; (c) real-time feedback to patients provides motivation due to visual/auditory/haptic feedback; and (d) combination of BCI with mechanical stimulation (eg, robotics) provides motor/sensory feedback that is beneficial.

We have conducted 3 pilot clinical studies involving 66 stroke patients, where we investigated how BCI was used in conjunction with other devices (robotics, haptic, and transcranial direct current stimulation) to help hemiplegic stroke patients in performing upper limb rehabilitation. In this talk, we will present the following results from the studies:

1. The clinical outcomes in various studies, measured by Fugl-Meyer assessment (FMA) scores
2. The fMRI study to measure the functional connectivity and comparison of the connectivity changes before and after the rehabilitation
3. The structural changes evidenced from diffusion tensor image (DTI) before and after the rehabilitation
4. The EEG coherence changes as a predictor for BCI-based stroke rehabilitation

In summary, we have observed statistically significant clinical outcomes in all 3 clinical studies comparing the pre- and postrehabilitation FMA measurements. Functional imaging shows statistically significant enhancement in functional connectivity after training. Initial indication of structural change might imply possible plasticity effects. EEG coherence provides possible prediction for clinical outcome.

Acknowledgments

This work was supported by the Science and Engineering Research Council of A*STAR (Agency for Science, Technology and Research), and the National Medical Research Council, Singapore.

References

1. Ang KK, Guan C. Computer interface in stroke rehabilitation. *J Comput Sci Eng.* 2013;7:139-146.
2. Ang KK, Guan C, Chua SG, et al. A large clinical study on the ability of stroke patients to use EEG-based motor imagery brain-computer interface. *Clin EEG Neurosci.* 2011;42:253-258.
3. Várkuti B, Guan C, Pan Y, et al. Resting state changes in functional connectivity correlate with movement recovery for BCI and robot-assisted upper-extremity training after stroke. *Neurorehabil Neural Repair.* 2013;27:53-62.

4. Daly JJ, Wolpaw JR. Brain-computer interfaces in neurological rehabilitation. *Lancet Neurol*. 2008;7:1032-1043.
5. Buch E, Weber C, Cohen LG, et al. Think to move: a neuromagnetic brain-computer interface (BCI) system for chronic stroke. *Stroke*. 2008;39:910-917.
6. Daly JJ, Cheng R, Rogers J, Litinas K, Hrovat K, Dohring M. Feasibility of a new application of noninvasive brain computer interface (BCI): a case study of training for recovery of volitional motor control after stroke. *J Neurol Phys Ther*. 2009;33:203-211.
7. Broetz D, Braun C, Weber C, Soekadar SR, Caria A, Birbaumer N. Combination of brain-computer interface training and goal-directed physical therapy in chronic stroke: a case report. *Neurorehabil Neural Repair*. 2010;24:674-679.
8. Sharma N, Pomeroy VM, Baron J-C. Motor imagery: a backdoor to the motor system after stroke? *Stroke*. 2006;37:1941-1952.
9. Prasad G, Herman P, Coyle D, McDonough S, Crosbie J. Applying a brain-computer interface to support motor imagery practice in people with stroke for upper limb recovery: a feasibility study. *J Neuroeng Rehabil*. 2010;7:60.
10. Zhou J, Yao J, Deng J, Dewald JP. EEG-based classification for elbow versus shoulder torque intentions involving stroke subjects. *Comput Biol Med*. 2009;39:443-452.
11. Ang KK, Chin ZY, Zhang H, Guan C. Mutual information-based selection of optimal spatial-temporal patterns for single-trial EEG-based BCIs. *Pattern Recogn*. 2011;45:2137-2144.
12. Ang KK, Guan C, Phua KS, et al. Transcranial direct current stimulation and EEG-based motor imagery BCI for upper limb stroke rehabilitation. *Conf Proc IEEE Eng Med Biol Soc*. 2012;2012:4128-4131.
13. Yang H, Guan C, Ang KK, Wang C, Phua KS, Yu J. Dynamic initiation and dual-tree complex wavelet feature-based classification of motor imagery of swallow EEG signals. Paper presented at: The IEEE International Joint Conference on Neural Networks; June 10-15, 2012; Brisbane, Queensland, Australia.
14. Ang KK, Guan C, Chua SG, et al. Clinical study of neurorehabilitation in stroke using EEG-based motor imagery brain-computer interface with robotic feedback. *Conf Proc IEEE Eng Med Biol Soc*. 2010;2010:5549-5552.

S10_3. Statistical Methods for Improving Brain-Computer Interface P300 Speller Speed and Accuracy in Disabled and Nondisabled Population

L. Collins¹, B. Mainsah¹, K. Colwell¹, K. Morton¹, D. Ryan², E. Sellers², K. Caves¹, and S. Throckmorton¹

¹Duke University, Durham, NC, USA

²East Tennessee State University, Johnson City, TN, USA

Recent research in P300 speller brain-computer interfaces (BCI) has focused less on P300 detection via improved classifiers and more on developing different speller interfaces and protocols that allow improved accuracy and speed. Research that was led by the East Tennessee State University (ETSU) team has demonstrated that the selection of speller layout can improve performance and a layout different from the standard row/column paradigm is often preferred. They have experimented with several other speller parameters in order to

optimize the interface for end users, and have tested their paradigms in disabled and nondisabled populations. Recent research led by the Duke team has demonstrated that a Bayesian dynamic stopping criteria where the number of flashes per character spelled is adjusted dynamically can statistically significantly improve accuracy and speed. In this talk, we will report on these dynamic stopping results for both disabled and nondisabled populations. In addition, we will present our recent research in which a dictionary-based language model is used in conjunction with the dynamic stopping paradigm to adjust the probabilities associated with the letters being flashed. Results are presented, which indicate a statistically significant improvement in speller speed when this probabilistic language model is included. Finally, we will report on our newest results in which the language model is used to perform spelling correction, and also on a study where a clustering approach is used to preselect from a group of trained classifiers, and demonstrate a dramatic reduction in the amount of time required to train the classifier with little degradation in speller accuracy.

Acknowledgments

This work was supported by NIH/NIDCD (R21 DC010470-01).

S10_4. Bridging Gaps: Independent Home Use of Brain-Computer Interfaces

A. Kübler¹, E.M. Holz¹, and C. Zickler²

¹Institute of Psychology, University of Würzburg, Würzburg, Germany

²Institute of Medical Psychology and Behavioural Neurobiology, University of Tübingen, Tübingen, Germany

Over the past 20 years, research on BCIs that can provide communication and control to individuals with severe motor impairment has increased almost exponentially. While considerable effort has been dedicated to off-line analysis for improving signal detection and translation, online studies with the target populations are far less common; there remains a great need for translational studies that examine BCI use by target populations. Furthermore, long-term studies with users in the field are required to improve reliability of BCI control. Thus, we are facing a translational and reliability gap. Further research is needed on usability, system robustness and convenience; training and technical support; subject inclusion criteria, recruitment, consent, and retention. The user-centered approach provides a framework to design and evaluate such studies in a standardized way that allows for comparison between different BCI-based applications for communication and control. It includes an iterative process of development and feedback between researchers and users which leads can lead to increasing refinement of the product. Within the user-centered design,¹ Usability is defined as effectiveness, efficiency, and satisfaction with regards to the assistive technology device of interest. For BCI-controlled applications, effectiveness can

be regarded equivalent to accuracy of selections and efficacy to the amount of information transferred per time unit and the effort invested (workload). Satisfaction with a device was assessed for general and BCI-specific aspects and included the match between user and technology. Results of first studies with severely motor impaired end-users mostly in their home environment, which implemented the respective evaluation metrics indicated high effectiveness and information transfer rate (ITR) with P300-based applications for communication and entertainment.^{2,3} While subjective workload was moderate to low, satisfaction was high to moderate. None of the end-users could imagine using BCI for communication, but most could for entertainment even when ITR was low. A high match between user and BCI could be achieved provided the BCI exactly met the individual user's needs. Using standardized evaluation metrics within the user-centered approach to device development will allow the BCI community to provide BCI-controlled applications for real end-users' needs in their daily life environment. Thus, the user-centered design appears to be suitable for bridging the translational and reliability gap and ultimately pave the way to independent home use.

Acknowledgments

This work is supported by the European ICT Program Project FP7-224631 (TOBI) and FP7-288566 (Backhome). This manuscript only reflects the authors' views and funding agencies are not liable for any use that may be made of the information contained herein.

References

1. DIS, I. 2008. 9241-210:2009. *Ergonomics of human system interaction—Part 210: Human-centred design for interactive systems (formerly known as 13407)*. Geneva, Switzerland: International Organization for Standardization (ISO); 2009.
2. Kübler A, Holz E, Kaufmann T. A user-centred approach for bringing BCI-controlled applications to end-users. In: Fazel-Rezaei R, ed. *Brain Computer Interfaces*. InTech Open Access. In press.
3. Kübler A, et al. The user-centered design in BCI research: a standardized procedure for evaluating the usability of BCI-controlled applications. In preparation.

S10_5. The Challenge of Communication in Complete Paralysis

E. Sellers¹, D. Ryan¹, K. Brown¹, K. Colwell², B. Mainsah², K. Caves², S. Throckmorton², and L. Collins²

¹East Tennessee State University, Johnson City, TN, USA

²Duke University, Durham, NC, USA

Noninvasive brain-computer interface (BCI) technology allows people to use scalp recorded electroencephalographic activity as a control signal to perform a variety of tasks (eg, cursor control, word processing, e-mail, environmental control). Because BCI communication does not depend on neuromuscular activity, it can be an effective means of communication for people with

severe motor impairments. In most cases, a BCI is the least preferred mode of communication due to functional limitations of these systems, modest rates of accuracy, and low speed—as compared with other augmentative and alternative communication solutions. Nonetheless, a BCI may be the only viable option of restoring independent communication and autonomy for some people who are severely disabled. However, the lack of effective communication makes it difficult, as a researcher, to know if the participant has understood protocols or if the participant has questions, can see clearly, etc. This talk will discuss effective means of overcoming communication barriers and presents work that has improved speed, accuracy, and reliability of BCI systems through systematic paradigm manipulation, as informed by cognitive neuroscience, visual attention, and psychophysiology.

Acknowledgments

Supported by NIH/NIDCD (R21 DC010470-01).

S11_1. Electromagnetic Source Imaging of Extended Cortical Sources: Reliability and Validity of Inverse EEG/MEG Applied to Human K-Complexes and Temporal Lobe Spikes

R. Wennberg¹

¹Krembil Neuroscience Centre, University Health Network, University of Toronto, Toronto, Ontario, Canada

Spontaneous electromagnetic potentials of interest for EEG and MEG source imaging (ESI/MSI) are typically generated by extended cortical sources at least 10 to 20 mm² in size. Sources of this size or larger are the intracranial EEG correlate for focal and generalized epileptiform discharges, the most common potentials modeled using inverse EEG/MEG. For ESI/MSI to provide added clinical benefit in the coming years, modeling results must be shown to be both reliable (ie, identical spikes give rise to identical source solutions) and valid (ie, localizations accurately represent the intracranial cortical source maxima). Moreover, ESI/MSI should provide localization accuracy better than can be achieved by simply looking at the raw data. True validity of source solutions can only be assessed by direct comparison with intracranially recorded fields. Reliability can be assessed by comparing source solutions obtained for repeated examples of identical potentials. An analysis of ESI/MSI performed on multiple identical spikes recorded from classical anterior temporal spike foci (10-20 mm² in size) showed limited reliability and validity when modeling single spikes, using either dipole or distributed inverse models. Modeling on averages of multiple ($n \geq 8$) identical spikes, however, significantly improved the validity and reliability of source solutions, with mm accuracy attained irrespective of data filtering, volume conductor or goodness-of-fit values. The benefits of spike averaging are presumably related to reduction of background noise, rendering the averaged spontaneous potential similar to an evoked potential. At the far end of the

spectrum of extended cortical source size is the human K-complex, topographically similar to the generalized spike/wave discharge. The largest spontaneous potential in the EEG, it is associated with an extended superficial bifrontal intracranial cortical field. An analysis of K-complexes showed a consistent propensity of ESI and MSI to return falsely localized deep midline source solutions, whether using dipole or distributed inverse models. The reliability of ESI/MSI results was high even when modeling single K-complexes (presumably due to high signal to noise ratio), however, the source localizations were consistently invalid. Thus, existing inverse EEG/MEG methods cannot provide valid solutions for the largest of extended cortical sources. The upper limit of cortical source size that can be accurately modeled remains to be determined, but must lie somewhere between the 10 to 20 mm² of the classical temporal lobe spike focus and the extended bifrontal cortical source of the human K-complex.

SI1_2. Complementary Properties of EEG and MEG

S.P. Ahlfors^{1,2}

¹Athinoula A. Martinos Center, Massachusetts General Hospital, Charlestown, MA, USA

²Harvard-MIT Division of Health Sciences and Technology, Cambridge, MA, USA

Electroencephalography (EEG) and magnetoencephalography (MEG) signals are generated by the same type of neural events, conceptually described as primary currents within local cortical neuron populations. However, the different sensitivity patterns of EEG and MEG suggest that these 2 measures provide complementary information about the brain activation. EEG and MEG have well-known differences in their sensitivity in terms of the orientation and the depth of focal source elements.¹ Experimental and theoretical studies have suggested relatively minor differences in the localization accuracy of isolated current dipoles. In contrast, complementary properties for EEG and MEG are expected to benefit source estimation for complex source patterns with extended and distributed sources. For a large proportion of cortical regions, substantial contributions from extended sources to the EEG signals are likely to originate from radial source components, to which MEG is insensitive. Because of selective cancellation, the sensitivity properties to different source orientations become more pronounced in determining differences between EEG and MEG when the sources are extended than when they are focal.² The complementary properties of EEG and MEG suggest that by combining these data in source estimation has the potential to enhance the identification, localization, and dissociation of source regions.

Acknowledgments

Supported by NIH grants NS057500, NS037462, HD040712, and NCRR P41RR14075.

References

1. Ahlfors SP, Han J, Belliveau JW, Hämäläinen MS. Sensitivity of MEG and EEG to source orientation. *Brain Topogr.* 2010;23:227-232.
2. Ahlfors SP, Han J, Lin FH, et al. Cancellation of EEG and MEG signals generated by extended and distributed sources. *Hum Brain Mapp.* 2010;31:140-149.

SI1_3. Evaluation of the Spatial Extent of the Sources of Epileptic Spikes in MEG

C. Grova^{1,2}, **R. Chowdhury**¹, **T. Hedrich**¹, **M. Heers**², **R. Zelman**², **J.A. Hall**², **J.M. Lina**^{1,3}, and **E. Kobayashi**²

¹Multimodal Functional Imaging Lab, Biomedical Engineering Department, McGill University, Montreal, Quebec, Canada

²Neurology and Neurosurgery Department, Montreal Neurological Institute, McGill University, Montreal, Quebec, Canada

³Département de Génie Électrique, École de Technologie Supérieure, Montreal, Quebec, Canada

Detection of spontaneous epileptic discharges in EEG or MEG from background brain activity requires synchronized neuronal activity over a minimum area of cortex to be detected from scalp recordings. A minimum area of 6 to 10 cm² has been suggested in EEG¹ and of 4 cm² in MEG.² We will present the principle of the maximum entropy on the mean (MEM) as a validated source localization method able to accurately recover the spatial extent of the generators of epileptic discharges. We carefully evaluated the ability of MEM to recover the extent of cortical area involved during interictal spikes, either from scalp EEG³ or from MEG data.^{4,5}

The first level of the validation was obtained using Monte Carlo simulations of realistic MEG data involving sources of several spatial extents and depths. MEM methods were compared with source localization methods based on hierarchical Bayesian (HB) models. For both MEM and HB frameworks, 2 types of spatial models have been investigated: (a) brain activity may be modeled using cortical parcels and (b) brain activity is assumed to be locally smooth within each parcel. Detection accuracy of each method was quantified using receiver operating characteristic analysis. Our results showed that MEM methods were sensitive to all spatial extents of the sources ranging from 3 cm² to 30 cm², whatever were the number and size of the parcels. To reach a similar level of accuracy within the HB framework, a model using parcels larger than the size of the sources should be considered.⁵

For the second level of validation, taking into account the limited spatial sampling of intracranial EEG (iEEG) depth electrodes, we proposed to estimate iEEG potentials from MEG sources, to assess what part of MEG sources could be seen by iEEG contacts. We evaluated five patients with focal epilepsy who had a preoperative MEG acquisition and iEEG with MRI-compatible electrodes. Individual MEG spikes were localized

along the cortical surface of each subject. Applying an iEEG forward model to MEG sources localized along the cortical surface, we obtained MEG-estimated iEEG potentials that were compared with real iEEG potentials recorded for each patient. Excellent MEG/iEEG correlation was found in the presumed focus for four patients. In one patient, the main MEG source could not be retrieved by iEEG implantation and the deep source found in iEEG could not be localized in MEG. MEM-based source localizations recovered accurately the sources' spatial extent with less spurious sources distant from the presumed focus. We demonstrated that MEG-estimated iEEG potentials allow quantification of the spatial extent of MEG generators that could be retrieved and validated with iEEG.

References

1. Tao JX, Baldwin M, Hawes-Ebersole S, Ebersole JS. Cortical substrates of scalp EEG epileptiform discharges. *J Clin Neurophysiol*. 2007;24:96-100.
2. Oishi M, Otsubo H, Kameyama S, et al. Epileptic spikes: magnetoencephalography versus simultaneous electrocorticography. *Epilepsia*. 2002;43:1390-1395.
3. Grova C, Daunizeau J, Lina JM, Bénar CG, Benali H, Gotman J. Evaluation of EEG localization methods using realistic simulations of interictal spikes. *Neuroimage*. 2006;29:734-753.
4. Lina JM, Chowdhury R, Lemay E, Kobayashi E, Grova C. Wavelet-based localization of oscillatory sources from magnetoencephalography data [published online March 6, 2012]. *IEEE Trans Biomed Eng*. doi: 10.1109/TBME.2012.2189883.
5. Chowdhury RA, Lina JM, Kobayashi E, Grova C. MEG source localization of spatially extended generators of epileptic activity: comparing entropic and hierarchical bayesian approaches. *PLoS One*. 2013;8(2):e55969.

SI 4. Validation and Clinical Application of Inverse ECG

T. Oostendorp¹, P. van Dam¹, P. Oosterhof², A. Linnenbank², R. Coronel², P. van Dessel², and J. de Bakker²

¹Donders Institute for Brain, Cognition and Behaviour, Radboud University Nijmegen Medical Center, Nijmegen, Netherlands;

²Academic Medical Center, Department of Clinical and Experimental Cardiology, Amsterdam, Netherlands

The activation sequence of the heart is an important parameter in clinical cardiology, for instance, in determining the site for ablation therapy. The estimation of activation times from measured surface electrocardiograms (ECGs) is far from trivial. Over the past decades, we have developed the equivalent surface source model,¹ in which the electric sources within the myocardium are presented by an equivalent dipole layer at the surface of the myocardium, whose source strength is proportional to the local transmembrane potential. In an inverse procedure, this model allows for the estimation of the activation

times at both epicardium and endocardium. Previous studies have shown that the estimated activation times found using this model correspond well to the expected activation sequence.² In our present study, the accuracy of the method is tested in an animal model and the method is applied to clinical data.

In the animal study, activation times were measured invasively in pigs, while recording the surface ECGs, for both sinus rhythm and single and dual beats paced at different sites. Individual volume conductor models were constructed on the basis of computed tomographic (CT) images. The site of earliest activation for paced beats found from the inverse procedure corresponds well to the pacing site (average distance 17 mm). For the left ventricle, the method performed well in determining whether the stimulation was endo- or epicardially (86% correct). The right ventricular wall is too thin to allow reliable single-sided activation. In the continuation of this study, measured and estimated activation times will be compared for the more complex dual site paced and sinus beats.

In the clinical study, the ECG was recorded in suspected Brugada patients who were subjected to an ajmaline stress test. Individual volume conductor models were constructed from magnetic resonance (MR) images. Brugada patients are prone to nonischemic sudden cardiac death. The test provokes the typical abnormalities in the ECG that may otherwise go unnoticed. The mechanism behind the Brugada syndrome is not well understood. One hypothesis states that in the outflow tract of the right ventricle the propagation of activation slows down, and more so on the epicardial than on the endocardial aspect.³

The inverse procedure was applied to successive beats while ajmaline was injected. The results show that the activation times increase in the right outflow tract, mainly epicardially, with increasing ajmaline concentration, and that the activation returns to normal when ajmaline washes out, which corroborates the hypothesis mentioned above.

The results of this study indicate that the equivalent surface source model allows noninvasive estimation of cardiac activation times.

Acknowledgments

This study was supported by the Dutch Technology Foundation STW grant 09201.

References

1. Huiskamp G, van Oosterom A. The depolarization sequence of the human heart surface computed from measured body surface potentials. *IEEE Trans Biomed Eng*. 1988;35:1047-1058.
2. Modre R, Tilg B, Fischer G, Wach P. Noninvasive myocardial activation time imaging: a novel inverse algorithm applied to clinical ECG mapping data. *IEEE Trans Biomed Eng*. 2002;49:1153-1161.
3. Coronel R, Casini S, Koopmann TT, et al. Right ventricular fibrosis and conduction delay in a patient with clinical signs of Brugada syndrome: a combined electrophysiological, genetic, histopathologic, and computational study. *Circulation*. 2005;112:2769-2777.

S12_1. The Nonhierarchical View of Face Perception in the Human Brain

B. Rossion¹

¹Institute of Research in Psychology and Institute of Neuroscience, University of Louvain, Louvain-la-Neuve, Belgium

The dominant view from psychophysics, computational modeling, and neuroscience (single-units, neuroimaging, and electromagnetic recordings) is that complex visual forms such as faces are processed through a hierarchical pathway in the primate brain: from lower level visual areas representing small facial elements to higher level areas representing the whole face. Here, I will argue that this view is incompatible with evidence from behavioral and electrophysiological studies in humans, showing that a face is processed primarily and initially as a Gestalt-like stimulus, with little or no part decomposition. I will also show that fMRI studies of normal observers and brain-damaged patients with prosopagnosia supports a nonhierarchical view of face perception in the human brain.

S12_2. Human Ventral Temporal Cortex: Corresponding Categorical Responses Across Electrocoricography and Functional Magnetic Resonance Imaging Arise Within 120 Milliseconds

C. Jacques^{1,2}, N. Witthoft^{1,3}, K.S. Weiner^{1,3}, B.L. Foster^{1,4}, K.J. Miller^{1,4}, D. Hermes⁴, J. Parvizi^{1,4}, and K. Grill-Spector^{1,3}

¹SHICEP, Stanford Human Intracranial Cognitive Electrophysiology Program, Stanford University, Stanford, CA, USA

²IPSY, Research Institute for Psychological Science, Université Catholique de Louvain, Louvain-la-Neuve, Belgium

³Department of Psychology, Stanford University, Stanford, CA, USA

⁴Neuroscience Institute, Stanford University, Stanford, CA, USA

Functional neuroimaging (fMRI) and electrocorticography (ECoG) research have revealed selective responses to faces, body parts, words, and places, in human ventral temporal cortex (VTC). However, the precise spatial organization of ECoG selective responses in VTC, as well as the nature of the coupling between ECoG and fMRI signals is poorly understood. We examined where and when categorical information arises in VTC by measuring responses to single and groups of images using both ECoG and fMRI in 6 subjects who were implanted with electrodes for evaluation prior to surgery. We find that in each subject VTC electrical signals measured with ECoG in the broadband gamma range (30-160 Hz) (*a*) show a categorical profile across many single images of a category, most strikingly for faces in the lateral fusiform; (*b*) show a similar spatial organization of selectivity across the VTC as measured with fMRI, with face-selective responses in the lateral fusiform and house-selective responses in the medial fusiform and collateral

sulcus; and (*c*) can be decoded to infer the category of single images within 120 ms, and even faster (90 ms) for faces. Notably, examination of the coupling between fMRI and ECoG signals in these subjects revealed that the strength of this coupling varies with time and frequency band. Early (100-200 ms) ECoG selectivity across all frequency bands was significantly and positively correlated with fMRI selectivity in VTC. However, at later times (400-800 ms), ECoG selectivity in the broadband range (30-160 Hz) remained positively correlated with fMRI selectivity, but ECoG selectivity in low frequencies (4-12 Hz) became negatively correlated with fMRI selectivity. These data indicate that the best coupling occurs between fMRI signals and broadband ECoG signals, suggesting that fMRI signals in VTC reflect local neural responses. Finally, our data suggest that information about the category of the visual stimulus, and in particular if it is a face, is processed rapidly in VTC, potentially giving rise to humans' remarkable visual classification and perception abilities.

Acknowledgments

Supported by Stanford NeuroVentures Program and R01 NS078396-01 to J. Parvizi; The Belgian Fund for Scientific Research (FNRS) to C. Jacques; NSF BCS 0920865 and R01 EY019279-01A1 to K. Grill-Spector.

S12_3. Spatial and Temporal Processing in the Core and Belt Auditory Cortex of Macaque Monkeys

G.H. Recanzone¹

¹Center for Neuroscience, University of California at Davis, Davis, CA, USA

Spatial and nonspatial information of acoustic stimuli has been hypothesized to be processed in parallel cortical streams, with spatial features selectively processed in caudal auditory cortical areas and nonspatial features selectively processed in rostral auditory cortical areas. This "dual-stream" hypothesis is similar in many ways to that proposed for the visual cortex, which has largely been supported experimentally over the past several decades. We have investigated this working hypothesis of auditory cortical function in a number of ways, concentrating primarily in the core and caudal belt of auditory cortex in the macaque monkey. We have also directly compared the responses of neurons with identical stimuli depending on whether the animal was selectively attending to the spatial or to the temporal features of the stimulus. Our results are to date inconclusive, providing evidence both for and against the dual stream hypothesis depending on a variety of factors, including the type of stimulus used, the behavioral state of the animal, and the recording location. These results, along with those from several other laboratories, prompt a refinement of the dual-stream hypothesis.

S12_4. Multisensory Processes Prompt New Conceptions of Sensory Cortices

M.M. Murray^{1,2,3}

¹Department of Clinical Neurosciences, University Hospital Center and University of Lausanne, Lausanne, Switzerland

²Department of Radiology, University Hospital Center and University of Lausanne, Lausanne, Switzerland

³The EEG Brain Mapping Core, Center for Biomedical Imaging (CIBM), University of Lausanne, Lausanne, Switzerland

I will summarize our efforts to identify the spatiotemporal brain dynamics and behavioral relevance of auditory–visual multisensory interactions in humans and the consequence such has had on our understanding of the functional selectivity of visual cortices. Across studies we have used a combination of psychophysics, event-related potentials (ERPs), functional magnetic resonance imaging (fMRI), and transcranial magnetic stimulation (TMS). Using these techniques in multisensory research often prompted (if not required) improvements in signal analysis methods that will likewise be briefly summarized in this talk and which can be used more generally for other domains of research. Several general conclusions about auditory–visual interactions in humans are supported relatively solidly from cumulative results of ourselves and others, in part because they derive from multiple brain imaging/mapping methods. First, low-level (likely primary) cortices are loci of multisensory convergence and interactions. Second, these effects occur at early latencies (ie, <100 ms poststimulus onset). Third, these effects directly affect behavior and perception. Finally, current unisensory (auditory or visual) object recognition and brain activity is incidentally affected by prior single-trial multisensory experiences; the efficacy of which is predictable from an individual's spatiotemporal dynamics of multisensory interactions. Together, these data underscore how multisensory research is changing long-held models of functional brain organization and perception.

S13_1. Decoding and Predicting Intentions From Patterns of Human Brain Activity: Lessons for the Architecture of Prefrontal Cortex

J.D. Haynes¹

¹Bernstein Center for Computational Neuroscience and Berlin Center for Advanced Neuroimaging, Charité–Universitätsmedizin Berlin, Berlin, Germany

The neural encoding of intentions plays a special role in the human brain. Because various cognitive subprocesses are orchestrated with the purpose of realizing intentions, the neural representation of an intention should be the best predictor of current and future brain activity. For this reason, our group has conducted a number of studies that attempt to identify the

neural code with which intentions are stored in the human brain. We applied multivariate pattern classifiers to brain signals recorded while subjects were holding certain intentions in mind.^{1–9} The aim was to identify brain regions where sub-components of intentions would be decodable. Following this approach, we assessed where it is possible to decode free-chosen versus cued intentions, where intentions can be decoded across delays (“prospective memory”), how intentions are reimplemented after delays and how complex intentions are coded based on simple constituent elements (“compositionality”). Our findings provide a complementary view to existing ideas on prefrontal coding. We neither found evidence for equipotentiality where a set of regions participates in coding a large number of intentions, without much differentiation, nor did we find evidence for a gradient of increasing complexity running from posterior to anterior prefrontal cortex (PFC). Instead, our results suggest a compositional view of PFC where different aspects of intentions (cues, tasks, timing, conditions, etc) are coded in different subregions. In another line of research we tried to predict which intention a person would choose to pursue even before subjects believed they were consciously making up their mind.^{1,8} Our results show that the specific outcome of free choices between different plans can be interpreted from brain activity, not only after a decision has been made but even several seconds before it is made. This suggests that a causal chain of events can occur outside subjective awareness even before a subject makes up his or her mind.

References

1. Soon CS, He AH, Bode S, Haynes JD. Predicting free choices for abstract intentions. *Proc Natl Acad Sci U S A*. 2013;110:6217–6222.
2. Reverberi C, Görgen K, Haynes JD. Distributed representations of rule identity and rule order in human frontal cortex and striatum. *J Neurosci*. 2012;32:17420–17430.
3. Heinze J, Wenzel MA, Haynes JD. Visuomotor functional network topology predicts upcoming tasks. *J Neurosci*. 2012;32:9960–9968.
4. Momennejad I, Haynes JD. Human anterior prefrontal cortex encodes the “what” and “when” of future intentions. *Neuroimage*. 2012;61:139–148.
5. Reverberi C, Görgen K, Haynes JD. Compositionality of rule representations in human prefrontal cortex. *Cereb Cortex*. 2012;22:1237–1246.
6. Haynes JD. Decoding and predicting intentions. *Ann NY Acad Sci*. 2011;1224:9–21.
7. Bode S, Haynes JD. Decoding sequential stages of task preparation in the human brain. *Neuroimage*. 2009;45:606–613.
8. Soon CS, Brass M, Heinze HJ, Haynes JD. Unconscious determinants of free decisions in the human brain. *Nat Neurosci*. 2008;11:543–545.
9. Haynes JD, Sakai K, Rees G, Gilbert S, Frith C, Passingham RE. Reading hidden intentions in the human brain. *Curr Biol*. 2007;17:323–328.

S13_2. Clinical Applications of Single-Subject Inference on Brain Graphs

J. Richiardi^{1,2} and M. Greicius¹

¹Stanford University, Stanford, CA, USA

²University of Geneva, Geneva, Switzerland

An important part of the neuroimaging community has embraced a “network” or “graph” view of brain imaging data. The terms can refer to functional magnetic resonance imaging (fMRI) or positron emission tomography (PET) (functional connectivity), diffusion weighted imaging (DWI)-based measures (structural connectivity), or even structural MRI (where covariation of regional thickness or surface area is known as morphological connectivity). Thus, very different modalities, representing very diverse biological processes at various temporal and spatial scales, can be viewed and analysed through the prism of a common mathematical representation, graphs.

A vast array of network modeling methods originating in the social sciences, complexity, and statistical physics, have been adapted and expanded for neuroimaging data.¹ These methods have yielded fascinating insights about large-scale organization of the brain, and about how it is disrupted by disease.² However, most methods and research have focused on group-level inference, rather than forming predictions for single subjects. Thus, very recently, analysis methods for brain graph data have started to evolve from mass-univariate to multivariate predictive modeling,³ mirroring at an accelerated pace the methodological trajectory of activation-based studies toward multivoxel pattern analysis.

This focus on single-subject inference opens the door to many clinical applications. In particular, brain graphs can form the basis of imaging markers with testable sensitivity and specificity, enabling diagnostic tools, prognostic tools, and surrogate endpoints for interventions and clinical trials.

These single-subject techniques have already yielded results for diagnosis in diseases as diverse as mild cognitive impairment or Alzheimer’s disease,⁴ multiple sclerosis⁵ (MS), schizophrenia, or obstructive sleep apnoea.⁶ We have, for example, shown good diagnostic accuracy for MS, and also found a link between attributes of the brain graphs and white matter lesion load, a clinically relevant quantity. In recent work, we have also started to link brain graphs with individual genomic data, paving the way for personalised medicine across biological scales and processes. Thus, brain graphs seem like a plausible avenue for linking modalities to bring out clinically relevant findings.

As with all data-driven techniques, the challenge with prognosis is the relative paucity of appropriate, large-scale longitudinal data sets, but preliminary group-level results (eg, on stroke⁷) indicate that single-subject inference on brain graphs has much potential as a predictor of patient evolution.

Acknowledgments

Supported by European Commission Marie Curie International Outgoing Fellowship #299500, NIH grant NS073498.

References

1. Sporns O. *Networks of the Brain*. Cambridge, MA: MIT Press; 2011.
2. Fox MD, Greicius M. Clinical applications of resting state functional connectivity. *Front Syst Neurosci*. 2010;4:19.
3. Richiardi J, Achard S, Bunke H, Van De Ville D. Machine learning with brain graphs: predictive modeling approaches for functional imaging in systems neuroscience. *IEEE Signal Proc Mag*. 2013;30(3):58-70.
4. Wang K, Jiang T, Liang M, et al. Discriminative analysis of early Alzheimer’s disease based on two intrinsically anti-correlated networks with resting-state fMRI. In: Larsen R, Nielsen M, Sparring J, eds. *Medical Image Computing and Computer-Assisted Intervention—MICCAI 2006. Lecture Notes in Computer Science: Vol. 4191*. Berlin, Germany: Springer; 2006:340-347.
5. Richiardi J, Gschwind M, Simioni S, et al. Classifying minimally disabled multiple sclerosis patients from resting state functional connectivity. *Neuroimage*. 2012;62:2021-2033.
6. Santarnecchi E, Sicilia I, Richiardi J, et al. Altered cortical and subcortical local coherence in obstructive sleep apnea: a functional magnetic resonance imaging study. *J Sleep Res*. 2013;22:337-347.
7. Carter AR, Shulman GL, Corbetta M. Why use a connectivity-based approach to study stroke and recovery of function? *Neuroimage*. 2012;62:2271-2280.

S13_3. Multivariate Decoding of Auditory Stimuli in Comatose Patients

M. De Lucia^{1,2}

¹Electroencephalography Brain Mapping Core, Centre for Biomedical Imaging (CIBM), Lausanne University Hospital and University of Lausanne, Lausanne, Switzerland

²Department of Radiology, Lausanne University Hospital and University of Lausanne, Lausanne, Switzerland

Assessing the degree of intact auditory functions in comatose patients can provide information about their chance of recovery and could be taken into account in clinics for improving their critical care. In this context, electroencephalography (EEG) is the most common neuroimaging technique as it can be used at bedside without disturbing the clinical practice. However, most EEG studies in coma research are based on a preselection of patients showing good signal quality and exhibiting stereotypical responses to auditory stimuli. This selection can systematically influence the results and typically produce a high percentage of patients that cannot be analyzed.

In an effort to provide an unbiased test for evaluating intact auditory functions, I will provide an overview of a multivariate decoding EEG analysis, which extracts the most discriminative voltage topographies at single-trial level. The method is data-driven and particularly suitable for clinical studies in which one cannot assume a priori a typical latency of the differential response to external stimuli.

Based on 3 auditory evoked potentials studies in postanoxic comatose patients, I will provide evidence of 3 main results. First, comatose patients during acute coma can discriminate frequent versus rare auditory stimuli in oddball paradigms as

well as categories of environmental sounds though their level of auditory discrimination is not predictive of their final outcome. Second, the progression from hypothermia to normothermia of auditory discrimination between frequent and rare types of stimuli is informative of patients' chance of awakening. Third, comatose patients can exhibit more accurate auditory discrimination than age-matched controls suggesting a critical role of therapeutic hypothermia and sedation in reducing physiological background activity unrelated to stimulus processing.

We are currently validating the application of this multivariate decoding analysis in mismatch negativity paradigms on a cohort of 100 patients. Another main direction of research is to further explore the role of therapeutic hypothermia. For this goal we plan to further validate our test in a cohort of postanoxic comatose patients during the first 2 days of coma without hypothermic treatment.

S13_4. Multimodal Imaging and Brain–Computer Interfacing

K.-R. Müller^{1,2}

¹Machine Learning Group, TU Berlin, Berlin, Germany

²Department of Brain and Cognitive Engineering, Korea University, Seoul, Korea

Learning to build universal decoders for brain–computer interfacing (BCI) is a great challenge (see Blankertz et al¹ and Lemm et al² for recent reviews on machine learning for BCI). While usually in multimodal imaging, we consider the modes to be different types of imaging devices such as EEG, NIRS, or fMRI (see, eg, Biessmann et al,³ Fazli et al,⁴ and Dähne et al⁵), we will interpret different subjects as imaging modalities to gain a zero training decoder from a database of subjects. The talk will briefly review prior work toward universal decoding such as optimization approaches where all features of the subject modalities are optimized within one large-scale L1 optimization problem⁶ or in an L1 mixed effects problem.⁷ Finally, we will discuss the similarities between different subjects aiming to compensate changes between a subjects' training and testing session in BCI, an issue of great importance for a robust BCI operation.⁸ We show that such changes are very similar between subjects, and thus can be reliably estimated using data from other users and utilized to construct an invariant feature space. This novel approach to learning from other subjects aims to reduce the adverse effects of common nonstationarities, but does *not* transfer discriminative information. This is an important conceptual difference to standard multisubject methods that, for example, improve the covariance matrix estimation by shrinking it toward the average of other users or construct a global feature space. These methods do not reduce the shift between training and test data and may produce poor results when subjects have very different signal characteristics. We compare our approach with 2 state-of-the-art multisubject methods on toy data and 2 data sets of

EEG recordings from subjects performing motor imagery. We show not only that it can achieve a significant increase in performance but also that the extracted change patterns allow for a neurophysiologically meaningful interpretation.

Acknowledgments

This is a joint work with Wojciech Samek, Frank Meinecke, Benjamin Blankertz, Gabriel Curio, Michael Tangermann, Carmen Vidaurre, Paul von Büna, Felix Biessmann, Siamac Fazli, and many other members of the Berlin Brain Computer Interface team. We gratefully acknowledge funding by BMBF, EU, DFG, and WCU.

References

- Blankertz B, Lemm S, Treder M, Haufe S, Müller K-R. Single-trial analysis and classification of ERP components—a tutorial. *Neuroimage*. 2011;56:814-825.
- Lemm S, Dickhaus T, Blankertz B, Müller K-R. Introduction to machine learning for brain imaging. *Neuroimage*. 2011;56:387-399.
- Biessmann F, Plis S, Meinecke FC, Eichele T, Müller K-R. Analysis of neuroimaging data. *IEEE Rev Biomed Eng*. 2011;4:26-58.
- Fazli S, Mehnert J, Curio G, et al. Enhanced performance by a hybrid NIRS-EEG brain computer interface. *Neuroimage*. 2012;59:519-529.
- Dähne S, Biessmann F, Meinecke FC, Mehnert J, Fazli S, Müller K-R. Integration of multivariate data streams with bandpower signals. *IEEE Trans Multimedia*. 2013; 15:1001-1013.
- Fazli S, Popescu F, Danoczy M, Blankertz B, Müller K-R, Grozea C. Subject independent mental state classification in single trials. *Neural Netw*. 2009;22:1305-1312.
- Fazli S, Danoczy M, Schellendorfer J, Müller K-R. L1-penalized models for high dimensional data with application to BCI. *Neuroimage*. 2011;56:2100-2108.
- Samek W, Meinecke FC, Müller KR. Transferring subspaces between subjects in brain-computer interfacing. *IEEE Trans Biomedical Eng*. 2013;60:2289-2298.

S13_5. Coding of Natural Sounds at Multiple Spectral and Temporal Resolutions in the Human Auditory Cortex

E. Formisano¹

¹Department of Cognitive Neuroscience and Maastricht Brain Imaging Center, Maastricht University, Maastricht, Netherlands

Functional neuroimaging research provides detailed observations of the response patterns that natural sounds (eg, human voices and speech, animal cries, environmental sounds) evoke in the human brain. The computational and representational mechanisms underlying these observations, however, remain largely unknown. Here, I will present research combining high spatial resolution (7 T) functional magnetic resonance imaging (fMRI) with computational modeling to reveal *how* natural sounds are represented in the human brain. With univariate regression, we compare competing models of sound representations and select the model that most accurately predicts fMRI

response patterns to natural sounds. With multivariate regression, we reconstruct the sounds' spectrogram and waveform from brain activation patterns and study the transformations of sound representations across auditory areas.

Our results show that the cortical encoding of natural sounds entails the formation of multiple representations of sound spectrograms with different degrees of spectral and temporal resolution. The cortex derives these multiresolution representations through frequency-specific neural processing channels and through the combined analysis of the spectral and temporal modulations in the spectrogram. Furthermore, our findings show that a spectral-temporal resolution trade-off governs the modulation tuning of neuronal populations throughout the auditory cortex. Specifically, our results suggest that neuronal populations in posterior auditory regions preferably encode coarse spectral information with high temporal precision. Vice versa, neuronal populations in anterior auditory regions preferably encode fine-grained spectral information with low temporal precision. We suggest that the unrevealed multiresolution analysis is crucially relevant for flexible and behaviorally relevant sound processing (eg, for sound recognition, sound localization and processing of sound motion) and may constitute one of the computational underpinnings of functional specialization in auditory cortex.

S14_1. Brain Functional and Structural Abnormalities Associated With Ongoing Psychosis: A Multimodal Approach

R. Smieskova^{1,2}, A. Schmidt^{1,2}, K. Bendfeldt², A. Walter¹, A. Riecher-Rössler¹, and S. Borgwardt^{1,2}

¹Department of Psychiatry (UPK), University of Basel, Basel, Switzerland

²Medical Image Analysis Centre, University Hospital Basel, Basel, Switzerland

Prefrontal and temporal structural alterations as well as specific cognitive network-related neural abnormalities have been identified as markers of psychosis. Their relation and causality are important issues to be studied in the at-risk mental state (ARMS) individuals and in the individuals who already fulfil the criteria for first-episode of psychosis (FEP). The Early Detection of Psychosis Clinic (FEPSY)¹ enables us to collect various modalities displaying clinical, brain structural and functional features in the ARMS and the FEP individuals.

Using the Biological Parametric Mapping (BPM)² toolbox implemented in the SPM8 (<http://www.fil.ion.ucl.ac.uk/spm/software/spm8>), we can evaluate neuroimaging data in conjunction with corresponding structural and/or functional imaging data on a voxel-wise basis. Additionally, we can correlate imaging and non-imaging data aiming to link pathophysiological and clinical features and explaining thus specific hypothesis.

First, we examined neural data from functional magnetic resonance imaging during working memory³ and reward learning paradigms in conjunction with structural information about gray matter volume (structural information). Second, we evaluated the influence of the neural differences in aberrant salience processing on the normal motivational salience processing (2 closely related functional modalities).

We showed that neural abnormalities were associated with structural deficits, particularly in insular and prefrontal regions evaluating working memory paradigm and in the striatum evaluating motivational salience paradigm. We used the multimodal approach to differentiate between vulnerability- and psychosis- associated abnormalities. Furthermore, we identified regions specifically sensitive to antipsychotic medication during motivational salience processing.

References

1. Riecher-Rössler A, Gschwandtner U, Aston J, et al. The Basel early-detection-of-psychosis (FEPSY) study—design and preliminary results. *Acta Psychiatr Scand.* 2007;115: 114-125.
2. Casanova R, Srikanth R, Baer A, et al. Biological parametric mapping: a statistical toolbox for multimodality brain image analysis. *Neuroimage.* 2007;34:137-143.
3. Smieskova R, Allen P, Simon A, et al. Different duration of at-risk mental state associated with neurofunctional abnormalities. A multimodal imaging study. *Hum Brain Mapp.* 2012;33: 2281-2294.

S14_2. Multimodal Imaging in People at High Risk for Psychosis

P. Fusar-Poli¹

¹Institute of Psychiatry London, London, UK

The onset of schizophrenia is usually preceded by a prodromal phase characterized by functional decline and subtle prodromal symptoms, which include attenuated psychotic phenomena, cognitive deterioration and a decline in socio-occupational function. Preventive interventions during this phase are of great interest because of the potential impressive clinical benefits. However, available psychopathological criteria employed to define a high-risk state for psychosis have a low validity and specificity. Consequently, there is an urgent need of reliable neurobiological markers linked to the pathophysiological mechanisms that underlie schizophrenia. Over the recent years, multimodal neuroimaging techniques have rapidly developed into a powerful tool in psychiatry as they provide an unprecedented opportunity for the investigation of both brain structure and function. We will review in this presentation the potentials of multimodal structural, functional, neurochemical imaging methods to address the core pathophysiological processes underlying psychosis onset.

S14_3. Multimodal Brain Imaging in 22q11.2 Deletion Syndrome: Unraveling the Brain Development Associated With Risk for Schizophrenia

S. Eliez^{1,2}

¹Office Médico-Pédagogique, Department of Psychiatry, University of Geneva School of Medicine, Geneva, Switzerland

²Department of Genetic Medicine and Development, University of Geneva School of Medicine, Geneva, Switzerland

22q11.2 deletion syndrome (22q11DS) is a genetic condition associated with a heightened risk for developing schizophrenia (~30%).¹ This syndrome thus offers a unique opportunity to study the cerebral mechanisms associated with the onset psychotic symptoms. We present here neuroimaging data acquired in a unique cohort of patients with 22q11DS, aged between 6 and 30 years, and followed up longitudinally with repeated scans over a period extending up to 10 years. The T1-weighted images comprised in this large longitudinal data set are exploited to identify deviances in the trajectories of brain maturation, using mixed-model at thousands of points over the cortex to measure the developmental course of cortical thickness changes with age. A specific emphasis is devoted to the integration of results stemming from different neuroimaging modalities (T1-weighted images, diffusion tensor imaging [DTI], resting-state fMRI, and EEG), to build up an integrated and detailed understanding of the pathogenesis of brain alterations in 22q11DS and in psychosis. Indeed, deviant trajectories of cortical thickness changes with age are observed in patients with 22q11DS, in a region where abnormal white matter structure is observed with an increased number of fibers observed using tractography.² Using resting-state fMRI in the same cohort, we further show functional alterations most prominent in the frontal lobes (Scariati et al, unpublished data), providing strong evidence for convergent frontal alterations across different imaging modalities in the syndrome. Within the group of patients with 22q11DS, similarly convergent multimodal alterations are associated with the onset of psychotic symptoms. Indeed, alterations to the temporal lobe and anterior cingulate cortex are observed using cortical thickness measurements, structural, and functional connectivity, task-related fMRI³ and EEG activity.⁴ This presentation will aim at building bridges between the results observed in the same cohort using multimodal brain imaging, to understand how structural and functional differences influence each other within the context of a neurodevelopmental condition.

References

1. Murphy KC, Jones LA, Owen MJ. High rates of schizophrenia in adults with velo-cardio-facial syndrome. *Arch Gen Psychiatry*. 1999;56:940-945.
2. Ottet MC, Schaer M, Cammoun L, et al. Reduced fronto-temporal and limbic connectivity in the 22q11.2 deletion syndrome:

vulnerability markers for developing schizophrenia? *PLoS One*. 2013;8(3):e58429.

3. Schneider M, Debbané M, Lagioia A, Salomon R, d'Argembeau A, Eliez S. Comparing the neural bases of self-referential processing in typically developing and 22q11.2 adolescents. *Dev Cogn Neurosci*. 2012;2:277-289.
4. Rihs TA, Tomescu MI, Britz J, et al. Altered auditory processing in frontal and left temporal cortex in 22q11.2 deletion syndrome: a group at high genetic risk for schizophrenia. *Psychiatry Res*. 2013;212:141-149.

S14_5. Dysconnectivity in Emerging Psychosis

A. Schmidt^{1,2}

¹Department of Psychiatry (UPK), University of Basel, Basel, Switzerland

²Medical Imaging Analysis Center (MIAC), University Hospital of Psychiatry, Basel, Switzerland

A key challenge in early detection of psychosis research is to find robust neural markers characterizing the onset of the illness. The identification of a clinical risk syndrome, an “at-risk mental state” (ARMS), that reflects a high-risk predisposition to psychosis is thus fundamental to research work in this area. Neurocognitive deficits are considered to be a central manifestation of the pathophysiology of psychosis with the most remarkable deficits in working memory (WM). Numerous functional magnetic resonance imaging (fMRI) studies have shown that WM deficits in psychosis were accompanied by reduced activation in frontal and parietal brain regions. It has been proposed that maybe not only focal brain abnormalities are characteristic for psychosis but also dysfunctional integration of task-related brain regions.¹ During WM processing, the prefrontal and parietal brain regions are functionally related. Indeed, recent studies reported dysfunctional frontoparietal effective connectivity in psychotic patients.² The extent of this dysconnectivity has often been linked to the severity of psychotic symptoms. In the current study,³ we aimed to explore whether modulation of effective connectivity during WM pre-dates the onset of psychosis. Furthermore, we also tested for the impact of antipsychotic treatment in patients with first-episode psychosis (FEP) and whether the connection strengths were related to the severity of psychotic symptoms. From healthy controls via ARMS subjects to patients with FEP, we observed a progressive reduction in WM-induced modulation of frontoparietal connectivity. Notably, the abnormal modulation of connectivity in FEP patients was normalized by treatment with antipsychotics. Moreover, the extent of disconnection in ARMS individuals was related to the severity of psychotic symptoms. Our findings suggest that the vulnerability to psychosis is associated with a progressive failure of functional integration of brain regions involved in WM processes and that treatment with antipsychotics may have the potential to counteract this. It further demonstrates that abnormal frontoparietal connectivity during WM processing is already evident in

ARMS subjects and related to severity of psychotic symptoms they experience.

References

1. Stephan KE, Friston KJ, Frith CD. Dysconnection in schizophrenia: from abnormal synaptic plasticity to failures of self-monitoring. *Schizophr Bull.* 2009;35:509-527.
2. Deserno L, Sterzer P, Wüstenberg T, Heinz A, Schlagenhauf F. Reduced prefrontal-parietal effective connectivity and working memory deficits in schizophrenia. *J Neurosci.* 2012;32:12-20.
3. Schmidt A, Smieskova R, Aston J, et al. Brain connectivity abnormalities predating the onset of psychosis: correlation with the effect of medication. *Arch Gen Psychiatry.* 2013;70:903-912.

S15_1. Difficulties and Pitfalls in Source-Space Connectivity Analysis

K. Sekihara¹ and S.S. Nagarajan²

¹Department of Systems Design and Engineering, Tokyo Metropolitan University, Tokyo, Japan

²Biomagnetic Imaging Laboratory, Department of Radiology, University of California, San Francisco, CA, USA

There has been tremendous interest in estimating the functional connectivity of neuronal oscillations across brain regions based on MEG/EEG. However, prior studies using EEG/MEG have largely employed sensor-space analysis, in which brain interactions have been analysed using raw sensor recordings. In sensor-space analysis, the field-spread across many sensors from a single brain region leads to uncertainties in interpreting the estimation results of brain interactions, as pointed out by Schoffelen and Gross.¹ Recently, a number of studies have begun to use source-space analysis in which voxel time courses are first estimated by solving the inverse problem and brain interactions are then analyzed using those estimated voxel time courses. The source-space analysis has the potential of providing more accurate information regarding which brain regions are functionally coupled. However, in source-space analysis, a serious problem arises from the spurious connectivity caused by the leakage of an inverse algorithm, which is more or less inevitable in any inverse algorithm.² In this talk, we discuss how the algorithm leakage causes the spurious connectivity, and how to avoid it.

The difficulties in source-space causality analysis are next discussed. Here, popular measures are Granger causality-based measures, which rely on the accurate modeling of the multivariate vector autoregressive (MVAR) process of the source time series. Since, in general, the causality analysis is performed using nonaveraged data, estimated time series inevitably contains large influence of brain background interference. However, the MVAR modeling, in general, does not take such interference into account, their existence may cause significant amount of errors in the estimated MVAR coefficients, leading to completely wrong estimation of causality relationships. One

approach to reduce such errors is to impose the sparsity constraint when estimating the MVAR coefficients.³ The key assumption here is that true brain interactions cause small number of MVAR coefficients to have nonzero values, and most of MVAR coefficients remain to be zero. This paper tests the effectiveness of a method that uses the sparsity constraint, and show that imposing the sparsity also causes the loss of detectability of causality relationships.

References

1. Schoffelen JM, Gross J. Source connectivity analysis with MEG and EEG. *Hum Brain Mapp.* 2009;30:1857-1865.
2. Sekihara K, Nagarajan SS. *Adaptive Spatial Filters for Electromagnetic Brain Imaging.* Berlin, Germany: Springer-Verlag; 2008.
3. Penny WD, Roberts SJ. Bayesian multivariate autoregressive models with structured priors. *IEE Proc Vis Image Signal Process.* 2002;149:33-41.

S15_2. Estimating Spurious Connectivity in MEG Source Space

J.M. Schoffelen^{1,2}

¹Donders Institute for Brain, Cognition and Behaviour, Donders Centre for Cognitive Neuroimaging, Radboud University Nijmegen, Nijmegen, Netherlands

²Max Planck Institute for Psycholinguistics, Nijmegen, Netherlands

Magnetoencephalographic (MEG) signals provide an account of brain activity at high temporal resolution. Signals picked up at the MEG sensors represent a mixture of the activity of the underlying sources, making the interpretation of connectivity estimates at the MEG sensor level nontrivial. For this reason, connectivity analysis is best done after reconstruction of the signals in MEG source space. The source reconstruction step results in an unmixing of the sensor signals based on biophysical constraints, but it will never be perfect. As a consequence, source space connectivity estimates can still be spurious.

This issue of spurious connectivity becomes particularly relevant when employing a so-called seed-based approach, where connectivity is evaluated between a set of predefined regions of interest (ROIs), or between a reference location and all other locations in the brain. Moreover, it will be argued that the interpretation of source space connectivity may be confounded when comparing 2 experimental conditions, when the source activity is different across conditions.

I will outline these issues and motivate the need for the reconstruction and evaluation of connectivity between all pairs of source locations. I will also outline a framework that may allow for the estimation of spurious connectivity. The latter approach would also be useful in situations where no experimental contrast is present, for example, in resting-state data or in clinical measurements.

S15_3. Behavioral and Clinical Relevance of EEG/MEG Functional Connectivity

A.G. Guggisberg¹

¹Department of Clinical Neurosciences, University Hospital Geneva, Geneva, Switzerland

Human brain function results from a dynamic equilibrium between segregation into specialized modules and information integration across brain areas. Integration is associated with synchronization of neural activity across space and can be studied with modern EEG and MEG analysis techniques. Intriguingly, synchronization seems to be a crucial determinant of behavior. Behavioral performance in several different motor and cognitive tasks can be predicted by the magnitude of resting-state functional connectivity between network nodes, in healthy subjects as well as in patients with brain lesions. Although the behavioral impact of resting-state synchrony has first been shown in fMRI studies, it can also be observed at the neural level with EEG and MEG. Furthermore, different neural oscillation frequencies and different measures of functional connectivity each seem to have a specific role in resting-state information integration. Correlated amplitude envelopes in the beta frequency band and correlated fMRI amplitudes are behaviorally relevant for interactions between homologous areas of both hemispheres, but not for interactions across networks. In contrast, phase-locking and coherence in the alpha frequency band is associated with behaviorally relevant integration across the entire brain. Hence, the brain seems to use at least 2 different communication channels responsible for integration across different spatial patterns within and across networks. This repertoire of synchronization types gives the brain flexibility in including brain regions required for a given integration process. EEG/MEG analyses of functional connectivity provide insights on integration that may not be accessible with fMRI.

S15_4. Causal Estimates in the Presence of Mixed and Colored Noise

G. Nolte¹

¹Department of Neurophysiology and Pathophysiology, UKE, Hamburg, Germany

Magnetoencephalographic (MEG) and electroencephalographic (EEG) data are a mixture of essentially unknown dependent and independent sources. Estimates of dynamical relations, including especially causal relations, are heavily confounded by mixing artifacts, often termed “artifacts of volume conduction,” and different signal-to-noise ratios. Misestimations due to mixing artifacts occur both on sensor and on source level, the latter being caused by the poor spatial resolution of EEG/MEG inverse calculations.

This problem was cast into a causality challenge where the goal was to estimate for 1000 simulated bivariate data sets the causal direction of a random linear unidirectional system to which a random mixture of independent noise sources, each with random spectral densities, was added. The signal-to-noise ratios were set randomly for each data set. The counting was +1 point for each correct result, -10 points for each wrong result, and 0 points if no result was given for that data set. This counting enforces to test whether a specific conclusion is based on sufficient evidence in this specific situation.

In this talk I will discuss why “standard” algorithms like Granger causality fail in this case and have a strong bias to estimate direction from high to low signal-to-noise ratios. If statistical significance is taken as evidence, Granger causality will almost always give a result which essentially amounts to guessing for very low signal-to-noise ratios.

The “phase slope index” is a measure of temporal order between 2 signals, which is interpreted as sign of a causal relation. It cannot be generated by instantaneous mixtures of independent sources regardless of number of sources and spectral content. I will discuss possibilities and limitations of the phase slope index in comparison with Granger causality for linear and nonlinear simulated data and for real MEG and EEG data.

As a general approach to address the mixing problem, I discuss the possibility to exploit temporal order by analyzing time inverted data, which should lead to inverted causal directions if, as is claimed for various causal measures, the estimated direction is based on the principle that the cause precedes the effects.

S16_1. Gamma Band Coherence in the EEG as Expression of Brain Connectivity in Unresponsive Wakefulness Syndrome (UWS)

S. Balazs¹, K. Kermanshahi², W. Kiesenhofer², H. Binder¹, and F. Rattay²

¹Neurologisches Zentrum, OWS, Vienna, Austria

²Institute for Analysis and Scientific Computing, Technische Universität Wien, Vienna, Austria

Background. Gamma band power and coherence in EEG increases during saccades in normal subjects.¹ Patients in unresponsive wakefulness syndrome (UWS)² display spontaneous, ballistic, conjugate eye movements (SBEM), reminiscent of saccades.³ **Aim.** To find connection between increasing gamma band coherence in patients in UWS and clinical (bedside) data as well as clinical scores. **Method.** Scalp EEG and simultaneous electro-oculogram were recorded in 45 patients in UWS continuously for 12 minutes. Silver/silvernitrate disc electrodes were placed according the international 10/20 system referenced to ear electrodes. We analyzed gamma activity centered on 37.5 Hz in the time period bracketing an acceptable eye movement. These time segments were divided in preintra- and

postsaccadic time windows, according the Bodis–Wollner^{1,4} method. To define timing and gamma frequency bands, we applied time/frequency analysis to decompose the EEG (wtEEG). We used continuous wavelet transform (CWT) with a complex Gaussian wavelet. Wavelet coefficients were entered into a Hilbert transform to quantify gamma power and its change with the progression of an eye movement. For statistical analysis, we used a custom-made software DataLab (Technical University Vienna). With these values we determined for each individual patient the eye movement-related gamma power and coherence over the electrodes. For bedside staging, we used the following scales: Glasgow Outcome Scale (GOS); Glasgow Coma Scale (GCS), and Coma Recovery Scale (CRS). The following variables determined our results: age, gender, recovery (yes/no), CRS, diagnoses (hypoxia, hemorrhage, and trauma)—diabetes, brain surgery, and inflammation were not of statistical relevance. Our software demonstrated wavelet coherence⁵ in connection with the different variables written above. **Results.** (a) In agreement with the previous pilot study,³ the most consistent wtEEG results are in the presaccadic period of eye movements; (b) during this period, patients in the process of recovery showed significant higher coherence; (c) higher or lower CRS values were not connected with significant differences in coherence; and (d) age, gender, and diagnosis seem do not seem to be relevant variables for outcome in UWS. **Conclusion.** The process of recovery itself produces higher values in coherence of gamma band EEG by patients in UWS independent of age, gender, or diagnosis.

References

1. Bodis-Wollner I, Von Gizycki H, Avitabile M, et al. Perisaccadic occipital EEG changes quantified with wavelet analysis. *Ann N Y Acad Sci.* 2002;956:464-467.
2. Laureys S, Celesia GG, Cohadon F, et al; European Task Force on Disorders of Consciousness. Unresponsive wakefulness syndrome: a new name for the vegetative state or apallic syndrome. *BMC Med.* 2010;8:68.
3. Balazs S, Stepan C, Binder H, et al. Conjugate eye movements and gamma power modulation of the EEG in persistent vegetative state. *J Neurol Sci.* 2006;246:65-69.
4. Forgacs PB, von Gizycki H, Selesnick I, et al. Perisaccadic parietal and occipital gamma power in light and in complete darkness. *Perception.* 2008;37:419-432.
5. Thatcher RW. Coherence, phase differences, phase shift, and phase lock in EEG/ERP analyses. *Dev Neuropsychol.* 2012;37:476-496.

SI6_2. Transcranial Near-Infrared Stimulation Induces Neuroplastic Changes in the Intact Human Cortex

A. Antal¹, L. Chaieb¹, and W. Paulus¹

¹Clinic for Clinical Neurophysiology, University Medical Center, Georg-August University, Goettingen, Germany

The primary target of applying infrared light as a therapeutic tool is for wound healing, inflammation, and chronic pain

relief. Applications have now been widened to include the potential of rehabilitative treatment for neurological disorders in animal models and in patients with stroke and traumatic brain injury. The aim of this study was to exploit the effect of transcranial near-infrared stimulation (tNIRS) as a tool to modulate cortical excitability in the healthy human brain.

Transcranial near-infrared stimulation was applied at a wavelength of 810 nm for 10 minutes over the hand area of the primary motor cortex (M1). Both single-pulse and paired-pulse measures of transcranial magnetic stimulation (TMS) were used to assess levels of cortical excitability in the corticospinal pathway and intracortical circuits. The serial reaction time task (SRTT) was used to investigate the possible effect of tNIRS on implicit learning. Altogether 50 right-handed healthy volunteers in the age range of 18 to 35 years participated in the study.

The mean amplitude of single-pulse TMS elicited motor-evoked potentials (MEPs) decreased significantly after verum stimulation up to 30 minutes poststimulation. The short interval cortical inhibition (SICI) was increased and facilitation (ICF) decreased significantly after the end of stimulation. The results of the implicit learning study show that there was no effect of stimulation in the collectivity of subjects but significant differences in the reaction times accuracies between female and male subjects were observed, being the female subject faster during stimulation. TNIRS did no induce serious side effects apart from light headache and fatigue. Nevertheless, 66% of the subjects were able to make difference between the active and sham stimulation conditions.

Here, we claim that tNIRS offers the potential to induce neuroplastic changes in the intact human cortex with a high spatial resolution. Since tNIRS is believed to modify mitochondrial respiration, it might offer hereby a possibility to aid in the management of a wide variety of disease pathologies originating from mitochondrial dysfunction.

SI6_3. Interaral Coupling in the EEG Modulated by Voluntary Saccades in Parkinson Disease

I. Bodis-Wollner¹

¹Downstate Medical Center, State University of New York, Brooklyn, NY, USA

Summary. Saccades are part of the overt attentional system of the brain.¹ We quantified EEG oscillatory changes activated by voluntary saccades in aged control and in PD subjects. We found attenuated coupling in the frontoparietal circuit in Parkinson disease (PD). **Introduction.** Visuospatial dysfunction is one of the prominent cognitive manifestations of PD.² Abnormalities of overt attention, saccades (S) in PD include increased latency and slowed and multisteped trajectories.³ Bold imaging shows hypoactive frontal but normal posterior parietal eye field activity in PD.⁴ **Aim.** To quantify oscillatory EEG changes accompanying S in PD. **Method.** The saccade activated EEG in PD. We introduced⁵ an EEG analysis method built on wavelet transform of the saccade-modulated

perisaccadic EEG epochs.⁶ A saccade consists of a stereotyped sequence of disengagement from fixation, saccade, and rest. We divided the EEG into a pre-, intra-, and postsaccadic period. Each was analyzed using wavelet transform with a Gaussian filter. Eye movements were recorded with an infrared reflection system (ISCAN) and with the EOG. *Subjects.* 14 age-matched controls and 14 PD patients (stage I-IV). *Results.* Controls: Gamma power increases with the onset of a saccade and decreases to baseline once the eye has reached fixation. Gamma power is higher frontally opposite the saccade and ipsilaterally posteriorly. PD: Intrascadic gamma power is desynchronized even in PD patients who execute interpretable S.⁷ Phase-amplitude correlation was attenuated for frontal delta and posterior gamma. *Conclusions.* In the resting state EEG there is increased corticocortical functional connectivity in the 8 to 10 Hz alpha range even in early PD. Gamma of the posterior EEG reveals decoupling from frontal delta.

References

1. Bodis-Wollner I, Yahr MD, Mylin LH. Non-motor functions of the basal ganglia. In: Hassler RG, Christ JR, eds. *Advances in Neurology: Vol. 40: Parkinson-Specific Motor and Mental Disorders*. New York, NY: Raven Press; 1983:289-298.
2. Cummings JL, Huber SJ. Visuo-spatial abnormalities in Parkinson's disease. In: *Parkinson's Disease: Behavioral and Neuropsychological Aspects*. New York, NY: Oxford University Press; 1992:59-73.
3. Chan F, Armstrong IT, Pari G, Riopelle RJ, Munoz DP. Deficits in saccadic eye movement control in Parkinson's disease. *Neuropsychologia*. 2005;43:784-796.
4. Rieger JW, Schoenfeld MA, Heinze HJ, Bodis-Wollner I. Different spatial organization of saccade related BOLD-activation in parietal and striate cortex. *Brain Res*. 2008;1233:89-97.
5. Bodis-Wollner I, Von Gizycki H, Avitable M, et al. Perisaccadic occipital EEG changes quantified with wavelet analysis. *Ann N Y Acad Sci*. 2002;956:464-467.
6. Forgacs P, Gizycki H, Selesnick I, et al. Perisaccadic parietal and occipital gamma power in light and complete darkness. *Perception*. 2008;37:419-432.
7. Javaid MA, Weeden J, Flom P, Avitable M, Glazman S, Bodis-Wollner I. Perisaccadic gamma modulation in Parkinson disease patients and healthy subjects. *Clin EEG Neurosci*. 2010;41:94-101.

S16_4. Gamma Activity Reveals Higher Cognitive Abilities in Man and Enables Abstract Thinking

K. Maurer¹

¹Department of Psychiatry, Psychosomatic Medicine and Psychotherapy, Goethe University, Frankfurt, Germany

In 1987 a symposium took place in Würzburg about "Topographic Mapping of EEG and Evoked Potentials." With brain mapping of EEG, we were able to search for topographical sites of brain areas, where sensory, cognitive, and behavioral phenomena took place. Also psychotic symptoms like hallucinations could be visualized. Walter Freeman and the

presenter could show for the first time the emergence of augmented activity in the 39- to 43-Hz band during a buzz. A subject was instructed to hold a buzzer and switch waiting for a buzz at an unexpected time. The emergence of gamma was concentrated in the part of the array over the sensory cortex and during pressing of the switch over the motor cortex. Later research on high-frequency gamma Activity had been continued in Frankfurt within our Brain Imaging Center (BIC) in cooperation with the Max Planck Institute (Prof W. Singer). In the framework of the Tandem Project, we concentrated on the analysis of high-frequency "gamma" of the EEG spectrum. Using so-called Mooney faces phenomena and deficits in high gamma-band oscillations were investigated in normal adult persons and under different psychiatric conditions where cognitive deficits were present, such as schizophrenia and also dementia of Alzheimer type. Since decay in "gamma" was linked to a poorer performance in the ability of abstract thinking, the presenter will explain his personal view of thinking with so-called "thinking cells," only observable in man. In the case of dementia, a convincing correlation could be found between loss of 4-dimensionality and disturbance of performing and thinking.

Within the laboratory and involved in the experiments the working group of Peter Uhlhaas has to be mentioned and the leader of the Tandem Project Prof Dr Wolf Singer; also Michael Wibral, Christine Grützner, Limin Sun, David Rivolta, and David Prvulovic and the person who brought the Mooney faces into our lab: Eugenio Rodriguez.

In adolescents, Uhlhaas could convincingly demonstrate alterations in corresponding neuronal networks pointing also to the leading role of high-frequency oscillations.

In Geneva, where Jean Piaget described the emergence of human behavior and thinking the presenter will not only be able to show how the human mind emerges with its abilities to think and to speak but also how the mind fades away.

S16_5. Resting State Synchrony as a Potential EEG Neurofeedback Treatment Target for Addiction

G. Fein^{1,2}, J. Camchong¹, J. Johnstone³, and V. Cardenas-Nicolson¹

¹Neurobehavioral Research Inc, Honolulu, HI, USA

²Department of Psychology, University of Hawai'i, Honolulu, HI, USA

³Q-Metrx Inc, Burbank, CA, USA

Alcohol dependence is a disorder with an impulsive and compulsive "drive" toward excessive alcohol consumption and an inability to control or inhibit such consumption despite considerable recurring negative consequences. Neuroimaging studies suggest that these behavioral components correspond to an increased involvement of regions that mediate appetitive drive and reduced involvement of regions that mediate executive inhibitory control. We have recently shown using functional connectivity fMRI that, compared with non-substance abusing controls, long-term abstinent alcoholics evidence (a) decreased

synchrony of limbic reward regions (eg, caudate and thalamus) with both the subgenual anterior cingulate cortex (ACC) and the nucleus accumbens (NAcc) and (b) increased synchrony of executive control regions (eg, dorsolateral prefrontal cortex) with both the NAcc and the subgenual ACC. These results are graded with duration of abstinence and are present both in cross sectional and longitudinal studies. This phenomenon is consistent with a compensatory mechanism that develops with abstinence such that, at rest, decision making networks are primed to be less responsive to appetitive drive stimuli and ready to exhibit inhibitory control. Facilitation of these adaptive changes may show promise as a treatment for individuals pursuing abstinence from alcohol and drugs. Studies to be reported here are extending these findings from fMRI to EEG using LORETA connectivity analysis with the goal of developing neurofeedback treatment supporting long-term abstinence from alcohol and drugs.

Free Oral Presentations

FCI_I. High-Resolution Forward Modeling Using Finite Element Method Head Models Based on 7-T MRI Data

L.D.J. Fiederer^{1,2,3}, F. Lucka^{4,5}, S. Yang⁶, J. Vorwerk⁵, M. Dümpelmann³, D. Cosandier-Rimé^{2,3}, A. Schulze-Bonhage^{2,3}, A. Aertsen^{1,2}, O. Speck⁶, C.H. Wolters⁵, and T. Ball^{2,3}

¹Neurobiology and Biophysics, Faculty of Biology, University of Freiburg, Freiburg, Germany

²Bernstein Center Freiburg, University of Freiburg, Freiburg, Germany

³Epilepsy Center, University Hospital Freiburg, Freiburg, Germany

⁴Institute for Computational and Applied Mathematics, University of Münster, Münster, Germany

⁵Institute for Biomagnetism and Biosignalanalysis, University of Münster, Münster, Germany

⁶Department of Biomedical Magnetic Resonance, Institute for Experimental Physics, Faculty of Natural Sciences, University of Magdeburg, Magdeburg, Germany

Evolution from analytical to finite element method (FEM) models has stressed the importance of high spatial detail for improving solutions of the neuro-electrical forward problem.¹ This evolution was supported by the continuous increase of field strength in magnetic resonance imaging (MRI), which allows creating complex individualized head models. Higher magnetic field strength improves signal-to-noise ratio and thus the quality of created head models.² The aim of the present study was to investigate the potential of cutting-edge high-field MRI at 7 T for creating more detailed FEM models with enhanced tissue differentiation, and to

examine the impact of increased FEM anatomical detail on forward modeling.

Our head model is based on 2 whole head MRI volumes acquired on a 7 T Siemens scanner using T1 magnetization-prepared rapid acquisition gradient echo and PD gradient echo sequences with 0.6 mm isotropic resolution. Segmentation was generated with FSL³ and a self-written 3D flood filling algorithm. To enhance the contrast of blood vessels, the volumes were preprocessed by 3D Frangi filtering. Segmentations were volume-meshed and solved with SimBio.⁴ The models used for the FEM simulations comprised >17.6 million nodes with an isotropic resolution of 600 µm. The hardware required were 2.8 GHz workstations with 16 GB of RAM under Linux.

As a main result, the present study demonstrates that high-resolution forward modeling using FEM volume conductor models based on 7-T MRI data at 0.6 mm isotropic resolution and over 17 million nodes is feasible. The segmentation yielded 12 compartments with distinct conductive properties; internal air, white matter, gray matter, cerebrospinal fluid, blood, dura mater, skull bone, fat, scalp, eyes, eye lens, and miscellaneous soft tissue. Special care was taken to segment an extensive vascular system ranging from the carotid to intracortical, diploe, and emissary vessels. Cranial vessels indeed create high-conductivity pathways between sources and head surface, thereby short-circuiting the highly resistive skull. We show that neglecting such vessels accounts for substantial EEG localization errors.

Model and results show that using submillimeter-resolution MRI data to build FEM models is possible and supported by some, but not all, state-of-the-art modeling tools and on mid-range computer hardware. To the best of our knowledge, the presented FEM model is the most highly resolved volume conductor head model up to now. Beyond blood vessels, the model can be used to investigate model errors induced by coarser resolution, such as 3 T-based head models, and to what extent those influence simulations.

Acknowledgments

Work supported by BMBF grants 01GQ0420 and 01GQ0830.

References

1. Ramon C, Schimpf PH, Haueisen J. Influence of head models on EEG simulations and inverse source localizations. *Biomed Eng Online*. 2006;5:10.
2. Duyn JH. The future of ultra-high field MRI and fMRI for study of the human brain. *Neuroimage*. 2012;62:1241-1248.
3. Smith SM, Jenkinson M, Woolrich MW, et al. Advances in functional and structural MR image analysis and implementation as FSL. *Neuroimage*. 2004;23(suppl 1):S208-S219.
4. Wolters CH, Grasedyck L, Hackbusch W. Efficient computation of lead field bases and influence matrix for the FEM-based EEG and MEG inverse problem. Part I. Complexity considerations. *Inverse Problems*. 2004;20:1099-1116.

FCI_2. Sensitivity of EEG and MEG for Extended Cortical Sources

M. Fuchs¹, M. Wagner¹, J. Kastner¹, and R. Tech¹

¹Compumedics Neuroscan, Hamburg, Germany

In a simulation study, we compared the sensitivity of MEG magnetometers, planar gradiometers, an EEG 10/20 montage, and the combined modalities for extended cortical sources. A realistically shaped boundary element method (BEM) head model with 3 compartments (6685 nodes overall: skin 1968, outer skull 1771, inner skull 2946 nodes) was used and sources on the folded cortical surface (30 381 nodes, mean node distance 2.8 mm) with Gaussian intensity profiles were investigated.

Relative sensitivities of the different MEG and EEG configurations normalized to point-like sources and averaged over all cortical positions were computed as a function of the source diameter (0–60 mm full-width at half-maximum [FWHM]). With increasing patch diameter cancellation of tangentially oriented sources on opposing sulcal walls leads to a more and more radial orientation of the overall activity and decreasing sensitivity. Due to the different sensitivities of MEG for radial and tangential current components as compared to the more homogeneous orientational sensitivity of EEG, increasing source sizes have a larger effect on MEG than on EEG. Areas with dominating radial orientations are better visible by EEG as compared to MEG as expected.

As an example sources in the central sulcus area were used and field/potential maps for different source extensions were computed. The overall source strength (integrated over the curved area of the cortical patch) was kept constant. From a purely tangential, point-like source, the EEG maps change from a tangential to a radial source map, whereas the MEG fields show decreasing intensities and even polarity inversion for larger source diameters. MEG exhibits superior sensitivity for superficial, tangential source locations, but strongly reduced sensitivity for radially oriented sources since it can detect only their decreasing tangential components.

Finally, single equivalent dipoles were fitted to the simulated extended source fields and dipole positions and strengths and field deviations were analyzed. Fitting single equivalent dipoles to extended cortical activity can result in misleading dipole orientations and positions due to cancellation (MEG and EEG) and invisible radial components (MEG). Combining both MEG and EEG modalities have advantages because of the orientational specificity of MEG and the more homogeneous sensitivity of EEG; however, it depends on the number of sensors used and their Signal-to-Noise Ratio (SNR). Comparing both modalities can exhibit virtual signal phase shifts between MEG and EEG when, for example, propagation or growing

extension of an epileptic zone is observed and tangential and radial components change differently.¹

Reference

1. Ebersole JS, Ebersole SM. Combining MEG and EEG source modeling in epilepsy evaluations. *J Clin Neurophysiol.* 2010;27:360–371.

FCI_3. Online Monitoring of Brain Activity

C. Dinh^{1,2}, J. Haueisen^{1,3}, D. Baumgarten¹, and M.S. Hämäläinen²

¹Institute of Biomedical Engineering and Informatics, Ilmenau University of Technology, Ilmenau, Germany

²Athinoula A. Martinos Center for Biomedical Imaging, Massachusetts General Hospital, Charlestown, MA, USA

³Biomagnetic Center, Department of Neurology, University Clinic Jena, Jena, Germany

Providing millisecond temporal resolution for noninvasive mapping of human brain functions, magnetoencephalography (MEG) is optimal to monitor brain activity in real time.¹ Real-time feedback allows the adaption of the experiment to the subject's reaction creating a whole set of new options and increasing time efficiency by shortening acquisition and offline analysis. Whereas data analysis to date is mostly done after the acquisition process, we introduce an approach to monitor brain activity online.

In order to handle the low signal-to-noise ratio (SNR) in single trials and at the same time cope with the high computational effort, the gain matrix is downsized. Since a low SNR reduces the number of distinguishable source localizations, regionwise clusters are calculated,² defined by Destrieux's brain atlas.³ Each cortical region is represented by a cluster dipole, that is, a standard mne-toolbox source space with 7498 dipoles is reduced to a sparse source space with 176 dipoles.

The reduced number of dipoles and a preserved variance of the gain matrix improve the ability to distinguish active regions and speeds up the localization calculation at the same time. Dynamic statistical parametric mapping (dSPM)⁴ is used as localization algorithm. This algorithm is able to handle Elekta Neuromag VectorView 306-channel MEG measurements and a sampling frequency of 1000 sps online with a small delay. In case the localization is applied directly to the raw data, the minimal measurement buffer for an ordinary mobile workstation of 80 samples results in an 80-ms delay. If a larger delay is acceptable, a moving average can be applied to increase the localization accuracy. The localization output is visualized in a stereoscopic real-time brain display.

First studies using both simulated and human MEG data show that the proposed real-time technique is accurate and fast. The responses to auditory and somatosensory stimuli can be

localized precisely. The stereoscopic display enables the clinician to follow the activation easily.

We conclude that online brain monitoring is a useful addition to common acquisition methods and allows acquisition of more information during the measurement. This can reduce the postprocessing effort dramatically.

References

1. Hämäläinen MS, Hari R, Ilmoniemi RJ, Knuutila J, Lounasmaa OV. Magnetoencephalography—theory, instrumentation, and applications to noninvasive studies of the working human brain. *Rev Mod Phys.* 1993;65:413-497.
2. Dinh C, Strohmeier D, Haueisen J, Güllmar D. Brain atlas based region of interest selection for real-time source localization using K-means lead field clustering and RAP-MUSIC. *Biomed Tech (Berl).* 2012;57(suppl 1).
3. Destrieux C, Fischl B, Dale A, Halgren E. Automatic parcellation of human cortical gyri and sulci using standard anatomical nomenclature. *Neuroimage.* 2010;53:1-15.
4. Dale AM, Liu AK, Fischl BR, et al. Dynamic statistical parametric mapping: combining fMRI and MEG for high-resolution imaging of cortical activity. *Neuron.* 2000;26:55-67.

FCI_4. Clustering of Interictal Events for Improved Source Imaging and fMRI Regressor Design in High-Density EEG–fMRI Investigations

S. Lau^{1,2,3,4}, S.J. Vogrin^{1,2}, W. D'Souza¹, J. Haueisen³, and M.J. Cook^{1,2}

¹Department of Medicine, St. Vincent's Hospital, University of Melbourne, Fitzroy, Queensland, Australia

²Centre for Clinical Neurosciences & Neurological R., St. Vincent's Hospital Melbourne, Fitzroy, Queensland, Australia

³Institute for Biomedical Engineering and Informatics, Technical University Ilmenau, Ilmenau, Germany

⁴NeuroEngineering Laboratory, Department of Electrical and Electronics Engineering, University of Melbourne, Parkville, Queensland, Australia

During presurgical planning in focal epilepsy, high-density EEG–fMRI of interictal activity can be used to locate epileptic foci in a multimodal context. The interevent variability in morphology and amplitude poses a problem for comprehensive identification of events and subsequent group analysis. Our objective is to develop a semiautomated method of identifying and clustering interictal events for improved electric source imaging (ESI) and fMRI regressor design.

A 128-channel EEG was recorded of a patient with left temporal lobe epilepsy in an electrically shielded room and during fMRI (1.5 T). The MR-gradient and cardiac pulse–related artifacts were removed. A representative interictal epileptic discharge (IED) from the shielded room recording was selected as the template and template matching using a set of indicative channels was performed to identify IEDs. The correlation and amplitude thresholds were relaxed to increase sensitivity. Intertrial correlations were calculated and used to cluster the

IEDs based on mean within-cluster correlation, which provided specificity. Clusters were averaged and a cortically constrained current density reconstruction (CDR, sLORETA) was performed using a boundary element model at the time period around the first peak and from that an equivalent dipole was derived. ESI-based cluster selections were used to define the regressor for the fMRI analysis (FSL FEAT, Gaussian smoothing FWHM 6 mm, double gamma HRF with +1 s, +3 s, +5 s, +7 s delays).

In the shielded room recording 456 events were detected over 35 minutes and in the scanner recording 233 in 25 minutes. Concordant event clusters could be identified as well as a separate group of spikes that occur within the sharp wave of a preceding spike. Weakly correlated events, for example, artifact corrupted or overlaid with other activity, could be separated and rejected. The left temporal blood oxygenation level–dependent (BOLD) activation was concordant with ESI. Selecting ESI-positive concordant event clusters for fMRI regression notably reduced spurious activation regions and isolated an otherwise unclear second contralateral precentral activation spatially concordant with the equivalent source of the postspike wave complex.

Semiautomatic event discovery and clustering can increase the sensitivity and specificity of IED analysis. ESI-based design of the fMRI regressor can notably improve BOLD contrast. Noninvasive ESI/fMRI of epileptic events shows promise in improving presurgical evaluation of epilepsy.

FCI_5. EEG Time-Resolved Source Imaging Based on General Linear Modeling and Nonparametric Statistical Testing

A. Custo¹, D. Van De Ville^{2,3}, S. Vulliemoz⁴, F. Grouiller^{1,5}, and C.M. Michel^{1,4}

¹Functional Brain Mapping Laboratory, Department of Fundamental Neurosciences, University of Geneva, Geneva, Switzerland

²Department of Radiology and Medical Informatics, University of Geneva, Geneva, Switzerland

³Institute of Bioengineering, Ecole Polytechnique Fédérale de Lausanne, Lausanne, Switzerland

⁴Presurgical Epilepsy Evaluation Unit and Functional Brain Mapping Laboratory, Neurology Department, University Hospital, Geneva, Switzerland

⁵CIBM, University Hospital, Geneva, Geneva, Switzerland

Electroencephalographic (EEG) data can be analyzed directly, for example, by looking at the moments of interictal spiking in epileptic patients, or, more interestingly, we can recover the underlying cortical sources of such spikes after computing the “spatial inverse” of the scalp measurements, that is, mapping the measurements to the brain generators. Working in such “source space” can be done by an inverse of the lead field operator, which expresses the physical laws to which electrical brain signal abides. However, a straightforward computation of EEG sources from the inverse of the lead field lacks of any

statistical significance and it is difficult to validate outside a simulation framework.

What we propose is a novel approach to EEG source imaging analysis—for which we coin the term “time-resolved source imaging” (TSI)—where we are able to quantify the significance of the results and additionally, by mimicking fMRI data analysis, further validate source localization against BOLD contrasts in a seamless manner, while fully exploiting EEG exceptionally high temporal resolution.

The main rationale of the method is inspired by fMRI data analysis. First, we use the general linear model (GLM) with regressors that are spatial maps (eg, instantaneous topographies of an epileptic spike) to fit to the EEG data and determine the associated temporal behavior. Next, we deploy a second GLM to the EEG data mapped into source space, where the solution of the first GLM is used as temporal regressors. We can then express “contrasts” of conditions, together with statistical significance, comparable to conventional fMRI analysis.

We validate our method by analyzing: (a) the EEG/fMRI recordings of 8 epileptic patients who later underwent surgery to remove the epileptic focus/foci and (b) the findings of simultaneous EEG/fMRI recording of 2 healthy subjects who performed an eyes-open/eyes-closed task to detect alpha activity.

We quantify the quality of TSI statistical threshold by comparing it with a range of ESI threshold values for the same simulated source, using LSMAC lead field and Laura inverse solution. We simulate a bilateral source in the secondary somatosensory area and plot the ROC of different ESIs’ threshold levels to show the extreme effect of compromising sensitivity for specificity and vice versa and finding the optimal balance (ROC saddle point). TSI matches ESI optimal solution’s sensitivity (ie, it does not miss more true positives) and is just below ESI’s best specificity level (ie, it has an increased false-positive rate by less than 0.005).

FCI_6. Independence of Bioelectric and Biomagnetic Signals

J. Malmivuo¹

¹Department of Electronics, Aalto University, Aalto, Finland

The first solution for the independence/interdependence of the bioelectric and biomagnetic signals was made by Malmivuo and Plonsey.¹ It was concluded that even though the dipolar electric and magnetic lead fields were orthogonal, that is, independent, the recorded signals are only partially independent. Actually, this is the case also with the 3 orthogonal dipolar ECG leads (or with the 3 orthogonal MCG leads). A clinical study where ECG and MCG were recorded from 313 subjects was also made and it confirmed the theoretical results.^{2,3}

In 2005, Iwasaki et al⁴ published a study where epileptic seizures were recorded with EEG and MEG from 43 patients. They came to very similar result demonstrating that part of the

seizures was recorded with only EEG, part of them with both EEG and MEG and the rest with only MEG.

It is the purpose of this paper to compare these 2 studies. It is concluded that because these 2 studies were made independently by different research groups, different instrumentation, and different patient material but similar results, they verify the conclusions of Malmivuo and Plonsey¹ on the independence/interdependence of bioelectric and biomagnetic signals.

References

1. Malmivuo J, Plonsey R. *Bioelectromagnetism—Principles and Applications of Bioelectric and Biomagnetic Fields*. New York, NY: Oxford University Press; 1995.
2. Malmivuo J, Nousiainen J, Oja OS, Uusitalo A. General solution for the application of magnetocardiography. In: Nowak H, Haueisen J, Giessler F, Huonker R, eds. *Proceedings of the BIOMAG 2002, 13th International Conference on Biomagnetism*; August 10-14, 2002; Jena, Germany. 2002:546-549.
3. Malmivuo J. Comparison of the properties of EEG and MEG in detecting the electric activity of the brain. *Brain Topogr*. 2012;25:1-19.
4. Iwasaki M, Pestana E, Burgess RC, Lüders HO, Shamoto H, Nakasato N. Detection of epileptiform activity by human interpreters: blinded comparison between electroencephalography and magnetoencephalography. *Epilepsia*. 2005;46:59-68.

FC2_1. Combined EEG/MEG Source Analysis of Epileptic Activity: Effects of Volume Conduction and Spike Averaging

Ü. Aydin¹, J. Vorwerk¹, P. Küpper^{1,2}, M. Heers³, H. Kugel⁴, J. Wellmer³, C. Kellinghaus², M. Scherg⁵, S. Rampp⁶, and C. Wolters¹

¹Institut für Biomagnetismus und Biosignalanalyse, Westfälische Wilhelms-Universität Münster, Münster, Germany

²Klinik für Neurologie, Klinikum Osnabrück, Osnabrück, Germany

³Ruhr-Epileptologie, Klinik für Neurologie, Universitätsklinikum Knappschaftskrankenhaus Bochum, Bochum, Germany

⁴Institut für Klinische Radiologie, Universitätsklinikum Münster, Münster, Germany

⁵BESA GmbH, Gräfelting, Germany

⁶Epilepsiezentrum, Universitätsklinikum Erlangen, Erlangen, Germany

We introduce a new experimental and methodological analysis pipeline for combining the complementary information in EEG and MEG using a calibrated anisotropic realistic finite element (FE) model of the patient’s head that was generated from simultaneously acquired somatosensory-evoked potential (SEP) and field (SEF) data and T1-weighted (T1w-), T2w-, and diffusion tensor (DT) MRIs. We apply the new methodology in presurgical epilepsy diagnosis to a case study of a patient suffering from refractory focal epilepsy with the goal to increase the reliability of the noninvasive estimation of the irritative zone by means of interictal spike reconstructions. We focus on the feasibility and reliability of combined EEG/MEG versus single modality EEG or MEG source reconstruction. We show

how to build and then investigate high-resolution FE head models, the most advanced consisting of 6 head tissue compartments (skin, skull compacta, skull spongiosa, cerebrospinal fluid, brain gray and white matter). Furthermore, it includes a conductivity-calibrated skull compartment that was individually determined from the SEP and SEF data and brain conductivity anisotropy that is derived on a new way from the DT-MRI data. We then study head tissue sensitivities of EEG, MEG, and combined EEG/MEG in the most advanced head model and in a variety of simplified head models that differ in terms of distinguished tissue types and their conductivities. In addition to volume conduction effects, we also present a comparison between 2 approaches that are widely used for determining the irritative zone.¹ The first approach is to reconstruct each single spike separately and estimate the irritative zone according to the clusters that those spikes produce.² The second approach is to average the spikes that belong to the same cluster and then perform source reconstruction. The advantage of the latter approach is that it allows an improved signal-to-noise ratio (SNR) if a sufficient number of spikes of the same cluster can be found and averaged, while the appeal of the first approach is that the spreading of the localizations might give an estimate on the size of the irritative zone.

Acknowledgments

This research has been supported by the German Research Foundation (DFG) through projects WO1425/2-1 and STE380/14-1, and by the Medical Faculty, Ruhr University Bochum, by a FoRUM research grant (K062-11).

References

1. Bast T, Boppel T, Rupp A, et al. Noninvasive source localization of interictal EEG spikes: effects of signal-to-noise ratio and averaging. *J Clin Neurophysiol.* 2006;23:487-497.
2. Chitoku S, Otsubo H, Ichimura T, et al. Characteristics of dipoles in clustered individual spikes and averaged spikes. *Brain Dev.* 2003;25:14-21.

FC2_2. Combining ESI, ASL, and PET for Quantitative Assessment of Drug-Resistant Focal Epilepsy

S.F. Storti¹, I. Boscolo Galazzo¹, A. Del Felice¹, F.B. Pizzini², C. Arcaro³, E. Formaggio³, R. Mai⁴, and P. Manganotti^{1,3,5}

¹Department of Neurological and Movement Sciences, University of Verona, Verona, Italy

²Department of Neuroradiology, AOUI of Verona, Verona, Italy

³Department of Neurophysiology, Foundation IRCCS San Camillo Hospital, Venice, Italy

⁴Epilepsy Surgery Center, Niguarda Hospital, Milan, Italy

⁵Clinical Neurophysiology and Functional Neuroimaging Unit, AOUI of Verona, Verona, Italy

When localization of the epileptic focus is uncertain, the epileptic activity generator may be more accurately identified with

noninvasive imaging techniques which could also serve to guide stereo-electroencephalography electrode implantation. Since arterial spin labeling (ASL) has been demonstrated to be useful for the characterization of different diseases,¹ it should be expected to detect perfusion changes related to the epileptic phenomena² as well, with advantages over nuclear medicine protocols. The aim was to assess the diagnostic value of perfusion MRI with ASL in the identification of the epileptogenic zone, as compared with the results obtained with more established imaging tools. A good agreement between the ASL data and those from other investigation methods, including PET, electrical source imaging (ESI), and electrophysiological data, could provide evidence for its flexible utility in clinical assessment protocols for epilepsy. In 6 patients with drug-resistant focal epilepsy, standard video-EEG was performed to identify clinical seizure semeiology, and high-density EEG, ASL, and FDG-PET to noninvasively localize the epileptic focus. A standardized source imaging procedure, low-resolution brain electromagnetic tomography constrained to the individual matter, was applied to the averaged spikes of high-density EEG.³ Quantification of cerebral blood flow (CBF) maps from the ASL data was performed using the Buxton equation⁴ and statistically compared with a CBF template based on a group of 17 healthy subjects, while the standardized uptake value (SUV), a PET quantifier, was calculated as the ratio of tissue radioactivity concentration at time t and injected dose, divided by body weight. The regions of interest identified using the Harvard-Oxford Atlas were used to calculate the mean values for current density (CD), CBF, and SUV in the same areas. In most of the patients, source in the interictal phase was associated with an area of hypoperfusion and hypometabolism. Conversely, in the patients presenting with early postictal discharges, the brain area identified by ESI as the generating zone appeared to be hyperperfused. The investigation allowed us to correctly identify the epileptogenic zone in 2 patients, in whom the results were confirmed by surgical resection and subsequent seizure freedom, 2 patients were excluded as surgery candidates, while the remaining 2 patients are waiting to be operated. As an innovative and more comprehensive approach to the study of epilepsy, the combined use of ESI, perfusion MRI, and PET may play an increasingly important role in the non-invasive evaluation of patients with refractory focal epilepsy.

References

1. Alsop DC, Dai W, Grossman M, Detre JA. Arterial spin labeling blood flow MRI: its role in the early characterization of Alzheimer's disease. *J Alzheimers Dis.* 2010;20:871-880.
2. Altrichter S, Pendse N, Wissmeyer M, et al. Arterial spin-labeling demonstrates ictal cortical hyperperfusion in epilepsy secondary to hemimegalencephaly. *J Neuroradiol.* 2009;36:303-305.
3. Michel CM, Murray MM, Lantz G, Gonzalez S, Spinelli L, Grave de Peralta R. EEG source imaging. *Clin Neurophysiol.* 2004;115:2195-2222.
4. Buxton RB, Frank LR, Wong EC, Siewert B, Warach S, Edelman RR. A general kinetic model for quantitative perfusion imaging with arterial spin labeling. *Magn Reson Med.* 1998;40:383-396.

FC2_3. The Dark Side of the Temporal Lobe: Mesial Sources Contribution on Simultaneous EEG-SEEG Recordings

L. Koessler^{1,2}, J. Vignal^{1,2,3}, T. Cecchin^{1,2}, S. Colnat-Coulbois⁴, H. Vespignani^{1,2,3}, G. Ramantani⁵, and L. Maillard^{1,2,3}

¹Université de Lorraine, CRAN, UMR 7039, Vandœuvre-lès-Nancy, France

²CNRS, CRAN, UMR 7039, Vandœuvre-lès-Nancy, France

³Centre Hospitalier et Universitaire de Nancy, Service de Neurologie, Nancy, France

⁴Centre Hospitalier et Universitaire de Nancy, Service de Neurochirurgie, Nancy, France

⁵Epilepsy Center, University Hospital Freiburg, Freiburg, Germany

Contribution of deep brain sources on scalp EEG is still under debate. Currently, it is widely accepted that localized hippocampal discharges do not correspond to a concomitant visible correlate in scalp EEG (ILAE's report¹). Thus, evidence of mesial temporal lobe (MTL) involvement in refractory partial epilepsy solely derives from seizure semiology and hippocampal sclerosis² and direct MTL resection is performed when the criteria of MTL epilepsy are fulfilled. In cases with no hippocampal lesion, the assessment of mesial temporal involvement still relies on invasive EEG recordings. The definition of scalp EEG biomarkers for mesial temporal sources could thus be crucial for the identification and differentiation of mesial from neocortical sources and constitute a potential surrogate of invasive recordings.

Seven patients undergoing presurgical evaluation of drug-resistant epilepsy were selected from a prospective series of 27 patients in whom simultaneous EEG-SEEG recordings had been performed since 2009. Interictal intracerebral spikes (IIS) were selected on depth EEG signals blinded to EEG signals. These IIS were triggered as temporally known (T0) brain sources. Then, after IIS characterization and classification, EEG signals were automatically averaged according to the T0 markers. Averaged interictal surface spikes (ISS) signals were finally characterized (3D mapping, duration, amplitude, and statistics) and clustered using hierarchical clustering method.

In mean in our population, 9 depth EEG electrodes and 16 surface EEG electrodes were simultaneously used. In total, 684 ± 186 IIS were selected by patients for a total number of spikes in our population of 4787. According to the anatomical distribution of the IIS, 21 foci were defined and classified according to 3 categories: mesial (limbic structures plus collateral fissure; M, n = 9), mesial and neocortical (M + NC, n = 5), and neocortical part of the temporal lobe (NC, n = 7). Overall, ISS had an average absolute amplitude of 15 µV, a duration of 78 ms, and a signal-to-noise ratio (SNR) of 18.2 dB. ISS generated respectively by M, M + NC, and NC networks had average amplitudes of 7.2, 36.1, and 10 µV; durations of 72, 78, and 87 ms; and SNR of 16.5, 22, and 17.7 dB, respectively. Concerning 3D map amplitude, negative pole of ISS were always seen on the ipsilateral temporo-basal electrodes for M, M + NC, and NC

networks whereas positive pole were only observed for M + NC and NC networks on the vertex electrodes.

Contribution of deep sources on surface EEG electrodes exists. Electrical sources from mesial temporal lobe cannot be considered as closed electrical field structures. The main problem to observe signals from these deep structures concerns the weak signal to noise ratio. Hierarchical clustering method and 3D amplitude maps of average EEG signals indicate that M contribution was different from M + NC and NC contributions.

References

1. Wieser HG; ILAE Commission on Neurosurgery of Epilepsy. ILAE Commission Report. Mesial temporal lobe epilepsy with hippocampal sclerosis. *Epilepsia*. 2004;45:695-714.
2. Chassoux F, Semah F, Bouilleret V, et al. Metabolic changes and electro-clinical patterns in mesio-temporal lobe epilepsy: a correlative study. *Brain*. 2004;127(pt 1):164-174.

FC2_4. Multimodal Studies of the Role of the Basal Ganglia (BG) in Temporal Lobe Epilepsy (TLE)

I. Rektor¹, R. Kuba¹, M. Brázdil¹, J. Chrastina¹, and I. Rektorova¹

¹Central European Institute of Technology (CEITEC) and the Brno Epilepsy Centre, First Department of Neurology and Department of Neurosurgery, Masaryk University, St. Anne's Hospital, Brno, Czech Republic

Epileptic activity may affect the basal ganglia (BG) as well as large-scale brain networks.

1. In the fMRI study, the impact of epilepsy on the functional brain connectivity (FC) of the BG in 2 large-scale networks, the default mode network (DMN), and somato-motor network (SMN), was studied in 10 healthy control subjects (HC) and 24 patients with temporal lobe epilepsy (TLE). Key findings: In HC, the BG was functionally negatively correlated with typical DMN regions, such as the posterior medial and prefrontal cortices. This negative correlation as well as the FC between the BG and SMN was significantly lower in patients.¹
2. SEEG studies: The human striatum and pallidum did not generate specific epileptic EEG activity, neither interictal nor ictal, not even when the seizures were generalized. The visually observed slowing and amplitude increase in the BG was found with the spread of the epileptic activity from the hippocampus to other areas.² Significant frequency components of 2 to 10 Hz, with the maximum in the 5- to 10-Hz range, were constantly observed in the BG.³ The frequency of this component slowed by around 2 Hz during seizures. There was a significant ictal increase of power spectral density in all frequency ranges. The changes in the BG were consistent while the seizure activity spread over the cortex, and they partially persisted after the clinical seizure ended. They

were inconsistently present in the first period after the seizure onset.

3. Significance: Unlike in HC, in TLE the BG are not correlated with a DMN component, and the FC of the BG is decreased with SMN. The epileptic process reduces the FC between the BG and large-scale brain networks. This may reflect an altered function of the BG in epilepsy. Based on our SEEG studies, the time course of the oscillatory activities together with the absence of the epileptiform EEG activities in the BG lead us to suggest an inhibitory role of the BG in temporal lobe seizures. This “filtering effect” of the BG may act as an obstacle to the spread of ictal activity. The BG should be seriously considered as a potential target for neuromodulatory and pharmacological treatment of TLE.

References

1. Rektor I, Tomčík J, Mikl M, Mareček R, Brázdil M, Rektorová I. Association between the basal ganglia and large-scale brain networks in epilepsy. *Brain Topogr.* 2013;6:355-362.
2. Rektor I, Kuba R, Brázdil M. Interictal and ictal EEG activity in the basal ganglia. *Epilepsia.* 2002;43:253-262.
3. Rektor I, Kuba R, Brázdil M, Halámek J, Jurák P. Ictal and perictal oscillations in the human basal ganglia in temporal lobe epilepsy. *Epilepsy Behav.* 2011;20:512-517.

FC2_5. Feasibility of Using Effective Connectivity to Localize the Seizure Onset Zone From Ictal Scalp EEG Recordings

P. van Mierlo¹, E. Carrette², G. Strobbe¹, V. Montes-Restrepo¹, K. Vonck², and S. Vandenberghe¹

¹iMinds, Department of Electronics and Information Systems, Ghent University, Ghent, Belgium
Reference Centre for Refractory Epilepsy, Ghent University Hospital, Ghent, Belgium

Epilepsy is a network disease in which multiple brain areas are simultaneously active during a seizure. The seizure onset zone (SOZ) is the brain area responsible for generating the seizures. Effective connectivity analysis of ictal intracranial EEG recordings has already proven to be valuable to localize the SOZ.¹⁻³ In a previous study⁴ in 8 patients we showed that the brain region depicted by effective connectivity using the adaptive directed transfer function (ADTF)^{3,5,6} corresponded both with the visual analysis of the epileptologist and with the resected brain region. However, the notion of an underlying ictal network during seizures is not commonly used in scalp EEG source reconstruction. In this study, we want to show the feasibility to couple effective connectivity analysis to EEG source analysis to localize the SOZ from ictal scalp EEG recordings.

First, we performed simulations in which ictal scalp EEG was constructed based on an underlying seizure network and a patient individual head model. We used the precorrelated and orthogonally projected multiple signal classification

(POP-MUSIC) algorithm⁷ to extract multiple simultaneously active sources from the scalp EEG. This method allows estimation of synchronous sources and their individual time courses. Afterward, we compared SOZ localization based on the energy of the sources and based on the estimated underlying network, derived using ADTF analysis. We also investigated 3 seizures of 1 patient with the proposed method.

The simulations revealed that it is advantageous to use network information to localize the SOZ. The SOZ was correctly localized by using effective connectivity in all 3 seizures recorded with scalp EEG. Hereby, we showed the feasibility of coupling EEG source reconstruction to network analysis to localize the SOZ. However, more research about the added value of incorporating connectivity analysis into EEG source analysis during the presurgical evaluation needs to be done. Nevertheless, the technique of coupling connectivity analysis with source reconstruction has the potential to ameliorate SOZ localization from ictal scalp EEG recordings.

References

1. Wilke C, van Drongelen W, Kohrman M, He B. Neocortical seizure foci localization by means of a directed transfer function method. *Epilepsia.* 2010;51:564-572.
2. Wilke C, Worrell G, He B. Graph analysis of epileptogenic networks in human partial epilepsy. *Epilepsia.* 2011;52:84-93.
3. van Mierlo P, Carrette E, Hallez H, et al. Accurate epileptogenic focus localization through time-variant functional connectivity analysis of intracranial electroencephalographic signals. *Neuroimage.* 2011;56:1122-1133.
4. van Mierlo P, Carrette E, Hallez H, et al. Ictal-onset localization through connectivity analysis of intracranial EEG signals in patients with refractory epilepsy. *Epilepsia.* 2013;54:1409-1418.
5. Wilke C, Ding L, He B. Estimation of time-varying connectivity patterns through the use of an adaptive directed transfer function. *IEEE Trans Biomed Eng.* 2008;55:2557-2564.
6. Astolfi L, Cincotti F, Mattia D, et al. Tracking the time-varying cortical connectivity patterns by adaptive multivariate estimators. *IEEE Trans Biomed Eng.* 2008;55:902-913.
7. Liu H, Schimpf PH. Efficient localization of synchronous EEG source activities using a modified RAP-MUSIC algorithm. *IEEE Trans Biomed Eng.* 2006;53:652-661.

FC2_6. Detection of Structural Brain Abnormalities in Single Patients: Focal Epilepsy

B. Ahmed¹, C. Brodely¹, C. Carlson², R. Kuzniecky², O. Devinsky², J. French², and T. Thesen^{2,3}

¹Department of Computer Science, Tufts University, Boston, USA

²Department of Neurology, New York University School of Medicine, New York, NY, USA

³Department of Radiology, New York University School of Medicine, New York, NY, USA

Advances in MRI have transformed the in vivo detection of brain abnormalities in neurological disease. However, many subtle structural abnormalities remain undetected, especially in

individual patients, where clinical relevance is highest. We present a quantitative, multifeature morphometry approach combined with machine learning algorithms for detecting structural cortical abnormalities in epilepsy patients with focal cortical dysplasia (FCD). FCD is a malformation of cortical development and is the most common etiology in pediatric epilepsy and the second most common etiology in adults with treatment resistant epilepsy. Lesions may occur anywhere in cortex. Seizure freedom after surgery is reported at 66% with a detected lesion, but only 29% in MRI-negative patients. Yet, 70% to 80% of histologically confirmed FCD cases go undetected by visual inspection of the MRI.

Sixty-one controls and 23 MRI-negative patients in whom no focal lesion was detected during routine visual radiological analysis and 7 MRI-positive patients were scanned before surgery at 3 T using a T1-weighted MRI sequence. All patients subsequently underwent intracranial EEG monitoring and resection of the epileptic focus and pathology confirmed FCD. Morphometric routines with surface-based spherical averaging techniques were used to align anatomical structures between individual brains and to calculate 6 features at each vertex, including *cortical thickness*, *gray-white contrast*, *local gyrification*, *sulcal depth*, *Jacobian distance*, and *curvature*. A logistic regression classifier was trained on normal control data and the data from the FCD region of MRI-positive patients to classify, in MRI-negative patients, vertices into lesional and nonlesional.

The logistic regression approach correctly classified lesions within the resection zone in 14 out of the 24 (58%) MRI-negative patients. The overall false positive rate (by vertex) was never greater than 1.05%. Quantitative MRI can aid in the presurgical detection of FCD lesions, even in patients whose clinical MRI was read as normal.

An automated, surface-based, multifeature, quantitative morphometry approach has the potential to increase the number of patients suitable for surgery and improve electrode placement and surgical outcome in patients with invisible lesions on routine clinical MRI. This method may have the potential to detect disease-characteristic structural abnormalities in single patients with other neurological diseases that are not spatially uniform across all patients.

FC3_1. Subthalamic Nucleus Activity Dissociates Proactive and Reactive Inhibition in Patients With Parkinson's Disease

D. Bénis^{1,2}, O. David^{1,2}, J.-P. Lachaux³, E. Seigneuret, P. Krack^{1,2,4}, V. Fraix^{1,2,4}, S. Chabardès^{1,2,5}, and J. Bastin^{1,2}

¹Fonctions Cérébrales et Neuromodulation, Université Joseph Fourier, Grenoble, France

²INSERM, U836, Grenoble Institut des Neurosciences, Grenoble, France

³INSERM, U1028, Centre de Recherche en Neurosciences de Lyon, Université Claude Bernard, Lyon, France

⁴University Hospital, Department of Neurology, Grenoble, France

⁵University Hospital, Department of Neurosurgery, Grenoble, France

Models of action selection postulate the critical involvement of the subthalamic nucleus (STN), especially in reactive inhibition processes when inappropriate responses to a sudden stimulus must be overridden.^{1,2} The STN could also play a key role during proactive inhibition, when subjects prepare to potentially suppress their actions.^{3,4} Here, we hypothesized that STN responses to reactive and proactive inhibitory control might be driven by different underlying mechanisms with specific temporal profiles.

Deep brain stimulation of the STN, used as a symptomatic treatment of Parkinson disease, allows direct recording of local field potentials (LFP) from STN stimulation electrodes with millisecond time precision.

Recordings in 12 Parkinson's disease patients during a modified stop signal task (SST) revealed a decrease of beta band activity (BBA, 13-35 Hz) in the STN during reactive inhibition of smaller amplitude and shorter duration than during motor execution. Crucially, the onset latency of this relative increase of BBA took place before the stop signal reaction time, and could thus be thought of as a "stop" signal inhibiting thalamo-cortical activity that would have supported motor execution. Finally, results also revealed a higher level of BBA in the STN during proactive inhibition, which correlated with patients' inhibitory performances. We propose that BBA in the STN would here participate to the implementation of a "hold your horse" signal to slow down motor responses, thus prioritizing accuracy as compared to speed. Taken together, our results provide strong electrophysiological support for the hypothesized role of the STN during proactive inhibitory control and rapid motor inhibition.

References

1. Aron A, Poldrack RA. Cortical and subcortical contributions to Stop signal response inhibition: role of the subthalamic nucleus. *J Neurosci*. 2006;26:2424-2433.
2. Li CS, Yan P, Sinha R, Lee TW. Subcortical processes of motor response inhibition during a stop signal task. *Neuroimage*. 2008;41:1352-1363.
3. Chikazoe J, Jimura K, Hirose S, Yamashita K, Miyashita Y, Konishi S. Preparation to inhibit a response complements response inhibition during performance of a stop-signal task. *J Neurosci*. 2009;29:15870-15877.
4. Ballanger B, van Eimeren T, Moro E, et al. Stimulation of the subthalamic nucleus and impulsivity: release your horses. *Ann Neurol*. 2009;66:817-824.

FC3_2. Reliability of Resting Brain Networks in BOLD and ASL fMRI Across Time and Platforms

K. Jann¹, D. Gee², E. Kilroy¹, T. Cannon³, and D.J. Wang¹

¹Department of Neurology, University of California, Los Angeles, CA, USA

²Department of Psychology, University of California, Los Angeles, CA, USA

³Department of Psychology, Yale University, New Haven, CT, USA

Since the seminal work by Biswal¹ in 1995, the study of resting brain networks (RBNs) based on functional connectivity (FC) in resting state fMRI (rs-fMRI) has experienced an upsurge from basic to clinical neuroscience. In addition to the widely used blood oxygen level-dependent (BOLD) contrast, RBNs can be detected using arterial spin labeled (ASL) perfusion MRI, which measures cerebral blood flow (CBF) using magnetically labeled blood water as an endogenous tracer. Compared with BOLD, perfusion-based FC analysis provides quantitative and more direct measures of the physiology and metabolism of specific networks. To date, however, no studies have systematically addressed the test-retest (TRT) reliability of RBNs detected using BOLD and ASL rs-fMRI across time and/or sites.

In the present study, we performed repeated 2D-EPI BOLD and background suppressed 3D GRASE pCASL² rs-fMRI scans in the same 10 healthy young subjects (6 females/4 males; age [mean \pm SD] = 22 \pm 3 years)—2 times on each of the 2 MR scanners—to evaluate the reliability of RBNs detected using each technique. After preprocessing, functional connectivity was assessed by means of a temporally concatenated group independent component analysis (ICA) approach that identified 5 common RBNs. Statistical analyses were performed on the network as well as on a voxel-wise level. Multivariate repeated-measures analyses of variance (ANOVAs) and post hoc *t* tests were computed to identify differences between modalities, scanners and sessions. TRT reliability of ASL and BOLD based RBNs was estimated using intraclass correlation coefficients (ICCs).

We found that CBF-based FC is feasible and yields a group RBNs similar to the BOLD-RBNs, but with significant differences in specific areas depending on the modality. Furthermore, TRT analysis indicates more reliable networks in BOLD (ICC = 0.900/0.925) than ASL (ICC = 0.625/0.550). However, while the spatial pattern of the DMN is more reliable using BOLD, ASL provides highly reproducible, network specific CBF measurements. Thus, the combination of ASL and BOLD rs-fMRI provides a powerful tool for characterizing RBNs.

Acknowledgments

Study funded by Garen and Shari Staglin and the International Mental Health Research Organization. K. Jann has a fellowship funded by SNSF/SSMBS (grant no. 142743).

References

1. Biswal B, Yetkin FZ, Haughton VM, Hyde JS. Functional connectivity in the motor cortex of resting human brain using echo-planar MRI. *Magn Reson Med*. 1995;34:537-541.
2. Fernández-Seara MA, Edlow BL, Hoang A, Wang J, Feinberg DA, Detre JA. Minimizing acquisition time of arterial spin labeling at 3T. *Magn Reson Med*. 2008;59:1467-1471.

FC3_3. Investigating the Effect of Functional Connectivity Definition on Graph Theoretical Metrics

J.R. Hale¹, S.D. Mayhew¹, I. Przeczdzik¹, T.N. Arvanitis², and A.P. Bagshaw¹

¹School of Psychology, University of Birmingham, Birmingham, UK

²School of Electronic, Electrical and Computer Engineering, University of Birmingham, Birmingham, UK

Brain function is thought to be mediated by integration of functionally specialised regions to form networks. Owing to their potential to characterise and summarise large-scale networks, graph theoretical methods are increasingly being applied to study the brain's functional networks.¹ Graphs are made by defining regions (nodes) and computing the functional connectivity (FC) strength between them (edges) to form an association matrix. While graph theory metrics are sensitive to several assumptions, to date there has been less consideration of the formation of the association matrix.² We examine several factors: node and edge characterisation, connectivity threshold (CT) and timeseries length (TL).

Eight healthy subjects underwent a 15-minute resting state fMRI scan. Standard preprocessing was performed.³ Data from a separate cohort were used to define a functional parcellation scheme using resting state networks (RSNs) identified from fMRI data using MELODIC.⁴ For each RSN, nodes were defined from 3x3x3 voxel cubes in each major functional region. FC was assessed between BOLD timecourses extracted from network nodes using Pearson correlation and partial correlation, computed for all pairs of nodes and averaged across subjects, forming association matrices. Matrices were constructed using the whole time series and data averaged over 2-minute and 30-second epochs. A range of thresholds were applied to binarise matrices and graph metrics computed as a function of CT using the Brain Connectivity Toolbox.¹

Pearson correlation FC analysis graph metrics displayed stability across TLs. With increased CT, the number of modules identified increased, reaching the number of RSNs expected from the parcellation scheme when CT = 0.2 to 0.3, becoming more variable thereafter. Clustering coefficient (C) and the characteristic path length (PL) of each RSN were also found to be stable up until CT = 0.3. As expected, connection strength for partial correlation analysis was lower, but showed stability across TL. Modularity was more variable across thresholds, and C and PL were more sensitive to changes in CT.

The choice of CT and edge definition greatly influenced graph metrics, which will have a major impact on subsequent interpretation of brain networks. Graph metrics were stable across TLs which is noteworthy for applications such as sleep where data are epoched when classifying stages. The functional parcellation scheme allows some internal validation of graph

theory quantities, for example, a low CT that estimates a low number of modules can be identified as inappropriate; which is particularly useful when summarising changes in FC between sleep stages, or between patient and control subjects.

Acknowledgments

Funded by the UK Engineering and Physical Sciences Research Council (EPSRC Grant Number EP/J002909/1).

References

1. Rubinov M, Sporns O. Complex network measures of brain connectivity: uses and interpretations. *Neuroimage*. 2010;52:1059-1069.
2. Smith SM. The future of fMRI connectivity. *Neuroimage*. 2012;62:1257-1266.
3. Fox MD, Snyder AZ, Vincent JL, Corbetta M, Van Essen DC, Raichle ME. The human brain is intrinsically organized into dynamic, anticorrelated functional networks. *Proc Natl Acad Sci U S A*. 2005;102:9673-9678.
4. Beckmann CF, Smith SM. Probabilistic independent component analysis for functional magnetic resonance imaging. *IEEE Trans Med Imaging*. 2004; 23:137-152.

FC3_4. Evaluating the Physiological Plausibility of Time-Varying Connectivity Methods Using Large-Scale Evoked Potentials in an Animal Model

G. Plomp¹, C. Quairiaux², L. Astolfi^{2,3}, and C.M. Michel^{1,4}

¹Department of Fundamental Neuroscience, University of Geneva, Geneva, Switzerland

²Department of Computer, Control, and Management Engineering, University of Rome "Sapienza", Rome, Italy

³Santa Lucia Foundation, IRCCS, Rome, Italy

⁴Neurology Clinic, University Hospital Geneva, Geneva, Switzerland

Time-varying connectivity measures are increasingly used to study directed interactions between brain regions from electrophysiological signals. These methods may show good results in simulated data but it is unknown to what extent connectivity results obtained from real data are physiologically plausible. Here, we compare time-varying connectivity measures on a benchmark data set of multichannel somatosensory evoked responses (SEPs) measured across rat cortex, where the structural and functional connectivity is relatively well-understood: Rat SEPs after whisker stimulation are exclusively initiated by contralateral primary sensory cortex (S1), at known latencies, and with known spread of activity from S1 to specific regions. This allows for a comparison of the physiological plausibility of time-varying connectivity measures according to fixed criteria. We evaluated the performance of four implementations of time-varying partial directed coherence (PDC), comparing

row- and column-wise normalization, and introducing a weighting by the spectral power. The different PDC approaches gave mostly converging results, but row-normalized, weighted PDC showed the largest effect sizes and best temporal resolution with results that were invariably physiologically plausible. The results provide a strong validation of information transfer methods in an animal model and suggest a driving role for ipsilateral S1 in the later part of the SEP. The benchmark SEP dataset will be made freely available so that the physiological plausibility of existing and future connectivity methods can be similarly evaluated.

FC3_5. Trial-by-Trial Global Modulation of BOLD Responses to Simple, Sensory Stimuli: Implications for Functional Brain Imaging and Understanding Positive and Negative BOLD Responses

S.D. Mayhew¹, K.J. Mullinger², A.P. Bagshaw¹, R. Bowtell², and S.T. Francis²

¹Birmingham University Imaging Centre, School of Psychology, University of Birmingham, Birmingham, UK

²Sir Peter Mansfield Magnetic Resonance Centre, School of Physics and Astronomy, University of Nottingham, University Park, Nottingham, UK

Unilateral stimulation induces contralateral positive (PBR) and ipsilateral negative (NBR) BOLD responses in primary visual (V1), motor (M1), and somatosensory (S1) cortices.¹⁻³ NBR are thought to reflect neuronal inhibition required to optimize task performance.¹⁻³ However, the functional significance of NBR and its balance with PBR has not been studied at the single-trial level, where signal modulations most relevant to dynamic network processing occur.⁴ We investigate the relationship between single-trial variability in PBR and NBR amplitude in V1, M1 and S1 for unilateral stimulation.

Three fMRI experiments were recorded in 14 subjects (age = 28 ± 5 years). *Visual*. Eighty trials of a 1-second duration left-hemifield checkerboard presented at 100% or 25% contrast with interstimulus interval (ISI) = 16 to 21 secnds. *Motor*. Five-second duration isometric contraction of right hand at 10% and 30% of maximum force. 40 trials of each force were recorded with ISI = 5 to 9 seconds. *Somatosensory*. Ten-second median nerve stimulation (MNS) was applied to the right wrist at 2Hz. Data were recorded over 40 trials with ISI = 20 seconds.

Blood oxygen level-dependent (BOLD) data were standardly preprocessed and GLM analyses performed using regressors of stimulus timings. Group-level ROIs were defined from a 3 × 3 × 3 voxel cube centered on the group peak voxel in contralateral (*c*) PBR and ipsilateral (*i*) NBR regions of V1, M1, and S1. Single-trial responses were extracted, baseline corrected, and single-trial amplitudes were measured as the

peak signal change within the time window: (mean response latency \pm TR*2). For each subject the linear correlation of single-trial PBR–NBR amplitudes was assessed between: $cV1-iV1$, $cM1-iM1$, and $cS1-iS1$.

Significant contralateral PBR and ipsilateral NBR were observed in V1, M1, and S1. In all three sensory modalities we found that the average magnitude of $cPBR$ and $iNBR$ were negatively correlated, while the natural modulations of single-trial PBR and NBR were positively correlated. Further GLM analyses showed that single-trial $cPBR$ amplitude was significantly positively correlated with the BOLD response to the stimulus in gray matter across widespread brain regions in all 3 data sets.

Single-trial PBR–NBR correlations form part of a global-brain positive correlation with the $cPBR$, that is strongest in stimulus-driven primary sensory cortex. This bilateral modulation may have neuronal origin, related to widespread, complex modulation of brain networks by simple sensory tasks.⁵ Physiological confounds of breathing and heart rate do not contribute. Additional work using resting-state fMRI data and also EEG–fMRI recordings is underway to quantify the potential contribution of vascular effects.

References

1. Shmuel A, Yacoub E, Pfeuffer J, et al. Sustained negative BOLD, blood flow and oxygen consumption response and its coupling to the positive response in the human brain. *Neuron*. 2002;36:1195–1210.
2. Allison JD, Meador KJ, Loring DW, Figueroa RE, Wright JC. Functional MRI cerebral activation and deactivation during finger movement. *Neurology*. 2000;54:135–142.
3. Klingner CM, Hasler C, Brodrecht S, Witte OW. Dependence of the negative BOLD response on somatosensory stimulus intensity. *Neuroimage*. 2010;53:189–195.
4. Scheibe C, Ullsperger M, Sommer W, Hecker HR. Effects of parametrical and trial-to-trial variation in prior probability processing revealed by simultaneous electroencephalogram/functional magnetic resonance imaging. *J Neurosci*. 2010;30:16709–16717.
5. Gonzalez-Castillo J, Saad ZS, Handwerker DA, Inati SJ, Brenowitz N, Bandettini PA. Whole-brain, time-locked activation with simple tasks revealed using massive averaging and model-free analysis. *Proc Natl Acad Sci U S A*. 2012;109:5487–5492.

FC3_6. Time Delays Cannot Be Estimated From the Phase–Frequency Relationship of Coherence

A.C. Schouten^{1,2}, S.F. Campfens², and H. van der Kooij^{1,2}

¹Department of Biomechanical Engineering, Delft University of Technology, Delft, Netherlands

²MIRA institute for Biomedical Technology and Technical Medicine, Twente University, Enschede, Netherlands

Coherence analysis is a popular tool in neuroscience to detect connectivity between spatially separated populations of neurons. The coherence indicates the linear relation between 2 signals as a function of frequency. By definition coherence varies between 0 and 1, where one indicates a perfect linear

noise-free relation. Coherence is the magnitude squared of the (complex) coherency. Coherency phase describes the relative timing between the signals and is often used to estimate the time delay between the signals.

Corticomuscular coherence (CMC) in the beta band demonstrates connectivity between the cortex (recorded with EEG or MEG) and the spinal motoneurons (recorded muscle activity with EMG). Typically, a linear phase–frequency relation is found, suggesting the presence of a time delay. In literature, 3 slopes of the phase–frequency relation are reported.^{1,2} Most studies report a negative slope (cortex leads muscle), which is often smaller than physiologically would be expected. A positive slope (muscle leads cortex) and a constant slope are also reported. Furthermore, these slopes typically have a nonzero intercept, which is awkward and not well explained.

Traditionally, CMC was considered a unidirectional coupling. With a unidirectionally coupled time delay, the phase–frequency relation would present as a straight slope with zero intercept. However, the underlying system could include feedback loops and also sensory information could be present in the cortical signal. Here, we analyzed how this affects the coherency phase and the estimation of time delays. We considered 4 scenarios: (a) a unidirectional (efferent) system with a time delay, (b) a system with a feedback loop with time delays in the forward (efferent) path and feedback (afferent) path, (c) a system without a feedback loop, but with additional sensory information in the cortical signal, and (d) the combination of (b) and (c). For the scenarios, we derived the coherency phase and estimated the time delay by fitting the slope of coherency phase in the beta band.

We found that both the presence of a feedback loop and the presence of afferent information in the cortical signal have a huge effect on the coherency phase, depending on the relative strength of the pathways and noise magnitudes. Within the beta band, the slope of the phase–frequency relation is reduced and has a nonzero intersect. If the afferent pathways are stronger than the efferent pathways even a phase advance will result, that is, the slope can become positive. In conclusion, the coherency phase depends on complex interactions within the sensorimotor loop, where the time delay cannot be simply estimated from the phase–frequency relationship.

References

1. Witham CL, Riddle CN, Baker MR, Baker SN. Contributions of descending and ascending pathways to corticomuscular coherence in humans. *J Physiol*. 2011;589(pt 15):3789–3800.
2. Schouten AC, Campfens SF. Directional coherence disentangles causality within the sensorimotor loop, but cannot open the loop. *J Physiol*. 2012;590(pt 10):2529–2530.

FC4_1. Phase Anomalies in the Cortical Source-Current Activity in Depression

Z. Koles¹, J. Lind², and P. Flor-Henry²

¹Department of Electrical and Computer Engineering, University of Alberta, Edmonton, Alberta, Canada

²Alberta Hospital Edmonton, Edmonton, Alberta, Canada

We have examined the coherences in the source-current activity between a number of cortical patches in a group of right-handed female patients diagnosed with depression. The analysis was completed in the 5 classical EEG bands: (2-3 Hz) delta, (4-7 Hz) theta, (8-13 Hz) alpha, (14-20 Hz) beta, and (21-50 Hz) gamma. The results, based on a study involving 93 patients and 87 right-handed female controls, indicate that there are significant differences in the coherences between the groups in all frequency bands but mostly in the delta and theta bands. In these bands, the differences were predominant in the left hemisphere and mainly in the frontal regions, while in the beta and gamma bands the differences were predominately right hemisphere. In many cases, the differences were attributable to the phase components of the coherences rather than their magnitudes. For example, in the theta band between the left prefrontal patch and the left frontal patch, there was a phase reversal between the groups with the prefrontal patch leading frontal patch in the patient group and lagging it in the control group. In the alpha band, there was no significant phase difference in the patient group between the left prefrontal patch and the left temporal patch but a significant phase lag of the temporal patch in the control group. In the beta band, there was a significant phase difference between the right prefrontal patch and a patch on the right sensory cortex not seen in the control group. To obtain the results, complex coherences were calculated in all of the frequency bands for each subject between all possible pairs of 14 patches located on homologous cortical regions of the 2 hemispheres. Evaluation of the results was based on scatter plots showing the complex coherences between pairs of patches for all of the subjects in the patient and control groups. The results of this study were obtained using a generic finite-element head model consisting of over 4 million elements and over 50 000 cortical locations.¹ The diameter of each cortical patch was about 2 cm and consisted of about 500 contiguous sources. The inverse solutions were obtained using a LORETA algorithm with a point-spread function approximately matching that of the patch diameters.

Reference

1. Koles Z, Lind JC, Flor-Henry P. Gender differences in brain functional organization during verbal and spatial cognitive challenges. *Brain Topogr.* 2010;23:199-204.

FC4_2. Protective Pathways? Cognitive and Physical Activity, Alzheimer's Disease Pathological Biomarkers and Cognitive Functioning in Cognitively Normal Older Adults

M. Wirth¹, C.M. Haase², S. Villeneuve¹, J. Vogel¹, and W.J. Jagust^{1,3}

¹Helen Wills Neuroscience Institute, University of California, Berkeley, CA, USA

²Institute of Personality and Social Research, University of California, Berkeley, CA, USA

³Life Sciences Division, Lawrence Berkeley National Laboratory, Berkeley, CA, USA

Objective. Cognitive and physical activities are proposed to protect against Alzheimer's disease (AD)-related pathology and associated cognitive impairment. Using path analysis, the study examined cross-sectional associations between cognitive and physical activities, AD-related biomarkers of beta-amyloid (A β) burden and neural integrity, cerebrovascular injury, and cognitive functioning in normal older adults. **Methods.** Ninety-two cognitively normal older adults (age, 75.2 ± 5.6 years; 58 women; education, 16.9 ± 1.9 years) were included. Cognitive activity (early life, middle life, and current) and current physical activity were measured using validated questionnaires. For each participant, we obtained cortical A β burden (quantified with [11C] Pittsburgh compound B (PIB)-PET), cerebrovascular injury (measured using white matter lesions [WML]), neural integrity within AD-affected regions (estimated using a multimodality neurodegenerative biomarker) and APOE genotyping. Cognitive functioning was measured combining memory and executive functioning tests. **Results.** Adjusting for age, gender, and education, higher (in particular middle life and current) cognitive activity as well as higher current physical activity was associated with lower WML, which were in turn associated with higher neural integrity and higher global cognitive functioning. Higher (in particular early and middle life) cognitive activity was confirmed to predict lower cortical PIB retention, which itself moderated the impact of neural integrity on cognitive functions. The APOE status interacted with early life cognitive activity, such that cognitively engaged ApoE4 carriers exhibited low PIB retention, comparable to ApoE4 noncarriers. **Conclusion.** The findings suggest that cognitive and physical activity may promote successful cognitive aging through AD-related neurobiological pathways, involving cerebrovascular injury, A β burden, and neurodegenerative pathology.

FC4_3. Association Between White Matter Hyperintensities and Resting State fMRI in Early-Stage Alzheimer's Disease

L. Kambeitz-Ilankovic¹, L. Simon-Vermot¹, B. Gesierich¹, M. Duerig¹, M. Ewers¹, and the Alzheimer's Disease Neuroimaging Initiative (ADNI)

¹Institute for Stroke and Dementia Research, Medical Centre, Klinikum der Universität München, Ludwig-Maximilians University, Munich, Germany

Background. Recent neuroimaging studies using resting state functional MRI (RS fMRI) demonstrated abnormal functional connectivity within the default mode network and other RS networks in mild cognitive impairment (MCI) and Alzheimer's disease (AD) dementia. Both beta-amyloid (A β) deposition and cerebrovascular pathology can be frequently observed in MCI and AD dementia. However, the independent effects of both types of pathologies on functional brain changes early in the course of AD are unknown. We aimed to test the independent effect levels of A β (¹⁸F-AV-45 PET) and cerebrovascular

disease (white matter hyperintensities [WMH]) and on functional connectivity (FC) of brain activity during resting state in elderly healthy controls (HC) and MCI. **Methods.** A total of 76 subjects, including 17 HC subjects (with normal low A β as measured by ^{18}F -AV-45-PET) and 59 MCI subjects were included from the multicenter biomarker study ADNI (<http://www.adni-info.org>). Based on RS fMRI, FC was assessed through a seed-based approach, including voxel-wise Pearson correlations between the low-frequency fMRI signal fluctuations in the left posterior cingulate cortex (PCC, ie, the seed) and each voxel within the gray matter. Using random effects analysis at the group level, the RS fMRI FC maps were divided into brain regions of positive correlations with the PCC (RSpos) and those with negative correlations with the PCC (RSneg). The mean FC of the RSpos and RSneg networks were regressed onto global WMH volume (segmented in FLAIR images) and global ^{18}F -AV45 PET binding, controlling for age, gender, and educational level across all subjects. **Results.** The RSneg network (showing negative correlations with the PCC) included the inferior parietal lobe, superior temporal and middle frontal gyri. The RSpos network (showing positive correlations with the PCC) included the precuneus/angular gyrus, middle temporal gyrus, orbitomedial frontal gyrus, and hippocampus, which overlapped with the known brain regions of the default mode network. Higher WMH volume was associated with reduced FC in the RSneg network ($P = .02$), whereas AV-45 PET was not a significant predictor. No significant associations were observed for the RSpos network. **Conclusion.** In MCI, cerebrovascular disease (WMH), but not A β , may contribute to reduced function of a temporoparietal and prefrontal network that has been previously implicated in attentional cognitive abilities and is anticorrelated to the default mode network.

FC4_4. Functional Imaging of the Default Mode Network in Cognitively Impaired Patients With Parkinson's Disease

I. Rektorova^{1,2}, L. Krajcovicova^{1,2}, R. Marecek^{1,2}, and M. Miki^{1,2}

¹Brain and Mind Research Program, CEITEC MU, Masaryk University, Brno, Czech Republic

²First Department of Neurology, School of Medicine, Masaryk University and St Anne's Hospital, Brno, Czech Republic

Background. Default mode network (DMN) decreases its activity when switching from rest to a task condition while activity of the network engaged in the task increases. Complex visual scene encoding task (VSET) evaluates visual processing that is typically disturbed in Parkinson's disease dementia (PDD). **Objective.** Using fMRI, we studied changes in the DMN connectivity in PDD as compared with healthy controls (HC) when switching from baseline to VSET. **Methods.** In all, 18 PDD and 18 age-matched HC participated. We used the psychophysiological interaction analysis with the posterior cingulate cortex (PCC) as a seed. The threshold

was set at $P < .05$ FWE (family-wise error) corrected. **Results.** Healthy controls showed greater PCC connectivity with bilateral middle temporal/ middle occipital gyri during the baseline than during the task condition. The correlation changed from positive to negative. In PDD, similar changes of PCC connectivity were observed with the left precentral gyrus (LPCG). LPCG was the only region with significant PCC connectivity changes between groups: reversed patterns of correlations were observed when switching from baseline to VSET. **Conclusion.** Parkinson's disease dementia expressed disturbed DMN connectivity with brain areas involved in the visual processing task. Instead, the primary motor cortex became engaged which may reflect malfunction caused by underlying PD brain pathology or inefficient compensation.

Acknowledgments

The study was supported by the grant of the Czech Ministry of Health, NT13499.

FC4_5. White Matter Microstructure Alterations of the Medial Forebrain Bundle in Major Depressive Disorder

T. Bracht¹, H. Horn¹, W. Strik¹, A. Federspiel², S. Schnell³, O. Höfle¹, K. Stegmayer¹, R. Wiest⁴, T. Dierks², T.J. Müller¹, and S. Walther¹

¹University Hospital of Psychiatry, University of Bern, Bern, Switzerland

²Department of Psychiatric Neurophysiology, University Hospital of Psychiatry, University of Bern, Bern, Switzerland

³Departments of Radiology and Biomedical Engineering, Feinberg School of Medicine, Northwestern University, Chicago, IL, USA

⁴Institute of Diagnostic and Interventional Neuroradiology, Inselspital, University of Bern, Bern, Switzerland

Background. The medial forebrain bundle (MFB) is a key structure of the reward system and connects the ventral tegmental area (VTA) with the nucleus accumbens (NAcc), the medial and lateral orbitofrontal cortex (mOFC, IOFC), and the dorsolateral prefrontal cortex (dlPFC). Previous diffusion tensor imaging (DTI) studies in major depressive disorder point to white matter alterations of regions that may be part of the MFB. Therefore, it was the aim of our study to probe white matter integrity of the MFB using a DTI-based probabilistic fibre tracking approach.

Methods. In our study, 22 patients with major depressive disorder (MDD) (12 melancholic MDD patients, 10 nonmelancholic MDD patients) and 21 healthy controls underwent DTI scans. We used a bilateral probabilistic fibre tracking approach to extract pathways between the VTA and NACC, mOFC, IOFC, dlPFC, respectively. Resulting probability indices forming part of a bundle of interest (PIBI) and mean fractional anisotropy (FA) values were used to compare structural connectivity between groups. **Results.** Patients with MDD had reduced PIBI

values in the right VTA–IOFC connection which may indicate an altered fibre tract course. Compared to healthy controls, only melancholic MDD patients had reduced mean-FA in the right VTA–IOFC and VTA–dlPFC connection. Mean-FA of MFB pathways was negatively correlated with total depression scale rating scores and with melancholic symptoms in MDD patients. **Conclusions.** Our results suggest white matter microstructure alterations of the MFB in the neurobiology of MDD, in particular in the melancholic subtype. White matter microstructure is associated with both depression severity and melancholic symptoms.

FC4_6. QEEG-Neurometric Analysis Guided Neurofeedback (NF) Treatment in Dementia: 20 Cases

T. Surmeli¹, A. Ertem¹, E. Eralp¹, and I.H. Kos¹

¹Living Health Center for Research and Education, Istanbul, Turkey

Dementia is characterized by a loss of cognitive function. Dementia patients may have comorbid mood problems, sleep problems, or agitation. They may need additional psychotropic drugs to address these problems. Therefore, an effective non-drug alternative would be very useful in this population that not only treats the cognitive symptoms but the comorbid symptoms associated with this disorder. In this study, we wanted to show the outcomes of a clinical case series using QEEG in the assessment and neurofeedback (NF) in the treatment of dementia. We studied 20 patients (9 males and 11 females). Before coming to our center, almost half of the subjects were on or had taken an antidementia drug and some of the subjects were on more than one psychotropic medication the most common being the concurrent use of an antipsychotic and an antidepressant. Evaluation measures included drug free QEEG analysis with the FDA-approved Nx-LINK data base, the Mini Mental State Exam (MMSE), Clinical Global Impressions scale (CGI), neuropsychological tests, and interviews with patients' families. Our hypothesis was that NF treatment targeted toward normalizing the deviations from norms seen in the QEEG would be the most beneficial treatment for this group. All the subjects showed improvement based on the CGI, MMSE, and in interviews with the patients' families. This is a study provides the first clinical evidence that NF treatment can produce improvements in patients with dementia. It is recommended that further controlled studies with additional outcome measures to be conducted.

FC5_1. Mathematical Problem Solving: Effects of Learning on Evoked EEG Frequencies

W. Skrandies¹, S. Flüggen¹, and A. Klein¹

¹Institute of Physiology, University of Giessen, Giessen, Germany

We investigated the change of evoked EEG frequencies induced by learning to solve mathematical tasks by divisibility rules. In a behavioral study on 48 healthy adults, we found a

significant increase in performance from 42% to 93% correct responses induced by learning.

Subsequently, the EEG data recorded from 29 volunteers was analyzed. The EEG experiment consisted of 2 parts: First, subjects had to solve 200 tasks without knowing the rules, followed by learning the divisibility rules. A time limit of 3 seconds was used. The EEG was measured simultaneously in 30 channels, artifacts were removed offline, and the data before and after learning were compared. For analysis the wavelet transformation with the Morlet wavelet was used, and the scalp topography of the maximal frequency and its occurrence time was compared.

Frequencies between about 7 and 13 Hz were observed, and after successful learning, the maximal frequencies were significantly smaller over left frontal areas. Similar changes were observed over right parietal regions. In addition, we observed lower frequencies for easy than for hard tasks.

In summary, our data illustrate a significant relation between successful learning and changes in the frequency content of the task-related EEG. These effects were observed after a very short training period of less than 10 minutes.

FC5_3. Microstate-Dependent Perceptual Awareness

J. Britz¹, L. Díaz Hernández^{1,2}, T. Ro³, and C.M. Michel¹

¹Department of Fundamental Neuroscience, University of Geneva, Geneva, Switzerland

²Department of Psychiatric Neurophysiology, University Hospital of Psychiatry, Bern, Switzerland

³Department of Psychology, The City College and Graduate Center, The City University of New York, New York, NY, USA

We investigated whether the differences in perceptual awareness for stimuli at the threshold of awareness can arise from different prestimulus EEG microstates. We used a metacontrast masking paradigm in which subjects had to discriminate between 2 stimuli and obtained measures of accuracy and awareness while their EEG was recorded from 256 channels. We used 4 interstimulus intervals (ISIs) and for each subject, we chose the ISI with nearly equal numbers of trials of correctly identified targets with and without awareness, which allows contrasting differences in awareness while keeping performance constant for identical physical stimuli. We determined the prestimulus microstates in the 2 conditions, and identified 2 microstate maps that doubly dissociated correct identification with and without awareness. The estimated intracranial generators associated with these maps were stronger in primary visual cortex before correct identification without awareness. This difference in activity cannot be explained by differences in alpha power. Analysis of alpha phase revealed that the prestimulus phase can be less reliably linked with differential prestimulus activation of primary visual cortex as previously claimed because of its variation with the reference. Our results shed a new light on the function of prestimulus activity in early visual cortex in visual awareness.

FC5_4. Concurrent EEG–fMRI Study of the Neural Substrates of Spatial Encoding in ADHD

A. Lenartowicz¹, E. Lau¹, C. Rodriguez¹, M.S. Cohen¹, and S.K. Loo¹

¹University of California, Los Angeles, Los Angeles, CA, USA

Attention deficit hyperactivity disorder (ADHD) is often associated with atypical performance on tasks requiring spatial working memory (WM). In the present study, we investigated the neural substrates of this deficit, with emphasis on the integrity of the encoding stage, which we had previously found to be associated with attenuated desynchronization of oscillations in the alpha (8–12 Hz) frequency band in ADHD. We hypothesized that this effect was indicative of atypical neural interactions of occipital, parietal, and prefrontal cortices during the encoding stage. To address this question, we tested 20 male adolescents (12–15 years), of whom half were diagnosed with ADHD, on a Sternberg spatial WM task. This task requires participants to encode the locations of dots presented on a screen, the accuracy of which is assessed after a 7- to 9-second delay with the presentation of a probe stimulus either in one of the previous shown location or in a novel location. During the task we concurrently recorded EEG and fMRI signals. We used the EEG indices to assess attention engagement during encoding as indexed by desynchronization of oscillations in the alpha (8–12 Hz) band. We used the fMRI measures to assess the interactions of then network involved in the process of spatial encoding. Our results indicate that alpha desynchronization during spatial encoding may be associated with the activities of occipital, parietal and prefrontal cortices, that these regions form a functional network and that these relationships vary as a function of difficulty during encoding. We describe the relationship of these measures with symptoms and performance. We conclude that alpha desynchronization and its relationship to occipito-parietal-frontal interactions may be used to characterize and refine the sources of deficits of spatial WM in ADHD.

Acknowledgments

This research was sponsored by NIMH Grant 1 R21/33 DA026109-01 (Cohen); NIMH Grant 1 R21 MH096239-01A1 (Cohen), and Support from the Klingenstein Third Generation Foundation (Lenartowicz).

FC5_5. EEG Functional Connectivity During Eye Movement Desensitization and Reprocessing Is Related With Psychological Tests

G. Di Lorenzo¹, M. Pagani², L. Monaco¹, A. Daverio¹, I. Giannoudas¹, P. La Porta³, A.R. Verardo³, C. Niolu¹, I. Fernandez³, and A. Siracusano²

¹Department of Systems Medicine, University of Rome “Tor Vergata”, Rome, Italy

²Institute of Cognitive Sciences and Technologies, CNR, Rome, Italy

³EMDR Italy Association, Bovisio Masciago, Italy

Background. Psychological tests were recently related with EEG functional connectivity changes in traumatized subjects treated with the Eye Movement Desensitization and Reprocessing (EMDR). The aim of this study was to extend this evidence, studying in a larger clinical sample of victims of psychological traumas the relation between the lagged phase synchronization (LPS) indexes and psychological tests, specifically aimed to trauma-related experience, depressive symptoms, and general psychopathology. **Methods.** A 37-channel EEG was used to record brain activity during whole EMDR sessions. Twenty-eight victims of psychological traumas were recorded at the first EMDR session and at the last one performed after processing the index trauma. EEG functional connectivity analysis was based on the LPS, derived by a 2-step eLORETA procedure: (a) a reduction of dimensionality of inverse matrix from 6239 voxels to 28 regions of interest (ROIs) and (b) computation of LPS index, for each spectrum band, in all possible ROI pairs. At the beginning of the first and the last EMDR session, 3 self-report psychological tests were administered: Impact of Event Scale (IES; total score, IES-T; intrusion score, IES-I; avoidance score, IES-A); Beck Depression Inventory (BDI); and Symptom Check List-90-R (SCL-90-R). To evaluate the association between the LPS indexes (LPSs) of the ROI pairs and psychological tests a correlation analysis was carried out using a nonparametric randomization technique of the p value correction for multiple comparisons. **Results.** All scores from psychological tests decrease significantly after EMDR therapy. IES-T scores showed a significant negative correlation with the LPSs in 3 pairwise interactions: left and right anterior cingulate cortex (ACC) (theta; $r = -0.401$), right posterior cingulate cortex (PCC), right inferior parietal lobe (IPL) (theta; $r = -0.417$), right ACC and right anterior frontal cortex (AFC) (alpha; $r = -0.418$). IES-I was found to correlate significantly with LPSs in left and right AFC (theta; $r = -0.383$), right ACC, and in right orbitofrontal cortex (OFC) (alpha; $r = -0.373$). IES-A correlated significantly with LPSs (theta) in left and right ACC ($r = -0.416$) and in right PCC and right IPL ($r = -0.459$). No other significant interactions between LPSs and the other 2 tests were found. **Conclusions.** After EMDR therapy, the decrease in trauma-related psychological discomfort, as reported by IES scores, is selectively associated with a functional connectivity enhancement in theta and alpha band of limbic and associative areas. These results confirm previous EEG findings of a shift of activation from emotional to cognitive cortex after EMDR therapy.

Acknowledgments

EMDR International Association (EMDRIA), EMDR Europe.

FC6_1. EEG Studies of Various Manifestations of Affective Disorders (Source Localization: LORETA and BEAMFORMER)

P. Flor-Henry¹, J. Lind¹, and Z. Koles²

¹Alberta Hospital Edmonton, University of Alberta, Edmonton, Alberta, Canada

²Department of Electrical and Computer Engineering, University of Alberta, Edmonton, Alberta, Canada

Major depression (males $n = 30$; females $n = 60$), mania (males $n = 17$; females $n = 27$), cyclothymia (males $n = 6$; females $n = 14$), psychotic depression (males $n = 11$; females $n = 23$), atypical depression (males $n = 8$; females $n = 17$), and bipolar depression (males $n = 28$; females $n = 35$), unmedicated patients, all dextral, were investigated and compared with 61 male and 83 female healthy controls: 48 channels, sampling rate 256 per second, Grass amplifiers. Twenty 1-second discontinuous artifact-free segments selected for fast Fourier transformation. All subjects were studied under 4 conditions: eyes open and eyes closed, resting condition, and during cognitive activation of the dominant hemisphere in a verbal task and of the nondominant hemisphere in a spatial task. The different EEG profiles of the various affective syndromes will be presented.

FC6_2. Spatial Working Memory in Attention Deficit/Hyperactivity Disorder

S. Bollmann^{1,2,3}, C. Ghisleni^{1,2,3}, R. O'Gorman^{1,2,4}, S.-S. Poil^{1,3}, P. Klaver^{2,3,5}, L. Michels^{1,6}, E. Martin^{1,2,3}, J. Ball⁷, D. Eich-Höchli⁸, and D. Brandeis^{3,7,9}

¹Center for MR Research, University Children's Hospital, Zurich, Switzerland

²Center for Integrative Human Physiology (ZIHP), University of Zurich, Zurich, Switzerland

³Neuroscience Center Zurich, University of Zurich and ETH Zurich, Zurich, Switzerland

⁴Pediatric Research Center, University Children's Hospital, Zurich, Switzerland

⁵Institute of Psychology, University of Zurich, Zurich, Switzerland

⁶Institute of Neuroradiology, University Hospital of Zurich, Zurich, Switzerland

⁷Department of Child & Adolescent Psychiatry, University of Zurich, Zurich, Switzerland

⁸Psychiatric University Hospital, University of Zurich, Zurich, Switzerland

⁹Central Institute of Mental Health Mannheim, Medical Faculty Mannheim/Heidelberg University, Mannheim, Germany

Attention deficit/hyperactivity disorder (ADHD) is a developmental psychiatric disorder affecting approximately 5% of the population.¹ Although working memory (WM) deficits due to ADHD are particularly prominent in spatial WM tasks, previous work has focused on verbal WM tasks. Thus, it is unknown whether neuronal activity is altered in ADHD during spatial WM, and particularly under high spatial WM load. We therefore developed a spatial WM task with 2 different set sizes to examine load dependent differences in brain activity between adults and children with ADHD and controls. We studied 18 children with ADHD, 21 control children, 20 adults with ADHD and 25 controls using functional MRI (fMRI). Displays consisted of 11 circles positioned on a circular grid. Positions of 2 (low cognitive load) or 4 (high cognitive load) filled circles had to be memorized (retention period). Typical WM regions were activated both in controls and in patients with ADHD.

Contrasting high and low load in the retention phase, we found positive and negative load effects in adult controls ($P < .05$, cluster extent corrected), but only negative load effects in adult patients with ADHD ($P < .05$, cluster extent corrected). These load effects were reduced in parietal and frontal regions for adult ADHD patients compared with controls ($P < .05$, cluster extent corrected). In ADHD children, load sensitivity in the right superior medial frontal gyrus was reduced compared with control children ($P < .05$, cluster extent corrected). Comparing ADHD-related load effect changes in adults and children revealed both age-invariant and age-dependent differences. Task performance was not impaired with ADHD. Our imaging results suggest that particularly adult patients with ADHD lack a reliable positive load effect in parietal and frontal regions. These results are in line with recent findings in the behavioral and imaging literature suggesting impaired spatial WM in ADHD.^{2,3} Our results may suggest that ADHD patients are not capable of synchronizing or recruiting a larger population of neurons to process high load conditions during spatial WM. Whether this result is caused by altered baseline perfusion or lacking synchronization in ADHD patients will further be explored in resting state perfusion and simultaneously recorded EEG data.

Acknowledgments

This cooperative project was funded by the Center for Integrative Human Physiology (ZIHP).

References

1. Polanczyk G, Rohde LA. Epidemiology of attention-deficit/hyperactivity disorder across the lifespan. *Curr Opin Psychiatry*. 2007;20:386-392.
2. Bayerl M, Dielentheis TF, Vucurevic G, et al. Disturbed brain activation during a working memory task in drug-naïve adult patients with ADHD. *Neuroreport*. 2010;21:442-446.
3. Fassbender C, Schweitzer JB, Cortes CR, et al. Working memory in attention deficit/hyperactivity disorder is characterized by a lack of specialization of brain function. *PLoS One*. 2011;6(11):e27240.

FC6_3. Intact Top-Down Modulation of the N400 ERP by Expectancy in Schizophrenia

D.F. Salisbury¹, T.K. Murphy¹, C.D. Butera¹

¹Clinical Neurophysiology Research Laboratory, Western Psychiatric Institute & Clinic, Department of Psychiatry, University of Pittsburgh School of Medicine, Pittsburgh, PA, USA

The N400 ERP is sensitive to semantic priming, and is typically smaller to related words than to unrelated words. Semantic priming and N400 are impaired in schizophrenia. Expectancy priming, where top-down expectations modulate automatic semantic priming, has been less studied in schizophrenia. This experiment examined whether schizophrenic subjects could develop expectancy for an unrelated exemplar after a specific category cue. Twenty-nine psychiatrically well and 25 schizophrenic participants matched for gender, age, PSES (parental

socioeconomic status), and WAIS Information and Vocabulary subscales performed a word pair lexical decision task based on Neely's classic experiment. Subjects first saw a category name followed by a category or noncategory exemplar, or a nonword. Subjects were cued to expect a noncategory exemplar for one specific category. N400 was measured to trained and untrained category exemplars. Significant reversal of the N400 effect was observed for healthy controls, and reaction time (RT) was significantly reduced to noncategory exemplars with expectancy. Although patients showed no automatic semantic N400 effect, the N400 effect showed a trend toward reversal and RT was significantly reduced with training. Both healthy controls and patients with schizophrenia can use top-down expectancy to modulate the automatic spread of activation. These findings run counter to the theorized inability of patients with schizophrenia to utilize top-down control mechanisms, and, when coupled with clear deficits in semantic priming, suggest the cognitive deficits must arise, at least in part, from early perceptual and network problems rather than only from executive deficits.

FC6_4. Deficient Default Mode Network Suppression During Working Memory Performance in Individuals at Clinical High Risk for Psychosis and in Early Schizophrenia

D.H. MATHALON¹, S.L. FRYER¹, K.A. KIEHL², V.C. CALHOUN², G.D. PEARLSON^{3,4}, B.J. ROACH^{1,2}, J.M. FORD^{1,2}, T.H. MCGLASHAN⁴, S.W. WOODS⁴

¹University of California, San Francisco and San Francisco VA Medical Center, San Francisco, CA, USA

²University of New Mexico and Mind Research Network, Albuquerque, NM, USA

³Olin Neuropsychiatry Research Center, Institute of Living, Hartford, CT, USA

⁴Department of Psychiatry, Yale University, New Haven, CT, USA

Background. The default mode network (DMN) is a set of brain regions typically activated at rest and suppressed during cognitive task performance. Schizophrenia is associated with a failure of normative DMN activity suppression, though the extent to which DMN alterations predate psychosis onset is unclear. This study examined task-related DMN suppression in youth at clinical high-risk (CHR) for psychosis, relative to healthy controls (HC) and early schizophrenia patients (ESZ). **Methods.** During performance of a multiloop Sternberg working memory task, fMRI data were collected from CHR ($n = 32$), ESZ ($n = 24$), and HC ($n = 54$) youth, aged 12 to 30 years. Group \times load interactions during working memory probes were identified within DMN regions-of-interest, to evaluate the hypothesis that ESZ would fail to suppress DMN activation at higher working memory loads relative to HC, and that CHR would show an intermediate pattern of DMN suppression. **Results.** Significant working memory retrieval group \times load interactions were observed within medial prefrontal, posterior cingulate, and right lateral parietal cortices. Follow-up testing, corrected

for multiple comparisons ($P < .05$), indicated that within posterior cingulate and right lateral parietal DMN network nodes, load \times group effects resulted from less suppression of higher load DMN activity in ESZ than HC, with CHR differing from neither group. In medial prefrontal cortex, both CHR and ESZ groups showed less higher load DMN suppression, relative to HC. **Conclusion.** While HC modulated DMN suppression by cognitive load, CHR individuals showed a reduction in higher load DMN suppression that was similar, but less pronounced, than ESZ patients. These data suggest that DMN dysfunction in schizophrenia predates psychosis onset.

FC6_5. Neural Circuits Involved in Reward Anticipation in Deficit and Nondeficit Schizophrenia

U. VOLPE¹, E. MERLOTTI¹, A. VIGNAPIANO¹, V. MONTEFUSCO¹, G.M. PLESCIA¹, O. GALLO¹, P. ROMANO¹, A. MUCCI¹, and S. GALDERISI¹

¹Department of Psychiatry, University of Naples SUN, Naples, Italy

In the past decade, several experimental studies investigating neurobiological underpinnings of anhedonia/avolition focused on the role of the ventral and dorsal striatal regions of the basal ganglia thought to mediate important aspects of the reward processing.^{1,2} No study to date has investigated the relationships between dysfunctions of these regions and primary and persistent negative symptoms.

The present study aimed to investigate reward anticipation in patients with deficit schizophrenia (DS), characterized by the presence of primary and persistent negative symptoms, as compared with those with nondeficit schizophrenia (NDS), and healthy controls (HC).

A functional magnetic resonance (fMRI) was recorded during a Monetary Incentive Delay (MID) task.³

We found that for cues anticipating reward, with respect to those anticipating neutral outcome, DS patients had significantly lower activation than HC in the left caudate nucleus, while NDS patients did not show any significant difference. For cues anticipating loss avoidance, with respect to those anticipating neutral outcome, DS patients showed a reduced activation in the right caudate, fusiform gyrus and parahippocampal gyrus, while no difference was observed between NDS patients and HC.

According to our findings, only DS patients demonstrate a reduced activation of the caudate during the anticipation of "salient" stimuli. Increasing evidence has been provided that the caudate mediates learning of action-values contingencies, subserving goal-directed behavior. Our findings are in line with the hypothesis that primary negative symptoms are related to difficulties using internal representations of values to motivate behavior for a dysfunction concerning the associations of action-outcome.

Acknowledgments

Funded by Compagnia San Paolo di Torino–Neuroscience Call.

References

1. Wacker J, Dillon DG, Pizzagalli DA. The role of the nucleus accumbens and rostral anterior cingulate cortex in anhedonia: integration of resting EEG, fMRI, and volumetric techniques. *Neuroimage*. 2009;46:327-337.
2. Harvey PO, Armony J, Malla A, Lepage M. Functional neural substrates of self-reported physical anhedonia in non-clinical individuals and in patients with schizophrenia. *J Psychiatr Res*. 2010;44:707-716.
3. Schlagenhauf F, Sterzer P, Schmack K. Reward feedback alterations in unmedicated schizophrenia patients: relevance for delusions. *Biol Psychiatry*. 2009;65:1032-1039.

FC6_6. Frequency Domains of Resting State Default Mode Network Activity in Schizophrenia

G. Mingoia^{1,2}, K. Langbein¹, M. Dietzek¹, G. Wagner¹, St. Smesny¹, S. Scherpiet¹, R. Maitra¹, Ch. Gaser^{1,3}, H. Sauer¹, and I. Nenadic¹

¹Department of Psychiatry and Psychotherapy, Jena University Hospital, Jena, Germany

²Brain Imaging Facility, IZKF, RWTH University Hospital, Aachen, Germany

³Structural Brain Mapping Group, Department of Psychiatry and Psychotherapy, Jena, Germany

Introduction. Recent studies have demonstrated altered low-frequency BOLD signal fluctuations during resting state (RS) in schizophrenia. It is unclear whether this alteration relates to DMN dysfunction. Here, we analyzed the power for different frequency bands from DMN time series extracted using a probabilistic independent component analysis (pICA) of fMRI data in order to test the hypothesis of altered frequency power in the DMN under RS conditions. **Methods.** We obtained RS fMRI series (3 T, $3 \times 3 \times 3$ mm resolution, 45 slices, TR 2.55 seconds, 210 volumes) in 25 schizophrenia patients (mean age 30 ± 7.3 years), on stable antipsychotic medication and 25 matched healthy controls (30.3 ± 8.6 years). Subjects were asked to lie in the scanner keeping eyes closed with no further specific instructions. Data were preprocessed using SPM5 (motion correction, co-registration, normalization, and smoothing). Band pass (0.009-0.18 Hz) frequency filters were applied. We applied FSL MELODIC (pICA) yielding 30 IC, and an automated routine to select for each subject the component matching the anatomical DMN definition. We then analyzed the frequency domains for this extracted DMN, estimating the power of a signal at different frequencies. The time course associated with each individual's DMN component was transformed from the time domain to the frequency domain using Welch's method. For this purpose we used pwelch, a Matlab signal processing toolbox. **Results.** We found a significant diagnosis \times frequency interaction, $F(11, 38) = 2.484$, $P = .019$. Comparison of the frequency bins between groups showed that the schizophrenia group exhibited significantly higher spectral power than controls at frequencies around 0.0784 Hz ($F = 5.938$, $P = .019$)

and 0.1725 Hz ($F = 5.463$, $P = .024$). **Conclusions.** Our results demonstrate that at least a part of the low-frequency alterations found in schizophrenia can be specifically attributed to DMN dysfunction, unrelated to cardiac or breathing artefacts, and task-driven cognitive activity. While the power differences in our results appeared to be rather specific to particular frequency bands, the role of these remains unclear and will need further investigations.

References

1. Fransson P, Metsäranta M, Blennow M, Åden U, Lagercrantz H, Vanhatalo S. Early development of spatial patterns of power-law frequency scaling in fMRI resting-state and EEG data in the newborn brain. *Cereb Cortex*. 2013;23:638-646.
2. Mingoia G, Wagner G, Langbein K, et al. Default mode network activity in schizophrenia studied at resting state using probabilistic ICA. *Schizophr Res*. 2012;138:143-149.
3. Raichle ME, Snyder AZ. A default mode of brain function: a brief history of an evolving idea. *Neuroimage*. 2007;37:1083-1090.
4. Welch PD. The use of fast Fourier transform for the estimation of power spectra: a method based on time averaging over short, modified periodograms. *IEEE Trans Audio Electroacoust*. 1967;AU-15:70-73.

Poster Presentations

P001. Electrical Neuroimaging of Emotional Decisions With IEEG and EEG

S. Gonzalez Andino¹ and R. Grave de Peralta Menendez^{1,2}

¹Electrical Neuroimaging Group, Geneva, Switzerland

²ENG-teCH, Geneva, Switzerland

Intracranial EEG (iEEG) is one of the most invasive approaches we can use to study the living human brain at high temporal resolution. In addition, invasive recordings are limited to epileptic patients and to structures potentially implicated in the disease. How does the disease or the diseased tissue affect the EEG signal and its relationship to high level cognitive processing is not yet clear. Fortunately, novel electrophysiological methods¹ allow the noninvasive estimation of intracranial potentials based on scalp EEG measurements. Here we explore to which extent noninvasive eLFP estimates correlate with iEEG during high level cognitive tasks.

Based on noninvasive eLFP (estimated local field potential) estimated with ELECTRA in 24 healthy controls playing the Trust Game we conclude that the rhinal cortex—more than the amygdala and orbitofrontal cortex (OFC)—is important for coding disappointment, retaining outcome related information across delays and updating behavior accordingly. We confirmed these results by iEEG recordings on 3 patients performing the same experiment.

These results show that non-invasive methods convey information about subcortical structures achieving spatial resolution in depth at the level of anatomical structures. Consequently,

eLFPs hold the promise to represent a noninvasive alternative to investigate high level cognition in humans at a high temporal resolution and full 3D coverage of cerebral structures unattainable with invasive recordings.

Note

1. LAURA, ELECTRA, EPIFOCUS methods were developed by S. Gonzalez and R. Grave de Peralta at the Electrical Neuroimaging Group. We thank enthusiast users (Michel, Blanke, Murray, Lantz, and others) who help disseminate results but, nevertheless, should not be blamed for the practical or theoretical (in)capabilities of these methods.

P002. Source Models for Electrical Neuroimaging: A Critical View of the (Quasi) Static Approximation

R. Grave de Peralta Menendez^{1,2}, M. Sanchez Vives³, B. Rebollo³, and S. Gonzalez Andino^{1,2}

¹Electrical Neuroimaging Group, Geneva, Switzerland

²ENG-teCH, Geneva, Switzerland

³Institut d'Investigacions Biomèdiques August Pi i Sunyer, Barcelona, Spain

The source model is an essential component of any inverse solution method/strategy.¹ Examples used so far vary from the simple equivalent dipole to multiple dipole models and distributed source models obtained by the discretization of the current density vector.

In this work we show that those source models are indeed based on the pure static approximation of Maxwell equations instead of the quasi-static approximation.

After presenting the theoretical and experimental evidences against the static approximation, we enumerate the advantages of a true quasi-static approximation and the full electrodynamics formulation as the only methods able to explain the dispersive behavior of local field potential (LFP) measured on brain slices. Theoretical evidences will be illustrated by some theoretical contradictions resulting from the assumption of static or quasi-static fields together with some source models (eg, cortical models or the basic equation general current density vector model). On the other side, experimental evidences will become evident from the delays observed in electro/chemically induced potentials that cannot be explained with static models. Finally, after highlighting the consequences of signal delays for connectivity methods based on the assumption of instantaneous volume conduction, we identify the only source model compatible with all approximations and present on all the problem statements from the static to the full electrodynamics modeling, that is, the irrotational source model of ELECTRA.

Note

1. Methods described here were developed by the Electrical Neuroimaging Group. We thank enthusiast users (Michel, Blanke, Murray, Lantz, and others) who help disseminate results but, nevertheless, should not be blamed for the practical or theoretical (in)capabilities of these methods.

P003. Classification of Independent Components of EEG Into Multiple Artifact Classes

L. Frølich¹, T.S. Andersen¹, and M. Mørup¹

¹Section for Cognitive Systems, DTU Compute, Technical University of Denmark, Lyngby, Denmark

The use of independent components (ICs) of EEG, extracted through IC, to clean EEG data is a standard preprocessing step. By removing contributions to data from artifactual ICs, a cleaner signal can be obtained. Presently, ICs of EEG data are classified manually, a lengthy and subjective task. While work on fully automatic supervised classification methods has increased over the past years, previous work has focused on distinguishing between neural and artifactual ICs.¹⁻³ By distinguishing between multiple types of artifacts such as eye movements and the pulse, more diverse uses of an automatic classification method can be imagined. Such uses include identifying changes in eye movements, for example, for drowsiness detection or removal of only specific types of artifacts.

Our aim is to classify ICs as belonging to 1 of the 6 classes of neural activity, 1 of 4 artifacts (horizontal eye movements, blinks, muscle, and pulse), or mixed. Mixed ICs represent mixed activity from artifacts, neural sources, and random noise.

Two data sets containing manually labeled ICs from 35 and 12 subjects were made available by Julie Onton and Klaus Gramann.^{4,5} The data sets differed in sample rates, electrode caps, recording lengths, and reference electrode. No subjects participated in both studies.

By choosing the features chosen more than 30 times by multinomial regression (MNR) with forward selection in leave-one-subject-out cross-validation over the data set with 35 subjects, 15 features were chosen from an initial pool of 65 features from the spatial, spectral, and temporal domains. All features were carefully constructed to be invariant to differences in experimental setup such as sample rate, electrode cap and analogue filter. MNR classifiers were trained and evaluated on each study and across studies using the established feature set. ICs were weighted by their inverse class proportions in all training.

The classifier performs on par with others' results when reducing classifications to neural versus artifactual ICs. In the multiclass case, our classifier is able to discriminate between the 6 different classes. In the between-subject, within-study case, we obtained 86.8% correct classifications averaged over classes and the 2 data sets. In the between-subject, between-study case, we obtained 81.7% correct classifications on average.

References

1. Winkler I, Haufe S, Tangermann M. Automatic classification of artifactual ICA-components for artifact removal in EEG signals. *Behav Brain Funct.* 2011;7:30.
2. Mogron A, Jovicich J, Bruzzone L, Buiatti M. ADJUST: An automatic EEG artifact detector based on the joint use of spatial and temporal features. *Psychophysiology.* 2011;48:229-240.

3. Nolan H, Whelan R, Reilly RB. FASTER: Fully Automated Statistical Thresholding for EEG artifact Rejection. *J Neurosci Methods*. 2010;192:152-162.
4. Onton J, Makeig S. High-frequency broadband modulations of electroencephalographic spectra. *Front Hum Neurosci*. 2009;3:61.
5. Gramann K, Töllner T, Müller HJ. Dimension-based attention modulates early visual processing. *Psychophysiology*. 2010;47:968-978.

P004. Changes in Scalp Potentials due to Fontanels in an Infant's Head Model

P. Belfiore¹, P. Gargiulo^{2,3}, C. Ramon^{3,4}, and S. Vanhatalo⁵

¹Department of Biomedical, Electronic and telecommunication Engineering, University Federico II of Naples, Naples, Italy

²Department of Science, Landspítali University Hospital, Reykjavik, Iceland

³Department of Bioengineering, Reykjavik University, Reykjavik, Iceland

⁴Department of Electrical Engineering, University of Washington, Seattle, WA, USA

⁵Department of Children's Clinical Neurophysiology, Helsinki University Central Hospital, Helsinki, Finland

Our objective was to study the effects of fontanel on neonatal scalp EEGs. We used a 3-D finite element method (FEM) model generated from 110 segmented axial MR slices of an infant. The hexahedral voxel resolution was $0.938 \times 0.938 \times 1$ mm. Majority of the tissues were identified that included: scalp, fat, muscle, dura layer, cerebrospinal fluid (CSF), cerebellum, gray and white matter, and hard and soft skull bone. The electrical activity of the whole cortex was represented by 2048 dipoles. The dipole intensity distribution was in the range of 0.0 to 0.4 mA meter with a uniform random distribution to represent the spontaneous brain activity. Each dipole vector was oriented normal to the local boundary between gray and white matter and they were pointing outward from white to the gray matter. Simulations were performed for 2 models. In one model, the conductivity of fontanel was equal to the conductivity of CSF (fontanel present) while in the other model it was equal to the hard skull bone (fontanel absent). The electrical conductivities of various tissues were obtained from the literature. Using an adaptive FEM solver, the potential and flux distributions in the whole head model were computed and scalp potentials (EEG) were extracted. Spatial contour plots of potentials on the scalp surface were made. Relative difference measure (RDM) and magnification factor (MAG) were computed between the 2 models. If the scalp potentials from two models are the same, the RDM and MAG will be zero and unity, respectively. Ten trial runs were performed with different uniform random distribution of dipolar intensities. Averaged over 10 trials, the RDM was 0.062 ± 0.016 and the MAG was 1.1 ± 0.31 . These values suggest that the 2 models yield very similar results. Closer inspection of spatial potential topographies, however, indicated up to 15% higher values above the fontanel area in the model with fontanels. This suggests a notable but local effect of fontanels on the EEG potentials in newborns.

P005. Influence of the Head Model on EEG and MEG Source Connectivity Analysis

J.-H. Cho¹, J. Vorwerk², C.H. Wolters², T.R. Knösche¹

¹Max Planck Institute for Human Cognitive and Brain Sciences, Leipzig, Germany

²Institute for Biomagnetism and Biosignalanalysis, University of Münster, Münster, Germany

Brain connectivity analysis using reconstructed source time courses derived from EEG and MEG data has been used to understand brain networks. Although previous studies have demonstrated the effects of different source localization methods and connectivity measures on connectivity analysis, additional investigation is still needed. Above all, the influence of the head model on source connectivity analysis has not been studied sufficiently, even though it has been well known that head modeling errors have a large influence on source analysis.^{1,2} The computer simulation study presented here used the finite element method (FEM) to construct realistic head models and investigated the influence of particular properties of that head model on the forward and inverse solutions as well as on source connectivity analysis in EEG and MEG. A detailed and anatomically realistic head model constructed from individual MR images was used as a reference model. Test head models were derived from the reference model to consider the effects of particular simplifications: the distinction between gray and white matter, the distinction between skull spongiosa and compacta, the inclusion of a cerebrospinal fluid (CSF) compartment, and the reduction to a simple 3-layer model comprising only skin, skull, and brain. The source time courses were reconstructed using a beamformer-based method³ and its source connectivity was estimated by partial directed coherence,⁴ which estimates effective connectivity. Our simulation study showed that the distortions of the volume current caused by the head modeling errors had an effect on the results of, both, the source localization and connectivity analysis. The errors in the reconstructed source time courses were reflected in the results of the source connectivity analysis. For EEG, the results were highly affected by different conductivities of the head compartments. In case of MEG, the skull modeling had no significant effect on the results, as it has already been known. However, the different conductivity of the gray and white matter and the CSF had an effect also on the MEG results. Large errors were found especially in the areas, where the source direction is radial to the head surface. In these areas, nonnegligible errors were also found in the results of the 3-layer model. Consequently, for the precise source connectivity analysis accurate head models have to be used in both EEG and MEG studies, and FEM-based forward approach can be a useful tool for this purpose.

References

1. Wolters CH, Anwander A, Tricoche X, Weinstein D, Koch MA, MacLeod RS. Influence of tissue conductivity anisotropy on EEG/MEG field and return current computation in a realistic head model: a simulation and visualization study using high-resolution finite element modeling. *Neuroimage*. 2006;30:813-826.

2. Dannhauer M, Lanfer B, Wolters CH, Knösche TR. Modeling of the human skull in EEG source analysis. *Hum Brain Mapp.* 2011;32:1383-1399.
3. Hui HB, Pantazis D, Bressler SL, Leahy RM. Identifying true cortical interactions in MEG using the nulling beamformer. *Neuroimage.* 2010;49:3161-3174.
4. Baccalá LA, Sameshima K. Partial directed coherence: a new concept in neural structure determination. *Biol Cybern.* 2001;84:463-474.

P006. Removal of Stimulus-Induced Artifacts in Functional Spinal Cord Imaging

T. Watanabe¹, Y. Kawabata¹, D. Ukegawa², S. Kawabata², Y. Adachi³, K. Sekihara¹

¹Department of Systems Design and Engineering, Tokyo Metropolitan University, Tokyo, Japan

²Department of Orthopedic Surgery, Tokyo Medical and Dental University, Tokyo, Japan

³Applied Electronics Laboratory, Kanazawa Institute of Technology, Kanazawa, Japan

A nerve conduction block of the cervical spinal cord compressed by intervertebral disks and ligaments may cause numbness and paralysis in the limbs, and such spinal cord disorders are very common.¹ Nonetheless, there are no effective methods for accurate diagnosis of such spinal cord lesions. This is primarily because compression and other spinal cord abnormalities found in patient's anatomical images (such as MRI or X-ray images) do not always cause spinal cord disorders. There has been growing interests in developing biomagnetometers optimized for measuring the spinal cord-evoked magnetic field (SCEF).^{2,3} Dynamic (spatiotemporal) source imaging of the spinal cord electrophysiological activity from its evoked magnetic field has also been investigated, aiming at developing a novel, diagnostic imaging tool for cervical spinal cord disorders.⁴

One serious problem in implementing such functional spinal cord imaging arises from large stimulus-induced artifacts, which exist immediately after the stimulus application and decrease to almost zero around 8 to 10 ms after the stimulus onset. Although exact causes of these artifacts are unexplored, we speculate that they are caused by combined effects of body electric currents induced by the stimulus and transient responses of receiver electronics. These artifacts overlap the SCEF signal, and distort imaging results of spinal cord activity, as shown in our experiments.

This paper proposes a novel method to reduce the influence of these artifacts in functional spinal cord imaging. The method consists of 2 steps; the first step acquires the artifact-alone data, the data containing only the artifacts. To obtain such data, we use exactly the same stimulus application procedure to measure SCEF with a stimulus electrode positioned a few centimeters away from the median nerve. The second step applies a method called common-mode subspace projection (CSP),⁵ which first estimates orthonormal basis of the interference subspace, and projects the measured SCEF data onto the subspace orthogonal

to the interference subspace. We validate the method effectiveness using SCEF data measured from a healthy volunteer.

References

1. Shinomiya K, Furuya K, Sato R, Okamoto A, Kurosa Y, Fuchioka M. Electrophysiologic diagnosis of cervical OPLL myelopathy using evoked spinal cord potentials. *Spine.* 1988;13:1225-1233.
2. Kawabata S, Komori H, Mochida K, Harunobu O, Shinomiya K. Visualization of conductive spinal cord activity using a biomagnetometer. *Spine.* 2002;27:475-479.
3. Adachi Y, Kawai J, Miyamoto M. et al. A SQUID system for measurement of spinal cord evoked field of supine subjects. *IEEE Trans Appl Supercond.* 2009;19:861-866.
4. Sato T, Adachi Y, Tomori M, Ishii S, Kawabata S, Sekihara K. Functional imaging of spinal cord electrical activity from its evoked magnetic field. *IEEE Trans Biomed Eng.* 2009;56:2452-2460.
5. Taulu S, Simola J. Spatiotemporal signal space separation method for rejecting nearby interference in MEG measurements. *Phys Med Biol.* 2006;51:1759-1768.

P007. Removal of Large Interferences in MEG Source Imaging

K. Sekihara¹ and S.S. Nagarajan²

¹Department of Systems Design and Engineering, Tokyo Metropolitan University, Tokyo, Japan

²Biomagnetic Imaging Laboratory, Department of Radiology, University of California, San Francisco, CA, USA

This paper proposes a simple but efficient method to remove interference magnetic fields in MEG source imaging. The principle of the method is similar to that of the spatiotemporal signal space separation method, often referred to as tSSS.¹ The key difference is that the proposed method does not require the vector spherical harmonic expansions. Instead, the proposed method makes use of the span of the source-space lead field. The method first estimates the orthonormal spatial basis vectors by applying the singular-value decomposition to the source-space lead field matrix, or equivalently, by applying the eigenvalue decomposition to the corresponding gram matrix. The eigenvectors corresponding to distinctively large eigenvalues are chosen, and the spatiotemporal MEG data containing large interferences is projected onto the inside and outside the span of these eigenvectors. Let us define the resultant (projected) data as B_{in} and B_{out} , and the subspaces spanned by the temporal singular vectors of B_{in} and B_{out} as S_{in} and S_{out} . The proposed method looks for the intersection of S_{in} and S_{out} . The orthonormal basis set of the intersection is obtained as the principal vectors between S_{in} and S_{out} whose principal angles are equal to zero.² Since this intersection represents the interference subspace, the method finally projects the original spatiotemporal MEG data onto the orthogonal subspace of the intersection. We show the method effectiveness by applying the proposed method to MEG data taken from a patient with a vagus nerve stimulator and to speech-affected auditory MEG data. Compared with

the original tSSS, the implementation of the proposed method is much easier, because it does not require “expensive” vector spherical harmonic expansions. The method, therefore, may be called “the poor man’s tSSS.”

References

1. Taulu S, Simola J. Spatiotemporal signal space separation method for rejecting nearby interference in MEG measurements. *Phys Med Biol*. 2006;51:1759-1768.
2. Golub GH, Van Loan CF. *Matrix Computations*. Baltimore, MD: Johns Hopkins University Press; 1996.

P008. Volume Conduction and Optimized Stimulation Protocols in Transcranial Current Stimulation

S. Wagner¹, Ü Aydin¹, J. Vorwerk¹, C. Herrmann², M. Burger³, C. Wolters¹

¹Institute for Biomagnetism and Biosignalanalysis, University of Münster, Münster, Germany

²Experimental Psychology Lab, University of Oldenburg, Oldenburg, Germany

³Institute for Computational and Applied Mathematics, University of Münster, Münster, Germany

Recently, sensor optimization approaches have received interest in the transcranial current stimulation (tCS) community. In several computer simulation studies, standard tCS approaches (2 big electrodes attached to the scalp) have been shown to induce a widespread current density activation pattern with often strongest current densities in nontarget brain regions.¹ Consequently, the aim of sensor optimization approaches is to optimize the focality, orientation, and intensity of current density at the target location, while minimizing current density in the remaining brain.²

Therefore, an optimized stimulation protocol for 2 or even more fixed electrodes is calculated using an inverse approach. For stimulation, we fix 74 electrode locations (the locations of a 10/10 EEG system) on the head surface. We model the volume conductor using a 6-compartment (skin, skull compacta, skull spongiosa, cerebrospinal fluid, gray and white matter) head model with white matter anisotropy in a geometry-adapted hexahedral finite element approach. Using this realistic head model, we present tCS volume conduction effects in a variety of simplified head models that differ in terms of distinguished tissue types and their conductivities. In order to achieve effective and well-targeted stimulation while ensuring patient safety, our sensor optimization approach, which is new to the tCS community, calculates an optimized applied current pattern at the fixed electrodes by minimizing an L_1 norm subject to appropriate constraints (eg, constraints with regard to patient safety). Direct validation of our approach is given by tCS forward calculation using the optimized stimulation protocol and visual inspection as well as quantification of the results, that is, the brain current density vector field. We evaluate our new optimization approach with regard to target focality, orientation,

and intensity and compare it with standard 2 big electrode tCS stimulation protocols.

Acknowledgments

This research has been supported by the German Research Foundation (DFG) through projects WO1425/2-1, 3-1.

References

1. Neuling T, Wagner S, Wolters CH, Zaehle T, Herrmann CS. Finite-element model predicts current density distribution for clinical applications of tDCS and tACS. *Front Psychiatry*. 2012;3:83.
2. Dmochowski JP, Datta A, Bikson M, Su Y, Parra LC. Optimized multi-electrode stimulation increases focality and intensity at target. *J Neural Eng*. 2011;8:046011.

P009. Hierarchical Fully Bayesian Inference for Combined EEG/MEG Source Analysis of Evoked Responses: From Simulations to Real Data

F. Lucka^{1,2,3}, Ü Aydin^{2,3}, J. Vorwerk^{2,3}, M. Burger^{1,3}, and CH Wolters^{2,3}

¹Institute for Applied Mathematics, University of Münster, Münster, Germany

²Institute for Biomagnetism and Biosignalanalysis, University of Münster, Münster, Germany

³Cells in Motion Interfaculty Center, University of Münster, Münster, Germany

Measuring the induced electromagnetic fields at the head surface to estimate the underlying, activity-related ion currents in the brain is a challenging, severely ill-posed inverse problem. Especially the recovery of brain networks involving deep-lying sources by means of EEG/MEG recordings is still a challenging task for most current density reconstruction (CDR) inverse approaches. Recently, hierarchical Bayesian modeling (HBM) emerged as a unifying framework for CDR approaches comprising most established methods as well as offering promising new methods. Our work examines the performance of fully Bayesian inference methods for HBM for source configurations consisting of few, focal sources when used with realistic, high-resolution finite element (FE) head models. In addition, using EEG and MEG alone is compared with a combined data analysis. In previous work,¹ we compared different aspects of fully Bayesian inference for HBM for EEG and MEG to established CDR methods like minimum norm estimation or sLORETA by extensive simulation studies. Encouraged by the good results of the HBM-based methods for simulated data, we proceeded to process experimental data, in particular simultaneous EEG/MEG recordings of the auditory late latency response N100(m) and somatosensory response N20(m). We used somatosensory N20(m) to test our algorithm for a single, superficial and mainly tangential source, while auditory N100(m) was used to test our algorithm for more difficult source scenarios (bilateral sources near planum temporale).² In addition, we examined several aspects of applying fully Bayesian inference for HBM

to real data like robustness against background activity and misspecification of the noise covariance matrix.

Acknowledgments

This research has been supported by the German Research Foundation (DFG) through project WO1425/2-1.

References

1. Lucka F, Pursiainen S, Burger M, Wolters CH. Hierarchical Bayesian inference for the EEG inverse problem using realistic FE head models: depth localization and source separation for focal primary currents. *Neuroimage*. 2012;61:1364-1382.
2. Pantev C, Lütkenhöner B. Magnetoencephalographic studies of functional organization and plasticity of the human auditory cortex. *J Clin Neurophysiol*. 2000;17:130-142.

P010. A Biomagnetic Head Phantom for the Investigation of Deep Auditory Brain Stem Sources

M. Bauer¹, L. Trahms¹, and T. Sander¹

¹Physikalisch-Technische Bundesanstalt, PTB, Berlin, Germany;

Hearing is one of the most vital senses and has to be protected against hazardous influences. Exposure to excessive noise can be a major threat leading to permanent hearing damage and there is a wide range of protection measures against noise exposure in the hearing range (20 Hz to 20 kHz). In contrast to hearable sounds in the audible frequency range the possible mechanisms of perceiving sounds in the infra- and ultrasonic range are not well understood. The aim of the project EARS is to investigate the interrelation between the perception of infra- and ultrasonic sound (sounds of a frequency below 20 Hz and above 20 kHz) and possibly associated brain responses measured by magnetoencephalography (MEG). As discussed by Oohashi et al,¹ there are centers deep in the brain stem along the auditory pathway, which might process these frequencies. Evoked responses from these centres have not yet been reported.

In order to explore the potential of electrophysiological methods to identify such sources, we investigated the depth sensitivity of our MEG measurement system, that is, a helmet-shaped 128-channel Yokogawa gradiometer system. In order to find thresholds of dipole strength and deepness for reliable source identification, we used 2 different approaches: First we simulated numerically the magnetic field generated by various electrical current dipoles with different alignments toward the sensor system in a homogeneous, single shell volume conductor model. The second approach is the experimental realization by the construction of a MEG head phantom filled with saline solution. The phantom mimics 4 prominent sources of the auditory pathway of the human brain—one is the auditory cortex itself and further 3 deep centres in brain stem corresponding to the auditory pathway as described by Krumbholz et al² and Herdman et al.³ The sources were simulated by 2 open platinum electrodes embedded in the volume conducting saline solution.

Simulation and measurement showed the same trend and the deepest sources could be estimated with an acceptable accuracy, so we are able to detect deep brain stem sources of the auditory pathway with a magnetic moment down to 25 nA m. According to the literature the cortical dipole moment ranges from 5 to 30 nA m.⁴

Acknowledgments

Financial support from the European Metrology Research Programme (EMRP) and help in manufacturing the phantom by Dirk Gutkelch as well as stimulating discussion with Christian Koch and the members of the HLT01 consortium is gratefully acknowledged (programme Health, grant EARS). The EMRP is jointly funded by the EMRP participating countries within EURAMET and the European Union.

References

1. Oohashi T, Nishina E, Honda M, et al. Inaudible high-frequency sounds affect brain activity: hypersonic effect. *J Neurophysiol*. 2000;83:3548-3558.
2. Krumbholz K, Schönwiesner M, Rübsamen R, Zilles K, Fink GR, von Cramon DY. Hierarchical processing of sound location and motion in the human brainstem and planum temporale. *Eur J Neurosci*. 2005;21:230-238.
3. Herdman AT, Lins O, Van Roon P, Stapells DR, Scherg M, Picton TW. Intracerebral sources of human auditory steady-state responses. *Brain Topogr*. 2002;15:69-86.
4. Williamson S, Okada Y. *Biomagnetism*. New York, NY: Plenum Press; 1983:399-408.

P011. Zen Meditation Versus No-Task Resting in a Frequency Band-Wise sLORETA Analysis

P.L. Faber^{1,2}, D. Lehmann^{1,2}, L.R.R. Gianotti^{1,2}, R.D. Pascual-Marqui^{1,2}, P. Milz^{1,2}, and K. Kochi^{1,2}

¹The KEY Institute for Brain-Mind Research, Zurich, Switzerland

²Department of Psychiatry, Psychotherapy and Psychosomatics, University Hospital for Psychiatry, Zurich, Switzerland

Peculiarities of individual meditation exercises might be considered as different routes to a comparably deep meditation state.¹ We studied 15 experienced right-handed Zen meditators (9 males) during Zazen, a typical open monitoring meditation with no special focus of attention.

A 58-channel EEG recorded during Zazen (60 minutes) and no-task resting (4 minutes) was analyzed. After artifact-correction and -rejection, an average of 116 seconds (SD = 20.9) of EEG data were available per subject for the resting condition and 1632 seconds (SD = 692) for the Zazen condition. Standardized low resolution brain electromagnetic tomography (sLORETA)² is a properly standardized discrete, linear, minimum norm, inverse solution that yields images of standardized current density with exact localization, albeit with low resolution. We used sLORETA to analyze the EEG data in 8 frequency bands: delta (1.5-6 Hz), theta (6.5-8 Hz), alpha-1 (8.5-10 Hz), alpha-2 (10.5-12 Hz), beta-1 (12.5-18 Hz), beta-2 (18.5-21 Hz), beta-3 (21.5-30 Hz), and gamma (35-44 Hz).

sLORETA functional images were computed for each subject, condition, and band. The frequency band-wise normalized and log-transformed sLORETA images were band-wise compared between Zazen and resting using *t* statistics (significances corrected for multiple testing).

Zazen current density power increased compared with resting in the theta and the 2 alpha bands in a right-hemispheric prefrontal–frontal–temporal cluster, and decreased in the 2 alpha bands in a small left-parietal–occipital cluster, and in the beta-1 and beta-2 bands in a large bilateral posterior cluster.

Thus, during Zazen meditation compared with resting, a remarkably exclusive right-hemispheric anterior area was engaged in routine processing, while a large bilateral posterior area showed decreased processing activity. In sum, this suggests that brain engagement in information processing is reduced during this meditation.

References

1. Lehmann D, Faber PL, Tei S, Pascual-Marqui RD, Milz P, Kochi K. Reduced functional connectivity between cortical sources in five meditation traditions detected with lagged coherence using EEG tomography. *Neuroimage*. 2012;60:1574-1586.
2. Pascual-Marqui RD. Standardized low resolution brain electromagnetic tomography (sLORETA): technical details. *Methods Find Exp Clin Pharmacol*. 2002;24(suppl D):5-12.

P012. State Classification Accuracy Based on Heart Rate Variability for Drug-Induced Distinct Autonomic States

S. Kaneko¹, S. Yamashita¹, K. Yana^{1,2}

¹Graduate School of Engineering Hosei University 1, Tokyo, Japan

²Department of Applied Informatics, Hosei University 1, Tokyo, Japan

The successive binary decision scheme has been examined and shown to be effective for the autonomic nervous activity (ANA) states classification based on the heart rate variability (HRV). HRV has been commonly utilized as a mean to assess the ANA non-invasively. However, a large individual variation makes it difficult to accurately classify the autonomic states in general. This work focuses on individualized classification of ANA states based on heart rate variability. Two sets of 5-minute heart rate time series are recorded for 14 young healthy male subjects. Atropine and Propranolol were applied to subjects to create clearly defined physiologic states of ANA. The feature vector consists of incremental HF, LF/HF, signal variance, mean heart rate, and MF (0.04-0.1 Hz) is adopted for the classification. Six distinct physiologic states are created by atropine administration and propranolol in different postures. The individualized relative heart rate indices are utilized for the state classification by the neural network. Successive binary decision showed good accuracy of correct average classification rate of 0.829 with specificity 0.966.

References

1. Ahmad S, Tejuja A, Newman KD, Zarychanski R, Seely AJ. Clinical review: a review and analysis of heart rate variability and the diagnosis and prognosis of infection. *Crit Care*. 2009;13:232.
2. Vuksanović V, Gal V. Heart rate variability in mental stress aloud. *Med Eng Phys*. 2007;29:344-349.
3. Heart rate variability: standards of measurement, physiological interpretation and clinical use. Task Force of the European Society of Cardiology and the North American Society of Pacing and Electrophysiology. *Circulation*. 1996;93:1043-1065.

P013 Source Analysis of Somatosensory Evoked Potentials of the Stimulated Fingers and Toes: Evaluation of Different Cortical Source Localization Methods

K. Kalogianni¹, A.N. Vardy¹, A.C. Schouten^{1,2}, F.C.T. van der Helm¹

¹Delft University of Technology, Delft, Netherlands;

²University of Twente, Enschede, Netherlands

Electrical stimulation of distal joints results in specific brain patterns, the so-called somatosensory-evoked potentials (SEP), which can be recorded with electroencephalography (EEG). Source localization algorithms try to find the underlying source in the brain responsible for the recorded SEP profile at the EEG electrodes on the scalp. The current study investigates the spatial resolution of source localization algorithms experimentally; SEPs are induced by electrical stimulation of the fingers of the right hand and the hallux of the right foot at subjects' comfort level. High-density EEG is recorded and sources are reconstructed using different source localization techniques and their results compared. To locate the sources, the forward bioimpedance model is firstly addressed with the use of boundary element method (BEM). The electrodes locations are recorded and aligned to the realistic head model. The location of the sources is then calculated using one of the algorithms widely used in the SEP literature¹⁻³: Dipole-fit, Minimum Norm Estimate, and MUSIC. In addition to the above-mentioned techniques, eLORETA⁴ is also applied to reveal the sources of the SEP, which to our knowledge was never applied with SEP. eLORETA is a quasi-linear inverse solution that has exact, zero error localization and included in the present study as the distinct locations for each finger will be the optimum solution. The current study will bring new knowledge to the field by addressing the following issues: First, the localization accuracy of the different source localization algorithms is assessed experimentally. The capability of each algorithm to reveal the somatotopy of the hand fingers and hallux in the primary somatosensory cortex is examined. Second, the spatial resolution of EEG enhanced by the electrodes digitization is being evaluated by comparing our results with fMRI findings in the literature. Finally, a comparison between different electrodes montages is made in order to examine to which extent the source localization accuracy is enhanced with the use of higher number of electrodes.

References

1. Baumgartner C, Doppelbauer A, Sutherling WW, et al. Somatotopy of human hand somatosensory cortex as studied in scalp EEG. *Electroencephalogr Clin Neurophysiol.* 1993;88:271-279.
2. Buchner H, Fuchs M, Wischmann HA, et al. Source analysis of median nerve and finger stimulated somatosensory evoked potentials: multichannel simultaneous recording of electric and magnetic fields combined with 3D-MR tomography. *Brain Topogr.* 1994;6:299-310.
3. Schaefer M, Mühlhnickel W, Grüsser SM, Flor H. Reproducibility and stability of neuroelectric source imaging in primary somatosensory cortex. *Brain Topogr.* 2002;14:179-189.
4. Pascual-Marqui RD, et al. *Neuroimage.* 2006;31:86.

P014. Adaptive Sequential Monte Carlo for Multidipole Estimation From a Single Topography in MEG

A. Sorrentino¹, G. Luria¹, and R. Aramini¹

¹Dipartimento di Matematica, Università di Genova, Genova, Italy

In MEG data analysis, brain activity can be conveniently described by dipole models, whereby each active area is a vector point source. However, most available methods for dipole estimation rely on subjective choices and initialization procedures, owing to the nonidentifiability of the dipole parameters and the uncertainty on the number of sources. In this connection, a Bayesian approach is preferable as it provides a theoretically sound framework to combine prior information, explicitly coded into a probability distribution, with the information content of the data.

Recently, Bayesian methods for estimation of multiple dipoles from MEG data are being investigated.¹⁻⁴ However, those currently available exploit the temporal continuity of the neural dynamics and therefore only apply to time series. In this work,⁵ we focus on Bayesian estimation of dipole parameters from a single MEG topography. This may include, for instance, dipole modeling from data taken at a single time point, from a single ICA component, at a single frequency in the Fourier domain, and so on.

We set up a prior distribution that is Poisson for the number of sources, uniform for the source locations and exponential for the dipole moments. As the posterior distribution is complex, we use a class of methods (sequential Monte Carlo [SMC] samplers⁶) that build a synthetic sequence of distributions, going smoothly from the prior to the posterior in a finite number of steps. We also employ an adaptation technique: the sequence is not predefined, but at each step the subsequent distribution is determined at runtime, with a trade-off between quality of the approximation and speed of computation.

We tested the algorithm with 100 synthetic data sets, with a variable number of sources (ranging from 1 to 4), random source locations, and different signal-to-noise ratios. The results show that the method can effectively recover the true dipole configuration in a wide range of conditions; the posterior distribution provides credibility regions whose size nicely decreases for outer sources, and generally depends on the noise

level. Expectedly, for high noise levels 2 nearby sources may be misinterpreted as a single one; this is a consequence of the Poisson prior on the number of sources, which is tuned to favor low-dimensional models.

When applied to MEG data from a median nerve stimulation, the adaptive SMC was able to find the same strong sources that were obtained by other methods (particle filtering, dSPM, sLORETA); our SMC also localized additional weak sources that appear to be in accordance with the results of Miao et al.⁷

References

1. Antelis JM, Minguez J. DYNAMO: concurrent dynamic multi-model source localization method for EEG and/or MEG. *J Neurosci Methods.* 2013;212:28-42.
2. Mauguière F, Merlet I, Forss N, et al. Activation of a distributed somatosensory cortical network in the human brain. A dipole modelling study of magnetic fields evoked by median nerve stimulation. Part I: Location and activation timing of SEF sources. *Electroencephalogr Clin Neurophysiol.* 1997;104:281-289.
3. Sorrentino A, Johansen AM, Aston JAD, Nichols TE, Kendall WS. Dynamic filtering of static dipoles in magnetoencephalography. *Ann Appl Stat.* 2013;7:955-988.
4. Sorrentino A, Parkkonen L, Pascarella A, Campi C, Piana M. Dynamical MEG source modeling with multi-target Bayesian filtering. *Hum Brain Mapp.* 2009;30:1911-1921.
5. Sorrentino A, Luria G, Aramini R. Bayesian multi-dipole modeling of single MEG topographies by adaptive sequential Monte Carlo samplers. arXiv:1305.4511 [stat.AP].
6. Del Moral P, Doucet A, Jasra A. Sequential Monte Carlo samplers. *J R Stat Soc B.* 2006;68:411-436.
7. Miao L, Michael S, Kowali N, Chakrabarti C, Papandreou-Suppappola A. Multi-source neural activity estimation and sensor scheduling: algorithms and hardware implementation. *J Signal Process Syst.* 2013;70:145-162.

P015. Sensitivity of EEG and MEG to Orientation Selective Source Strength Variations

A. Hunold¹, M. Funke², R. Eichardt¹, J. Haueisen¹

¹Institute of Biomedical Engineering and Informatics, Ilmenau University of Technology, Ilmenau, Germany

²Department of Pediatrics, University of Texas Health Science Center at Houston, Houston, TX, USA

Clinical applications of simultaneous electroencephalography (EEG) and magnetoencephalography (MEG) recordings of interictal epileptic spikes revealed situations where both modalities showed different sensitivities to the epileptic-form activity. In previous studies, we showed that for focal and extended sources EEG and MEG provided varying sensitivities depending on the depth and the orientation of the spike source.

Here, we extend this work to effects of background source strength variations depending on the source orientation on the spike detectability in EEG and MEG simulations.

We build realistic 3-compartment boundary element method head models for 2 participants with 5120 triangles per layer.

The vertices in a triangular grid of the segmented boundary between white and gray matter provided the base points for single dipole sources. For each dipole, the angle between the source vector and the surface normal in the closest point of the inner skull mesh defined the source orientation. The Euclidean distance to the closest scalp vertex defined the source depth. In the baseline simulations, single dipoles generated interictal activity with a maximal strength of 600 nA m and approximately 30 000 randomly distributed dipoles contributed to normal brain activity as background noise with an individual strength of 10 nA m. In further simulations, we selectively increased the strength of radial and tangential background sources to 300% of baseline strength. As detectability measure we calculated a linear ratio between spike and background amplitudes as signal-to-noise ratio (SNR) in the EEG/MEG channel with the maximal spike amplitude.

In the baseline simulations, spikes from radially oriented single dipole sources generated the highest SNR in EEG and tangential sources dominated the SNR in MEG responses for superficial source locations. With 3 times stronger radial background activity, the SNR in EEG responses marginally decreased and the SNR profiles of MEG simulations remained almost stable. Opposing, the increase of tangential background activity strongly lowered the SNR in MEG responses and also affected the SNR in EEG simulations.

Our simulations show complementary sensitivity profiles of EEG and MEG to superficial sources depending on their orientation. Due to the MEG's orientation selectivity, only increased tangential background activity lowered the SNR in MEG simulations.

The complementary SNR profiles of EEG and MEG to superficial sources indicate the benefit of simultaneous recording of both modalities.

P016. Cardiac Output on Skin Level by Biomagnetic Blood Pressure Records Assessments

F. Gómez-Aguilar¹, S. Vázquez-Olvera², T. Cordova-Fraga³, J. Castro-López^{2,3}, M.A. Hernández-Gonzalez², S. Solorio-Meza², M. Sosa-Aquino³, J.J. Bernal-Alvarado³, and M. Vargas-Luna^{1,3}

¹Departamento de Ingeniería Eléctrica–DICIS, Universidad de Guanajuato campus Irapuato-Salamanca, Comunidad de Palo Blanco Salamanca, GTO, Mexico

²Unidad de Investigación y Epidemiología Clínica, UMAETI Bajío, León, GTO, Mexico

³Departamento de Ingeniería Física–DCI, Universidad de Guanajuato campus León, León, GTO, Mexico

An alternative method for the estimation of cardiac output measured at the skin level is presented. A recently patented medical device was used in this study, which was performed by measuring the cardiac output of 10 patients (40 measures in total).

This technique has the advantage of avoiding the direct damage to the vessels because it measures the variations of the magnetic field generated by a magnet fixed on the skin, just over the blood vessels. The above process is performed in order to convert the mechanical motions of the blood inside the vessels to an analogue signal and then, with a magnetometer at a fixed distance of 2.5 cm. The measure is recorded and converted to digital signal. The formula applied is $CO = SVE \times CF$, where CO is cardiac output, SVE is systolic volume ejection and CF is heart rate (SVE is under normal conditions, CF is the average value of signal). The cardiac output is obtained by measuring variations in the intensity of a magnetic field generated by the magnetic marker. Correlation parameters around $r = 0.9$ and $P < .05$ were found in this study using the new evaluation modality for the cardiac output versus thermodilution method.

P017. The FieldTrip–SimBio Pipeline for Finite Element EEG Forward Computations in MATLAB: Validation and Application

J. Vorwerk¹, L. Magyari², J. Ludewig¹, R. Oostenveld², and C.H. Wolters¹

¹Institute for Biomagnetism and Biosignalanalysis, University of Münster, Münster, Germany

²Donders Institute for Brain, Cognition and Behaviour, Radboud University Nijmegen, Nijmegen, Netherlands

We present a MATLAB pipeline that allows for an easy computation of EEG forward solutions using the finite element method (FEM) in combination with realistic multicompartment head models. Previous studies have shown that FE methods achieve a very good numerical accuracy.^{1,2} The major advantage is the possibility to handle nearly arbitrarily complex geometries, allowing the distinction of compartments of different conductivity in the head with a complex shape, for example, the cerebrospinal fluid (CSF),³ skull spongiosa,⁴ or holes in the skull.⁵ The high computational effort required for the FEM has been strongly reduced by the introduction of transfer matrices and fast algebraic multigrid solvers (AMG-CG).⁶ The remaining main arguments against the practical application of FEM were the effort for the setup of realistic head models, that is, models with more than just skin, skull, and brain as conductive compartments, and the necessity to use a variety of software and toolboxes rather than a single pipeline.

We have integrated the iso-parametric implementation of the Venant FE approach in the SimBio (<http://www.simbio.de/> or <https://www.mrt.uni-jena.de/simbio> or <http://fieldtrip.fcdonders.nl/development/simbio>) toolbox¹ into the FieldTrip (<http://www.ru.nl/donders/fieldtrip>) toolbox. Among others, this allows the use of the FEM with geometry-adapted hexahedral meshes in a fully MATLAB-based EEG source analysis. The implementation was realized using native MATLAB code and mex files, ensuring that no additional external binaries need to be compiled by the end-user.

Starting from a segmented MRI of the head tissues, we included the possibility to (a) easily generate a geometry-adapted hexahedral head model, (b) construct an individual source space fitted to the needs of the FEM, and (c) calculate a lead-field using the FEM. Thereby, our pipeline allows the user to combine the high accuracy and flexibility of FE methods with the convenient evaluation pipeline provided by FieldTrip. Using the complete set of functions in the FieldTrip toolbox, EEG preprocessing, FE leadfield computation, and subsequent inverse analysis can now be performed in a single MATLAB-based pipeline.

Acknowledgments

This research has been supported by the German Research Foundation (DFG) through projects WO1425/2-1, 3-1. The authors gratefully acknowledge the support of the BrainGain Smart Mix Programme of the Netherlands Ministry of Economic Affairs and the Netherlands Ministry of Education, Culture and Science.

References

1. Wolters CH, Anwander A, Berti G, Hartmann U. Geometry-adapted hexahedral meshes improve accuracy of finite-element-method-based EEG source analysis. *IEEE Trans Biomed Eng.* 2007;54:1446-1453.
2. Vorwerk J, Clerc M, Burger M, Wolters CH. Comparison of boundary element and finite element approaches to the EEG forward problem. *Biomed Tech (Berl)*. 2012;57:795-798.
3. Wolters CH, Anwander A, Tricoche X, Weinstein D, Koch MA, MacLeod RS. Influence of tissue conductivity anisotropy on EEG/MEG field and return current computation in a realistic head model: a simulation and visualization study using high-resolution finite element modeling. *Neuroimage*. 2006;30:813-826.
4. Dannhauer M, Lanfer B, Wolters CH, Knösche TR. Modeling of the human skull in EEG source analysis. *Hum Brain Mapp.* 2011;32:1383-1399.
5. Lanfer B, Scherg M, Dannhauer M, Knösche TR, Burger M, Wolters CH. Influences of skull segmentation inaccuracies on EEG source analysis. *Neuroimage*. 2012;62:418-431.
6. Wolters CH, Grasedyck L, Hackbusch W. Efficient computation of lead field bases and influence matrix for the FEM-based EEG and MEG inverse problem. Part I. Complexity considerations. *Inverse Problems*. 2004;20:1099-1116.

P018. A Mixed Finite Element Approach to Solve the EEG Forward Problem

J. Vorwerk¹, C. Engwer², J. Ludwig^{1,2}, and CH Wolters¹

¹Institute for Biomagnetism and Biosignalanalysis, University of Münster, Münster, Germany

²Institute for Applied Mathematics, University of Münster, Münster, Germany

The finite element (FE) method has been shown to achieve high accuracies in solving the EEG forward problem,^{1,2} while offering high flexibility with regard to the modeling of

different head compartments and anisotropic conductivities.³⁻⁶ It allows for the accurate distinction of arbitrarily complex geometries like the strongly folded cortex surface that is needed for the distinction between cerebrospinal fluid (CSF) and brain tissue, which was shown to have an important influence on the volume conduction due to the much higher conductivity of the CSF.^{3,6} Further applications are the modeling of skull holes—natural ones like the foramen magnum or those due to surgery⁵—or the 3-layeredness of the skull.⁴ Furthermore, FE methods enable the incorporation of anisotropic conductivities, for example, for modeling white matter anisotropy.³ A crucial point in the implementation of FE methods to solve the EEG forward problem is the treatment of the strong singularity at the source position due to the model of the current dipole. Different approaches to solve this problem have been developed, for example, the Venant approach, the partial integration approach, the subtraction approach (see recent comparison in Vorwerk et al²) or an approach based on Whitney elements.⁷ These approaches rely on a discretization of the unknowns using classical Lagrange elements (hat functions) to solve the Poisson equation that is known as the EEG forward problem. We present a novel approach to solve the EEG forward problem based on so-called mixed finite elements.⁸ Here, the Poisson equation is treated as 2 first-order equations and the unknowns are discretized using 2 sets of trial functions, Lagrange elements for scalar variables and vector-valued elements for vector valued variables. Mixed finite elements have achieved a high accuracy and shown great robustness in a variety of applications. In our case, they furthermore enable us to directly introduce an atomic current source instead of approximating this by a distribution of electrical monopoles like it is done in the Venant or partial integration approach. The implementation was carried out using the open source software package DUNE-PDELab (<http://www.dune-project.org/pdelab>).

Acknowledgments

This research has been supported by the German Research Foundation (DFG) through project WO1425/2-1, 3-1.

References

1. Wolters CH, Anwander A, Berti G, Hartmann U. Geometry-adapted hexahedral meshes improve accuracy of finite-element-method-based EEG source analysis. *IEEE Trans Biomed Eng.* 2007;54:1446-1453.
2. Vorwerk J, Clerc M, Burger M, Wolters CH. Comparison of boundary element and finite element approaches to the EEG forward problem. *Biomed Tech (Berl)*. 2012;57:795-798.
3. Wolters CH, Anwander A, Tricoche X, Weinstein D, Koch MA, MacLeod RS. Influence of tissue conductivity anisotropy on EEG/MEG field and return current computation in a realistic head model: a simulation and visualization study using high-resolution finite element modeling. *Neuroimage*. 2006;30:813-826.
4. Dannhauer M, Lanfer B, Wolters CH, Knösche TR. Modeling of the human skull in EEG source analysis. *Hum Brain Mapp.* 2011;32:1383-1399.

5. Lanfer B, Scherg M, Dannhauer M, Knösche TR, Burger M, Wolters CH. Influences of skull segmentation inaccuracies on EEG source analysis. *Neuroimage*. 2012;62:418-431.
6. Lanfer B, Paul-Jordanov I, Scherg M, Wolters CH. Influence of inferior cerebrospinal fluid compartments on EEG source analysis. *Biomed Tech (Berl)*. 2012;57:623-626.
7. Pursiainen S, Sorrentino A, Campi C, Piana M. Forward simulation and inverse dipole localization with the lowest order Raviart-Thomas elements for electroencephalography. *Inverse Problems*. 2011;27(4):045003.
8. Fortin M, Brezzi F. *Mixed and Hybrid Finite Element Methods*. New York, NY: Springer-Verlag; 1991.

P019. Characterization of Circadian Trend Change in QT Intervals of Diabetic Patients

K. Sato¹, T. Nishibe¹, M. Furuya¹, K. Yamashiro¹, K. Yana², and T. Ono³

¹Graduate School of Engineering, Hosei University 1, Tokyo, Japan

²Faculty of Science and Engineering, Hosei University 2, Tokyo, Japan

³Department of Cardiology, Nippon Medical School, Tokyo, Japan

A new method of characterizing circadian changes in QT intervals of type 2 diabetic patients (T2DM) has been proposed. Although QT intervals are extensively utilized for characterizing T2DM pathological conditions, their long term circadian changes are not fully studied. The cosinor method has been utilized in the preliminary work describing the relation between circadian QT interval changes and insulin resistance. This work proposes to utilize weighted spline smoothing technique for more precise characterization of the circadian variation of the QT interval sequences. The method aims to cope with both smoothness and tracking capability at rapidly changing period of the data. Circadian changes of QT intervals for 19 T2DM patients and 20 normal subjects are analyzed by the proposed method. The estimated trends yield new indices QTCA (QT circadian transition amplitude). Proposed method showed QTCA difference QT in intervals/day for T2DM patients and normal subjects are 57.0 ± 23.3 mS and 86.8 ± 24.8 mS ($P < .001$). QT-CAs of T2DM patients are significantly smaller than normal subjects. The circadian amplitude obtained by the standard cosinor method showed significant difference between the 3 groups. However, the significance level is much higher with the new method.

References

1. National Institutes of Health. *National Diabetes Statistics* (NIH Publication No. 11-3892). Bethesda, MD: National Institutes of Health; 2011.
2. Tanaka K, et al. *The Autonomic Nervous System*. 2010. Suppl pp. 220.
3. Ong JJ, Sarma JS, Venkataraman K, Levin SR, Singh BN. Circadian rhythmicity of heart rate and QTc interval in diabetic autonomic neuropathy: implications for the mechanism of sudden death. *Am Heart J*. 1993;125:744-752.

P020. Fractal-Based Wavelet-ICA Method for Automatic Artifact Rejection in Scalp EEG

N. Puthanmadam Subramaniyam¹ and J. Hyttinen¹

¹Department of Electronics and Communications, Tampere University of Technology, Tampere, Finland

Independent component analysis (ICA) has been extensively used to remove artifacts from electroencephalogram (EEG) signals. Using ICA, EEG components are first demixed into independent components (IC) and then artifactual independent components (AIC) are identified (visually or automatically) to be rejected before reconstructing the denoised EEG. It has been shown recently that the IC as separated by ICA are not truly independent.¹ To address this issue, wavelet-enhanced ICA (wICA) technique was proposed that involves wavelet denoising of AIC using common applied universal wavelet thresholding to suppress only the artifacts in AIC.¹

However there are some issues with wICA method that have not been addressed. First, the performance of different wavelet thresholding techniques (heuristic Stein's unbiased risk estimate [hSURE], rigorous Stein's unbiased risk estimate [rSURE], minimax) for wICA to suppress artifacts in EEG has not been tested. Second, in real EEG recordings along with electro-oculography (EOG) artifacts, electromyography (EMG) artifacts are also commonly present which are more challenging to remove. Automatic removal of EMG artifacts using wICA-like approach has hitherto not been addressed. Third, since wICA relies on ICA decomposition and in order to achieve completely automatic artifact rejection it was suggested by Castellanos and Makarov¹ that all the components (artifactual and nonartifactual) may be passed through wavelet thresholding by assuming that components having no high magnitude artifacts will pass unaffected.

To address the above-mentioned issues, we first propose a method to automatically identify the AIC containing artifactual activity (EOG or EMG) based on fractal dimensions (FD), derived and extended from the work of Gomez-Herrero et al² and then we propose a fractal-based wavelet denoising method along the lines of wICA to denoise the automatically identified AIC. Our method (F-wICA) differs from wICA in 2 aspects: (a) it uses stationary wavelet decomposition and (b) it uses fractal-based wavelet thresholding and only for automatically identified AICs.

Using semisimulated EEG recordings, we quantitatively compared the performance both in time and frequency domain of the proposed F-wICA method with ICA/wICA method. Our results show that F-wICA outperforms ICA/wICA with minimum distortion in time and frequency domain. We also show that wavelet thresholding techniques benefit by preselection of the AIC based on some reliable estimators before denoising.

In conclusion, we have proposed a completely automatic artifact rejection method that to suppress artifacts from EEG signals, which is a better alternative to ICA or wICA methods.

References

1. Castellanos NP, Makarov VA. Recovering EEG brain signals: artifact suppression with wavelet enhanced independent component analysis. *J Neurosci Methods*. 2006;158:300-312.
2. Gomez-Herrero G, De Clercq W, Kara O, et al. Automatic removal of ocular artifacts in the EEG without an EOG reference channel. In: Proceedings of the 7th Nordic Signal Processing Symposium, NORSIG; 2006.

P021. Influence of Skull Defect Conductivity on MEG Signal and Source Reconstruction in an In Vivo Animal Experiment

S. Lau^{1,2,3,4}, D. Güllmar⁵, L. Flemming², and J. Haueisen¹

¹Institute of Biomedical Engineering and Informatics, Technical University Ilmenau, Ilmenau, Germany

²Biomagnetic Center, Department of Neurology, Jena University Hospital, Jena, Germany

³NeuroEngineering Laboratory, Department of Electrical & Electronics Engineering, University of Melbourne, Parkville, Queensland, Australia

⁴Department of Medicine, St. Vincent's Hospital, University of Melbourne, Fitzroy, Queensland, Australia

⁵Medical Physics Group, Department of Diagnostic & Interventional Radiology, Jena University Hospital, Jena, Germany

While the influence of skull defects on the electroencephalogram (EEG) has been reported, the magnetoencephalogram (MEG) is thought to have a negligible sensitivity to skull defects. However, quantitative experimental evidence under realistic conditions is rare. Our objectives are to experimentally investigate the influence of skull defects of varying conductivity on the MEG and EEG using a controlled current source under a defect and to develop a finite element head model representing the skull defect influence.

Ethics approval was obtained (Freistaat Thüringen, Germany, 02 034/08). We measured a 64-channel EEG simultaneously to a 16-channel MEG produced by a miniaturized artificial co-axial dipole implanted in a rabbit brain tangentially to the inner skull surface in vivo. Following a recording with intact skull, a skull defect was introduced above the dipole and successively filled with agar of increasing conductivity and recorded. Finally, the dipole was shifted in 0.35-mm steps from a position next to the skull defect to a position under the defect and further to the opposite side and a recording was taken at each step. The body, ocular humour and lens, compact and cancellous bone, skull defects and grey matter, white matter, cerebrospinal fluid (CSF), and intracranial blood vessels were segmented from a co-registered CT (0.4 mm³) and a T2 MRI (0.4 mm³). A node-shifted cubic mesh was derived (Vgrid). The EEG and MEG were forward simulated using a blurred dipole approach (SimBio). Source reconstruction from the MEG was performed using an unconstrained moving dipole fit.

Both EEG and MEG were significantly influenced by a conductive skull defect. The amplitude and topography change

increased nonlinearly with increasing defect conductivity in measurement and simulation. Both, the EEG and to a smaller degree also the MEG topography, were altered in a fashion that is spatially corresponding to the skull defect location and geometry. The sources from the skull defect MEGs reconstructed with an intact skull model were displaced away from the defect. Their orientation was altered from the implanted source direction to point more radial to the skull defect boundary. When the sources were instead reconstructed with a head model incorporating the skull defects, the displacement was increasingly reduced as the modeled defect conductivity approaches the actual conductivity and the dipole orientation is gradually restored.

A realistic finite element head model is able to represent a skull defect and to compensate its influence on the MEG source reconstruction. We conclude that skull defects need to be accounted for in realistic volume conductor models.

P022. Leakage Effect in Hexagonal FEM Meshes of the EEG Forward Problem

H. Sonntag¹, J. Vorwerk², C.H. Wolters², L. Grasedyck³, J. Haueisen⁴, and B. Maß¹

¹Max Planck Institute for Human Cognitive and Brain Sciences, Leipzig, Germany

²Institute for Biomagnetism and Biosignalanalysis, University of Münster, Münster, Germany

³Institut für Geometrie und Praktische Mathematik, RWTH Aachen, Aachen, Germany

⁴Institute of Biomedical Engineering and Informatics, Ilmenau University of Technology, Ilmenau, Germany

When solving the EEG forward problem with high spatial resolution it is recommended to model spongy and compact bone of the skull as separate tissues.¹ Both are very thin layers and have different conductivities. Consequently, it may occur that during the finite element method (FEM) some holes in these layers are meshed and cause a current leakage. Our main goal is to introduce an algorithm for finding and fixing such holes causing leakage. We use a model with a 6-compartment structure (gray matter, cerebrospinal fluid [CSF], inner compacta, spongiosa, outer compacta, and skin) for a spherical head model digitized via regular hexagonal elements (cubes) of 1 mm³. We use the same settings for thickness and conductivity as reported by Rampersad et al.,² which are based on Akhtari et al.³ and consistent with the findings of Tang et al.⁴ Rampersad et al.² assumed the following values for the thickness: 1.2, 2.3, and 1.5 mm, respectively, for outer compacta, spongiosa, and inner compacta, resulting in a total skull thickness of 5 mm. The size of the finite elements (FEs) is in the order of the thickness of the compacta. Hence, we found that current leakage occurs in 6% of FE nodes of the compacta structure (in 1% of all FE nodes). We can show that the forward solution from this leaky mesh results in higher errors against the analytical solution (overall relative difference measure: RDM* > 0.07 and magnification: MAG > 1.15) compared to the findings of Wolters et al.⁵ In a second setup, the leaks are

closed by relabeling leaky spongiosa into compacta. With this repair mechanism, we achieve significantly smaller errors in the RDM* and MAG. In a third setup, we use the so-called node-shift approach, described by Wolters et al.,⁶ to reshape the hexagonal elements which are involved in the leakage effect and relabeled spongiosa and CSF or skin to compacta in the respective elements. Results are further improved as demonstrated by smaller errors (RDM* and MAG) compared to the analytical solution.

We conclude that the leakage effect in hexagonal FEM meshes needs to be corrected by closing the leaks via the suggested relabeling and node shifting at the relevant elements.

Acknowledgments

Partially funded by DFG-project KonnekFEM: WO 1425/3-1, GR 3179/3-1, HA 2899/14-1, MA 4940/1-1.

References

1. Dannhauer M, Lanfer B, Wolters CH, Knösche TR. Modeling of the human skull in EEG source analysis. *Hum Brain Mapp.* 2011;32:1383-1399.
2. Rampersad S, Stegeman D, Oostendorp T. On handling the layered structure of the skull in transcranial direct current stimulation models. *Conf Proc IEEE Eng Med Biol Soc.* 2011;2011:1989-1992.
3. Akthari M, Bryant HC, Mamelak AN, et al. Conductivities of three-layer live human skull. *Brain Topogr.* 2021;14:151-167.
4. Tang C, You F, Cheng G, et al. Correlation between structure and resistivity variations of the live human skull. *IEEE Trans Biomed Eng.* 2008;55:2286-2292.
5. Wolters CH, Köstler H, Möller C, Härdtlein J, Anwander A. Numerical approaches for dipole modeling in finite element method based source analysis. *Int Congr Ser.* 2007;1300:189-192.
6. Wolters CH, Anwander A, Berti G, Hartmann U. Geometry-adapted hexahedral meshes improve accuracy of finite-element-method-based EEG source analysis. *IEEE Trans Biomed Eng.* 2007;54:1446-1453.

P023. EEG Artifact Detection Using Spatial Harmonic Analysis and Support Vector Machines

S. Freitag¹, U. Graichen¹, P. Fiedler¹, D. Strohmeier¹, and J. Haueisen^{1,2}

¹Institute of Biomedical Engineering and Informatics, Ilmenau University of Technology, Ilmenau, Germany

²Biomagnetic Center, Department of Neurology, University Clinic Jena, Jena, Germany

Introduction. Electroencephalography (EEG) is an important clinical and research method. Artifacts overlaying the original signals are a reoccurring problem in EEG. Due to the increasing number of EEG electrodes and high sampling rates, efficient methods for signal analysis and artifact detection are required. **Materials and methods.** A promising approach enabling online artifact detection is the spatial harmonic analysis (SHA) of EEG data. This method

allows signal decomposition based on the eigenspace of the Laplace–Beltrami operator of the triangulated surface of the electrode positions. The resulting signal components are utilized for detecting artifacts in EEG data. We propose a method combining SHA and support vector machines (SVM) for artifact detection. The spatial harmonic signal components are classified binary by a previously trained SVM resulting in one group containing the artifact affected components and one group including the artifact free ones. Spontaneous EEG signals of 10 healthy male volunteers were recorded using a 256-channel cap with an equidistant electrode layout and 2 coupled 128-channel amplifiers (ANT BV, Enschede, The Netherlands). Data were sampled at 2048 Hz and band-pass (1-300 Hz) and notch (50 Hz and 4 harmonics) filtered. The recorded resting EEG signals were manually checked for eye blink and swallowing artifacts. Those were individually segmented from the data sets resulting in EEG segments with (134) and without (185) eye blinks as well as with (52) and without (86) swallowing artifacts. The segments consist of 800 ms on average. The EEG segments for each type of artifact were divided into two thirds acting as test data and one third available as training data. To train the SVMs equal amounts of artifact-containing and artifact-free EEG data were randomly selected from the training data sets. **Results.** With a training data set of 5,000 ms a correct classification rate (CCR) of 95% was achieved for the eye blink test data. The swallowing artifact test data were classified correctly with a CCR of 83%, using 10 000 ms training data. **Conclusion.** The proposed method using SHA and SVM for artifact detection in EEG data enables an efficient identification of artifact-containing and artifact-free EEG segments, respectively. Due to the low computation times for SHA and SVM, the method is well suited for online artifact detection.

Acknowledgments

This research was supported by the German Federal Ministry of Education and Research (03IPT605A) and the German Federal Ministry of Economics and Technology (KF2250111ED2).

P024. MEG/EEG Resolution Metrics With Noise: From Linear Estimators Toward Estimates

M. Stenroos^{1,2} and O. Hauk¹

¹MRC Cognition and Brain Sciences Unit, Cambridge, UK

²Aalto University, BECS, Aalto, Finland

In MEG/EEG inverse problems, neural sources that give rise to measured signals are estimated. To solve this ill-posed problem, various constraints are used. The effects of these constraints on linear estimators can be studied using point-spread and cross-talk functions (PSF, CTF) that are formed by applying the inverse model to the topographies of the forward model.^{1,2} Resolution metrics characterise features of the PSF and CTF, such as localisation error and spatial spread. In conventional resolution analysis, the measurement noise

is taken into account in the inverse operator but not in the topographies. The noise has earlier been shown to have a major role on measurement sensitivity.^{3,4} In this work, we extend the concept of resolution metrics by taking the noise into account in the topographies.

A 3-shell realistic boundary element model and cortical source model were built and co-registered with the Elekta MEG/EEG system using FreeSurfer and MNE software. Signal-to-noise ratio (SNR) maps were made according to Goldenholz et al.⁴ A minimum-norm (MN) estimator was built using measured noise covariance matrix as whitener, setting the regularization according to the assumed SNR of 3. Brain noise and measurement noise with the mean SNR of 3 were simulated, and MN estimates for the simulated data were computed. Statistical PSFs were obtained by taking the standard deviation of the estimates in all source locations. Resolution metrics were computed for both conventional PSFs and for the simulated noisy ones.

For sources with good SNR, the conventional and statistical metrics were very similar, but for sources with low SNR (especially SNR < 1), the spread of the statistical estimates increased. For MEG, the spread increased especially in bottoms of sulci and on tops of gyri and in deepest brain regions, following the patterns of the SNR maps and well-known MEG sensitivity profiles. The statistical metrics showed the benefit of adding EEG to MEG more clearly than the conventional ones in Molins et al.¹: When the modalities were combined, the spread of the estimates at low SNR regions decreased considerably.

Conventional resolution metrics may yield overoptimistic results for sources with low SNR. Adding the measurement noise to resolution analysis removes this bias and shifts the focus from the estimator toward the source estimate, thus increasing the value of resolution analysis in experimental use. At regions of low MEG SNR, adding EEG may increase resolution considerably.

References

1. Molins A, Stufflebeam SM, Brown EN, Hämäläinen MS. Quantification of the benefit from integrating MEG and EEG data in minimum l2-norm estimation. *Neuroimage*. 2008;42:1069-1077.
2. Hauk O, Wakeman DG, Henson R. Comparison of noise-normalized minimum norm estimates for MEG analysis using multiple resolution metrics. *Neuroimage*. 2011;54:1966-1974.
3. Haueisen J, Funke M, Güllmar D, Eichardt R. Tangential and radial epileptic spike activity: different sensitivity in EEG and MEG. *J Clin Neurophys*. 2012;29:327-332.
4. Goldenholz DM, Ahlfors SP, Hämäläinen MS, et al. Mapping the signal-to-noise-ratios of cortical sources in magnetoencephalography and electroencephalography. *Hum Brain Mapp*. 2009;30:1077-1086.

P025. Efficient Spatial Filter Approach Permits Single-Trial Decoding of Speech Items From M/EEG Recordings

M. Grigutsch¹, M. Felber¹, B. Maess¹, and B. Herrmann²

¹Department of Neuropsychology, Max Planck Institute for Human Cognitive and Brain Sciences, Leipzig, Germany

²Max Planck Research Group "Auditory Cognition", Max Planck Institute for Human Cognitive and Brain Sciences, Leipzig, Germany

Low-frequency neuronal oscillations in the human auditory system might be entrained by intensity modulations of ongoing speech.¹ Assessing cortical speech tracking using electrophysiological measurements is challenging because of the low SNR due to interferences from background activity. Here, we applied an efficient filtering approach for the detection of stimulus-entrained cortical activity driven by aperiodic speech stimuli. We employed ICA and multivariate linear regression to optimize spatial filters which maximize the covariance between the projected signal and the stimuli. The filters effectively suppress background activity and provide a hypothesis-driven data reduction of high-dimensional M/EEG measurements. Filter weights can be interpreted as sensor topographies and used to localize the underlying brain activity. Filtered time courses allow decoding of stimulus properties from single trial electrophysiological recordings. This was demonstrated on simultaneously recorded MEG and EEG data from 33 participants of a prior study. The stimuli were the same as in Eckstein et al.² Participants actively listened to sentences and had to perform a judgement task on linguistic syntax and prosody. Speech envelopes extracted from the sound waveforms were used to estimate spatial filters from a subset of the data (training). The obtained filter weights were then applied to a test data set to decode speech items from single-trial M/EEG measurements. Decoding was based on Pearson correlation between the projected signals and the real speech, assigning the label of the stimulus with the highest correlation coefficient.

Analyses revealed that speech envelopes were best tracked by low-frequency neural activity at time lags of about 75 ms and 160 ms. The early effect had a sensor topography very similar to that observed from temporal brain activity distributions generating the N1/N1m ERP components. It most likely represents onset responses to sudden intensity changes at word or syllable onsets. Speech items could be successfully decoded with high accuracy from a variety of single-trial measurements. Accuracy improved with increasing length of the utterances. Interestingly, MEG measurements from magnetometers and planar gradiometers yielded comparable decoding accuracy. EEG measurements were least informative, requiring significantly longer speech items for reliable decoding. In summary, our spatial filter approach proved to be efficient in detecting

brain activity entrained to speech and was successfully applied to decode speech stimuli even from single-trial measurements.

References

1. Luo H, Poeppel D. Phase patterns of neuronal responses reliably discriminate speech in human auditory cortex. *Neuron*. 2007;54:1001-1010.
2. Eckstein K, Friederici AD. It's early: event-related potential evidence for initial interaction of syntax and prosody in speech comprehension. *J Cogn Neurosci*. 2006;18:1696-1711.

P026. EEG Source Reconstruction Using Realistic Finite Difference Forward Models Based on a MRI Template

G. Strobbe¹, P. van Mierlo¹, S. Vandenberghe¹

¹iMinds, Department of Electronics and Information Systems, MEDISIP, Ghent University, Ghent, Belgium

In this study, we used the parametric empirical Bayesian (PEB) framework for distributed source reconstruction in EEG/MEG implemented in the Statistical Parametric Mapping (SPM) software to compare forward models using real EEG data.¹ The current forward modeling in the framework comprises a 3-layered boundary element method (BEM) approximation of the head, including a skull, scalp, and brain compartment constructed based on a high-resolution anatomical MRI template. Here we introduce forward models constructed using the finite difference reciprocity method (FDRM)² within the framework. This method allows using more realistic volume conductor models segmented from the template. First, we numerically verified the FDRM technique in a 3-layered spherical volume conductor model using standard metrics such as the relative difference measure (RDM).³ After verification, 2 aspects were investigated: (a) the influence of using FDRM or BEM based forward modeling assuming the same 3-layered default BEM volume conductor model used in SPM and (b) the effect of using a FDRM forward model including the 3-layered volume conductor model extended with CSF and air cavities. For all the models we assumed the same source space. Based on 8 grand average ERP data sets across subjects and assuming multiple sparse priors,⁴ the models were compared using the Bayesian log-evidence corresponding with the reconstructions. Also the reconstructed activity was compared to the activity reported in previous studies of equivalent ERP waveforms. The results indicate that FDRM forward modeling and the use of a more realistic volume conductor model both improve the reconstructed activity compared to the 3-layered BEM approximation. For equal volume conductors we found strong evidence in 6 of the 8 ERP datasets in favor of the FDRM. For the extended FDRM volume conductor model we found strong evidence for all the datasets in favor of the FDRM. These results emphasize the influence of the forward model on the reconstructed activity

and show that EEG source reconstruction can benefit from the use of realistic MRI-based FDRM volume conductor models

References

1. Henson RN, Mattout J, Phillips C, Friston KJ. Selecting forward models for MEG source-reconstruction using model-evidence. *Neuroimage*. 2009;46:168-176.
2. Vanrumste B, Van Hoey G, Van de Walle R, D'Havé MR, Lemahieu IA, Boon PA. The validation of the finite difference method and reciprocity for solving the inverse problem in EEG dipole source analysis. *Brain Topogr*. 2001;14:83-92.
3. Gramfort A, Papadopoulos T, Olivi E, Clerc M. OpenMEEG: open-source software for quasistatic bioelectromagnetics. *Biomed Eng Online*. 2010;9:45.
4. Friston K, Harrison L, Daunizeau J, et al. Multiple sparse priors for the M/EEG inverse problem. *Neuroimage*. 2008;39:1104-1120.

P027. Selecting Volume Conductor Models for EEG Source Localization of Epileptic Spikes: Preliminary Results Based on 4 Operated Epileptic Patients

G. Strobbe¹, D. Cárdenas-Peña², V. Montes-Restrepo¹, P. van Mierlo¹, G. Castellanos-Dominguez², and S. Vandenberghe¹

¹iMinds, Department of Electronics and Information Systems, MEDISIP, Ghent University, Ghent, Belgium

²Signal Processing and Recognition Group, Universidad Nacional de Colombia, Campus La Nubia, Manizales, Colombia

In order to reconstruct the underlying active neural sources of epileptic spiking activity measured with scalp-EEG, it is necessary to construct a volume conductor model (VCM) reflecting the geometrical and electromagnetic properties of the head. Often 3-shell spherical VCMs are used.¹ Based on boundary element methods (BEM) the patient's anatomy can be approximated better. In these models, the head is modeled as a 3-layered VCM, including scalp, skull, and brain tissue.² The most realistic models can be constructed using finite element or finite difference techniques (FDM).³ Using these techniques many extra tissue types can be incorporated such as cerebrospinal fluid (CSF), gray and white matter based on MRI tissue segmentation techniques. In this study, we investigated the effect of the VCM on spike localization. We used a FDM forward solver to compare 4 types of models: (a) 3-layered spherical models, (b) 3-layered BEM-like models, (c) 5-layered models using SPM segmentation, and (d) 5-layered models using a segmentation method based on level-set (LS).⁴ For each of the models we assumed the same conductivity for equivalent tissue classes and constrained the solution space to the gray matter subspace segmented from the MR.⁴ We used a single dipole model to reconstruct 27-channel EEG spiking activity in 4 patients who underwent epilepsy surgery and have been seizure-free since then.

CT images were available to extract the electrode positions. We applied single dipole spike localization using least squares minimization and validated the estimated sources against the resected area, as indicated by the postoperative MRI and serving as our ground truth. The closest distance of the estimated dipole to the resected area was used as a measure of localization accuracy. In all 4 patients we found the smallest distances using the most realistic 5-layered VCMs (c) and (d). The maximum error was 5 mm. We did not find significant differences between level-set and SPM segmentation. For the BEM and the spherical models, the error was bigger ranging from 5 mm to 40 mm from the resected zone. We can therefore preliminarily conclude that it is worth the effort to build realistic VCMs including more tissue types, based on the MRI segmentation of the patient's head. This is especially useful in the presurgical evaluation of patients with refractory epilepsy, where the precise determination of the ictal onset zone is very important.

References

1. Brodbeck V, Spinelli L, Lascano AM, et al. Electroencephalographic source imaging: a prospective study of 152 operated epileptic patients. *Brain*. 2011;134(pt 10):2887-2897.
2. Gramfort A, Papadopoulou T, Olivi E, Clerc M. OpenMEEG: open-source software for quasistatic bioelectromagnetics. *Biomed Eng Online*. 2010;9:45.
3. Vanrumste B, Van Hoey G, Van de Walle R, D'Havé MR, Lemahieu IA, Boon PA. The validation of the finite difference method and reciprocity for solving the inverse problem in EEG dipole source analysis. *Brain Topogr*. 2001;14:83-92.
4. Boykov Y, Kolmogorov V. An experimental comparison of min-cut/max-flow algorithms for energy minimization in vision. *IEEE Trans Pattern Anal Mach Intell*. 2004;26:1124-1137.

P028. Automatic MRI-Based Generation of Head Models for EEG Source Analysis

B. Lanfer^{1,2}, I. Paul-Jordanov¹, M. Scherg¹, and C.H. Wolters²

¹BESA GmbH, Gräfelfing, Germany

²Institute for Biomagnetism and Biosignalanalysis, University of Münster, Münster, Germany

Electroencephalographic (EEG) source analysis greatly benefits from using individual, realistically shaped head models for the solution of the forward problem.^{1,2} Routine application of individual models is still impeded by the difficulty of correctly segmenting MRI data, especially bone and cerebrospinal fluid (CSF). For this reason, we propose a new, automated segmentation procedure on the basis of MR images. The good performance of this approach is demonstrated by exemplary segmentation results and validation against a computed tomographic (CT) reference segmentation.

The segmentation procedure is formulated in a Bayesian framework in which multimodal image data as well as a priori

information on the anatomy is evaluated to achieve optimal segmentation performance. A Markov random field (MRF) model³ incorporates the a priori knowledge that the head can be described as a structure with consecutive layers of 8 different tissues.

The optimal segmentation, which best fits the MRF model and the measured data, is determined using an expectation-maximization (E-M) type algorithm.

Our approach was applied to 3 exemplary data sets: the first containing a T1- and a T2-MRI, and the second only containing a T1-MRI. The outlines of the segmented regions were overlaid onto the original MRI to show the accuracy of the segmentation. In addition, we computed a segmentation for a third subject where also a CT image was available. A reference skull segmentation was derived from the co-registered CT image. The overlap of the skull segmented from the MR data using the proposed approach and the CT-based reference skull mask was quantified using the Dice coefficient D .⁴

Visual inspection revealed that scalp, skull, CSF, and brain tissue were accurately identified. CSF was precisely delineated even when only a T1-MRI was available. Still, the results indicate that it is advantageous to also incorporate a T2-MRI into the segmentation.

A good agreement of $D = 0.86$ was found between the skull segmentation for the third subject and the CT-based reference skull. In a comparable validation study⁵ previously published, skull segmentation approaches only reached agreements of $D = 0.75$ and below.

In summary, we propose an automatic segmentation approach, which proves to be accurate especially with regard to skull segmentation. The approach was implemented into an easy-to-use software pipeline allowing the effortless generation of individual, 4-compartment realistic head models. By doing so, our development removes a substantial obstacle for the use of realistic head models in EEG source analysis.

References

1. Lanfer B, Paul-Jordanov I, Scherg M, Wolters CH. Influence of interior cerebrospinal fluid compartments on EEG source analysis [published online August 30, 2012]. *Biomed Tech (Berl)*. doi:10.1515/bmt-2012-4020.
2. Yvert B, Bertrand O, Thévenet M, Echallier JF, Pernier J. A systematic evaluation of the spherical model accuracy in EEG dipole localization. *Electroencephalogr Clin Neurophysiol*. 1997;102:452-459.
3. Li SZ. *Markov Random Field Modeling in Image Analysis*. Berlin, Germany: Springer; 2009.
4. Dice LR. Measures of the amount of ecologic association between species. *Ecology*. 1945;26:297-302.
5. Wang D, Shi L, Chu WC, Cheng JC, Heng PA. Segmentation of human skull in MRI using statistical shape information from CT data. *J Magn Reson Imaging*. 2009;30:490-498.
6. Besag J. On the statistical analysis of dirty pictures. *J R Stat Soc Ser B (Methodological)*. 1986;48:259-302.

P029. Biomagnetic Field Measurements With an Optically Pumped Atomic Magnetometer Using a Hybrid Cell of K and Rb Atoms

Y. Ito¹, D. Sato¹, K. Kamada^{1,2}, and T. Kobayashi¹

¹Graduate school of Engineering, Kyoto University, Kyoto, Japan

²Japan Society for the Promotion of Science, Tokyo, Japan

In recent years, optically pumped atomic magnetometers (OPAMs) have gained practical interest as magnetic sensors for biomagnetic measurements because of their ultra-high sensitivity without cryogenic cooling.^{1,2} We have developed an OPAM using a hybrid cell with K and Rb atoms (hereafter called a hybrid OPAM).³ The hybrid OPAM is based on spin exchange collisions between optically thin and dense atoms, so that we can achieve wider sensing area suitable for imaging modalities.⁴ In this study, we developed the ultra-high sensitivity hybrid OPAM whose sensitivity reached about $100 \text{ fT}_{\text{rms}}/\text{Hz}^{1/2}$ at 10 Hz. In the case, the sensitivity was limited by the system noise. In addition, we found that the homogeneity of the sensing area of the hybrid OPAM was higher than that of the conventional OPAM using a single Rb cell by varying the position of the probe beam path. This result indicates that the hybrid OPAM is more effective in realizing simultaneous signal measurements at different locations with the uniform sensitivity.

First, we applied the hybrid OPAM for human magnetocardiogram (MCG) measurements to demonstrate its feasibility as a biomagnetic sensor.⁵ MCGs from a healthy male subject (23 years old) were measured for 10 seconds in a 3-layer magnetic shield room. Since the hybrid OPAM has a certain frequency response, and measured data contained slow fluctuations originating from subject's breathing and 60 Hz power line noise, the data were corrected by the frequency response curve and a 0.5 to 50 Hz band-pass filter. The measured signals show typical features of a human MCG, such as periodic heart beats, the QRS complexes, the T waves. Second, we carried out simultaneous multipoint mapping with the hybrid OPAM toward practical biomagnetic measurements. We measured magnetic field distributions generated from a loop coil and a dipole electrode placed inside a saline-solution-filled phantom. Although the achieved sensitivity was lower than that of single channel sensing, we could measure magnetic field distributions agreeing well with theoretical calculations.

Consequently, these results demonstrate the feasibility of the hybrid OPAM for biomagnetic measurements. In future, we plan to apply the hybrid OPAM to magnetoencephalograms (MEGs) improving its sensitivity by lock-in detection and gradiometric configuration.

Acknowledgments

This work was supported in part by the Innovative Techno-Hub for Integrated Medical Bio-imaging of the Project for Developing Innovation Systems, Grant-in-Aid for Scientific Research (A) (24240081) and Grant-in-Aid for Challenging Exploratory Research

(24650221) all from the Ministry of Education, Culture, Sports, Science, and Technology (MEXT), Japan.

References

1. Allred JC, Lyman RN, Kornack TW, Romalis MV. High-sensitivity atomic magnetometer unaffected by spin-exchange relaxation. *Phys Rev Lett*. 2002;89(13):130801.
2. Budker D, Romalis M. Optical magnetometry. *Nat Phys*. 2007; 2:227-234.
3. Ito Y, Ohnishi H, Kamada K, Kobayashi T. Sensitivity improvement of spin-exchange relaxation free atomic magnetometers by hybrid optical pumping of potassium and rubidium. *IEEE Trans Magn*. 2011;47:3550-3553.
4. Ito Y, Ohnishi H, Kamada K, Kobayashi T. Effect of spatial homogeneity of spin polarization on magnetic field response of an optically pumped atomic magnetometer using a hybrid cell of K and Rb atoms. *IEEE Trans Magn*. 2012;48:3715-3718.
5. Ito Y, Ohnishi H, Kamada K, Kobayashi T. Development of an optically pumped atomic magnetometer using a K-Rb hybrid cell and its application to magnetocardiography. *AIP Advances*. 2012;2:032127.

P030. Improved MEG/EEG Source Reconstruction Quality With Accurate Sensor Positions Captured With a Novel 3D Scanning Device

S.S. Dalal¹, S. Rampp², F. Willomitzer³, O. Arold³, S. Fouladi-Movahed³, G. Häusler³, H. Stefan², and S. Ettl³

¹Zukunftscolleg & Department of Psychology, University of Konstanz, Konstanz, Germany

²Department of Neurology, University Hospital Erlangen, Erlangen, Germany

³Institute of Optics, Information and Photonics, University of Erlangen-Nuremberg, Erlangen, Germany

Introduction. The novel 3D scanning technique “Flying Triangulation” (FlyTri) enables rapid and motion-robust optical 3D scanning with a resolution of $\sim 150 \mu\text{m}$. Using phantom measurements and simulations, we evaluated the use of FlyTri for EEG electrode localization and coregistration with MRI. We hypothesized that this new technology would enable improved source localization in comparison to the current standard technique that employs a digitization stylus. **Methods.** An independent high-resolution 3D-scanning technique (FaceSCAN^{3D}, 3D-Shape GmbH, Erlangen, Germany) was used to scan a real subject wearing a 68-channel EEG cap and create a digital 3D model. With this, a true-to-size physical model was then created via 3D printing. “True” locations of electrodes were then reacquired using FaceSCAN^{3D} to compensate for any inaccuracies of the printing process. Electrodes were then localized using a digitization stylus (Polhemus Fastrak, Polhemus, Colchester, VT) as well as FlyTri. Using NUTMEG (nutmeg.berkeley.edu), a dipole was simulated and projected to the EEG electrode array via a BEM-based forward model

constructed with the FaceSCAN electrode coordinates. The sources were then reconstructed using an LCMV beamformer and BEM-based forward models from the Polhemus coordinates and from the FlyTri coordinates. **Results.** Electrode coordinates recorded by the Polhemus deviated from the true locations by an average of 3.5 mm, while FlyTri coordinates deviated by only 0.9 mm. The simulated source location and time course were accurately reconstructed using FlyTri with only minor signal degradation. Source analysis using Polhemus coordinates failed with a diffuse source map and heavily corrupted time series. **Conclusions.** Accurate registration of EEG electrode positions is critical, particularly for the detection and reconstruction of low-SNR sources, for example, high-frequency activity. The FlyTri technique provides significantly improved electrode registration accuracy, thereby effectively boosting the SNR of EEG source reconstructions.

P031. Simulation of MCG Localization With a Current Dipole

S. Zhang^{1,2}, Y. Zhang^{1,2}, H. Li^{1,2,3}, and X. Kong^{1,2}

¹State Key Laboratory of Functional Materials for Informatics, Shanghai Institute of Microsystem and Information Technology (SIMIT), Chinese Academy of Sciences (CAS), Shanghai, China

²Joint Research Laboratory on Superconductivity and Bioelectronics, Collaboration between CAS-Shanghai and FZJ, Shanghai, China

³Graduate University of the Chinese Academy of Sciences, Beijing, China

The influence of measuring plane and signal-to-noise ratio (SNR) to the MCG localization was investigated. A current dipole was applied to simulate the cardiac electric source. By adjusting the distance of measuring plane and the dipole, MCG signals were recorded and used to compute the cardiac sources. The computed source matched the known dipole perfectly, indicating no correlation with the measuring distance. However, MCG signal with a poor SNR showed an obvious localisation error. The results give a helpful instruction for data exclusion during the clinical research.

Acknowledgments

Knowledge Innovation Program of the Chinese Academy of Sciences (Grant No: KGCX2-YW-906 and KGCX2-EW-105), One Hundred Person Project of the Chinese Academy of Sciences and Strategic Priority Research Program (B) of the Chinese Academy of Sciences (Grant No. XRD04020300).

P032. Effects of Conductivity Perturbations of the Trilayered Skull on EEG Source Analysis

V. Montes-Restrepo¹, G. Strobbe¹, P. van Mierlo¹, and S. Vandenberghé¹

¹iMinds, Department of Electronics and Information Systems, MEDISIP, Ghent University, Ghent, Belgium

Electroencephalographic (EEG) source analysis relies on an accurate model representing the human head. In this head model, the skull plays an important role due to its complex structure and low conductivity compared to the other tissues inside the head. The skull has often been modeled as a single compartment with isotropic conductivity. However, the actual structure of the skull is trilayered, consisting of a spongiform layer surrounded by 2 compact layers. Not only spongy and compact bones are part of this structure but also air-filled cavities. Therefore, the skull has different conductivities and thicknesses throughout its whole structure and so it is *inhomogeneous*.¹

In this work, we analyze the effect of conductivity perturbations of the inhomogeneous skull compartment on EEG source analysis. For this purpose, a data set with co-registered magnetic resonance (MRI) and computed tomography (CT) images of one patient was used. A head model with an accurately segmented skull, including spongy and compact bone as well as some air-filled cavities, was incorporated in the analysis. The conductivity values for the compact ($\sigma_c = 0.0068$ S/m) and spongy ($\sigma_{sp} = 0.0298$ S/m) bone compartments of the skull were selected as the average measurements of Akhtari et al.,² yielding a ratio of 4.38 ($\sigma_{sp} : \sigma_c$) for the reference model. We perturbed these values by (a) multiplying both conductivities by the same factor, that is, keeping the ratio constant and (b) doubling and halving the ratio. These perturbed conductivity values resulted in a total of seven test head models. Simulated EEG data was computed on the reference model. These data were compared with the forward solutions of the test models through the RDM and MAG error measures. The finite difference method with reciprocity (FDRM)³ was used to calculate the forward problem in all models. To solve the inverse problem, a single dipole localization based on the minimization of a least squares cost function was performed. The source localization error was computed for dipoles placed at clinically significant brain areas: cingulate cortex, fronto-basal and mesio-temporal regions.

The results suggest that conductivity perturbations of the compact bone have the strongest influence on EEG source localization. Conversely, the perturbations of the spongy bone did not show a noticeable influence on the dipole estimation. This means that more than the spongy to compact bone conductivity ratio, the correct determination of the compact bone conductivity can improve the accuracy of the forward solution. For deep sources (cingulate cortex), the effects of conductivity perturbations were larger than for sources located at fronto-basal or mesio-temporal regions.

References

1. Law S. Thickness and resistivity variations over the upper surface of the human skull. *Brain Topogr.* 1993;6:99-109.
2. Akhtari M, Bryant HC, Mamelak AN, et al. Conductivities of three-layer live human skull. *Brain Topogr.* 2002;14:151-167.
3. Hallez H, Vanrumste B, Van Hese P, D'Asseler Y, Lemahieu I, Van de Walle R. A finite difference method with reciprocity used to incorporate anisotropy in electroencephalogram dipole source localization. *Phys Med Biol.* 2005;50:3787-3806.

P033. Examining the Contribution of Hippocampus Activity to Surface ECoG

D.D.E. Wong¹, A. Bidet-Caulet², R.T. Knight³, N.E. Crone⁴, and S.S. Dalal¹

¹Department of Psychology, University of Konstanz, Konstanz, Germany

²Brain Dynamics and Cognition Team, Lyon Neuroscience Research Center, Lyon, France

³Helen Wills Neuroscience Institute and Psychology, University of California, Berkeley, CA, USA

⁴Department of Neurology, Johns Hopkins University School of Medicine, Baltimore, MD, USA

The localization of neural generators of hippocampal activity can be performed using intracranial electroencephalography (icEEG) depth electrodes. However, due to the limited spatial resolution of this modality, electrocorticography (ECoG) grids would greatly aid in spatially localizing neural generators of these oscillations. While the detection of hippocampal activity using ECoG is feasible, the relationship between oscillations measured by icEEG and ECoG is uncertain. Furthermore, the oscillations measured by ECoG are believed to be generated by multiple neural populations with overlapping activations, making it more difficult to isolate individual sources.

We present a novel method, based on factor analysis, to identify the contribution of sources detected by icEEG to the ECoG signal, as well as additional sources of overlapping activation. This method allows for the representation of the ECoG data as weighted contributions of icEEG sources, thereby yielding the forward potential topography of the detected sources to the ECoG grid.

The proposed method is first validated using simulated data. Using continuous hippocampal data recorded from an epilepsy patient, we then demonstrate that (a) a correlation exists between icEEG and ECoG data, and as such it should be possible to reconstruct the forward potentials of sources detected by icEEG and (b) the proposed method is able to determine, on an 8 × 8 ECoG grid, the forward potentials of oscillatory sources within the hippocampus measured by two icEEG depth electrodes, as well as those of sources of overlapping activity. These forward potentials are then used to localize the neural generators using a boundary element head model. The localization results are ultimately compared to the positions of the icEEG depth electrodes to assess the effectiveness of the head model in representing the sources.

While this method demonstrates that it is indeed possible to localize hippocampal sources using an ECoG grid, it still relies on icEEG electrodes for primary source identification. This study, however, provides a first step in developing the necessary head models and source localization procedures to reconstruct hippocampal neural generators from ECoG data alone.

P034. Electrical Source Imaging in Epilepsy: A Comparison of 3 Head Models

G. Birot¹, L. Spinelli², S. Vulliémot², M. Seeck², and C.M. Michel¹

¹Department of Fundamental and Clinical Neurosciences, University of Geneva, Geneva, Switzerland

²EEG and Epilepsy Unit, Neurology Clinic, University Hospital of Geneva, Geneva, Switzerland

Electrical source imaging (ESI) is the reconstruction of the electrical brain activity from recordings of scalp electroencephalography (EEG). When applied on interictal epileptic spikes (IES), this technique is of great interest for identifying the irritative zone in partial epilepsy.¹ ESI is based on the inversion of the so-called EEG forward model, which describes how electrical currents generated in the brain propagate to the scalp electrodes. Forward modeling errors may strongly influence ESI² and lead to mis-localization of IES generators. In this context, head models used for solving the EEG forward problem have been greatly enhanced this past 20 years.³ It was in the beginning made of a simple single sphere and consists nowadays of a sophisticated voxel-based realistic mesh of the head obtained from MRI. Various head models are nevertheless still used: layered pseudo-spherical model, layered realistic model or voxel-based realistic model. The cohabitation of these models is partially due to technical reasons but most importantly to the lack of study on the influence of head model on ESI in a clinical context.

Thus, we propose here to do this comparison using a data set of 58 epileptic patients who have undergone surgery and/or intracranial recordings. They also had either 128 or 256 electrodes high-density EEG, preoperative and postoperative MRI scans, as well as CT scans with implanted intracranial electrodes. We compared localization accuracy resulting from a 3-layers (brain, skull, skin) locally spherical head model LSMAC,⁴ a 3-layer realistic head model (BEM),⁵ and a 4-media (adding CSF) voxel-based realistic head model (FEM) (BESA MRI, BESA GmbH, Germany). All these head models were computed from individual MRI, and ESI was performed for each of them on averaged IES. The estimated location of the spikes generators was set at the maximum of brain activation map, and its distances from resected area (using postoperative MRI) and from the maximum activation recorded during IES by intracranial electrodes (using implanted CT scan) were calculated.

We found that realistic head models provided less ghost sources than LSMAC, which were particularly present in temporal polar regions. When the maximum activation was not in a ghost source, its distance from the most activated intracranial electrodes slightly decreased as the head model became more complex. Despite its increased computational load, we think that ESI using voxelized head model should be preferred to others in order to increase both detection rate and localization accuracy of epileptogenic area in partial epilepsy.

Acknowledgment

Supported by Swiss National Science Foundation: SPUM Grant No. 140332.

References

1. Brodbeck V, Spinelli L, Lascano AM, et al. Electroencephalographic source imaging: a prospective study of 152 operated epileptic patients. *Brain*. 2011;134(pt 10):2887-2897.
2. Akalin Acar Z, Makeig S. Effects of forward model errors on EEG source localization. *Brain Topogr*. 2013;26:378-396.
3. Hallez H, Vanrumste B, Grech R, et al. Review on solving the forward problem in EEG source analysis. *J Neuroeng Rehabil*. 2007;4:46.
4. Brunet D, Murray MM, Michel CM. Spatiotemporal analysis of multichannel EEG: CARTOOL. *Comput Intell Neurosci*. 2011;2011:813870.
5. Gramfort A, Papadopoulos T, Olivi E, Clerc M. OpenMEEG: open-source software for quasistatic bioelectromagnetics. *Biomed Eng Online*. 2010;9:45.

P040. EEG Topography and LORETA Tomography in Neuropathology and Treatment of Genetic Epilepsy: Two Patients With Attentional, Affective and Anorexic Behaviors

H. Emory¹, C. Wells¹, and N. Mizrahi¹

¹Emory Neurophysiological Institute, Los Angeles, CA, USA

Genetic epilepsies in adolescents are diverse in etiology and complex in presentation. We report the electroencephalographic (EEG) and quantitative EEG (QEEG) topography paired with low-resolution brain electromagnetic tomography (LORETA) data of 2 young females with dysphoric moods, attentional difficulties, and anorexic behaviors. Neurophysiologic evaluations were performed before and during treatment.

An initial EEG and QEEG of 4 frequency bands (delta = 1.5-3.5 Hz, theta = 3.5-7.5 Hz, alpha = 7.5-12.5 Hz, and beta = 12.5-25.0 Hz) showed increased theta activity and decreased relative alpha and/or low alpha mean frequencies. Anatomical distribution by LORETA showed bilateral theta decreases in medial and basal prefrontal areas. Alpha was significantly decreased bilaterally in the precuneus, posterior cingulate and superior parietal lobule. Each patient's neurophysiologic data and physiologic parameters at follow up guided the selection and dosing of their regimen.

Treatment with minimal dosage of antiepileptic drug(s) combined with a catecholamine agent normalized the overall spectral composition of EEG topography and LORETA tomography. Significant decrease of theta activity was evident in medial and lateral parts of the cortex above the level of the basal ganglia, and statistically significant increases in alpha activity were observed in the posterior cortices. The patients' decreased theta and increased alpha tomographic activities were in accord with their EEG/QEEG changes and consistent with the clinical outcomes including seizure remission. This study provides preliminary evidence for a medical model that can be empirically tested.

P041. High Temporal Resolution EEG in EEG-fMRI Investigation of Epileptiform Brain Activity

S.J. Vogrin^{1,2}, S. Lau^{1,2,3,4}, and M.J. Cook^{1,2}

¹Department of Medicine, St. Vincent's Hospital, University of Melbourne, Fitzroy, Queensland, Australia.

²Centre for Clinical Neurosciences & Neurological Research, St. Vincent's Hospital Melbourne, Fitzroy, Queensland, Australia

³Institute for Biomedical Engineering and Informatics, Technical University Ilmenau, Ilmenau, Germany.

⁴NeuroEngineering Laboratory, Department of Electrical and Electronics Engineering, University of Melbourne, Parkville, Queensland, Australia.

Localizing the source of seizures from cortical activity observed in electroencephalogram (EEG) is common clinical practice. However, the features of the reconstructed source can be significantly impacted by the quality of the EEG signal recorded. Simultaneous EEG-fMRI offers unique insights from two independent modalities, but is hampered by the sensitivity of the EEG to artifact sources caused by interactions of electrodes and cables with the strong magnetic fields, both static and rapidly switching gradients. We aimed to acquire the EEG at higher temporal and spatial resolution to improve the characterization of these artifacts for subsequent signal processing and clinical review toward more accurately defining epileptiform discharges and seizures.

High-density EEG-fMRI using a 128-channel Maglink system (Compumedics Neuroscan, Charlotte, NC) was performed on a 3T Skyra MRI scanner in a 32-channel head coil (Siemens, Erlangen, Germany). EEG data were sampled at 20 kHz, with a bandwidth of DC-3500 Hz (-6 dB/Oct) and synchronization of the EEG amplifier to the MR clock ensuring time locked sampling of the gradient artifacts during the EPI sequence. Electrodes with high impedances were excluded from further analysis. PCA projection artifact removal was performed using Curry Neuroimaging Suite 7 (Compumedics Neuroscan, Hamburg, Germany) prior to average artifact subtraction using a rolling average and no digital filtering was applied to directly assess efficiency of artifact subtraction. A control EEG was recorded in an electrically shielded room of the same participant with the same cap preparation to rule out hardware-related artifact sources.

Unfiltered MR gradient switching artifacts showed peak spectral power centered on 772 Hz and notable power for third and fifth harmonics. MRI gradient subtraction techniques per channel provided significant reduction of these artifacts revealing that residual variability arose from high electrode impedances and spectral profiles from individual electrodes relative to their position within the MRI head coil. The variability in EPI artifact morphology can be classified into systematic and subject-dependent sources.

The higher power residual harmonics could be clearly attributed to the EPI artifact and removed, preventing aliasing of these components onto clinically relevant EEG bands used for display of epileptiform spike activity. High temporal sampling

of the EEG can improve detection, classification and characterization of clinically relevant waveform morphologies as well as subsequent localization of cortical and subcortical generators of abnormal activity.

P042. Detecting Interictal Epileptic Discharges With Total Activation

F.I. Karahanoglu^{1,2}, F. Grouiller², C. Caballero-Gaudes³, M. Seeck⁴, S. Vulliemoz⁴, and D. Van De Ville^{1,2}

¹Institute of Bioengineering, École Polytechnique Fédérale de Lausanne, Lausanne, Switzerland

²Department of Radiology and Medical Informatics, Université de Genève, Geneva, Switzerland

³Basque Center on Cognition, Brain and Language, San Sebastián, Spain

⁴Department of Neurology, Université de Genève, Geneva, Switzerland

Electroencephalography (EEG) is one of the most prominent methods to diagnose and monitor epilepsy noninvasively. Interictal epileptic discharges (IEDs) are analyzed to locate possible sources of epileptic activity. However, EEG alone lacks the spatial resolution to localize the sources, therefore simultaneous recording of EEG and functional magnetic resonance imaging (fMRI) is often proposed for presurgical exploration.^{1,2} Conventional methods typically deploy an EEG-informed analysis of the fMRI data; that is, EEG-derived IED onset timings are used to setup regressors for linear regression. Recently we have proposed a new fMRI analysis method, *total activation* (TA), which is able to deconvolve the underlying activity-inducing signal without prior information on the onset timing and duration of events.³ Here, we demonstrate that TA can locate the epileptogenic regions from fMRI data of 5 patients with epilepsy. The fMRI data were acquired by a Siemens 3T TIM Trio MR scanner with gradient echo EPI while resting (eyes-closed). EEG signals were recorded with a 64 MR-compatible EEG cap (EasyCaps, Falk Minnow Services, Herrsching, Germany) according to the 10-20 system. Two patients did not have any epileptic spikes during simultaneous EEG-fMRI; therefore, IED onset timings were driven from the long-term EEG recordings using topographic mapping approach.⁴ TA analysis was performed on the fMRI data; the resulting activity-inducing signals were correlated with the IEDs driven either from the EEG-fMRI or long-term EEG measurements using topographic mapping. Finally, nonparametric hypothesis testing revealed the possible brain regions related to the epileptic activity. We compared our results with conventional methods performed by experts prior to surgery.

Acknowledgments

This work was supported in part by the Swiss National Science Foundation (under grants PP00P2-123438, 310030-132952, 122073, 141165, SPUM 140332) and in part by Center for Biomedical Imaging (CIBM) of the Geneva–Lausanne Universities and the EPFL.

References

1. Gotman J, Kobayashi E, Bagshaw AP, Bénar CG, Dubeau F. Combining EEG and fMRI: a multimodal tool for epilepsy research. *J Magn Reson Imaging*. 2006;23:906-920.
2. Millerand JW, Gotman J. The meaning of interictal spikes in temporal lobe epilepsy: should we count them? *Neurology*. 2008;71:392-393.
3. Karahanoglu FI, Caballero-Gaudes C, Lazeyras F, Van de Ville D. Total activation: fMRI deconvolution through spatio-temporal regularization. *Neuroimage*. 2013;73:121-134.
4. Grouiller F, Thornton RC, Groening K, et al. With or without spikes: localization of focal epileptic activity by simultaneous electroencephalography and fMRI. *Brain*. 2011;134(pt 10):2867-2886.

P043. The Accuracy of Electric Source Imaging in Localizing Epileptic Activity Relative to the Preoperative Gold Standard of Intracranial EEG

L. Spinelli¹, P. Megevand¹, M. Genetti^{1,2}, K. Schaller³, C. Michel², S. Vulliemoz¹, and M. Seeck¹

¹EEG and Epilepsy Unit, Neurology Division, Geneva University Hospital, Geneva, Switzerland

²Basic Neuroscience Division, Geneva University Medical School, Geneva, Switzerland

³Neurosurgery Division, Geneva University Hospital, Geneva, Switzerland

Rationale. Electric source imaging (ESI) of interictal epileptic discharges using high-density EEG is a prospectively validated method to help localizing the epileptogenic zone in candidates for epilepsy surgery. However, its accuracy relative to the preoperative gold standard of intracranial EEG (icEEG) has not been reported. Furthermore, it is debated whether using interictal activity, as ESI does, in order to localize the source of ictal activity is adequate. **Methods.** Retrospective study of 35 candidates to epilepsy surgery who underwent icEEG monitoring. ESI was performed using 125- or 204-electrode EEG, a 3-shell spherical model with anatomical constraints (SMAC) and a distributed linear inverse solution (LAURA). **Results.** The median distance from the ESI maximum to the nearest intracranial electrode involved in an irritative zone (IZ) was 19 mm (interquartile range 12-23 mm), that to the most irritative electrode 30 mm (26-48 mm), that to the nearest electrode in the seizure onset zone (SOZ) 22 mm (14-30 mm). The ESI-to-nearest IZ and ESI-to-maximal IZ distances were strongly correlated with the ESI-to-SOZ distance ($P < .0001$ and $P < .01$, respectively). There were no significant differences in ESI accuracy in patients with medial temporal lobe, lateral temporal lobe, or extratemporal epilepsy. The ESI maximum was included in the resected brain volume more often in patients with favorable postoperative outcome (9 of 18 patients in Engel classes I and II) than in those with unfavorable outcome (1 of 8 patients in Engel classes III and IV; difference in proportions 0.375, 95% confidence interval 0.0278 to 0.6667). Furthermore, the maximal IZ electrode was more often within the resected brain

volume in the patients with favorable outcome (15 of 18 patients) than in those with unfavorable outcome (3 of 8; difference in proportions 0.4583, 95% confidence interval 0.0833 to 0.8194). *Discussion.* Put together, our results indicate that the localization of interictal spikes by ESI closely corresponds to the localization of irritative zones by intracranial EEG; that irritative zones are often part of the seizure onset zone or lie close to it; and that localizing interictal spikes by ESI helps localizing the seizure onset zone. Additionally, including the ESI maximum in the resected brain volume is correlated with favorable postoperative outcome. We propose that future studies on the accuracy of non-invasive methods in localizing epileptic activity report direct measures of localization error with respect to intracranial EEG in addition to the margins of resected brain volume whenever feasible.

P044. Presurgical Functional Mapping in Patients With Epilepsy

M. Genetti¹, R. Tyrand¹, F. Grouiller², S. Vulliemoz³, L. Spinelli³, M. Seeck³, K. Schaller⁴, and C.M. Michel¹

¹Department of Neurology and Fundamental Neurosciences, Geneva University Hospitals, Geneva, Switzerland

²Department of Radiology and Medical Informatics, Geneva University Hospitals, Geneva, Switzerland

³Department of Neurology, Geneva University Hospitals, Geneva, Switzerland

⁴Department of Neurosurgery, Geneva University Hospitals, Geneva, Switzerland

Aims. Despite its invasiveness, electrocortical stimulation (ECS) remains the gold standard for the localization of crucial areas in presurgical planning of epileptic patients. To overstep the limitations of ECS (epileptic afterdischarges, several hours of testing, collaboration of the patients), additional functional brain mapping methods have emerged as reliable tools for building a preliminary functional map: functional magnetic resonance imaging (fMRI), time-frequency analysis and evoked potentials based on electrocorticographic (ECoG) recordings. This study investigates their respective contribution to the preliminary functional map in the left hemisphere in relation to extraoperative ECS and the surgical outcome. *Methods.* We recorded subdural ECoG during an auditory semantic decision task in twelve patients with intractable epilepsy. We compared language areas in the left hemisphere suggested by ECoG power in the gamma band (70-160 Hz) with that suggested by ECoG evoked potentials, fMRI ($n = 8$) on the same task, and by ECS. *Results.* Electrocortical stimulation could not identify any language-related sites in 5/12 patients. Language-related changes in ECoG gamma power were found in 10/12 patients. In one left-handed patient (familial sinistrality), the lack of language-related gamma site was consistent with ECS and fMRI. Across the ten patients with language-related gamma responses, on average 6 electrode sites showed significant

gamma activity. We found significant evoked potentials sites (11, on average) in all but one ambidextrous patient and fMRI-related sites (10, on average) in 7/8 patients. The sensitivity and specificity of gamma activity ($n = 6$) with respect to ECS were 41% and 85%, respectively, whereas those of evoked potentials ($n = 7$) were 30% and 72%. Furthermore, the sensitivity and specificity of fMRI ($n = 5$) was 63% and 75%, respectively. Postsurgical MRI revealed that language-related sites (all modalities) were spared by the resection in 8/12 patients: 6 showed no deficit, 2 had slight transient language impairments (verbal fluency and naming). Resection included language-related sites in 4/12 patients: 1 showed no deficit, 2 had moderate language impairments, and 1 had moderate to severe language impairments also due to surgical complications. *Conclusion.* These results suggest that fMRI together with time-frequency analysis of ECoG can be a reliable complementary tool for presurgical language mapping, particularly when ECS results are missing. This enables a shorter and more flexible functional mapping by delineating the electrode sites of interest for ECS.

P045. Quadrimodal Localization of Epileptic Focus Using Simultaneous EEG, MRI, and PET Imaging

F. Grouiller¹, S. Heinzer², B. Delattre², F. Lazeyras¹, L. Spinelli³, F. Pittau³, M. Seeck³, O. Ratib¹, M. Vargas¹, V. Garibotto¹, and S. Vulliemoz³

¹Department of Radiology and Medical Informatics, Geneva University Hospital, Geneva, Switzerland

²Philips Healthcare, Zurich, Switzerland

³EEG and Epilepsy Unit, Department of Neurology, Geneva University Hospital, Geneva, Switzerland

Background. In patients suffering from pharmaco-resistant focal epilepsy, resection of the epileptic focus can lead to seizure-freedom or significant improvement in most well-selected cases. The localisation of the epileptic focus relies on structural and functional brain imaging and multimodal concordance is associated with a better postoperative outcome. The existence of epileptogenic lesions detectable on structural MRI and the presence of focal hypometabolism on FDG-PET, especially after fusion with MRI are widely accepted localizing findings. In addition other tools for localising epileptic activity, such as EEG-based electric source imaging (ESI) and simultaneous EEG and functional MRI (EEG-fMRI) are increasingly used. We here report combined EEG-PET, MRI, EEG-fMRI, and ESI based on data recorded in a single session using high-density EEG (Electrical Geodesics Inc.) and a PET-MRI hybrid scanner (Philips Ingenuity TF PET/MR) in 6 patients with pharmaco-resistant epilepsy.¹ *Methods.* An MR-compatible high-density (256 electrodes) EEG system was used for EEG-fMRI and for excluding subclinical seizures during uptake of the PET tracer (FDG). The structural MRI was performed after removal of the EEG cap for allowing the full epilepsy imaging protocol and improving comfort. ESI on interictal epileptiform discharges used an individual

head model and a distributed inverse solution.² Haemodynamic changes correlated to interictal epileptiform discharges or to the presence of epileptic-specific EEG topography were mapped using EEG–fMRI.³ **Results.** The whole multimodal recording could be performed in 2 hours of scanner time. In 4 patients we obtained concordant focal results of at least 2 modalities that were also concordant with electroclinical ictal semiology of unilateral temporal lobe epilepsy. In one patient with a posterior cingulate cavernoma, multimodal imaging was concordant with an epileptogenic zone in the same localisation. In one patient, multimodal imaging allowed to diagnose generalised epilepsy despite localising EEG features. **Discussion.** This single-session quadrimodal imaging provided reliable interictal clinical data with reduced scanning time and good patient comfort. This procedure avoids multiple scanning sessions and markedly improves the workflow of presurgical epilepsy evaluations. Irradiation was reduced compared to the use of PET–CT. Additional functional mapping of eloquent cortex (motor, language) could be added in individual cases with little duration increase.

Acknowledgments

We acknowledge the financial support of the Swiss National Science Foundation (No. 33CM30-140332 and 320030-141165).

References

1. Garibotto V, Heinzer S, Vuilleumoz S, et al. Clinical applications of hybrid PET/MRI in neuroimaging. *Clin Nucl Med*. 2013;38:e13–e18.
2. Brodbeck V, Spinelli L, Lascano AM, et al. Electroencephalographic source imaging: a prospective study of 152 operated epileptic patients. *Brain*. 2011;134(pt 10):2887–2897.
3. Grouiller F, Thornton RC, Groening K, et al. With or without spikes: localization of focal epileptic activity by simultaneous electroencephalography and fMRI. *Brain*. 2011;134(pt 10):2867–2886.

P046 Strategies to Optimize EEG Quality During EEG–fMRI in Severe Childhood Epilepsies.

S.J. Vogrin¹, C.A. Bailey², M. Kean¹, A.E. Warren⁴, A. Davidson⁵, M. Seal^{1,2}, A.S. Harvey^{2,3}, and J.S. Archer⁴

¹Developmental Imaging, Murdoch Children's Research Institute, Parkville, Queensland, Australia.

²Department of Neurology, Royal Children's Hospital, Parkville, Queensland, Australia

³Department of Paediatrics, University of Melbourne, Parkville, 3052, Australia

⁴Department of Medicine, Austin Health, University of Melbourne, Parkville, Queensland, Australia

⁵Department of Anaesthesia, Royal Children's Hospital, Parkville, Queensland, Australia

Background. Characterizing the source of seizure activity in epilepsy is central to accurately describing epilepsy syndromes and choosing suitable treatments. In young children, the immature brain is associated with EEG waveforms that vary significantly from adults. In symptomatic generalised epilepsies like the

Lennox–Gastaut syndrome, morphologically unique discharges are interspersed continuously throughout the EEG recording complicating clinical review of subtle differences and isolating superimposed features. Simultaneous EEG–fMRI provides an opportunity to investigate electrical and hemodynamic changes across widespread cerebral regions involved with these scalp electrical phenomena. However technical artifacts can impact reliable discrimination of such differences. Our aim was to better define EEG–fMRI artifacts prior to discriminating complex interictal epileptiform discharges (IEDs). **Methods.** We performed simultaneous EEG–fMRI on 15 children lightly anesthetized with remifentanyl and <0.7% isoflurane, in a Siemens 3T Trio MR scanner using a 32-channel headcoil and a 64-channel cap Maglink system (Compumedics Neuroscan, Australia). EEG data were sampled at 5 kHz, during continuous EPI acquisition with 64 × 64 matrix × 44 slices, EPI repetition time 3200 ms, and EEG clock synchronization to MRI scanner. Removal of MR gradient and ballistocardiogram artifacts performed using a combination of PCA Projection and Average Artifact Subtraction, in Curry 7 (Compumedics Neuroscan, Germany). Postcorrected EEG artifacts were assessed with and without band-pass filtering at 1 to 100 Hz. **Results.** The spectral power of residual artifacts from MR gradient switching predominated above 600 Hz; however, the fundamental frequency and harmonics of the slice repetition frequency remained at ~14Hz when assessing EEG mean global field power. Individual spectra of EEG channel artifacts demonstrated a correlation of residual higher power with high impedances, but efficient removal at low impedances. **Discussion.** Anesthetized EEG–fMRI offers improved EEG quality, and less motion artifacts in fMR images through reduced subject motion. Retaining more EEG frequencies ensures capture of higher order harmonics to improve discrimination of other sources from faster cerebrally generated transient and oscillatory activity. Characterising EEG–fMRI artifacts with sufficiently temporally sampled data and greater bandwidth increases confidence during review and classification of all discharge types, allowing more accurate fMRI regressors for investigating hemodynamic correlates of complex IEDs in severe childhood epilepsies.

P048. Strategies for the Application of DCM to Intracranial EEG in Epilepsy

M. Papadopoulou¹, M. Leite², P. van Mierlo³, K. Vonck⁴, P. Boon⁴, K. Friston⁵, and D. Marinazzo¹

¹Department of Data Analysis, Faculty of Psychology and Pedagogical Sciences, Ghent University, Ghent, Belgium

²UCL Institute of Neurology, Department of Clinical and Experimental Epilepsy, London, UK

³Medical Image and Signal Processing Group, Electronics and Information Systems Department, Ghent University, Ghent, Belgium

⁴Laboratory for Clinical and Experimental Neurophysiology, Ghent University Hospital, Ghent, Belgium

⁵The Wellcome Trust Centre for Neuroimaging, University College London, London, UK

Dynamical causal modeling (DCM) is used to infer connectivity patterns from intracranial EEG (iEEG) recordings from a patient with refractory epilepsy. DCM provides posterior estimates of neurobiological interpretable quantities, which can shed light on which neuronal populations and which connections among them result in specific features and patterns in the data. DCM is mainly used as a confirmatory method, and a specific range of hypotheses needs to be formulated. For this patient, the presurgical evaluation based on invasive EEG monitoring highlighted the left hippocampus as the putative epileptogenic focus. We use this information to confine the regions of interest and to extract smaller networks of these interconnected regions on which DCM models have been applied.

The considered patient is implanted bilaterally with intracranial electrodes: 2 amygdalo-occipital depth electrode and 2 subdural strips over the anterior temporo-basal, the posterior temporo-basal and the temporo-lateral brain region.

We build 2- and 3-node networks where the nodes in this case are the recording sites of iEEG. For this study we focus our analysis on recorded electrodes of the left hemisphere, mainly the contacts of the depth electrode which covers the ictal onset zone localized by an experienced team of neurologists.

Coherence analysis initially conducted on segments of 2 seconds before and during the seizure revealed information on how dependent or not the different recorded neighboring regions are, and how this relationship is modulated in those different segments. DCM analysis is then applied on the same segments providing further information not only on how the time series corresponding to each recorded node are coupled/decoupled at preictal/ictal states, but also on the connections and on the cortical hierarchy of the neural populations associated with them. This information might be crucial for the investigation of putative seizure pathways and to provide hypothesis of the neuronal mechanism which originates the seizure.

P049. Increased Phase Clustering in Epileptogenic Areas Measured With dEEG

C. Ramon^{1,2} and M. Holmes³

¹Department of Electrical Engineering, University of Washington, Seattle, WA, USA

²Department of Bioengineering, Reykjavik University, Reykjavik, Iceland

³Department of Neurology, University of Washington, Seattle, WA, USA

Our objective was to examine if spatial phase clustering patterns are different in epileptogenic zones which can be used to localize epileptogenic areas from high-density interictal scalp EEGs. We studied one patient with refractory epilepsy who underwent intracranial EEG to establish the localization of seizures. This subject had seizures in midline frontal and parietal areas. Prior to invasive EEG studies the subject underwent dense array 256-channel EEG (dEEG) recordings. Three minutes of interictal dEEG data from first day was selected for analysis. The selected segment was at least 2 hours from an epileptic seizure and, based on visual analysis, free

of interictal epileptiform patterns. Excessively noisy channels were removed and replaced with averages of surrounding electrodes. Data were imported into MATLAB for analysis. The EEG data were filtered in the low gamma (30-50 Hz) band. The phase was computed after taking Hilbert transform of the EEG data. Contour plots with 4-ms intervals were constructed using a montage layout of 256 electrode positions. Spatial plots did show formation of cone-like structures which changed in spatial shapes from one frame to the next. Also, the peak intensity varied from one frame to the next. In general, more stronger and stable patterns were observed in the seizure area as compared with nearby surrounding brain areas. A clustering of spatial patterns was also observed which was more dense in the seizure areas as compared with nearby surrounding areas. These preliminary results show that the spatiotemporal dynamics and clustering of phase cone patterns have a potential to localize the epileptic sites from the scalp dEEG data.

P050. Electrical Source Imaging: An Aid to Localize the Epileptogenic Zone in the Cortical Malformations

L. Koessler¹, E. Rikir², M. Gavaret³, F. Bartolomei³, J.P. Vignal⁴, H. Vespignani⁴, and L. Maillard¹

¹CRAN, CNRS UMR 7039, Nancy, France

²Centre Hospitalier Universitaire de Liège, Liège, Belgium

³INS, UMR 1106, Marseille, France

⁴Centre Hospitalier Universitaire de Nancy, Nancy, France

Malformations of cortical development (MCD) are frequently associated with drug-resistant epilepsy. Although increasingly recognized using high-resolution MRI and scalp EEG (typical dysplastic fast activity), localizing the epileptogenic zone (EZ) associated with MCD still relies on intracerebral EEG recordings. Our purpose was to study the spatial correlations between the modeled electrical sources of interictal events (irritative zone = IZ) recorded with high-resolution scalp EEG (HR-EEG) and the EZ defined by stereo-EEG (SEEG) in MCD.

This prospective, bicentric study enrolled 30 consecutive patients (26 in Nancy and 4 in Marseille) with established or suspected MCD undergoing pre-surgical investigations between 2008 and 2012 and comprising a HR-EEG (64 channels) with electrical source imaging using 3 different inverse problem methods (equivalent current dipole, MUSIC, and sLORETA). Stereo-EEG (SEEG) recordings using multicontact depth electrodes implanted in the brain were used in this study as the reference method.

Three patients were excluded from the analysis because of missing data (no SEEG seizure recording in 2 cases and no HR-EEG interictal paroxysm registration in 1 case).

The mean age at the time of SEEG recordings was 28 years. Twelve out of 27 patients (44%) had temporal lobe epilepsy (TLE), 15 (55%) had extratemporal lobe epilepsy: 11 frontal lobe epilepsy (FLE) and 4 posterior epilepsy including occipito-temporal or posterior parietal epilepsy. The structural MRI

was negative in eleven patients (41%) and showed a structural lesion suggesting a MCD in 16 patients (59%): a focal cortical dysplasia (type I or II FCD) in 6, a dysembryoplastic neuroepithelial tumor (DNE) in 4, a schizencephaly and polymicrogyria (SCZ/PMG) in 3, a ganglioglioma in 2 and a Bourenville's tuberous sclerosis (BTS) in a single case.

ESI-IZ co-localized with the EZ in 10 patients (37%) and 7 of them were MRI negative. ESI-IZ and SEEG-EZ were completely or more often partially overlapping in 92.5% (25/27). In 6 cases, ESI-IZ completely included and extended to the propagation zone in 4/6. ESI-IZ was completely included in SEEG-EZ in 3, and partially overlapped the SEEG-EZ in 6. In these cases, ESI often missed the medial part of the EZ.

In negative MRI subgroup ($n = 11$), ESI-IZ was perfectly concordant with SEEG-EZ in 63.6% (7/11), never discordant and partially concordant in 4 patients.

Concerning the inverse problem method: rotating dipoles localize correctly in 93%, sLORETA in 81%, moving dipole and MUSIC in 75%.

Electrical source imaging (ESI) helps localize and target the EZ in MCD with a concordance of 92.5% and a perfect concordance of 37%. All inverse problem methods gave at least 75% of precise source localizations. One important point is that ESI compared with depth EEG recording is quite rare in the literature (Koessler et al., 2010). ESI is particularly relevant in MRI negative cases where the at least partial concordance is 100% and the perfect concordance 64%.

P052. Default Mode Network Dysfunction in a Patient With Epilepsy in the Precuneus

M. Centeno¹, S. Perani¹, K. St Pier², L. Lemieux³, J. Clayden¹, C. Clark¹, R. Pressler², H. Cross^{1,2}, and D.W. Carmichael¹

¹Imaging and biophysics, UCL Institute of Child Health, London, UK

²Epilepsy Unit, Great Ormond Street Hospital NHS Foundation Trust, London, UK

³Department of Clinical and Experimental Epilepsy. UCL Institute of Neurology, London, UK

Background. Default mode network (DMN) deactivations have been reported in patients with epilepsy associated with ictal and interictal activity.¹ This network is involved in cognitive processes and conscious rest.² Failure to suppress the DMN during a task is associated with poor performance.³ Here, we investigated a patient with focal epilepsy located in the precuneus, a key hub within the DMN. We used EEG–fMRI to compare areas involved in interictal epileptiform discharges (IEDs) and analysed the functional connectivity of the DMN during rest and an attention-directed task. **Methods.** A 17-year-old male with focal epilepsy was studied. MRI showed an abnormality in the right precuneus. Ictal onset on scalp and intracranial EEG confirmed the epileptic focus location to right precuneus. Postsurgical tissue analysis revealed focal cortical dysplasia. Seizures recurred after surgery. Four EEG–fMRI sessions were recorded in 1.5-T MRI. During 2/4 sessions a paradigm was shown with alternat-

ing blocks of movie and rest. For the remaining sessions the patient was told to rest with eyes closed. The same EEG–fMRI protocol was repeated in 8 controls. Three types of analyses were applied: (a) Visually identified IEDs were entered into a general linear model (GLM) using SPM8 along with movement and cardiac confounds. IED-related BOLD responses were found with an F-test across all 4 sessions. (b) The paradigm blocks were entered into a GLM using SPM8. Attention-directed task responses were found in each individual and then entered in a second level analysis to compare responses between the patient and controls. (c) The DMN was separated using independent component analysis as implemented in FSL. DMN connectivity compared both between sessions and between controls and the patient. **Results.** EEG–fMRI IED-correlated analysis revealed areas of significant ($P < .001$ unc) BOLD change in the right precuneus concordant with the epileptic focus. During the movie periods, the patient showed activation of the DMN in addition to the attention networks differently that the control group ($P < .05$ FWE). Patient's functional connectivity of DMN was increased within the network and to other cognitive networks during rest and the task. **Conclusion.** EEG–fMRI revealed a focus consistent with other localisation methods and also suggested a wider extent of FCD than was resected consistent with the outcome. In a patient with an abnormality in the right precuneus we observed an aberrant activation of the DMN network in response to a task. Characterization of the dysfunction of DMN in a patient with epilepsy in one of the key nodes of this network may help us to understand its role and relationship to IEDs.

References

1. Laufs H, Hamandi K, Salek-Haddadi A, Kleinschmidt AK, Duncan JS, Lemieux L. Temporal lobe interictal epileptic discharges affect cerebral activity in "default mode" brain regions. *Hum Brain Mapp.* 2007;28:1023-1032.
2. Voets NL, Beckmann CF, Cole DM, Hong S, Bernasconi A, Bernasconi N. Structural substrates for resting network disruption in temporal lobe epilepsy. *Brain.* 2012;135:2350-2357.
3. Raichle ME, Snyder AZ. A default mode of brain function: a brief history of an evolving idea. *Neuroimage.* 2007;37:1083-1090.

P053. Interictal Localization of the Seizure Onset Zone Using High-Frequency Oscillations and Visibility Graphs

A. Spring¹, R. Bessemer¹, D. Pittman¹, Y. Aghakhani^{1,2}, P. Federico^{1,2,3}

¹Hotchkiss Brain Institute, University of Calgary, Calgary, Alberta, Canada

²Department of Clinical Neurosciences, University of Calgary, Calgary, Alberta, Canada

³Department of Radiology, University of Calgary, Calgary Alberta, Canada

Rationale. High-frequency oscillations (HFOs) in the ripple (80-250 Hz) and fast ripple (250-500 Hz) ranges are hypothesized to reflect increases in neural synchrony. In epileptic syndromes, this increase is pathological, and localized to the

seizure onset zone. Interictal HFOs have been proposed as a marker for the identification of the seizure onset zone. Recently, the graph index complexity (GIC) of visibility graphs has been introduced as a measure of HFOs, and has been shown to increase ictally at the seizure focus. However, the properties of the GIC have yet to be investigated interictally. **Methods.** The interictal intracranial electroencephalograms of 4 patients with focal epilepsy were analyzed during 5 to 10 minutes of continuous slow-wave sleep. The data were bandpass filtered for ripples and labeled using an automated detection algorithm: The filtered data were normalized by the root mean square of a sliding 1-second epoch, and ripples were identified wherever the signal exceeded a threshold of 3 standard deviations from the mean during a minimum of 6 consecutive half-cycles. A visibility graph was constructed for each 1-second epoch of the filtered time series, with a one half overlap. The GIC was calculated from each visibility graph, resulting in a time series of GIC values for each channel. The channels corresponding to the seizure onset zone were identified clinically. The mean GIC and number of ripples per minute (ripple rate) for all channels within the seizure onset zone, as well as the mean for all channels without, were calculated for each patient. A paired-sample *t* test was performed to determine whether the GIC and ripple rate were greater within the seizure onset zone across patients. **Results.** The mean ripple rate for each channel group ranged from 1.32 to 27.93 ripples/min, and was significantly greater for channels within the seizure onset zone in all patients, with a mean difference between the seizure onset zone and other channels of 10.81 ripples/min ($P = .0267$). The mean GIC values for each channel group ranged from 0.0228 to 0.0306, and was significantly greater for channels within the seizure onset zone in all patients, with a mean difference of 0.0023 ($P = .0143$). **Conclusions.** The rate of ripple occurrence and the GIC of visibility graphs exhibited similar behaviour during slow wave sleep. Both measures of high frequency oscillations were significantly greater at the seizure onset zone in all patients during interictal slow-wave sleep. Therefore, both the identification of ripple events and the calculation of the GIC from visibility graphs may be useful in the localization of the seizure onset zone in patients with focal epilepsy.

P054. Regional Homogeneity in Mesial Temporal Lobe Structures Affected by Epilepsy

F. Pittau¹, F. Grouiller¹, S. Vulliémot¹, and J. Gotman²

¹Unité d'EEG et d'exploration de l'épilepsie, Service de Neurologie/Hôpitaux Universitaires de Genève, Geneva, Switzerland

²Montreal Neurological Institute, McGill University, Montreal, Quebec, Canada

Rationale. Regional homogeneity (ReHo) measures the degree of regional coherence of BOLD (blood oxygen level dependent) time courses in different brain regions. In unilateral mesial temporal lobe epilepsy (MTLE) the epileptogenic area is

confined to the mesial temporal structures of one side. The aim of this study is to compare ReHo of the affected mesial temporal structures of a group of MTLE patients during the interictal period with the unaffected ones and with the homologous areas of a group of healthy control subjects. **Methods.** We selected electroencephalography–functional magnetic resonance imaging (EEG–fMRI) resting state data without EEG spikes from 16 patients with right and 7 patients with left MTLE. EEG–fMRI resting state data of 23 healthy subjects matched for age, sex, and manual preference were selected as controls. Four volumes of interest in the left and right amygdalae and hippocampi (LA, RA, LH, and RH) were manually segmented in the anatomic MRI of each subject. fMRI preprocessing included realignment, coregistration, segmentation, normalisation. REST toolbox of SPM12 was used to calculate ReHo in each seed. Group differences between patients and controls were estimated. **Results.** ReHo of the affected hippocampus, but not of the amygdala, was higher than one in the unaffected side ($P = .034$), whereas there were no statistically significant differences between affected hippocampus/amygdala of the MTLE and the hippocampus/amygdala of the healthy control group. **Conclusions.** Affected hippocampus in unilateral MTLE has a higher level of BOLD coherence compared to the healthy one. This finding can reflect the hyper synchronous neuronal activity found by intracranial electroencephalography in the hippocampus of MTLE patients.

P055. Localization of Ictal Events in MEG With BeamForming Techniques

J.M. Badier^{1,2}, C.-G. Bénar^{1,2}, F. Bartolomei^{1,2,3}, C. Cruto^{2,3,4}, P. Chauvel^{1,2,3}, and M. Gavaret^{1,2,3}

¹INSERM UMR 1106, Institut de Neurosciences des Systèmes, Marseille, France

²Aix-Marseille Université, Faculté de Médecine, Marseille, France

³Service de Neurophysiologie Clinique, AP-HM, Hôpital de la Timone, Marseille, France

⁴Service de Neurologie, Centro Hospitalar do Porto, Porto, Portugal

Background. Analysis of interictal activity with MEG has been proven to be an efficient tool in the presurgical investigation of epileptic patients. Because of constraints such as immobility, MEG is not the technique of choice for recording ictal activity. However, ictal events can incidentally be recorded during MEG investigations. In these cases, if movement at the beginning of seizure is sufficiently small, source localization could provide important information on the epileptogenic zone. However, the standard “equivalent current dipole” (ECD) may not be the most practical technique for localizing the origin of this activity. **Aims.** Our goal was to evaluate beamforming techniques in the temporal domain (LCMV) for the localization of ictal events recorded with MEG. **Material and methods.** MEG ictal recordings were obtained for 9 patients with pharmacoresistant partial epilepsy, using a whole head 248-channel biomagnetometer

system (4D neuroimaging). Six of them were under presurgical evaluation. For 3 other patients, MEG seizures were recorded after a first epilepsy surgery. Different localization strategies have been applied. The results of the localizations have been compared with intracerebral SEEG recordings. For LCMV, we investigated the impact of baseline selection and time window of analysis. Frequency localization has been performed after time/frequency transform of the signals. *Results and conclusion.* We have shown that beamforming techniques can be used in order to localize the ictal activity, whereas ECD technique failed. In all patients but one, localizations were in agreement with the information obtained from SEEG recordings.

P060. Additional Topographic Feature in Resting-State EEG of Grapheme Colour Synaesthetes: EEG Microstates in Source Space

V. Brodbeck¹, T. van Leeuwen², E. Tagliazzuchi¹, L. Melloni^{2,3}, H. Laufs^{1,4}

¹Brain Imaging Center, Department of Neurology, University of Frankfurt am Main, Frankfurt am Main, Germany

²Max Planck Institute for Brain Research, Frankfurt am Main, Germany

³Department of Psychiatry, Columbia University, New York, NY, USA

⁴Neurology Department, University of Kiel, Kiel, Germany

Purpose. In synaesthesia, specific sensory stimuli (eg. graphemes) inevitably lead to unusual, additional sensations (eg. color). Whether the neural mechanisms are rather structural or functional is under debate.^{1,2} Few EEG studies exist examining synaesthesia. Here, we used EEG microstate analysis of spontaneous EEG at rest and applied a new approach using source analysis of EEG microstates. *Methods.* EEG recordings at wakeful rest (30 channels, 3 minutes, eyes closed) of 17 grapheme-color synaesthetes and 16 matched nonsynaesthetes were analysed using an EEG microstate approach.³ Number of cluster maps, map topographies and microstate parameters after fit-back of cluster maps into the EEG were compared between the 2 groups. As a new methodological approach we calculated source estimations (LAURA) of timeframes with very high (>0.9) spatial correlation of each cluster map and averaged these source estimates for each subject and each cluster map, allowing to contrast corresponding maps' source estimations between the 2 groups (2-sample *t* test). *Results.* Synaesthetes showed overall higher numbers of optimal cluster maps at the individual level. On the group level, the common 4 standard map topographies were present in both groups, synaesthetes however showed a fifth cluster map, which was not identified in controls. Mean duration of microstates did not differ between the groups. Contrasting of corresponding source estimations led to significant differences for all 4 standard maps ($P < .05$). Fitting the 5 synaesthesia cluster maps into both groups and contrasting the corresponding sources revealed significant differences only for the synaesthesia specific fifth map. Differences

were present in right dorsolateral prefrontal cortex (stronger source estimates for synaesthetes). *Discussion.* Synaesthetes show an additional topographic feature in spontaneous EEG at wakeful rest. As these results are present in the absence of any task, they support the hypothesis that structural differences are the basis of synaesthetic experiences, rather than altered processing of incoming stimuli. The identified differences in source space in right dorsolateral prefrontal cortex might indicate involvement of higher cognitive functions.

Acknowledgments

This study was funded by LOEWE-Neuronale Koordination Forschungsschwerpunkt Frankfurt (NeFF).

References

1. Rouw R, Scholte HS, Colizoli O. Brain areas involved in synaesthesia: A review. *J Neuropsychol.* 2011;5:214-242.
2. Mulvenna CM, Walsh V. Synaesthesia: supernormal integration? *Trends Cogn Sci.* 2006;10:350-352.
3. Brodbeck V, Kuhn A, von Wegner F, et al. EEG microstates of wakefulness and NREM sleep. *Neuroimage.* 2012;62:2129-2139.

P061. Twenty-Hertz Auditory Steady-State Response: Should Subject's Age Be Taken Into Account?

I. Griskova-Bulanova¹ and K. Dapsys^{1,2}

¹Department of Neurobiology and Biophysics, Vilnius University, Vilnius, Lithuania

²Department of Electrophysiological Investigations and Treatment Methods, Republican Vilnius Psychiatric Hospital, Vilnius, Lithuania

The physiological significance of 40-Hz activity that is generated along with 20-Hz auditory steady-state responses (ASSRs) in response to 20-Hz periodic auditory stimulation was recently stressed out. As this activity, further termed 20-Hz ASSR-related 40-Hz activity, is frequently analyzed together with 20-Hz ASSRs and 40-Hz ASSRs in various experimental conditions, it is tempting to evaluate its relationship to subjects' age. Thus, it is aimed to identify the effects of aging on phase-locking of 20-Hz ASSR and 20-Hz ASSR-related 40-Hz activity and to compare it with 40-Hz ASSR results.

The effect of aging was tested in a sample of 45 healthy male subjects (20-57 years old, divided into 4 groups: 20-30 years, 30-40 years, 40-50 years, 50-60 years) during eyes closed condition. Auditory stimuli were click trains, made of brief white noise bursts, which were presented pseudorandomly in trials of 20 Hz and 40 Hz for 500 ms with intertrial intervals of 1 to 3 seconds. Phase-locking index values, as measured after wavelet transform, were decomposed by nonnegative multiway factorization for 100-ms duration windows to assess temporal dynamics and evaluate the relation to aging.

The temporal dynamics of the responses did not differ between the age-groups. However, in disagreement with previously published data, phase-locking index of 40-Hz ASSR was

diminishing with age. The same was observed for 20-Hz ASSR-related 40-Hz activity—phase-locking index diminished with increasing age of the subjects. No effect of aging was seen for 20-Hz ASSRs.

It is concluded that phase-locking measures of brain's ability to synchronize to external periodic stimulation at 40-Hz frequency and to generate 40-Hz activity in response to 20-Hz stimulation diminishes with increasing age. Additionally, similar modulation of 40-Hz ASSR and 20-Hz ASSR-related 40-Hz activity by aging, confirms the physiological importance of 40-Hz responses elicited by periodic auditory stimulation at 20-Hz.

References

1. Griskova I, Morup M, Parnas J, Ruksenas O, Arnfred SM. Two discrete components of the 20 Hz steady-state response are distinguished through the modulation of activation level. *Clin Neurophysiol.* 2009;120:904-909.
2. Griskova-Bulanova I, Ruksenas O, Dapsys K, Maciulis V, Arnfred SM. Distraction task rather than focal attention modulates gamma activity associated with auditory steady-state responses (ASSRs). *Clin Neurophysiol.* 2011;122:1541-1548.
3. Poulsen C, Picton TW, Paus T. Age-related changes in transient and oscillatory brain responses to auditory stimulation in healthy adults 19-45 years old. *Cereb Cortex.* 2007;17:1454-1467.

P062. The Influence of a High-Density EEG Cap on T1- and T2*-Weighted MR Images

C. Klein¹, J. Hänggi¹, and L. Jäncke¹

¹Division of Neuropsychology, Institute of Psychology, University of Zurich, Zurich, Switzerland

Magnetic resonance imaging (MRI) techniques as well as electroencephalographic (EEG) measurements are well established and widely used in the field of clinical and cognitive neuroscience. Bringing together these two imaging methods to benefit from both the high spatial resolution of the MRI and the high temporal resolution of the EEG has gained increasing interest and advantages in the past few years.

Much effort has been spent to develop an algorithm aimed at successfully cleaning EEG data from MRI-related ballistocardiological and gradient artefacts.

However, previous studies have also shown that the EEG has a negative influence on MRI data quality. In particular, the interaction of the magnetic field and the EEG channels leads to susceptibility artefacts, which create magnetic field inhomogeneities and hence cause a signal loss or dropout in the MRI data, especially in parietal areas. To the best of our knowledge, with this study we provide first evidence on the influence of a high-density EEG net on T1- and T2*-weighted (echoplanar) images at 3 T. The evaluation of the signal-to-noise ratio (SNR) for both the structural and functional images revealed a consistently higher value for the measurements of subjects not wearing an EEG cap compared with when wearing the net, whereas regions of activity were comparable with and without the EEG net. In addition, the results also show an intense influence of the

EEG cap on cortical thickness measurements derived from surfaced-based morphometry. In summary, our findings strongly advise against the measurement of T1-weighted images simultaneously with EEG, despite the benefit in MRI preprocessing and for reasons of time.

Acknowledgments

Supported by SNF Sinergia Grant No. 136249.

P063. I Like to Move it (Move It): EEG Correlates of Mobile Spatial Navigation

B.V. Ehinger¹, P. Fischer¹, A.L. Gert¹, L. Kaufhold¹, F. Weber¹, M. Marchante Fernandez¹, G. Pipa¹, and P. König^{1,2}

¹Institute of Cognitive Science, University of Osnabrück, Osnabrück, Germany

²Institute of Neurophysiology and Pathophysiology, University Medical Center Hamburg-Eppendorf, Hamburg, Germany

In everyday life navigation, active movement generates visual, vestibular, and kinesthetic information. Yet, studies of human orientation commonly employ stationary setups with obvious consequences on vestibular and kinesthetic feedback. Here, we demonstrate a fully immersive virtual reality with systematic control of vestibular and kinesthetic information combined with high density mobile EEG to investigate cortical processing in a spatial navigation task.

The experiment is based on a modified triangle completion task: Participants traversed one leg of a triangle, did an on-the-spot-turn and continued along the second leg. They then had to point back to their starting position with a virtual arrow that was presented in front of them. We employed a 2 × 2 intra-subject design, manipulating vestibular and kinesthetic information. The 128-electrode EEG data of all subjects (n = 5) were analyzed by clustering blind source separated independent components (ICs) dipoles with their respective event-related spectral perturbations (ERSP).

We select 9 IC clusters, partially replicating earlier studies, localized in occipital, parietal, motor, and frontal areas. Occipital clusters A and B show specific desynchronization in alpha band frequencies during the turn compared with the first straight segment. These clusters show the strongest effect in the vestibular condition. The medial parietal clusters C, D, E, and F show similar specific alpha desynchronization, but stronger in those conditions that involve movement: kinesthetic, vestibular, and active. Clusters G and H show heterogeneous alpha modulation with synchronization (increase) in the vestibular condition and desynchronization in the active condition. The final cluster I in areas around the right medial premotor cortex shows specific alpha synchronization in the passive and vestibular condition, which did not involve active walking of the subjects. The task-related alpha modulation in spatial navigation tasks during the passive condition in clusters A–F and I closely reproduces previous studies, which suggest that alpha

suppression is associated with an increased demand concerning visuo-attentional processing in navigational settings. However, cluster- and condition-specific modulations are present, which are related to the additional vestibular and kinesthetic information provided. We can conclude that navigational brain dynamics do not only depend on visual information but also on the access to kinesthetic and vestibular input.

P064. A Novel Method of Computing Resolution for Neuromagnetic Imaging Systems

K. Sekihara¹, E. Hiya¹, and R. Koga¹

¹Department of Systems Design and Engineering, Tokyo Metropolitan University, Tokyo, Japan

Modern MEG systems are capable of whole-head coverage with simultaneous measurements of nearly 300 sensors. Such whole-head sensor arrays, together with advanced signal processing algorithms, now enable imaging of dynamic brain activity—referred to as neuromagnetic source imaging.^{1,2} One problem with neuromagnetic imaging is that no clear measure exists to assess the performance of imaging systems. At present, an index commonly used for assessing imaging system's general ability is the number of sensors. Although one can imagine that a system with a larger number of sensors should have performances better than the performances of a system with smaller number of sensors, there is no clear method to quantitatively assess the performance improvements due to the increase in the number of sensors. Meanwhile, the resolution has traditionally been used to assess the performance of wide variety of imaging systems. It is, however, difficult to define the resolution for neuromagnetic imaging systems because the resolution changes depending on the locations and orientations of sources due to the space variant nature of this imaging method. This paper proposes a novel definition on resolution, and develops a method based on Monte Carlo simulation to compute the resolution for neuromagnetic imaging systems. Using the resolution as a performance measure, various types of sensor hardware are compared.

We analyse the performance changes due to changes in the gradiometer baseline and find that, compared to the 5-cm baseline case, 34% and 11% resolution losses are, respectively, caused if we use a gradiometer with 1.6-cm and 3.2-cm baselines. Use of a gradiometer with a 5-cm baseline causes only 10% loss of spatial resolution, compared with the use of a magnetometer sensor. We also analyse the influence of the sensor helmet size on resolution, and find that sensor helmets with 11.5-cm and 10-cm radii, respectively, provide nearly 20% and 35% better resolution than the helmet with a 13-cm radius. We find that planar and axial gradiometer systems attain almost the same resolution. We also compare performances between the radial and vector sensors, and find that, the resolution improvement due to the use of the vector sensor system is only 10% to 15%. Finally, we compute the resolution of 2 significantly

different existing MEG systems, MEGvision (Yokogawa Electric Corporation, Tokyo, Japan)³ and Elekta-Neuromag TRIUX (Elekta Corporate, Stockholm, Sweden),⁴ and find that these 2 systems have almost the same resolution.

References

1. Sekihara K, Nagarajan SS. *Adaptive Spatial Filters for Electromagnetic Brain Imaging*. Berlin, Germany: Springer-Verlag; 2008.
2. Baillet S, Mosher JC, Leahy RM. Electromagnetic brain mapping. *IEEE Signal Process Mag*. 2001;18:14-30.
3. Uehara G, Adachi Y, Kawai J, et al. Multi-channel SQUID, systems for biomagnetic measurement. *IEICE Trans Electron*. 2003;E86-C:43-54.
4. <http://www.elekta.com/healthcare-professionals/products/elekta-neuroscience/functional-mapping/elekta-neuromag-product-specifications.html>.

P065. Electrical Neuroimaging of ERPs in Response to Different Sensory Input From the Tongue

E. Iannilli¹, C.M. Michel², A.-L. Bartmuss¹, N. Gupta¹, and T. Hummel¹

¹Smell & Taste Clinic, Department of Otorhinolaryngology, University of Dresden Medical School, Dresden, Germany

²Functional Brain Mapping Laboratory, Department of Neuroscience, University of Geneva, Geneva, Switzerland

Taste, texture, temperature, and flavours are the quality of a food that in combination can produce an enjoyable meal. The objective investigation (without the subjective evaluation of the participant) of this process is technically limited. Using a dedicated taste stimulus delivery system (gustometer) with special characteristic able to elicit ERPs (quasi-squared pulsed stimuli, constant temperature of 38°C) we aimed to characterize the event related potentials (ERPs) in response to taste, temperature, and mechanosensory input. For this we studied microstate segmentation, source estimation and latencies and amplitudes of the main classical electrode sites. We applied a 128-channel EEG system and registered the signal from 25 healthy volunteers (mean age 24 years). Normal gustatory and olfactory functions of the subjects were ascertained by means of "Sniffin' Sticks" and taste spray tests.

The classical ERPs peak measurement showed a faster response for the temperature and mechanosensory stimulation compared with taste stimulation (N1-cold = 283 ± 43 ms; N1-somatosensory = 293 ± 44 ms; N1-salt = 396 ± 59 ms) ($P < .01$, $F[2, 72] = 5.15$).

The comparative microstate segmentation of the 3 conditions revealed 5 conclusive maps to describe the processes. For the taste conditions the sources were located in primary and secondary taste cortices along with some other areas in left temporal and right prefrontal lobe. For temperature and mechanosensory conditions the estimated sources were coherently located in left and right somatosensory cortex, but we found also involved left and right prefrontal cortex and right temporal

lobe. Moreover, the cold condition differed from the somatosensory with one map. The last had one of the main sources located in the right frontal operculum. The same map was shared by the taste condition within a slightly earlier time frame. This is in agreement with other studies, mainly using fMRI technique, which suggested the frontal operculum/ insula as site for both taste and temperature processing.

In conclusion, these findings offer new important insights in the brain processes related to the cross-modal integration of multisensory input on the tongue by emphasizing for the first time the spatiotemporal dynamic of them in synchronization.

P067. Impact of Early Life Adversity on Reward Processing in Young Adults: EEG–fMRI Results From a Prospective Study

R. Boecker¹, N. Holz¹, A.F. Buchmann¹, D. Blomeyer¹, M.M. Plichta², I. Wolf¹, S. Baumeister¹, A. Meyer-Lindenberg², T. Banaschewski¹, D. Brandeis^{1,3,4,5}, and M. Laucht^{1,6}

¹Department of Child and Adolescent Psychiatry and Psychotherapy, CIMH Medical Faculty Mannheim/Heidelberg University, Mannheim, Germany

²Department of Psychiatry and Psychotherapy, CIMH Medical Faculty Mannheim/Heidelberg University, Mannheim, Germany

³Department of Child and Adolescent Psychiatry, University of Zurich, Zurich, Switzerland

⁴Center for Integrative Human Physiology, University of Zurich, Zurich, Switzerland

⁵Neuroscience Center Zurich, University of Zurich and ETH Zurich, Zurich, Switzerland

⁶Department of Psychology, University of Potsdam, Potsdam, Germany

Introduction. Adversity in early childhood can impair human brain development, and promote the development and persistence of mental disorders, like attention deficit/hyperactivity disorder (ADHD) or addiction. Alterations of the mesolimbic reward pathway have been suggested to play a major role in this development. The present study examined the impact of early family adversity on different stages of reward processing in young adults. **Methods.** A total of 162 healthy young adults (mean age = 24.4 years) from a longitudinal study participated in a simultaneous EEG–fMRI measurement using a monetary incentive delay task.^{1,2} The task probes reward anticipation and outcome processing, and requires a button press after a flash, cued either by a laughing or a scrambled smiley to receive either a monetary or a verbal feedback. Data were recorded using a 3-T MRI scanner and a 64-channel MRI-compatible EEG-system. Early family adversity (EFA) was assessed at the age of 3 months with a standardized parent interview. **Results.** Robust fMRI task effects in areas related to reward anticipation (VS, supplementary motor area and anterior cingulate cortex) and reward delivery (putamen, caudate, left inferior frontal gyrus, right dorsolateral prefrontal cortex) revealed higher activation

for monetary versus verbal reward and for win versus no-win trials (all $P_{\text{FWE}} < .0001$). Region-of-interest fMRI analysis revealed a decreasing activation with increasing EFA during reward anticipation in reward-related areas (ie, ventral striatum, putamen, thalamus). EEG analysis demonstrated a similar effect for the contingent negative variation (CNV) which decreased with increasing EFA. In contrast, during reward delivery, activation of the bilateral insula, right pallidum, bilateral putamen, and left superior temporal gyrus increased with the level of EFA. **Conclusion.** The reliable task effects consistent with the literature^{1,2} also reflect the long-term impact of early life adversity on both reward processing stages, with parallel ERP and fMRI findings, implicating a hyporesponsiveness during reward anticipation and a hyperresponsiveness when receiving a reward. Similar alterations in ADHD³ or substance dependent^{4,5} patients suggest an association between early adversity and psychopathology, mediated by a dysfunctional reward pathway.

Acknowledgments

This work was supported by grants from the German Research Foundation (DFG LA 733/1-2) to ML, DB, TB, and AML.

References

1. Kirsch et al. *Neuroimage*. 2003;20:1086-1095.
2. Knutson et al. *J Neurosci*. 2001;21:1-5.
3. Ströhle et al. *Neuroimage*. 2008;39:966-972.
4. Wrase et al. *Neuroimage*. 2007;35:787-794.
5. Bjork et al. *Neuroimage*. 2008;42:1609-1621.

P068. On an fMRI Detecting Oscillating Neural Magnetic Fields Toward fMRI–MEG Combination

S. Natahara^{1,2}, M. Ueno¹, and T. Kobayashi¹

¹Department of Electrical Engineering, Graduate School of Engineering, Kyoto University, Kyoto, Japan

²Japan Society of the Promotion of Science, Tokyo, Japan

Recently, a new method of fMRI that can detect neural activities directly has been focused on. It observes neural magnetic fields and does not depend on hemodynamic changes.¹ Nonetheless, there are no successful fMRI experiments reported, although some researchers claim that neural magnetic fields are observable with MRI scanners.¹⁻³ fMRI imaging detecting neural magnetic fields are considered to be suitable to fMRI–MEG combination because of its measurement principle.

Magnetic resonance imaging with spin-lock sequence is a method which has potential to detect neural magnetic field dependent (NMFD) changes in MR signal intensities as fMRI; hereafter, we call it NMFD-fMRI. Studies suggesting its possibility to detect oscillating magnetic fields have been reported.^{4,5} The spin-lock sequence consists of spin-lock module, including two $\pi/2$ pulses and a spin-lock pulse between them, and the conventional spin-echo sequence. If there is a magnetic field oscillating at the same frequency with the Larmor frequency of spin-lock pulse, the magnetization of protons decreases owing

to the secondary magnetic resonance. Consequently, oscillating magnetic field decrease the MR signals.

In this work, we observed the secondary magnetic resonance occurring between the spin-lock pulses and oscillating magnetic fields assuming neural magnetic fields with a loop coil phantom. A 7-T MRI scanner was used to observe the signal decrease originating from secondary magnetic resonance. The phantom consists of a single loop coil and a cylindrical plastic tube. It was filled with a solution of saline. We used a standard spin-echo sequence preceded by the spin-lock module. During the spin-lock pulse, the oscillating magnetic fields were generated around the loop. Its amplitude and the frequency were set to 47 nT at the center of the loop and 0 to 200 Hz, respectively, to see the secondary magnetic resonance. Moreover, we focused on minute magnetic fields such as neural magnetic fields and obtained MR images while originating the magnetic fields of sub-nT from the loop coil.

We could observe the signal decrease when the frequency of the oscillating magnetic field and the spin-lock pulse satisfy the condition for secondary magnetic resonance. Moreover, we also figured out that magnetic fields of approximately 200 pT could be observed by repeating the imaging and increasing the duration of spin-lock pulse. In the future study, we plan to use ultra-low-field (ULF) MRI⁶ for NMFD-fMRI to avoid BOLD contamination and/or susceptibility artifacts. The NMFD-fMRI under ULF is expected to provide possibilities of implementing not only fMRI-MEG combination but also fMRI-MEG simultaneous measurements.

Acknowledgments

Ministry of Education, Culture, Sports, Science and Technology, Japan, Dr Ito, Dr Imai, and Dr Takayama.

References

1. Bodurka J, et al. *Magn Reson Med*. 2002;47(6):1052-1058.
2. Park T, et al. *Neuroimage*. 2007;35(2):531-538.
3. Jay W, et al. *Med Biol Eng Comput*. 2012;50(7):1-7.
4. Witzel T, et al. *Neuroimage*. 2008;42(4):1357-1365.
5. Halpern-Manners N, et al. *Proc Natl Acad Sci U S A*. 2010;107:8519-8524.
6. Cassara A, et al. *Magn Reson Imaging*. 2009;27(8):1131-1139.

P069. Topographic Associations of EEG Theta and Gamma Oscillations With Task Positive and Negative Resting State Networks During Working Memory Processing

M. Kottlow^{1,2}, A. Bänninger¹, and T. Koenig¹

¹Department of Psychiatric Neurophysiology, University Hospital of Psychiatry, University of Bern, Bern, Switzerland

²Institute of Pharmacology and Toxicology, University of Zurich, Zurich, Switzerland

Working memory processing is an important indicator of cognitive functioning and can yield information about the mental

condition in health and disease. Theta and gamma oscillations are both engaged in working memory processing showing load-dependent activity.¹ In addition, several task negative and positive fMRI-BOLD resting state networks (RSNs) as, for example, the default mode network (DMN) and a left-lateralized working memory network (l-WMN) respectively were shown to systematically change during the execution of a Sternberg working memory task.²

We therefore used an approach of temporally correlating the fluctuations of the dynamics of spatially high-resolving fMRI-RSNs with the dynamics of temporally high-resolving EEG spectral amplitudes. This so-called covariance mapping yielded the spatial distribution of frequency domain EEG fluctuations associated with the dynamics of RSN networks.³ In a preliminary single-trial analysis of data obtained during a visual Sternberg working memory task, covariance maps of EEG theta and gamma oscillations from retention periods and the dynamics of the DMN and the l-WMN were computed.

The DMN showed negative correlations with theta frequency amplitude, while no correlations between this RSN and gamma could be seen. In contrast, the l-WMN correlated negatively with gamma but not theta amplitudes.

Our results support the involvement of both EEG spectral fluctuations in the theta and gamma range as well as task negative and positive resting state networks in working memory. Further analyses may be able to reveal the interaction of theta and gamma spectral fluctuations during different working memory processes as well as their associations with task positive and task negative RSNs.

Acknowledgments

Supported by SNF Sinergia Grant No. 136249.

References

1. Brookes MJ, et al. *Neuroimage*. 2011;55:1804-1815.
2. Kim DI, et al. *Hum Brain Mapp*. 2009;30:3795-3811.
3. Jann K, et al. *PLoS One*. 2010;5(9):e12945.

P070. Thalamic Relay of Frequency-Specific EEG Scalp Field Maps

S. Schwab¹, T. Koenig¹, A. Federspiel¹, T. Dierks, and K. Jann²

¹Department of Psychiatric Neurophysiology, University Hospital of Psychiatry, University of Bern, Bern, Switzerland

²Department of Neurology, Ahmanson-Lovelace Brain Mapping Center, University of California, Los Angeles, CA, USA

The thalamus is a fundamental relay structure of the brain that transfers sensory and motor signals to distinct zones of the cerebral cortex. The thalamus has also been argued as the pace-maker of cortical rhythms observed by EEG. Recently, EEG microstates that represent states of synchronized brain activity and EEG spectral fluctuations have been associated to fMRI resting state networks (RSNs). However, the emergence of

specific scalp field oscillations and associated thalamic BOLD signal fluctuations has not yet been studied. In the present work, we aimed to define the frequency specific thalamic areas generating distinct synchronized cortical networks, as indexed by EEG scalp fields oscillating with a common phase. Fourteen healthy subjects (6 females/8 males, mean age 26 ± 2.7 years) underwent simultaneous EEG/fMRI in a no-task condition. The EEG was subjected to a topographic time–frequency algorithm that decomposed the EEG into 6 classes of transient states of synchronized oscillations. First, in single-subject GLMs, the BOLD response was fitted by using the 48 time courses (6 classes of states \times 8 frequency bands) as predictors, which were previously convolved with the canonical haemodynamic response function. In the group analysis, we used voxel-wise one-way ANOVA with the 8 frequency bands as within factor to fit the beta values of the GLM. For each of the 6 state-classes, a statistical map with F values of the main effect of frequency was created (Bonferroni, $P < .05$). Frequency-specific areas were identified for the different state-classes (maps) in distinct medial and lateral thalamic subregions, such as dorsomedial nucleus, ventral–posterolateral n., ventral lateral n., pulvinar, and lateral posterior n. In the past, cortical BOLD fluctuations have successfully been correlated with thalamic BOLD to determine the functional thalamocortical connectivity. In this study, we have identified a consistent topological mapping of thalamic regions to a set of spatially defined patterns of cortical common phase oscillations at specific frequencies. Since thalamic activity itself is not visible in the EEG, the observed EEG–BOLD relations must be functional, attributing the thalamus a role of mediator, modulator and coordinator of cortical oscillatory activity that is visible in EEG. Synchronization of cortical oscillations is an important candidate mechanism for network formation and feature binding. Therefore, our study provides a novel way to elucidate the systematics of subcortical effects on the formation of large scale cortical networks.

P072. A Normalized Integrative fMRI–MEG Study on Cortical Activations Associated With Determination of Depth Order in Motion Transparency

H. Natsukawa¹ and T. Kobayashi

¹Graduate School of Engineering, Kyoto University, Kyoto, Japan

When visual patterns drifting in different directions and/or at different speeds are superimposed on the same plane, observers perceive transparent surfaces on planes of different depths. This phenomenon is known as motion transparency depth rivalry.¹ Although electrophysiological studies have investigated how the visual system extracts transparent surfaces from 2D motion,^{2–4} the relationship between dynamic cortical activity and motion transparency depth rivalry remains to be elucidated. In this study, to determine which regions of the brain are involved in motion transparency depth rivalry and when this phenomenon occurs, cortical activities were measured during a motion transparency

depth rivalry task under depth attention and a control coherent motion task using functional magnetic resonance imaging (fMRI) and magnetoencephalography (MEG). Eleven healthy subjects (10 males and 1 female, age range: 21–27 years) participated in the fMRI measurement portion of the study, and 7 subjects (6 males and 1 female, age range: 21–27 years) of those 11 participated in the MEG measurement portion of the study. In addition, eye movements were measured. MEG and fMRI data were analyzed by a normalized integrative fMRI–MEG method⁵ that enables reconstruction of time-varying dipole moments of activated regions from MEGs and extract data regarding cortical activity commonly observed in subjects using the clustering technique and the Montreal Neurological Institute and Hospital (MNI) coordinates. The activated regions were used as spatial constraints during reconstruction using the integrative fMRI–MEG method. By comparing the responses obtained for both the control and experimental tasks, the dynamic brain processes involved in determination of depth order in motion transparency depth rivalry were investigated. For interpretation of the results, we referred to behavioral indicators determined from eye movement measurements, that is, time of occurrence of motion transparency depth rivalry. Dynamic recurrent neural activities in the visual dorsal pathway, including the human middle temporal area, intraparietal sulcus, and those in the anterior cingulate and lateral occipital cortices were observed for the periods between behavioral indicators. These results suggest that the initial eye movements and accompanying cortical activations played an important role in determining the depth order of transparent motion.

Acknowledgments

Dr Oida, Dr Matsushashi, Dr Fukuyama.

References

1. Chopin A, Mamassian P. *J Vis.* 2011;11(7):1–8.
2. Qian N, Andersen RA. *J Neurosci.* 1994;14:7367–7380.
3. Rosenber A, Wallisch P, Bradley DC. *Vis Neurosci.* 2008;25:187–195.
4. Muckli L, et al. *Neuroimage.* 2002;16:843–856.
5. Natsukawa H, Kobayashi T. *Adv Biomed Eng.* 2012;1:27–35.

P073. ICA-Based Artifact Correction of Sleep EEG Recordings During Arterial Spin Labeling–MRI Measurements

L. Tüshaus^{1,2}, T. Koenig³, M. Kottlow^{1,3}, and P. Achermann^{1,2}

¹Institute of Pharmacology and Toxicology, University of Zurich, Zurich, Switzerland

²ZNZ Neuroscience Center Zurich, University of Zurich, Zurich, Switzerland

³Department of Psychiatric Neurophysiology, University Hospital of Psychiatry Bern, Bern, Switzerland

Simultaneous measurements of electroencephalography (EEG) and magnetic resonance imaging (MRI) have increased

in the past years as both modalities complement each other and the combination provides higher resolution in the temporal as well as in the spatial regime. Correction of artefacts in the EEG, caused by the scanner gradients, has been approached with several different techniques. However, these methods are mostly tailored to fit the correction of the commonly used echo planar imaging gradient artefacts while simultaneous measurements of EEG and arterial spin labeling (ASL)-MRI are very rare.

Sleep studies conducted in MRI scanners have been emerging more and more in the recent past. Simultaneous sleep EEG-MRI studies exist but the sleep EEG is mainly used to define sleep stages without any further EEG analysis. To our knowledge, so far no study has been published employing the ASL-MRI technique during sleep.

In this study, healthy participants were subjected to a night of sleep restriction (4 hours of sleep) and extended wakefulness. In the following night, we simultaneously measured EEG and ASL-MRI data for several hours (maximum 4 hours), while subjects were instructed to sleep in the scanner.

The simultaneously acquired EEG data were then preprocessed, including the following steps: scanner artefact removal by template correction, cardioballistogram detection and removal, downsampling and filtering.

To clean the EEG of the ASL gradient artefacts, we combined sleep EEG data from outside the scanner (during a night in the sleep lab) with the simultaneously acquired sleep EEG data. A similar approach has been used by Jann et al¹ with simultaneous wake EEG data acquired from epilepsy patients.

As the high sampling rate needed in simultaneous measurements and the duration of our recordings create demanding amounts of data challenging to process, we created a subset of the data, consisting of several minutes of “outside” and “inside” data each to yield a balanced sample data set.

On this combined data subset, we performed an independent component analysis (ICA) and created an artefact-specific filter. The combination of “outside” and “inside” data enhanced the identification of scanner-related artefacts on the basis of ICA components’ power spectra and map topographies. This filter was then used to remove the artifact-rich components identified by the ICA from the simultaneous EEG data.

With this approach, we could remove artefacts created by the simultaneous measurements and were able to show corrected sleep EEG power spectra that resembled power spectra found in “normal” sleep EEG studies performed outside an MRI scanner.

Acknowledgments

Supported by SNF Sinergia Grant No. 136249.

Reference

1. Jann K, et al. *Neuroimage*. 2008;42:635-648.

P074. The Effect of Epoch Length on Functional Connectivity Within the Default Mode Network

R. S. Wilson^{1,2}, S.D. Mayhew¹, S. Asseondi¹, T.N. Arvanitis², and A.P. Bagshaw¹

¹School of Psychology, University of Birmingham, Birmingham, UK

²School of Electronic, Electrical and Computer Engineering, University of Birmingham, Birmingham, UK

Functional connectivity (FC) identifies low frequency BOLD signal correlations between brain regions.¹ Exploiting correlations in spontaneous fMRI signals enables the identification of intrinsic connectivity networks (ICNs), such as the default mode network (DMN).² To calculate FC, standard methodology uses scan durations of several minutes to calculate correlation, although it has been suggested that shorter temporal intervals (epochs) could enable the study of dynamic changes in ICNs.³ By using shorter epochs we could investigate the link between ICNs and dynamic changes in behaviour, such as during sleep⁴. However, shorter epochs could compromise the reliability of FC measurements⁵. The current study investigated this by examining how the DMN FC strength was affected by varying the epoch length from 15 minutes to 8 seconds.

Eight healthy adult volunteers (5 males, age 32 ± 6 years) underwent a single fifteen minute resting state (RS) scan and the data underwent standard preprocessing.² The DMN was defined from 6 minute RS fMRI scans from a separate cohort of 55 subjects (28 males, age 25 ± 4 years). Data were preprocessed and decomposed using a group temporal concatenated ICA.⁶ The DMN component was divided into individual nodes and Regions of Interest (ROIs) defined as $3 \times 3 \times 3$ voxel centred on the maximum z-statistic voxel.

In the 8 subjects with the longer scans, FC was measured between posterior cingulate cortex seed region and all DMN ROIs using six different epoch durations with a sliding window: 15 minutes, 2 minutes (1-minute overlap), 1 minute (30-second), 30 seconds (15-second), 16 seconds (8-second), and 8 seconds (4-second). The mean FC for each epoch length was compared to random datasets created from the actual data by randomizing the time course.

For each epoch length the DMN was robustly identified. A similar pattern of group average FC was observed across ROIs for all epoch lengths, although the FC strength decreased as the epoch length decreased. A 2-way ANOVA (Epoch, Region) showed significant main effects of Epoch ($P < .001$) and Region ($P < .001$) with significant interaction between Epoch and Region ($P = .001$). Dynamic changes in FC were similar within individual subjects across the different epochs, suggesting that even at the short epoch lengths physiological variation was being assessed.

Our results show that FC could be analyzed using a sliding window as short as 30 seconds or less without the risk of spurious correlations. The source of dynamic variability in FC strength remains to be clarified, but examining FC on shorter timescales allows a more coherent link with behaviour and a clearer assessment of changes in patient populations.

Acknowledgments

Funded by the UK Engineering and Physical Sciences Research Council (EPSRC Grant Number EP/J002909/1).

References

1. Fox MD, Greicius M. *Front Syst Neurosci*. 2010;4.
2. Fox MD et al. *Proc Natl Acad Sci U S A*. 2005;102:9673-9678.
3. Allen EA, et al. *Cereb Cortex*. 2012. In press.
4. Spoormake VI, et al. *J Neurosci*. 2010;30:11379-11387.
5. Van Dijk KRA, et al. *J Neurophysiol*. 2010;103:297-321.
6. Beckmann CF, Smith SM. *IEEE Trans Med Imaging*. 2004;23:137-152.

P075. The Effect of Prematurity on Maturation of the Auditory Network in Newborns Using EEG and Functional MRI

A. Darque¹, T.A. Rihs², F. Grouiller³, F. Lazeyras³, R. Ha-Vinh Leuchter¹, C. Caballero³, C.M. Michel², and P.S. Hüppi¹

¹Division of Development and Growth, Department of Pediatrics, University of Geneva, Geneva, Switzerland

²Functional Brain Mapping Laboratory, Department of Fundamental Neurosciences, University of Geneva, Geneva, Switzerland

³Department of Radiology and Medical Informatics, University of Geneva, Geneva, Switzerland

Background and aims. Premature birth has an impact on brain maturation that can be measured at term equivalent age (TEA) with neuroimaging techniques. The aim of our study is to determine the neural pathways and processes that are activated in term babies and preterm infants (gestational age [GA] < 32 weeks) at term after listening to their mother's voice and a stranger's voice with EEG and fMRI techniques. Our secondary aim is to differentiate innate (genetically determined) and acquired (determined by experience) networks. Here, we present the results of the EEG analysis and preliminary results of fMRI in newborns. **Methods.** High-density EEG (Electrical Geodesics Inc, 109-channel) and fMRI (Siemens 3T) recordings were performed for subsequent analysis on newborns while listening to their mother's voice and the voice of an unknown woman. Two groups were tested: premature newborns tested at TEA (41 weeks) and full term controls (GA = 40 weeks). **Results.** For preterm and full-term babies, the event related potentials (ERPs) results showed significant differences on left temporal electrodes during the first 200 ms when they listened to their mother's voice compared to a stranger's voice (t test; $P < .05$). The topographic maps showed that the mother voice implies an almost similar map for preterm and full-term babies; however, the unknown voice seems to be clearly processed only in the preterm group. Preliminary fMRI results will be presented. **Conclusions.** By showing specific activation in preterm babies at TEA when they listen a known and an unknown voice, our results suggest that the maturation of the auditory network can be influenced by these early ex utero experiences resulting in

an early differentiation between their mother's voice and the voice of a stranger.

P076. Dissociating Cortical Midline Time Courses in Decision Making: Results From a Simultaneous EEG-fMRI Study

T.U. Hauser^{1,2,*}, L.T. Hunt^{3,*}, R. Iannaccone^{1,4}, P. Stämpfli⁵, D. Brandeis^{1,6,7}, R.J. Dolan³, S. Walitza^{1,6}, and S. Brem¹

¹University Clinics for Child and Adolescent Psychiatry (UCCAP), University of Zurich, Zurich, Switzerland

²Neuroscience Center Zurich, University of Zurich and ETH Zurich, Zurich, Switzerland

³Wellcome Trust Centre for Neuroimaging, University College London, London, UK

⁴PhD Program in Integrative Molecular Medicine, University of Zurich, Zurich, Switzerland

⁵MR-Center of the Psychiatric University Hospital and the Department of Child and Adolescent Psychiatry, University of Zurich, Zurich, Switzerland

⁶Zurich Center for Integrative Human Physiology, University of Zurich, Zurich, Switzerland

⁷Department of Child and Adolescent Psychiatry and Psychotherapy, Central Institute of Mental Health, Medical Faculty Mannheim/Heidelberg University, Mannheim, Germany

*These authors equally contributed to the study.

Adaptive learning and decision making is essential for survival, and several subregions of the medial cortical wall are strongly implicated in these skills. Ventromedial prefrontal cortex (vmPFC) and posterior cingulate cortex (PCC) are crucially involved in the valuation and evaluation of decision options. Dorsal regions of the medial frontal cortex (MFC—incorporating dorsal anterior cingulate and presupplementary motor areas), by contrast, are implicated in action selection and adaptive response behaviour. There is extensive knowledge about the functions of these regions in humans based on functional magnetic resonance imaging (fMRI) studies. By contrast, little is known about the differential temporal dynamics of these regions' activity, and the interaction between them. Notably, conditions that elicit the feedback-related negativity (FRN) component in electroencephalogram (EEG)—which is frequently modeled as a single dipole in MFC—can elicit widespread activation in many other nodes of the medial wall in fMRI. It is unclear whether the temporal dynamics of these nodes can be disentangled from that of MFC activity.

Here, we use simultaneous EEG-fMRI to dissociate the contributions of subregions of the medial wall to the electroencephalogram. First, we localize trial-by-trial FRN variability to MFC and evaluate its relation between the FRN and reward prediction errors, which reflect the inappropriateness of decisions. Second, we use a novel methodological approach which adopts trial-by-trial variability in fMRI data in timecourses of vmPFC and MFC and PCC activity to explain the dynamics in EEG data. Using this approach, these areas were revealed

to be active with different temporal dynamics. Strikingly, the distinct spatial topographies of fMRI-informed event related potentials could successfully be relocalized to each of the regions of origin in an unconstrained dipole fit, providing strong support that the dynamics observed were generated by the 3 regions under consideration. These findings crucially advance the understanding of cortical midline regions, and our new approach to fMRI-EEG analysis reveals the temporal dynamics of regions whose activity might be hidden via traditional EEG methodology.

P077. Spatial Harmonic Analysis of EEG Data: A Comparison With PCA and ICA

U. Graichen¹, R. Eichardt¹, P. Fiedler¹, D. Strohmeier¹, S. Freitag¹, F. Zanow², and J. Haueisen^{1,3}

¹Institute of Biomedical Engineering and Informatics, Faculty of Computer Science and Automation, Ilmenau University of Technology, Ilmenau, Germany

²eemagine Medical Imaging Solutions GmbH, Berlin, Germany

³Biomagnetic Center, Department of Neurology, University Clinic Jena, Jena, Germany

Introduction. In the analysis of multichannel EEG data, the spatial distribution of the measured potentials is of particular interest. We present a method for the spatial harmonic analysis (SHA) of irregularly sampled data, which can be regarded as a generalization of the Fourier analysis. Our objective is to compare SHA with the principal component analysis (PCA) and the independent component analysis (ICA) for the decomposition of EEG data. **Materials and methods.** The basis functions of SHA are computed by solving the Laplacian eigenvalue problem. The required Laplace–Beltrami operator was discretized by a FEM approach. The EEG data are decomposed by projection into the space of basis functions. This is similar to PCA or ICA, where projections into the space of principal or independent components are used. For the comparison, we use an own implementation of PCA and the FastICA¹ algorithm. Somatosensory-evoked potentials were recorded in eleven healthy volunteers. The median nerve of the right forearm was stimulated by bipolar electrodes. EEG signals were recorded with 256 channels (equidistant electrode layout) and 2 coupled 128 channel amplifiers. The positions of the EEG electrodes were digitized. The data were sampled at 2048 Hz and high-pass (2 Hz) and notch (50 Hz and 2 harmonics) filtered. All trials were manually checked for artifacts; the remaining trials were averaged. **Results.** The SEP data was decomposed by the 3 methods. The computational time to determine the SHA basis functions and the PCA components was below one second. The computational effort to determine the independent components by ICA was significantly higher (in the range of minutes). The time for data decomposition was similar for all three approaches. Three principal components (PCA), seven basis functions (SHA) and 98 independent components (ICA)

out of 256 were required, on average, to describe 90% of the original signal's energy. **Conclusions.** The best result in reducing the data dimensionality in our application was achieved by PCA, closely followed by SHA. The advantage of SHA is that the basis functions can be computed prior the recording of the time series, because only the sensor positions are required for its determination. This is particularly beneficial for time critical applications.

Acknowledgments

This work was supported by the German Federal Ministry of Economics and Technology (KF225011ED2).

Reference

1. Hyvärinen, A. *IEEE Trans Neural Netw.* 1999;10(3):626-634.

P078. Modulation of Resting-State Brain Networks in Newborns by Newborn Screen Heel Prick

L. Lordier¹, F. Grouiller², D. Van de Ville^{2,3}, A. Sancho Rossignol⁴, I. Cordero⁴, F. Lazeyras², F. Ansermet⁴, and P. Hüppi¹

¹Division of Development and Growth, Department of Pediatrics, University of Geneva, Geneva, Switzerland

²Department of Radiology and Medical Informatics, University of Geneva, Geneva, Switzerland

³Institute of Bioengineering, Ecole Polytechnique Fédérale de Lausanne, Lausanne, Switzerland

⁴Division of Child and Adolescent Psychiatry, Department of Pediatrics, University of Geneva, Geneva, Switzerland

There is a growing interest in the nature of spontaneous brain activity observed during so-called “resting state.” Specifically, using resting-state functional magnetic resonance imaging (RS-fMRI) it is possible to establish resting-state networks (RSNs) that show temporally coherent (typically low frequency) BOLD signal fluctuations. Functional connectivity between brain regions in RSNs is linked to the development of white matter pathways occurring early in brain development that are maturing throughout childhood. However, little is known about the development and role of those RSNs in newborns. To date, only few studies have explored RSNs in newborns.¹ Furthermore, even if very similar RSNs than those found in adults have been found, the role of these RSNs in newborns is not well understood. Previous studies reported that spontaneous brain activity can be modulated not only by learning, training, but also by behavioral states, which is supporting the idea that low-frequency BOLD signal fluctuations are modulated by recent experience.^{2,3}

The aim of this study is to map RSNs in newborns and to investigate if these low-frequency BOLD signal fluctuations reflecting behavioral state could be modified after a painful event.

We acquired 2 runs of RS-fMRI (Siemens 3T) in nine healthy term newborns (mean gestational age: 39 4/7 weeks) at 3 to 4 days of life during natural sleep or while resting quietly

in the scanner without any sedation. Between these 2 runs of 8 minutes, each newborn underwent a “Guthrie test,” which is a heel prick to get a few drops of blood for metabolic screening.

Resting-state fMRI data, acquired immediately before and after this painful and stressful event, were preprocessed (realigned, normalized and smoothed) and analyzed using group-level independent component analysis (ICA). RSNs consistent with those previously described in infants and in adults have been found. We compared functional network connectivity between each RSN before and after the stressor, and detected alteration of connectivity between cuneus and superior frontal regions.

However, analyses on a larger cohort of babies are needed to better understand these low-frequency BOLD signal fluctuations after a painful event.

References

1. Smyser CD, et al. *Neuroimage*. 2011;56:1437-1452.
2. Harrison BJ, et al. *Plos One*. 2008;3(3):e1794.
3. van Marle HJ, et al. *Neuroimage*. 2010;53(1):348-354.

P079. Shared and Task-Specific Brain Mechanisms Underlying Different Response Inhibition tasks: A Simultaneous EEG–fMRI Study

A. Schläpfer^{1,2}, K. Rubia³, and D. Brandeis^{1,4,5}

¹University Clinics for Child and Adolescent Psychiatry, (UCCAP), University of Zurich, Zurich, Switzerland

²Neuroscience Center Zurich, University of Zurich and ETH Zurich, Zurich, Switzerland

³Department of Child and Adolescent Psychiatry, King's College London, London, UK

⁴Zurich Center for Integrative Human Physiology, University of Zurich, Zurich, Switzerland

⁵Department of Child and Adolescent Psychiatry and Psychotherapy, Central Institute of Mental Health, Medical Faculty Mannheim/Heidelberg University, Mannheim, Germany

Response inhibition is an essential executive function required to inhibit inappropriate behaviors. Functional magnetic resonance imaging (fMRI) has revealed that inhibition mainly activates frontal lobe regions. Event-related potentials (ERPs) are characterized by a centrally positive activation (NoGo-P300) after 300 to 600 ms with frontal source localization. Although different response inhibition tasks share these inhibitory fMRI and ERP activation patterns, localization within the frontal cortex in fMRI and temporal aspects of the ERP appear dependent on the nature of the specific response inhibition task.

Here, we applied simultaneous 64-channel EEG–fMRI (3T) recordings to study shared and task-specific activation patterns in two inhibition tasks, a tracking Stop task and a Flanker/NoGo task, in the same individuals to compare spatial and temporal aspects of inhibitory processing patterns in the brain.

Preliminary results (n = 4, study ongoing) suggest that these inhibitory tasks have both common and task-specific neural activations. The fMRI data clarified that response inhibition in both tasks elicited overlapping frontal activation, while the

ERPs revealed a common central positive NoGo P300 after response inhibition. However, a timing difference of the NoGo P300 between the tasks was detected.

These findings suggest that particularly the timing of neural mechanisms supporting response inhibition may be task-dependent. The common frontal activation in both tasks suggests that activation of these regions within a relatively narrow time window is necessary and critical for inhibition, irrespective of additional task-specific demands. Further analyses will focus on relating the timing differences, and the additional regions activated to task-specific aspects of response inhibition.

Acknowledgments

Supported by SNF Sinergia Grant No. 136249.

P080. EEG Source Connectivity Changes in Eye Movement Desensitization and Reprocessing

G. Di Lorenzo¹, M. Pagani², L. Monaco¹, A. Daverio¹, I. Giannoudas¹, A.R. Verardo³, P. La Porta³, C. Niolu¹, I. Fernandez³, and A. Siracusano²

¹Department of Systems Medicine, University of Rome, Rome, Italy

²Institute of Cognitive Sciences and Technologies, CNR, Rome, Italy

³EMDR Italy Association, Bovisio Masciago (MB), Italy

Background. Changes in brain connectivity have been recently demonstrated in victims of psychological traumas treated with the Eye Movement Desensitization and Reprocessing (EMDR). The aim of this study was to implement principal component analysis (PCA) to investigate EEG source connectivity during bilateral ocular stimulation (BS) before and after EMDR therapy. **Methods.** A 37-channel EEG was used to record brain activity during whole EMDR sessions. Twenty-eight victims of psychological traumas were investigated at the first EMDR session (T0) and at the last one performed after processing the index trauma (T1). Electrical source images were analyzed for each EEG band by eLORETA. Source current density values of 6239 voxels, for each band of both sessions, were reduced to 28 ROIs and standardized before performing PCA (extracted factor minimum eigenvalue = 1; factor rotation = varimax). **Results.** In all bands, the performed PCA resulted in 4 to 6 factors explaining between 86% for delta band to 93% for alpha band of the total variance. Relevant decreased connectivity, especially between limbic structures, was found in T1 as compared to T0 in delta, theta, and gamma bands. As for delta band the first factor including at T0 several limbic structures as bilateral anterior (ACC) and posterior (PCC) cingulate cortex, parahippocampal gyri (PHG), right insula (INS-R), and orbitofrontal cortex (OFC-R) explaining the 43% of the variance was reduced at T1 to bilateral PCC and PHG explaining only the 28% of the variance. The same was found for theta band in which factor 1 containing the most of the anterior limbic structures (bilateral INS and ACC, right PHG and right anterior, AFC, and lateral, LFC, frontal cortex) and explaining the 45% of the variance broke up at T1 reducing considerably the explained

variance. For gamma band, as well, the 2 factors, including the most of the limbic areas (bilateral ACC, PCC, PHG, OFC and AFC) and explaining a combined variance of 50%, were disrupted at T1. **Conclusions.** These findings suggest that EMDR efficacy in victims of psychological traumas is associated to electrical brain connectivity changes during BS. In particular, after positive clinical outcomes electric activity is reduced in areas involved in the cortical hyperactivation state of trauma-related disorder. Our results suggest that successful EMDR and hence processing of the traumatic event is related to decreased functional connections between intralimbic and corticolimbic regions involved in the emotional elaboration of the index trauma. PCA is useful to explore functional brain connectivity and enables to assess functional networks activated during BS of EMDR therapy.

Acknowledgments

EMDR International Association (EMDRIA), EMDR Europe.

P081. EEG Response to Subjects' Own Name in Patients With Severe Motor and Intellectual Disabilities

K. Tamura¹, C. Karube¹, T. Mizuba¹, M. Matsufuji², S. Takashima², and K. Iramina¹

¹Graduate school of Systems Life Sciences, Kyushu University, Fukuoka, Japan

²Yanagawa Institute for Developmental Disabilities, Yanagawa, Fukuoka, Japan

Severe motor and intellectual disability (SMID) is a term used to describe a heterogeneous group of disorders with severe physical disabilities and profound mental retardation which is caused by a disturbance of central nervous systems. Patients with SMID cannot express their feelings in language. It is difficult to understand what they think about, or how they feel, even if they appear to attempt a response. In order to expand our understanding, we investigated the brain activity in patients with SMID by measuring and analysing their Electroencephalography (EEG). By analysing inter-trial coherence we found that theta phase-locked activity increased in response to subjects' own names specifically in patients with SMID. These results indicate that theta phase-locked activity in patients with SMID is strongly associated with their own names. Our study suggests the existence of specific neural markers that signal an attentional shift in patients upon hearing their own names.

P082. Characterization of Information Coding in Simulated EEG-fMRI Data Sets

S. Asseondi¹, D. Ostwald², and A.P. Bagshaw¹

¹School of Psychology, University of Birmingham, Edgbaston, Birmingham, UK

²Center for Adaptive Rationality (ARC), Max Planck Institute for Human Development, Berlin, Germany

Transmission, encoding, and decoding of internal and external stimuli enable an individual to interact with the external world. The study of the basic mechanisms of information coding in healthy subjects is required for a better understanding not only of the healthy brain but also of clinical populations where these basic mechanisms may be impaired. EEG-fMRI is a noninvasive technique that can be safely used with healthy volunteers and clinical populations to address these questions. However, a consensus on the most efficient approach to combine the data sets has not yet been reached.

Information coding is well characterized by the estimation of information theoretic quantities.¹ Information theory (IT) primarily differs from more traditional approaches such as the general linear model (GLM) in that while the GLM assumes a linear relationship amongst variables, IT allows the exploitation of linear as well as nonlinear dependencies. IT thus enables us not only to study the relation between brain activity and stimuli but also to exploit the interplay between EEG and fMRI in encoding and decoding the stimuli.²

Unfortunately, entropy and information estimates suffer from the fact that an accurate estimate requires a large number of samples, which is not always available from neuroimaging recordings. While techniques to correct for this bias have been proposed, they have mainly been used with invasive neuronal data, which differ from EEG-fMRI recordings in terms of number of samples, number of recording sites and underlying distributions.

We used simulated signals to reproduce salient features of typical EEG-fMRI recordings, to explore the dependencies of the information theoretic estimates on parameters (number of samples, amount of correlation, binning strategy, and bias correction), and on the underlying multivariate "true" distribution (with normal, uniform, and gamma marginals). We drew samples from distributions with several degrees of correlation and estimated information quantities using several combinations of bias correction techniques and binning strategies. We found that the particular combination of binning strategy and bias correction affected the information estimate. Moreover, when the correlation of the model increased, a higher number of samples was required to obtain an unbiased estimate of the information, regardless of the bias correction, the binning strategy or the underlying distribution. These simulations provide a framework to optimize the accuracy of information estimates for the specific experimental parameters and distributions expected within an EEG-fMRI experiment.

Acknowledgments

Support for this research was provided by the Dr Hadwen Trust for Humane Research (DHT), the United Kingdom's leading medical research charity that funds and promotes exclusively human-relevant research that encourages the progress of medicine with the replacement of the use of animals in research.

References

1. Cover TM, Thomas JA. *Elements of Information Theory*. Hoboken, NJ: Wiley Interscience; 2006.
2. Ostwald D, Bagshaw AP. *Magn Reson Imaging*. 2011;29:1417-1428.

P083. Spatio-temporo-spectral Patterns of EEG and Brain Hemodynamics Using Bayesian Approach

R. Marecek¹ and M. Brazdil¹

¹Central European Institute of Technology—CEITEC, Masaryk University, Brno, Czech Republic

In the past decade, several articles describing the relationships between brain hemodynamics and spectral patterns in EEG power have been published. Most of these works utilize rather severe priors in the stage of EEG preprocessing, for example, dealing only with few electrodes disregarding information contained in the others or by restricting the spectral band of interest by sharp edges.^{1,2} These severe priors could be the cause for certain degree of inconsistency in results across papers. Moreover, temporal nonstationary of this approach was showed by Meyer et al.³ These methodological issues may be overcome by the Parallel Factor Analysis (Parafac) method introduced by Bro.⁴ This method works blindly without any constraints on frequency pattern or electrode selection and thus draws natural spatio-temporo-spectral patterns from EEG spectrum (STSp). Temporal features of STSp could be then used to find brain regions with correlated brain hemodynamics. So far, the alternating least squares (ALS) method was used for Parafac estimation. This approach shows stable and reliable results when small number of STSp is estimated (eg, 4 or 5 STSp for EEG data acquired in MR). With increasing number of STSp, the reliability and stability of ALS rapidly decreases.

In our work, we introduce a method for Parafac estimation based on variational Bayesian statistic (VB).⁵ We used a large set of simulated 3-dimensional data that were subjected to the Parafac estimation using either ALS or VB and show its better performance in particular when more than 10 STSp is estimated from EEG data. Additionally, we show the utilization of VB based Parafac on EEG–fMRI data of epileptic patient acquired before successful surgical treatment (according to 1-year outcome). 30 STSp were drawn from EEG data and for each we found brain regions with correlated brain hemodynamics. One of them was the expected occipital alpha which correlated negatively with hemodynamics in occipital lobe. Another was the STSp with peak at 4 Hz in spectral pattern which correlated with brain region later resected.

The VB-based Parafac is a powerful blind decomposition method which could draw natural STSp from EEG data with better performance than ALS. It could add valuable contribution to the studying physiological relationship between EEG and hemodynamics. Moreover, it may help with evaluating the epileptic patients planned for surgical treatment.

Acknowledgments

The research was supported by the grant GAČR P304/11/1318.

References

1. Laufs H, et al. *Neuroimage*. 2003;19:1463-1476.
2. Laufs H. *Hum Brain Mapp*. 2008;29:762-769.
3. Meyer MC, et al. *Brain Topogr*. 2013;26:98-109.
4. Bro R. *Chemometr Intell Lab*. 1997;38:149-171.
5. Chappell MA, et al. *IEEE Trans Signal Proces*. 2009;57:223-236.

P084. Identification of Epileptic Foci Using ICA in Simultaneous fMRI/EEG Data

M. Lamoš¹, T. Slavíček¹, R. Marecek², and J. Jan¹

¹Department of Biomedical Engineering, Brno University of Technology, Brno, Czech Republic

²Central European Institute of Technology—CEITEC, Masaryk University, Brno, Czech Republic

The contribution aims to the investigation of relationships between manifestation of epileptic activity in the brain and its reflection into the fMRI and the EEG data, enabling better understanding of this neural activity. Independent component analysis (ICA) has advantage of being a completely data-driven approach. However, no idea on the importance of a particular independent component (IC) is available without some prior knowledge about processes, the signs of which we are looking for.¹ First step before ICA is data reduction by principal component analysis (PCA), which has a strong connection to the variability in the data; thus there is another uncertainty because effects of interest (in this case the epileptic activity) can be minor compared to common processes in the brain and then we can remove them accidentally. We tried to show that it is possible to find ICs that correspond to epileptic activity.

Simultaneous fMRI/EEG resting-state data were measured by 1.5-T MRI tomograph with MR compatible 30-channel EEG. The data were obtained before surgical resection and complemented with 3D resection mask after surgery. The study contains 13 patients with different types of focal epilepsy, and good 1-year outcome after surgery. Preprocessing was performed in standard way using SPM and BrainVision software.

Preprocessed data from both modalities were separately analysed by ICA (temporal ICA for EEG, spatial ICA for fMRI). EEG ICs were characterized by features like power, entropy and Hurst coefficient respecting higher temporal resolution than fMRI ICs. The reduction degree in fMRI ICA was based on data variability. There was 98% of variability represented by approximately 220 ICs (depends on specific subject). Only stable ICs (approximately 70) were used in the subsequent data processing. The stability was tested by Icasso.² Thereafter, the resection mask was spatially applied to stable fMRI ICs (individually for each subject) and the IC, most representative for epileptic activity, was chosen using similarity criteria of sensitivity, positive predictive value and cosine criterion. The reliability of such epileptic fMRI IC identification was verified by comparison with results of healthy subjects. The last step was then finding the EEG IC, which would

correspond to the selected fMRI IC. The relation is assessed by correlation coefficient and mutual information.³

We have demonstrated that ICA is capable of separating epileptogenic processes from the rest of the brain activity in fMRI and EEG data, and that the EEG power is the best feature for finding links between fMRI and EEG ICs via mutual information.

Acknowledgements

The research was supported by the Grant No. GAČR P304/11/1318.

References

1. Hyvärinen A, Oja E. *Neural Netw.* 2000;13:411-430.
2. Himberg J, Hyvärinen A, Esposito F. *Neuroimage.* 2004;22(3):1214-1222.
3. Jan J. *Medical Image Processing, Reconstruction and Restoration: Concepts and Methods.* Boca Raton, FL: CRC Press; 2005.

P085. Is Excessive EEG Beta Activity Associated With Delinquent Behavior in Adult Subjects With ADHD?

N.M. Meier^{1,2}, W. Perrig^{1,3}, and T. Koenig^{2,3}

¹Department of Psychology, Division of Experimental Psychology and Neuropsychology, University of Bern, Bern, Switzerland

²Department of Psychiatric Neuropsychology, University Hospital of Psychiatry, University of Bern, Bern, Switzerland

³Center for Cognition, Learning, and Memory, University of Bern, Bern, Switzerland

Objective. The attention deficit/hyperactivity disorder (ADHD) shows an increased prevalence in delinquents. In recent studies, a subgroup of subjects with ADHD and delinquents displayed excessive EEG beta activity, which has been associated with antisocial behavior in ADHD children. We investigated whether delinquent behavior in adult ADHD subjects is related to excessive beta activity. **Methods.** We compared the resting state EEGs of delinquent and nondelinquent subjects with ADHD and controls regarding power spectra and topography of the EEG. **Results.** Offenders with ADHD showed more beta power at frontal, central and parietal brain regions than nondelinquents with ADHD. **Conclusion.** Excessive beta power may represent a risk-factor for delinquent behavior in adults with ADHD. The awareness of such a risk-factor may be helpful in the assessment of the risk for delinquent behavior in a psychiatric context and provide a neurobiological background for therapeutic interventions.

P086. Oscillatory Brain Activity Correlates With Disambiguation of Hidden Figures

T. Minami¹, Y. Noritake², and S. Nakauchi¹

¹Electronics-Inspired Interdisciplinary Research Institute (EIIRIS), Toyohashi University of Technology, Toyohashi, Aichi, Japan

²Department of Information and Computer Sciences, Toyohashi University of Technology, Toyohashi, Aichi, Japan

Sudden insight into an object's identity often occurs following a period of ambiguity. While magnetoencephalography and electroencephalography (EEG) studies have shown that increased gamma-band oscillations are associated with object identification or recognition, little is known about the brain activity that occurs during disambiguation of a visual perception. Our aim was to determine whether this transition was associated with specific changes in oscillatory brain activity. Beta-band oscillations have been hypothesized to reflect the transition of cognitive states. We therefore hypothesize that beta-band oscillations are related to the process of disambiguation, and here we investigated oscillatory activity during the disambiguation process of 2-tone images using EEG. We identified oscillatory activity to detect temporal changes, and compared brain activity that occurred during a perceptual transition with activity that occurred when no perceptual transition occurred. In the beta band, we observed a decrease over posterior-parietal and temporal areas (0.2-0.5 seconds after stimulus onset). To characterize the beta-power decrease further, we applied a beamforming approach. Source analysis indicated the beta-power decrease was around the parietal-posterior regions, mainly in the precuneus. We propose that beta-band desynchronization in the parietal-posterior regions reflects the disambiguation process, and our findings provide additional support for the theory that beta-band activity is related to maintenance of the current cognitive state.

Acknowledgments

Grants-in-Aid for Scientific Research from the Japan Society for the Promotion of Science (grant number 22300076, 25330169), the Global COE Program "Frontiers of Intelligent Sensing" from the Ministry of Education, Culture, Sports, Science, and Technology, the SCOPE from the Ministry of Internal Affairs and Communications, Japan.

P087. Steady State Visually Evoked Potential Is Modulated by the Difference of Recognition Condition

K. Azuma¹, T. Minami², and S. Nakauchi¹

¹Department of Computer Science and Engineering, Toyohashi University of Technology, Toyohashi, Aichi, Japan

²Electronics-Inspired Interdisciplinary Research Institute, Toyohashi University of Technology, Toyohashi, Aichi, Japan

Recent researches revealed that the EEG component caused by flickering visual stimulus, which is called steady state visually evoked potential (SSVEP), might be a potential index for object recognition. This study examined whether SSVEP reflects different states during object recognition.

In one trial, a binary image (BI) which is difficult to recognize was followed by a grayscale image (GI) of the same object as the answer. Both BI and GI were presented in flickering manner at frequency of 7.5 Hz and 12Hz. Participants were first asked to answer whether they could recognize BI. Then, after GI was presented, participants were requested to answer whether they had correctly recognized BI. EEG recorded during BI and GI presentation was classified into

two of recognition condition in each image type according to participants' behavioral responses. We investigated SSVEP from the two recognition conditions to see whether SSVEP could reflect different states of object recognition.

For unrecognized BI, SSVEP was stronger and the middle frontal gyrus was more activated. This might be resulted from activation of theta activity during memory search, which subsequently amplified the 7.5 Hz activity in SSVEP and working memory access. On the other hand, when participants could correctly recognize objects in the images after GI presentation, brain activity was suppressed and the activities were localized in the middle temporal gyrus and middle occipital gyrus. A previous study suggested that suppression of the 6- to 8-Hz activity in the occipito-parietal area reflects the semantic processing. Therefore, the decrement of SSVEP found in this study might be a result of semantic memory retrieval. In conclusion, this study suggests that SSVEP reflects the different recognition states and shows the possibility that SSVEP might be a potential tool for extraction of human's introspective information.

Acknowledgments

Grants-in-Aid for Scientific Research from the Japan Society for the Promotion of Science (grant number 22300076, 25330169), the Global COE Program "Frontiers of Intelligent Sensing" from the Ministry of Education, Culture, Sports, Science, and Technology, the SCOPE from the Ministry of Internal Affairs and Communications, Japan.

P088. An EKG-Free Method for Extracting BCG Timing From the EEG Signal

C. Rodriguez¹, A. Lenartowicz¹, and M.S. Cohen¹

¹University of California Los Angeles, Los Angeles, CA, USA

Second to the gradient artifact, the ballistocardiogram (BCG) is the largest contaminant of the EEG recording acquired within the MRI environment. This is of particular importance for EEG signals in the sub-25-Hz frequency range as this is where the majority of the spectral power for this BCG artifact lies. Removal of BCG artifact typically depends on cardiac timing from a simultaneously acquired electrocardiogram (EKG) recording. Implementing the simultaneous EKG however introduces additional sources of error: The EKG recording device can induce artifacts in both the EEG and MRI recordings; it must be synchronized to the EEG device, a process subject to timing slips; and its success depends on an estimate of timing lag between EKG and BCG, the delay of which is not fixed within channel from heartbeat to heartbeat. To eliminate all of these confounds, especially the timing variability of the BCG artifact, we have developed EKG-free algorithms that locate and characterize the BCG artifacts in the EEG data on a channel-by-channel and event-by-event basis. There are believed to be 3 main sources of the BCG; head rotations and translation due to cardiac motion, scalp pulsation, and the Hall effect.¹ It is the scalp pulsation portion of the BCG that we have found to

be the most temporally stable with respect to the heartbeat. We have found this pulsatile signal to be highly pronounced in the L-R signal. Most likely this is due to the locations of the facial arteries. So, to extract our cardiac timing from the EEG we begin by creating a left minus right (L-R) mean signal and apply a high-order band pass filter in the range of the BCG. Next we apply a constrained peak detection algorithm with built-in error checking to identify the EKG "R-wave" equivalent in the BCG. Multiple layers of automatic error checking and correction are applied here and at each stage of the algorithm to prevent propagation of errors. Due to both the built-in error checking and using the L-R mean signal the timing between the BCG events from the L-R mean and EKG r-wave peak is extremely stable with $\sigma \approx 0.002$ seconds, on a 1-kHz recording this approaches the limit of detection. The range of the mean latency for the individual channels "r-wave" peaks within a 10-20 channel setup when compared to the L-R mean is $\sim \pm 1\%$ while the variance within channel for each event $\sim \pm 5\%$ of the channel's mean latency.

Acknowledgments

This research was sponsored by NIMH Grant 1 R21/33 DA026109-01 (Cohen); NIMH Grant 1 R21 MH096239-01A1 (Cohen), and Support from the Klingenstein Third Generation Foundation (Lenartowicz).

References

1. Debener S, Mullinger K, Niazzy R, Bowtell R. *Int J Psychophysiol.* 2008;67:189-199.

P089. A Novel MRI-Based Method for Automatic Electrode Location and Identification

C. Rodriguez¹, A. Lenartowicz¹, and M.S. Cohen¹

¹University of California Los Angeles, Los Angeles, CA, USA

Increasingly important, and key to the advancement of electroencephalographic (EEG) work, is the technique of source imaging/localization of activity within the cortex. Determination of source locations is difficult, and is limited significantly by indeterminacy of the electrode locations. There thus exists a need for accurate knowledge of the location of each electrode channel with respect to the brain. Current methods can be cumbersome, tedious and time-consuming, prone to errors, and register the locations of the electrodes to the scalp/skull, but not to the brain; our new method circumvents each of these limitations without manual interaction. We take advantage of that fact that when high-resolution source space imaging is required, anatomical MRI scans frequently are acquired as well. Our process has 2 steps, location and identification. Location is determined by extracting the electrodes from a high-resolution magnetic resonance imaging (MRI) scan of the head, with the electrodes in place, using a structural scan. Identification is performed by registering a mask with known channel numbers using a combination of linear and nonlinear transforms to the locations of the extracted electrodes. The algorithm relies on

form rather than intensity, thereby removing the need for markers. This also makes this method robust against RF parasitic signal losses that are inevitable with high-density electrode arrays and their wiring. Because the electrodes themselves are detected, and not markers, the need for estimation of the actual electrode location with respect to the marker location is eliminated. The automated labeling of dense arrays saves considerable time and effort. This method eliminates user bias increasing stability of the measurements across samples. We are currently testing the method against multiple head shapes and hairstyles as well as validating against the scalp registered and manual methods currently on the market.

Acknowledgments

This research was sponsored by NIMH Grant 1 R21/33 DA026109-01 (Cohen); NIMH Grant 1 R21 MH096239-01A1 (Cohen).

P090. Measurement of Neuronal Activity of the Mentally Retarded Child Without Restraint Using Wireless EEG, ECG, NIRS

K. Iramina¹, H. Kinoshita¹, K. Tamura¹, C. Karube¹, M. Kaneko¹, J. Ide², and Y. Noguchi²

¹Graduate School of Systems Life Sciences, Kyushu University, Fukuoka, Japan

²Department of Human Sciences, Seinan Gakuin University, Sawaraku, Fukuoka, Japan

The purpose of this study is the measurement of brain activities in usual behavior without restraint. We developed the measurement system of brain activity without restraint and we acquired the physiological information such as EEG, ECG and cerebral blood of a subject, even if the subject walked around or moved freely. We invited a 12-year-old boy with mental retardation to cooperate in our study, and measured the EEG, ECG, NIRS and moving activity while he was being in education program for 30 minutes. EEG electrodes were placed according to international 10-20 system at Fz (frontal cortex) and Pz (parietal cortex). The hemodynamic response was also measured at the forehead by NIRS. At the same time, we measured the electrocardiograph (ECG). After removing the body movement artifact from the EEG data, we analyzed the time-frequency response of EEG. As a result, we observed differences in the time course of EEG power at alpha band (8-12 Hz) and theta band (13-20 Hz), between the concentrating-state (studying) and rest-state.

P091. Advancing EEG/fMRI: Cleaning Signals and Integrating Data

M.S. Cohen¹, P.K. Douglas¹, C.M. Rodriguez¹, and H.J. Xia¹

¹University of California, Los Angeles School of Medicine and Laboratory of Integrative Neuroimaging Technology, Los Angeles, CA, USA

Approaches to the joint recording of EEG and fMRI have been described since at least 1994, yet stable and reliable technology, and principled means for data integration, remain elusive. This presentation will highlight important steps that our lab has taken toward these challenging goals.

We will consider:

1. Solutions to support accurate source space solutions. We have developed a rapid means of EEG electrode location based on MRI data that operates without user intervention, providing accurate three dimensional coordinates in high density EEG recordings. This tool has the additional advantage that the electrode locations are resolved automatically in brain space, as opposed to scalp space. It therefore intrinsically minimizes errors in inverse solutions. We will also show a novel electrode configuration that provides much improved 3-dimensional coverage of the brain without resulting in significant patient discomfort.
2. An accurate means to colocalize fMRI and EEG sources, using a surjective mapping procedure. We will show validation data to indicate accurate projection in both sensory and cognitive tasks, and reveals source dynamics in tomographic space.
3. It is well known that ballistocardiographic (BCG) artifacts are large contaminants of concurrently acquired EEG and fMRI data. We will demonstrate that the popular adaptive means of artifact suppression greatly alter the true EEG signals, at times more than doubling the quantitative errors present before correction that are particularly prominent in continuous (as opposed to event-driven) studies that seek better understanding of brain rhythms. We show that this is based on false assumption of mutual orthogonality between BCG and EEG sources. We will then present a novel hardware/software method based on group sparsity, which can reduce such errors more than 14-fold when high-density EEG is available.

P092. Relationship Between Thalamic Asymmetry and Right-Hemisphere Theta Abnormalities

E.M. Zimmerman¹, C.J. Konopka², P.S. Epstein³, and L.M. Konopka^{2,4}

¹The Chicago School of Professional Psychology, Chicago, IL, USA

²Loyola University, Chicago, IL, USA

³Advanced Neurodiagnostics, Wheeling, IL, USA

⁴Yellowbrick Foundation, Evanston, IL, USA

Objective. The right hemisphere of the brain plays a significant role in the experience and expression of emotions and is often deregulated in psychiatric patients. The thalamus influences cortical and subcortical activity in both hemispheres via widespread thalamocortical/corticothalamic projections. Asymmetrical thalamic activity may impact function in one hemisphere. In our population of psychiatric patients studied with a combination of positron emission tomography (PET)

and quantitative EEG (qEEG), most patients demonstrated reduced metabolic activity in their right thalamus. We hypothesized greater right-sided ($R < L$) thalamic asymmetry in metabolic activity would significantly correlate with focal EEG abnormalities in the right hemisphere. **Methods.** We analyzed archival PET and qEEG data of 48 patients from a community-based psychiatric outpatient clinic. Patients presented with a variety of symptoms, often with complex and comorbid diagnoses. Statistical evaluation for PET images was obtained with BRASS software (HERMES software, total count adjustment). Significant focal EEG abnormalities were identified using low-resolution brain electromagnetic tomography (LORETA). Significance was set at ± 2 standard deviations. Independent t tests ($P < .05$) were utilized to compare percent differences between right and left thalamic count/voxel ratios as well as normalized asymmetry z -scores between patients with focal EEG abnormalities in the right hemisphere and those without. **Results.** Thirty-five ($n = 35$) patients demonstrated decreased activity in the right thalamus as compared to the left. Of these patients, 12 ($n = 12$) demonstrated one or more right-hemispheric focal EEG abnormalities in theta (θ) frequencies and 23 ($n = 23$) did not have any right-sided focal θ findings. A significant difference was found in percentage difference of right/left metabolic activity between patients with right focal θ abnormalities ($M = 8.90$, $SD = 4.92$) and those without ($M = 5.36$, $SD = 4.07$); $t = -2.268$, $P = .030$. There was also a significant difference in normalized asymmetry z -scores for patients with right focal θ abnormalities ($M = 3.31$, $SD = 1.49$) and those without ($M = 2.00$, $SD = 1.38$); $t = -2.590$, $P = .014$. **Conclusions.** The findings support the hypothesis in that right-sided thalamic asymmetry is correlated to presence of right-hemispheric focal θ abnormalities in EEG. The results offer implications for relationships between thalamic function and electrophysiological activity. This study supports a multimodality approach combining nuclear imaging and EEG to enhance identification of abnormal function in psychiatric patients.

P094. Positive and Negative Correlations Between Cerebral Blood Flow and Fractional Anisotropy in Brain White Matter

S. Giezendanner¹, M. Fisler¹, L. Soravia¹, J. Andreotti¹, R. Wiest², T. Dierks¹, and A. Federspiel¹

¹Psychiatric University Hospital, Department of Psychiatric Neurophysiology, Bern, Switzerland

²Institute of Diagnostic and Interventional Neuroradiology, University of Bern, Bern, Switzerland

Introduction. Little is known about white matter (WM) perfusion. Recently, a study investigated the relationship between cerebral blood flow (CBF) and WM properties on a tract-specific basis and showed an inverse correlation between CBF and fractional anisotropy (FA).¹ In the present study, we probe

for a relationship between CBF and FA using a voxel-based approach with tract-based spatial statistics (TBSS). **Methods.** A total of 32 healthy subjects were included in the study (mean age: 28.7 ± 8.2 years). All MRI scanings were performed on a 3T Siemens TRIO TIM scanner. DTI was performed with a spin echo EPI using two 180° pulses along 42 non-collinear directions. Preprocessing of the FA data was carried out using TBSS,² part of FSL.³ Pseudocontinuous ASL (pCASL) sequence was acquired.^{4,5} MatLab/SPM8 was used for preprocessing of imaging data. After motion correction, CBF was quantified, co-registered to the FA maps in native space and smoothed. SNR of the 50 CBF time series was estimated. The nonlinear warps and skeleton projections from the FA maps were applied to the CBF and SNR images. A correlation analysis between FA and CBF values in each voxel of the WM skeleton across subjects was performed masking for low SNR and FA. The significance was estimated using AlphaSim program.⁶ **Results.** Clusters with significant negative correlations comprised in total 210 voxels and were located in parts of the left and right cingulum (hippocampus), the left uncinate fasciculus, the genu and the splenium of the corpus callosum (CC), the right superior longitudinal fasciculus (SLF) and the right corticospinal tract (CST). Clusters with significant positive correlations comprised 218 voxels and were located in parts of the left anterior and posterior infero fronto-occipital fasciculus, the genu of the CC, the left forceps major, the left superior and posterior corona radiata, the left cingulum (cingulate gyrus), the left SLF and the right CST. **Conclusions.** The present study investigated perfusion and microstructural properties within WM in healthy controls. In line with a previous study it shows significant negative correlations between CBF and FA values. However, the as-yet unreported in literature positive correlations might indicate that fiber bundles having differing functional purposes display different metabolic properties.

References

1. Aslan S, et al. *Neuroimage*. 2011;56:1145-1153.
2. Smith SM, et al. *Neuroimage*. 2006;31:1487-1505.
3. Smith SM, et al. *Neuroimage*. 2004;23(suppl 1): S208-S219.
4. Wu WC, et al. *Magn Reson Med*. 2007;58(5):1020-1027.
5. Dai W, et al. *Magn Reson Med*. 2008;60(6):1488-1497.
6. Cox RW. *Comput Biomed Res*. 1996;29(3):162-173.

P095. ASL-Based Functional Connectivity in Schizophrenia Spectrum Disorders Relates to Disease Severity

N. Razavi¹, A. Federspiel¹, T. Dierks¹, M. Hauf², and K. Jann^{1,3}

¹Department of Psychiatric Neurophysiology, University Hospital of Psychiatry/University of Bern, Bern, Switzerland

²Institute of Diagnostic and Interventional Neuroradiology, University of Bern/Inselspital, Bern, Switzerland

³Department of Neurology, University of California, Los Angeles, CA, USA

Functional connectivity (FC) of the human brain has become a widely used method to investigate brain function. Recently, arterial spin labeling (ASL) based cerebral blood flow (CBF) measurements has attained interest to estimate FC. Compared to the conventional BOLD fMRI that is a complex mixture of perfusion, metabolic and oxygenation status of the brain, the CBF measurements represent absolute quantitative brain perfusion. Especially in the diseased brain, this additional information helps to better classify the pathological alterations and explain inter-individual differences in disease symptoms and their severity.

In this study, we aimed to explore the potential of CBF-based functional connectivity maps in schizophrenia spectrum disorder in comparison to BOLD. To this end, pCASL^{1,2} and standard BOLD fMRI data from 11 schizophrenia spectrum disorder patients (SZ; 30.5 ± 6.3 years; 9 males/2 females) were acquired. For comparison, BOLD data of 11 age-matched healthy controls (HC) was also analyzed. Psychopathology and the severity of symptoms were assessed by the PANSS interview.

We ran 3 separate group ICAs⁴ to compute group components (GC) and single subject components (SC) for HC_{BOLD}, SZ_{BOLD} and SZ_{ASL}. In all data sets, the default mode network (DMN) was identified. The DMN-GC of all 3 analyses showed a highly similar pattern (spatial correlations: HC_{BOLD} to SZ_{BOLD} $r = 0.74$; SZ_{BOLD} to SZ_{ASL} $r = 0.56$; HC_{BOLD} to SZ_{ASL} $r = 0.55$). CBF and BOLD single subject maps also showed a consistent spatial pattern for individual patients ($r = 0.73$). Mean CBF in DMN was 50.0 ± 17.7 mL/100 g/min. The spatial similarity of the SZ_{ASL}-SC to the SZ_{ASL}-GC was negatively correlated to the PANSS positive scores ($r = -0.66$, $p = 0.03$). Finally, partial correlation between SZ_{ASL}-SC and DMN-CBF values (using GrayMatter-CBF as control variable) yielded a negative trend ($r = 0.61$, $P = .06$).

Our results showed that pCASL and BOLD yield spatially similar DMNs, while pCASL provides additional information about the absolute perfusion of the brain and the specific network.

Furthermore, the degree of similarity of an individuals' DMN to the GC may reflect the severity of specific disease symptoms as assessed by PANSS positive scores. Thus it could be argued that spatially altered DMN in schizophrenia reflects deficits in self-monitoring, causing a disturbed capacity of an individual in the integration of external stimuli and internal cognition to a whole concept. Furthermore, higher CBF values in the altered DMNs suggest a state of hyperactivity that may relate to how processing errors occur due to constant overload.

References

1. Dai et al. *Magn Reson Med*. 2008.
2. Wu et al. *Magn Reson Med*. 2007.
3. Deichmann et al. *Neuroimage*. 2004.
4. Calhoun et al. *Hum Brain Mapp*. 2001.

P096. A Phantom Study Toward MEG Measurements by a Newly Developed Compact Module of Atomic Magnetometer

K. Kamada^{1,2}, D. Sato¹, Y. Ito¹, K. Okano³, N. Mizutani³, and T. Kobayashi¹

¹Graduate school of Engineering, Kyoto University, Nishikyo-ku, Kyoto, Japan

²Japan Society for the Promotion of Science, Tokyo, Japan

³Canon Inc, Ohta-ku, Tokyo, Japan

Biomagnetic field measurements, such as magnetocardiograms (MCGs) and magnetoencephalograms (MEGs), are widely used for non-invasive imaging of biological functions. Recently, optically pumped atomic magnetometers (OPAMs) based on electron-spin polarization of alkali-metal atoms have attracted significant attention for the biomagnetic field measurements as alternative sensors to those based on superconducting quantum interference devices (SQUIDS).^{1,2} We developed a compact module of high-sensitivity OPAM for the biomagnetic field measurements.³ Here, we evaluated it by measuring magnetic fields generated by dipole-electrodes placed inside a phantom modelling the human head.

The module has a Pyrex glass cell (8 cm³) containing potassium metal and buffer gases as a sensor head. To achieve high sensitivity, the module was operated under spin-exchange relaxation-free (SERF) conditions.^{2,4,5} The module was placed in a 3-layer magnetic shield and the cell was heated to 180°C inside the module to obtain high atomic density. The laser beams used to generate electron-spin polarization and to detect spin rotation were irradiated via optical fibers. The distance between the sensing area and surface of the module was about 2 cm. A phantom consisted of a spherical glass, normal saline solution, and 3 dipole electrodes with different positions.⁶ The diameter of the spherical phantom was 100 mm and the length of the each dipole electrode was 6 mm. A sinusoidal wave current was applied to 1 of the 3 electrodes to reproduce magnetic fields caused by neural activities (pseudo-MEGs). The frequency of the current was set 10 Hz and its magnitude was changed from 1 μ A to 10 μ A.

The magnetic field sensitivity of the module and noise floor of the probe beam at 10 Hz were 20 fT_{rms}/Hz^{1/2} and 5 fT_{rms}/Hz^{1/2}, respectively. This result indicated that ambient magnetic field noise limited the sensitivity of the module at 10 Hz. The pseudo-MEGs with amplitudes of several hundreds fT generated by the phantom could be successively measured by using this module. Although more miniaturization of the module and multi-channel array detections are required to achieve more practical measurement systems, these results demonstrated the feasibility of the newly developed OPAM module for MEG measurements.

Acknowledgments

Ministry of Education, Culture, Sports, Scientist and Technology, Japan.

References

1. Budker D, Romalis MV. *Nat Phys*. 2007;3:227-234.
2. Allred JC, Lyman RN, Kornack TW, Romalis MV. *Phys Rev Lett*. 2002;89:130801.
3. Okano K, Terao A, Ban K, Ichihara S, Mizutani N, Kobayashi T. *Proc IEEE Sensors*. 2012;2012:1-4.
4. Happer W, Tang H. *Phys Rev Lett*. 1973;31:273-276.
5. Kominis IK, Kornack TW, Allred JC, Romalis MV. *Nature*. 2003;422:596-599.
6. Taue S, Sugihara Y, Kobayashi T, Ichihara S, Ishikawa K, Mizutani N. *IEEE Trans Magn*. 2010;46:3635-3638.

P097. Predicting Benefits of Multisensory Memories

A. Thelen¹ and M. Murray^{1,2,3,4}

¹FENL, Department of Clinical Neurosciences, CHUV, Lausanne, Switzerland

²Radiology Department, CHUV, Lausanne, Switzerland

³Electroencephalography Brain Mapping Core, Center for Biomedical Imaging of Lausanne and Geneva, Switzerland

⁴Department of Hearing and Speech Sciences, Vanderbilt University Medical Center, Nashville, TN, USA

Single encounters with multisensory auditory-visual pairings are sufficient to impact subsequent unisensory object recognition (Thelen et al., 2012). Recognition accuracy for images that had been paired with a meaningless sound upon their initial encounter (V+) is generally impaired when compared with recognition accuracy of images encountered only visually (V-) during a continuous recognition task. This behavioral decrement correlates with differential neuronal activity at 270 to 310 ms post-stimulus onset within middle temporal cortices. Moreover, activity within these areas appears to be linked to the episodic nature of the meaningless encounters and/or to behavioral outcome, rather than reactivation processes of initial encounter context as proposed by the “reintegration” theory. In order to address this hypothesis directly, we divided subjects into groups according to whether recognition accuracy for images paired with a meaningless sound upon initial encounter (V+) was impaired (group 1) or enhanced (group 2) with respect to images encountered only visually (V-).

We computed sensitivity (d') and response bias (c') measures to investigate differences between groups in terms of perception and response strategy. Data were submitted to a 2×2 ANOVA with between-subject factor of group and within-subject factor of modality (V- and V+). A significant group \times modality interaction for d' and post hoc paired t tests revealed a significant decrease of d' in group 1 (mean \pm s.e.m.: $d'(V-) = 2.96 \pm 0.28$; $d'(V+) = 2.27 \pm 0.30$; $t = 3.218$; $P = .024$). Analyses on relative criterion (c') revealed a significant group \times modality interaction, and post hoc paired t tests revealed a significant effect for c' for group 2 (mean \pm s.e.m.: $c'(V-) = -0.23 \pm 0.03$; $c'(V+) = -0.18 \pm 0.03$; $t = -4.189$; $P = .009$). This pattern suggests the 2 groups use distinct strategies to perform the task, either relying on perception or adopting a lax response criterion. To examine the neural bases of these strategies, we analyzed event-related potentials (ERPs).

In terms of initial multisensory presentations, we observed a significant group by condition interaction at 270 to 316 ms post-stimulus for the GFP. Further, this group difference was also observed at the level of source estimations. A significant group by condition interaction within right temporal regions at 270 to 346 ms post-stimulus was observed, suggestive of differential underlying multisensory processing that may explain the opposing behavioral outcome during unisensory repetition discrimination.

P098. Quantitative EEG During Hyperbaric Oxygen Breathing in Professional Divers

L. Pastena¹, E. Formaggio^{2,*}, S.F. Storti^{3,*}, F. Faralli⁴, M. Melucci⁴, R. Gagliardi⁴, L. Ricciardi⁴, and G. Ruffino⁴

¹Department of Neurological Sciences, University of Rome, La Sapienza, Rome, Italy

²Department of Neurophysiology, Foundation IRCCS San Camillo Hospital, Venice, Italy

³Department of Neurological and Movement Sciences, University of Verona, Verona, Italy

⁴Italian Navy Medical Service Comsubin Varignano, Le Grazie (La Spezia), Italy

*These authors equally contributed to this work.

The use of oxygen mixture and closed circuit apparatus in diving augments the risk of central nervous system oxygen toxicity (CNS O₂T); it is known that the pattern of electroencephalogram (EEG) changes during saturation dives¹. In fact breathing oxygen at various depths, especially between 8 and 18 m seawater (msw), can increase the toxicity of oxygen on central nervous system. The aim of this study was to investigate and define the possible alterations of cerebral activity during a prolonged hyperbaric oxygen exposure and decompression compared to a baseline activity. The EEG was recorded inside the hyperbaric chamber by a Holter apparatus equipped with Bluetooth technology (Ates Medica Device, Italy; Electrical Geodesic, Inc, USA). A 32-channel EEG was recorded with a Bluetooth system in 11 subjects. A 20-minute EEG recording was carried out under three different conditions: breathing air inside a hyperbaric chamber at sea level (1 ATA); breathing O₂ at 18 m (2.8 ATA); during decompression (rate of descent and ascent 9 m/min; overall time 60 minutes). EEG data were analyzed using fast Fourier transform. Relative power was estimated for delta (1-4 Hz), theta (5-7 Hz), alpha (8-12 Hz), beta1 (13-15 Hz), and beta2 (15-30 Hz) frequency ranges. The relative power and statistical tests were represented using topographic maps²: one map for each band in the air condition (1-20 minutes) and 7 maps for O₂ and decompression conditions indicating the intervals of analysis (1, 2, 5, 8, 10-12, 15-17, and 18-20 minutes). While breathing oxygen, brain activity shows an early fast delta decrease in the posterior regions with a synchronous and significant increase of alpha in the same regions (post hoc paired sample 2-tailed t test with Bonferroni correction, $P < .05$). During decompression, the delta relative

power decrease, compared to baseline, is uniformly distributed over the cerebral cortex until minute 8. At minute 10-12 this decrease is principally localized in the posterior regions. The EEG power in alpha activity is maximal in the same posterior regions during the first 2 minutes of decompression and only returns to baseline after 20 minutes. The findings (ie, a decrease of delta and an increase of alpha activity) showed an opposite behaviour compared to hypoxia condition. Decrease in delta activity observed during oxygen breathing would be a sign of reduced performance of cortical inhibitory mechanisms. Thus, it is possible to detect an increase in alpha activity in the central regions where this activity is normally very low. Results may be relevant in order to establish a reference point in future studies on O₂ sensitive patients who reported problems during oxygen diving.

Acknowledgments

This study has been funded by a grant SMD L-023: Rilevazioni elettrofisiologiche in immersione; Cap. 1322, Italian Ministry of Defense, Direzione Generale della Sanità Militare, 2010.

References

1. Pastena L, et al. *Aviat Space Environ Med.* 1999;70:270-276.
2. Formaggio E, et al. *J Neuroeng Rehabil.* 2013. doi:10.1186/1743-0003-10-24.
3. Papadelis C, et al. *Clin Neurophysiol.* 2007;118:31-52.

P099. Assessment of Dynamic Effective Connectivity of Epileptic Networks in Temporal Lobe Epilepsy Using Scalp EEG

A. Coito¹, P. Macku¹, R. Tyrand¹, L. Astolfi², B. He³, R. Wiest⁴, M. Seeck⁵, C. Michel¹, G. Plomp⁵, and S. Vulliemoz^{1,5}

¹Functional Brain Mapping Lab, Faculty of Medicine, University of Geneva, Geneva, Switzerland

²Department of Physiology and Pharmacology, University of Rome La Sapienza, Rome, Italy

³Department of Biomedical Engineering, University of Minnesota, Minneapolis, MN, USA

⁴Support Center for Advanced Neuroimaging, University Institute for Diagnostic and Interventional Neuroradiology, Inselspital-Bern University Hospital, University of Bern, Bern, Switzerland

⁵Epilepsy Unit, Department of Clinical Neuroscience, University Hospital and Faculty of Medicine of Geneva, Geneva, Switzerland

Objective. We aimed to analyze the dynamic behavior of epileptic networks through the study of effective connectivity using scalp EEG signals, in order to improve the understanding of pathologic neural activity in particular spikes, seizures, and their electro-clinical and cognitive manifestations. **Methods.** In 10 patients, 5 with right temporal lobe epilepsy (RTLE) and 5 with left temporal lobe epilepsy (LTLE), we assessed the connectivity of large-scale cortical networks during interictal spikes at high temporal resolution, using high density (96-256 channels) EEG recordings. The cortical electric source activity was obtained for 82 cortical regions of interest (ROI) using

an individual head model and a distributed linear inverse solution. A multivariate, time-varying (millisecond resolution), and frequency-resolved (1-50 Hz) Granger causality analysis (partial directed coherence) was applied to the source signal of all ROIs. In all patients, the results were validated by subsequent intracranial recordings or postsurgical outcome. Afterward, a grand average for RTLE and LTLE groups was computed. **Results.** The key driving structures were located in the medial temporal regions. This time-frequency analysis of source activity revealed changes in 2 frequency bands: 7.5-35 Hz around the spike and 50-80 Hz before the spike. Peak information transfer occurred before the spike maximum, sometimes with a different structure being the key driver at the time of spike maximum and the following slow wave. Both in individual cases and group analyses, we observed an increase in information outflow from the key driver around the spike. The peak of this information transfer occurred before the spike maximum (10-20 ms before), which supports the fact that the key drivers should be identified before the spike peak. Furthermore, we observed a different temporal dynamics between LTLE and RTLE. The results were concordant with the postoperative MRI—the key driver overlapped with the removed region. **Conclusion.** EEG-based time-varying effective connectivity of epileptic spikes was able to identify the major contributors to interictal epileptic activity. This was concordant with invasive electro-clinical findings and supports the fact that the key drivers should be identified before the spike maximum. This enhanced characterization of the epileptic networks could have major clinical implications for tailoring resective, disconnective and functional surgery.

Acknowledgments

Study funded by Swiss National Foundation (SNF) grants 33CM30-140332, 141165, 144529, 122073.

P100. Optimum Gradient Artifact Removal From Simultaneously Acquired fb-EEG/fMRI Data Using FACET

F.Ph.S. Fischmeister^{1,2}, J. Glaser³, V. Schöpf⁴, H. Bauer³, and R. Beisteiner^{1,2}

¹Study Group Clinical fMRI, Department of Neurology, Medical University of Vienna, Vienna, Austria

²High Field MR Center of Excellence, Medical University of Vienna, Vienna, Austria

³Faculty of Psychology, University of Vienna, Vienna, Austria

⁴Department of Neuro- and Musculoskeletal Radiology, Medical University of Vienna, Vienna, Austria

Throughout recent years simultaneous recordings of EEG and fMRI has turned into a viable tool for clinical applications. However, elimination of scanner-induced artifacts is still challenging. For event related potentials (ERP) the practicability of several software algorithms to compensate these imaging artifacts has been shown repeatedly. Slow cortical potentials (SCP), however, form a special class of ERPs induced by

temporally extended cognitive processes representing changes in the frequency range below 0.1 Hz. In case of SCPs, existing artifact reduction methods fail since they modify the DC changes in the EEG signal. Here, we present an optimum multistep algorithm which combines various correction steps for the removal of gradient artifacts preserving slow potential variations present in the EEG signal.

FACET is a modular toolbox for fast and flexible correction and evaluation of imaging artifacts. Within this toolbox an optimum algorithm (OptGAR) was constructed by combining various preprocessing steps—like slice onset detection and sub-sample alignment—with an adaptive template generation approach to optimally describe the gradient artifact. Residual artifacts are removed using PCA and ANC. This algorithm was first developed and evaluated by automatic comparison to existing algorithms via stepwise evaluation and then applied to simultaneously acquired fb-EEG data.

Fb-EEG was recorded from 64 locations using a NEURO PRAX MR full-band EEG amplifier while participants were visually stimulated using a slowly rotating propeller (presented for 8 seconds) repeated 40 times with a 7-second black screen interstimulus interval. Signals were sampled at 2000 smp/s within a frequency range from DC to 1200 Hz. In order to evaluate OptGAR on fb-EEG data, this paradigm was performed twice, one run without and one run with simultaneous fMRI acquisition.

Overall the algorithm presented here not only outperforms existing tools but also shows a unique performance in reducing the content of slice frequency and its harmonics while preserving slow endogenous fluctuations in full-band EEG data. Corrected fb-EEG data show a clear negative SCP that can be easily depicted at occipital recording sites.

Since SCP changes and the BOLD signal show high positive correlations, our new correction approach allows for simultaneously investigate endogenous fluctuations of cortical excitability within functional systems. Thus OptGAR together with FACET provides a valuable tool for the removal of imaging artifacts from concurrently recorded fb-EEG.

References

1. Bauer H. Slow potential topography. *Behav Res Methods Instrum Comput.* 1998;30(1):20-33.
2. He BJ, Snyder AZ, Zempel JM, Smyth MD, Raichle ME. Electrophysiological correlates of the brain's intrinsic large-scale functional architecture. *Proc Natl Acad Sci U S A.* 2008;105(41):16039-16044.
3. Khader P, Schicke T, Röder B, Rösler F. On the relationship between slow cortical potentials and BOLD signal changes in humans. *Int J Psychophysiol.* 2008;67(3):252-261.
4. Ritter P, Villringer A. Simultaneous EEG-fMRI. *Neurosci Behav Rev.* 2006;30(6):823-838.

PI01. Quantitative Agreement Between fMRI and EEG Brain Connectivity Matrices in Different Frequency Bands

F. Deligianni¹, M. Centeno¹, D.W. Carmichael¹, and J. Clayden¹

¹Imaging and Biophysics Unit, UCL Institute of Child Health, London, UK

It has been shown that the resting-state (rs) networks observed with fMRI reflect electrophysiological activity.¹⁻³ However, questions remain regarding which EEG features most closely reflect rs fMRI networks. For example, significant spatial agreement with fMRI-derived networks emerged from MEG data filtered in β and α frequency bands.^{1,2} Whereas, work in anesthetised animals with intracranial EEG suggested that the rs fMRI signal correlated with the EEG power coherence in low-frequency bands.³ Here, we quantify the agreement of whole-brain connectivity matrices derived from rs fMRI and EEG frequency-filtered bands.

Simultaneous EEG-fMRI was acquired from one healthy volunteer. Scalp EEG was recorded using a 64-channel MR-compatible electrode cap (BrainCap MR). A T2*-weighted gradient-echo EPI sequence with 300 volumes was acquired at 1.5 T: TR/TE = 2160/30, 30 slices with thickness 3.0 mm (1-mm gap), effective voxel size $4.0 \times 3.3 \times 3.3$ mm, flip angle 75° , FOV $210 \times 210 \times 120$ mm. A T1-weighted structural image was also obtained.

EEG was corrected for scanner and cardiac pulse related artefacts using Brain Vision Analyzer 2. It was downsampled to 250 Hz and frequency filtered into 5 bands: δ (1-4 Hz), θ (4-8 Hz), α (8-13 Hz), β (13-30 Hz), and γ (30-70 Hz). Frequency filtered EEG data were projected into source space using beamforming as implemented in SPM12b.^{2,4} The signal was segmented in (fMRI) TR epochs. The average envelope of the signal was estimated for each segment based on the absolute value of the Hilbert transform.

Preprocessing of the fMRI data involves removing the first 5 volumes, motion correction, low pass filtering and spatial smoothing with FSL. Both preprocessed fMRI and the averaged envelope of the EEG signals were averaged within cortical gray matter regions derived from Freesurfer's anatomical parcellation of the T1-weighted image. Between region connectivity matrices were derived based on the correlation coefficient calculated between each regions averaged time series and all other regions. We estimated the similarity between connectivity matrices based on a distance metric that quantifies differences in the space of correlation matrices.^{5,6}

Our results demonstrate that the distance between the fMRI connectivity matrix and the EEG connectivity matrix derived from β band is an order of magnitude less than the distance from the other bands. The γ and α bands show the next-smallest distances. The highest distance was observed for δ and θ bands.

Our analysis of rs fMRI and EEG provides quantitative evidence that supported the hypothesis that β band activity reflects spontaneous cognitive operations during conscious rest.⁷

References

1. Brookes MJ, et al. *Proc Natl Acad Sci U S A*. 2011;108:16783-16788.
2. Brookes MJ, et al. *Neuroimage*. 2011;56:1082-1104.
3. Lu H, et al. *Proc Natl Acad Sci U S A*. 2007;104:18265-18269.
4. Brookes MJ, et al. *Neuroimage*. 2012;63:910-920.
5. Forstner W, et al. *Qua vadis geodesia*. 1999;113.
6. Deligianni F, et al. *IPMI*. 2011;296-307.
7. Laufs H, et al. *Proc Natl Acad Sci U S A*. 2003;100:11053-11058.

PI02. Gender Affects Activity of the Brain's Default Mode Network at Rest

G. Mingoia^{1,2}, K. Langbein¹, M. Dietzek¹, G. Wagner¹, St Smesny¹, S> Scherpiet¹, R. Maitra¹, Ch. Gaser^{1,3}, H. Sauer¹, and I. Nenadic¹

¹Department of Psychiatry and Psychotherapy, Jena University Hospital, Jena, Germany

²Brain Imaging Facility, IZKF, RWTH University Hospital, Aachen, Germany

³Structural Brain Mapping Group, Department of Psychiatry and Psychotherapy, Jena, Germany

Introduction. The default mode network (DMN) has been studied in a number of psychiatric and neurological conditions. The changes detected in these disorders are assumed to reflect task-independent basic alterations of brain function. However, there is little data on physiological variation, in particular effects of gender. Given the structural differences in male and female brains, it appears conceivable that basic functional differences might emerge even in the absence of cognitive task. We tested the hypothesis that DMN activity under resting state (RS) conditions differs between male and female healthy volunteers. **Methods.** We obtained RS fMRI series (3 T, $3 \times 3 \times 3$ mm resolution, 45 slices, TR 2.55 seconds, 210 volumes) in 67 healthy, right-handed subjects: 33 females (mean age 31.6 ± 8.8 years), and 34 males (29.8 ± 7.9 years), matched for age (T test: $P = .39$). All subjects were asked to lie in the MRI scanner keeping their eyes closed with no further specific instructions. Data were preprocessed using SPM8. Band pass (0.009-0.18 Hz) frequency filters were applied. We applied FSL MELODIC yielding 30 IC, and an automated routine to select for each subject the component matching the anatomical DMN definition. We then analyzed the frequency domains for this extracted DMN, estimating the power of a signal at different frequencies. The time course associated with each individual's DMN component was transformed from the time domain to the frequency domain using Welch's method.¹ **Results.** Our method

reliably identified a DMN component in every subject, with no differences of the goodness of fit between groups ($P = .77$). We found significant differences ($P < .05$ FDR) with males showing larger extent of the network in left superior frontal gyrus (BA10) and left superior temporal gyrus (BA 39) and in women versus men in a large prefrontal medial area including medial and superior frontal gyrus (BA10/11). We found a significant diagnosis \times frequency interaction ($F(12, 54) = 2.485$, $P = .011$). T tests performed post-hoc at each frequency bin showed that the women exhibited significantly higher spectral power than men at a frequency bin around 0.0784 Hz ($F = 8.038$, $P = .006$) and 0.1098 Hz ($F = 6.254$, $P = .015$). **Conclusions.** Our findings provide robust evidence for gender-related modulation of DMN activity under RS. They contradict findings of a recent study² suggesting that male and female brains show no difference in DMN activity. In addition power spectrum analysis suggests different power distribution in frequency domain of DMN during RS between genders. Our results suggest that sexual dimorphisms in the brain are detectable already under RS conditions.

References

1. Welch PD. The use of fast Fourier transform for the estimation of power spectra: a method based on time averaging over short, modified periodograms. *IEEE Trans Audio Electroacoust*. 1967;AU-15:70-73.
2. Weissman-Fogel I, Moayed M, Taylor KS, Pope G, Davis KD. Cognitive and default-mode resting state networks: do male and female brains "rest" differently? *Hum Brain Mapp*. 2010;31:1713-1726.

PI06. Cortical and Subcortical Phase-Amplitude Cross-Frequency Coupling Tracks Human Motor Adaptation in Skill Learning

S. Dürschmid^{1,2}, T. Zaehle^{1,2}, H. Pannek³, H.F. Chang⁴, J. Voges¹, J. Rieger⁵, R.T. Knight^{5,6}, H.-J. Heinze^{1,2,7}, and H. Hinrichs^{1,2,7}

¹Department of Neurology, Otto-von-Guericke University, Magdeburg, Germany

²Leibnizinstitut of Neurobiology (LIN), Magdeburg, Germany

³Epilepsiezentrum Bethel, Bielefeld, Germany

⁴Department of Neurological Surgery, University of California, San Francisco, CA, USA

⁵Department of Psychology, University of California, Berkeley, CA, USA

⁶Helen Wills Neuroscience Institute, University of California, Berkeley, CA, USA

⁷German Center for Neurodegenerative Diseases (DZNE), Magdeburg, Germany

Motor skill acquisition is proposed to be supported by tuning of neural networks constituted by (1) motor cortex, (2) subcortical structures as the Nucleus Accumbens (NAcc) and (3) dispersed cortical regions (eg, temporal areas) in which information are increasingly integrated to adapt to external needs. We assessed

Phase-Amplitude Cross-Frequency Coupling (PAC) between theta (θ) and high gamma (HG) oscillations as an integrating mechanism facilitating motor adaptation. To address this issue we investigated changes of PAC during motor skill acquisition in three studies involving (1) presurgical electrocorticographic recordings (ECoG), (2) recordings from DBS procedure and (3) whole-head MEG recordings. (1) To assess whether PAC tracks motor learning on a cortical level we recorded from subdural electrodes from 6 patients learning motor tasks requiring coordination of finger movements with an external cue (Serial Response Task [SRT], auditory motor task, Go/No-Go). In (2) we conducted the SRT with varying levels of cognitive control. We recorded intracranial field potentials directly from the bilateral human NAcc in three patients to assess PAC in the NAcc. In a magneto-encephalographic study (3) we studied 11 healthy subjects and assessed whether θ activity synchronization (phase locking [PLV]) between MEG sensors correlated with cognitive control.

In (1), performance improved in all subjects and all tasks during the first block and plateaued in subsequent blocks. Skill learning was paralleled by increasing neural changes in the trial-to-trial PAC between θ (4-8 Hz) phase and HG (80-180 Hz) amplitude. Electrodes showing this covariation pattern were located contralateral to the limb performing the task and were observed predominantly in motor brain regions. We observed stable PAC when task performance asymptoted. In parallel θ networks, acting on long distances, increased while HG networks, working on short distances decreased as indicated by between electrode PLV.

In (2), PAC was observed in the human NAcc, transiently occurring contralateral to a movement following the motor response. Importantly, PAC correlated with the level of cognitive control needed to monitor the action performed.

The MEG study (3) showed that following stimulus onset θ activity (de-)synchronization reflects the level of cognitive control and predicts the upcoming reaction times. MEG sensors showing the PLV variation as a function of cognitive control were bilaterally located in the temporal cortex. Subcortical PAC reached its maximum when cortical phase locking was minimal. These findings support a key role of PAC in the evaluation of motor programs during adaptive behavior.

PI 107. Dimension Reduction for Individual ICA to Decompose fMRI During Real-World Experiences: Principal Component Analysis vs. Canonical Correlation Analysis

V. Tsatsishvili¹, F. Cong¹, T. Puoliväli¹, V. Alluri^{1,2}, P. Toiviainen², A.K. Nandi^{1,3,4}, E. Brattico⁴, and T. Ristaniemi¹

¹Department of Mathematical Information Technology, University of Jyväskylä, Jyväskylä, Finland

²Finnish Centre of Excellence in Interdisciplinary Music Research, Department of Music, University of Jyväskylä, Jyväskylä, Finland

³Department of Electronic and Computer Engineering, Brunel University, Uxbridge, Middlesex, UK

⁴Institute of Behavioral Sciences, Cognitive Brain Research Unit, University of Helsinki, Helsinki, Finland

Group independent component analysis (ICA) with special assumptions is often used for analysing functional magnetic resonance imaging (fMRI) data. Before ICA, dimension reduction is applied to separate signal and noise subspaces. For analyzing noisy fMRI data of individual participants in free-listening to naturalistic and long music, we applied individual ICA and therefore avoided the assumptions of Group ICA. We also compared principal component analysis (PCA) and canonical correlation analysis (CCA) for dimension reduction of such fMRI data. We found interesting brain activity associated with music across majority of participants, and found that PCA and CCA were comparable for dimension reduction.

PI 110. Altered N400 Correlates With Reduced Neuronal Activity in Anterior Temporal Lobes in Dementia

M. Grieder¹, R.M. Crinelli², K. Jann³, A. Federspiel¹, M. Wirth⁴, T. Koenig¹, M. Stein¹, L.-O. Wahlund², and T. Dierks¹

¹Department of Psychiatric Neurophysiology, University Hospital of Psychiatry, University of Bern, Bern, Switzerland

²Department NVS, Division of Clinical Geriatrics, Karolinska Institute, Stockholm, Sweden

³Department of Neurology, University of California Los Angeles, Los Angeles, CA, USA

⁴Jagustlab, Helen Wills Neuroscience Institute, University of California Berkeley, Berkeley, CA, USA

With the progressing course of Alzheimer's disease (AD), deficits in declarative memory increasingly restrict the patients' daily activities. Besides episodic memory impairments, semantic memory is affected by this dementia subtype. In contrast, patients suffering from semantic dementia (SD) show isolated semantic memory impairments. With the aim to establish biological markers for the early differentiation of symptom dimensions in dementia subtypes, the present study compared 14 early AD and 5 mild SD patients with 19 healthy, age-matched controls.

In particular, the participants' electrophysiological brain activity during semantic word processing was correlated with their baseline cerebral blood flow (CBF). In detail, a voxel-wise linear regression between regional CBF of each participant at rest and individual event-related potential (ERP) topographies, obtained while the participants performed lexical decisions in a semantic priming task, was conducted.

The analysis revealed that a deviant topography of the N400, an ERP sensitive to semantic word retrieval, was related to decreased CBF mainly in the anterior temporal lobes. Although the altered N400 topography was not specific for AD and SD, it differentiated dementia patients from healthy controls with a sensitivity of 0.8. Thus, the present study proposed N400-topography alterations as a possible candidate marker for impaired semantic word retrieval occurring in early dementia.

PII1. Relationship of Mood States With Prefrontal Cortex Activation During Working Memory Tasks Performed by Participants in Return-to-Work Program

H. Atsumori¹, R. Yamaguchi², Y. Okano², H. Sato¹, T. Funane¹, K. Sakamoto^{2,3}, and M. Kiguchi¹

¹Central Research Laboratory, Hitachi, Ltd, Hatoyama, Saitama, Japan

²MDA-JAPAN, Shinagawa, Tokyo, Japan;

³Department of Psychiatry, Tokyo Women's Medical University, Shinjuku, Tokyo, Japan

Increasing the number of mental disorder patients has become a significant problem. To solve this problem, it is important to explore a biomarker related to mental state for supporting the patients. Previous studies¹⁻³ have shown the relationship between mood states of healthy Japanese adults measured with questionnaire and prefrontal cortex (PFC) activity during working memory (WM) tasks measured with optical topography (OT) which is a functional imaging technique for brain activities based on near-infrared spectroscopy. In this study, we investigated mood states of participants in return-to-work program using the previous studies' procedure¹⁻³ for developing a novel healthcare method in rehabilitation for mental disorder. Volunteers were participants in return-to-work program in which a nonprofit organization provides support and education for those with mood disorders. We scheduled measurement session in this program once a week, and recorded PFC activities during verbal and spatial WM tasks with OT and measured subjective mood with the Profile of Mood States (POMS) for the same volunteers over time. The results show that the correlation coefficients between changes in PFC activities and those in depressive mood scores of individual volunteers over successive sessions are higher at the last period of the program when they are ready for return-to-work than the first period to start the program. Our results suggested that the relationship between PFC activities and mood states will be useful for evaluating mental state of mood disorder patients in rehabilitation for return-to-work.

References

1. Aoki R, et al. *Neurosci Res.* 2011;70(2):189-196.
2. Sato H, et al. *J Biomed Opt.* 2011;16(12):126007.
3. Aoki R, et al. *Psychiatr Res Neuroimage.* 2013;212:79-87.

PII2. High-Resolution 7-T MR Imaging of the Human Subgenual Prefrontal Cortex In Vivo: Development of a Segmentation Algorithm and Its Application in Major Depressive Disorder

A. Tränkner¹, S. Schindler¹, F. Schmidt¹, M. Strauß¹, R. Trampel², U. Hegerl², R. Turner², S. Geyer², and P. Schönknecht¹

¹Klinik und Poliklinik für Psychiatrie und Psychotherapie, Universitätsklinikum Leipzig AöR, Leipzig, Germany

²Max Planck Institut für Kognitions- und Neurowissenschaften, Leipzig, Germany

The subgenual prefrontal cortex (SGPFC) as part of the limbic system plays a crucial role in mood regulation as demonstrated in structural and functional brain imaging studies. Previous research of SGPFC volumes revealed a reduction in patients with major depressive disorder (MDD) mainly in the left SGPFC. However, contradicting findings are biased by imaging methods and magnetic field strengths, and the SGPFC has never been investigated by high-resolution MRI.

In the present study, we aimed to investigate the SGPFC using 7-T MRI.

First, we developed a reliable segmentation protocol of the SGPFC (ICC > 0.90 for 2 independent raters) and our preliminary results of the method being applied in a sample of MDD patients compared to matched healthy controls will be presented and perspectives of high-resolution imaging in mood disorders will be discussed.

PII3. Structural and Functional Alterations in Presymptomatic Alzheimer's Disease Revealed by Multivariate Pattern Analysis

V. Kebets^{1,2}, M. van Assche^{1,2}, R. Goldstein^{1,2}, M. van der Meulen^{1,2}, P. Vuilleumier¹, J. Richiardi^{3,4,5}, D. Van De Ville^{3,4}, and F. Assal²

¹Laboratory for Neurology and Imaging of Cognition, University of Geneva, Geneva, Switzerland

²Department of Neurology, Geneva University Hospital, Geneva, Switzerland

³Institute of Bioengineering, Ecole Polytechnique Fédérale de Lausanne, Lausanne, Switzerland

⁴Department of Radiology and Medical Informatics, University of Geneva, Geneva, Switzerland

⁵Functional Imaging in Neuropsychiatric Disorders Laboratory, Stanford University, Stanford, CA, USA

Pattern recognition tools offer a novel way to detect patterns in imaging data associated with brain disease and to eventually predict individuals' patient status. We employed these methods using structural and functional magnetic resonance imaging (MRI) to distinguish amnesic mild cognitive impairment (aMCI) patients from elderly controls (EC). Specifically, MRI was acquired in 13 aMCI patients and 13 age-/gender-/education-matched healthy ECs during an associative memory task using picture pairs. We deployed binary support vector machine (bSVM) and binary Gaussian process classifier (bGPC) to discriminate MR scans of controls versus aMCI patients. We found structural alterations in hippocampus and parahippocampal gyrus bilaterally with accuracies up to 73% (bGPC, $P = .03$). Functionally, activity in the left parahippocampal gyrus at the encoding task yielded the highest prediction accuracies (85% using bGPC, $P = .01$; and 77% using bSVM, $P = .006$); at retrieval, activity in the right precuneus (77% using bSVM, $P = .008$), right cingulate cortex (73%, $P = .01$ with bSVM and bGPC), and left thalamus (73%, $P = .02$ using bSVM) successfully identified aMCIs from ECs. Importantly all those regions play a critical role in declarative memory formation. The prediction performance obtained from functional MRI data thus

outperformed the one obtained by using structural MRI. This work shows the potential of using multivariate pattern analysis applied to neuroimaging data in a clinical setting; that is, we show early identification of brain changes symptomatic of pre-Alzheimer's disease at an individual level.

PI 14. The Influence of 10-Hz Repetitive Transcranial Magnetic Stimulation Treatment on Resting EEG Activity in Patients With Bipolar and Major Depressive Disorder

A. Wozniak- Kwasniewska¹, D. Szekely², S. Harquel³, T. Bougerol², and O. David¹

¹Fonctions Cérébrales et Neuromodulation, Grenoble Institut des Neurosciences, Chemin Fortune Ferrini, La Tronche, France

²Clinique Universitaire de Psychiatrie, Pôle Psychiatrie Neurologie, Centre Hospitalier Universitaire, Grenoble, France

³UMS IRMaGe, Grenoble, France

Repetitive transcranial magnetic stimulation (rTMS) is being developed to treat depressive disorders. The mechanisms of action of rTMS are still not entirely understood. It is particularly interesting to understand why some patients respond to the therapy while others do not.

In this open study, rTMS guided by neuronavigation was combined with EEG as a tool to compare short and long-term plasticity induced by 10-Hz stimulation. Ten patients with bipolar (BP) and 8 with major depressive disorder (MDD) were included in rTMS therapy with additional EEG recording. Ten-hertz rTMS over the left dorsolateral prefrontal cortex stimulation with 120% of motor threshold intensity was applied as a standard procedure of depression treatment (2000 pulses, 20 sessions). The EEG signals were recorded at baseline (before rTMS) and at poststimulus period. Recordings were repeated 3 times: during the first session, the middle session and the last session of the treatment. Patients remained still and awake, with eyes closed during EEG. Resting state EEG signals were analyzed in terms of relative power in δ , θ , α , and β frequency bands. Statistical analyses of EEG changes induced by rTMS were computed with statistical parametric mapping (SPM) for EEG, in every frequency band. A $3 \times 2 \times 2$ ANOVA of baseline recordings over patients was used to assess significant differences between conditions. The factors were: "Time condition" (session 1, 2, 3), "responders – nonresponders" and "MDD – BP." Then, to be able to verify short-term changes in the brain plasticity we also ran second $3 \times 2 \times 2$ ANOVA, using baseline and poststimulus recordings for MDD and BP patients separately. Here, the factors were: "Time condition" (session 1, 2, 3), "responders – non-responders" and "baseline – poststimulus."

Analyses revealed higher activity in δ and θ bands in MDD and BP responders than in non-responders ($P < .05$ FWE). However, nonresponders showed increased activity in higher frequencies, α ($P < .05$ FWE) and β ($P < .05$ uncorrected). Interestingly, comparing MDD with BP only α band appeared to

be significant, showing higher relative power for MDD patients ($P < .05$ FWE). In remaining frequency bands BP patients tend to show greater relative power than MDD, however it did not reach significance. The analysis of short-term responses did not demonstrate significant differences in relative power between baseline and post-stimulus EEG. However, when the first baseline was compared with third one, we noticed higher relative α power in the first baseline in occipital regions ($P < .05$ uncorrected).

These results strongly suggest that baseline EEG recordings can be useful to predict patient's response to rTMS therapy, both for MDD and BP.

PI 16. A Longitudinal Assessment of White Matter Integrity of the Medial Forebrain Bundle in Unipolar and Bipolar Depressed Patients

T. Bracht^{1,2}, D.K. Jones², H. Horn¹, T.J. Müller¹, and S. Walther¹

¹University Hospital of Psychiatry, University of Bern, Bern, Switzerland

²Cardiff University Brain Research Imaging Centre (CUBRIC), School of Psychology, Cardiff University, Cardiff, UK

Background. Recent diffusion tensor imaging (DTI) studies suggest white matter microstructure alterations of the medial forebrain bundle (MFB) in major depressive disorder (MDD). However, DTI suffers from inaccuracies in regions of crossing fibers. The damped Richardson–Lucy algorithm (dRL) enables the reconstruction of crossing fibre populations in a single voxel and therefore partially overcomes these limitations. It is the aim of our study to investigate white matter microstructure of the MFB in unipolar and bipolar depression. We hypothesize white matter microstructure alterations of the MFB during depression, that is, reduced fractional anisotropy (FA). Furthermore, we assume that these alterations normalize with remission of depression. **Methods.** A total of 21 unipolar depressed patients, 14 bipolar depressed patients and 30 healthy controls underwent diffusion weighted magnetic resonance imaging (MRI) scans (42 diffusion encoding directions). "ExploreDTI" was used for data analyses. The MFB was reconstructed using the damped Richardson–Lucy algorithm (dRL). Furthermore, we reconstructed the optic radiation as control tract. Mean-fractional anisotropy (FA), mean diffusivity as well as axial and radial diffusivity were averaged over the MFB and compared between depressed patients and healthy controls using independent t tests. Furthermore, we tested in the structural data at baseline, whether alterations were predictive of treatment response after 4 weeks by comparing responders and non-responders in independent t tests. Paired t tests were used to compare mean-FA of 15 patients that were scanned during depression and after remission. **Results.** Data analyses are not yet completed. Results will be presented at the conference.

PI 17. Influence of Subanesthetic Dose of Ketamine on Theta Cordance in Unipolar Depression

P. Sos¹, M. Klirova¹, T. Novak¹, M. Brunovsky¹, J. Horacek¹, M. Bares¹, and C. Hoschl C.¹

¹Prague Psychiatric Centre, Prague, Czech Republic

Background. A series of clinical studies demonstrated that QEEG prefrontal theta cordance value decreases after 1 week of treatment in responders to antidepressants and precedes clinical improvement.¹ Ketamine, a non-competitive antagonist of NMDA receptors, has a unique rapid antidepressant effect² but its influence on theta cordance is still unknown. To date predictive value of cordance³ in response to single infusion of ketamine in depressive subjects has not been studied. We hypothesized in our study that the changes in prefrontal cordance 24 hours after the infusion will predict sustained antidepressant response fourth day after the infusion. **Methods.** In a double-blind, cross-over, randomized, placebo-controlled experiment we studied the influence of ketamine (0.54 mg/kg) on theta cordance in a group of 27 right-handed hospitalized depressive patients on stable antidepressant medication. Antidepressant response was defined as 50% decrease of depressive symptoms evaluated fourth and seventh day after infusion by means of Montgomery-Åsberg Depressive Rating Scale (MADRS). Psychotomimetic symptoms were evaluated by the Brief Psychiatric Rating Scale before and after the infusion.⁴ Three EEG segments obtained before, after the infusion and 24 hours after the dosing were entered into spectral analyses. QEEG cordance values in theta frequency band were calculated according to UCLA algorithm³ from 3 prefrontal electrodes (Fz, Fp1, Fp2). **Results.** Responders (n = 11) to ketamine in comparison to nonresponders (n = 16), showed significant difference in cordance values at the end of ketamine infusion (Spearman, $P = .039$). The cordance decrease, measured between the end of infusion and next day, positively correlated with ketamine antidepressant response (MADRS decrease) fourth day after infusion (2-tailed Fisher's exact test, $df = 1$, $P = .0076$) with NPV 90.9% (95% CI 64.3% to 99.5%) and PPV 62.5% (95% CI 44.2% to 68.4%). **Conclusions.** Our data indicate that ketamine (glutamatergic-based drug) infusion immediately induces similar changes as monoaminergic-based antidepressants do gradually after a series of downstream signalling steps. The reduction in theta prefrontal cordance could serve as a marker of ketamine's sustained antidepressant response, a hypothesis that should be tested in larger depressive population.

Acknowledgments

This study was supported by the Internal Grant Agency, Ministry of Health of the Czech Republic (IGA MH CR) [Grant No. NT13403-4]. The study was registered with EU Clinical Trials Register (EudraCT No. 2009-010625-39).

References

1. Bares M, et al. The change of prefrontal QEEG theta cordance as a predictor of response to bupropion treatment in patients who had failed to respond to previous antidepressant treatments. *Eur Neuropsychopharmacol.* 2010;20(7):459-466.
2. Zarate CA Jr, et al. A randomized trial of an N-methyl-D-aspartate antagonist in treatment-resistant major depression. *Arch Gen Psychiatry.* 2006;63(8):856-864.
3. Leuchter AF, et al. Cordance: a new method for assessment of cerebral perfusion and metabolism using quantitative electroencephalography. *Neuroimage.* 1994;1(3):208-219.
4. Sos P, et al. Relationship of ketamine's antidepressant and psychotomimetic effects in unipolar depression. *Neuroendocrinol Lett.* 2013;34(4):101-107.

PI 20. Effects of Image Quality and Neurodegenerative Disorders on the Automated Brain Segmentation

I. Fellhauer¹, F.G. Zöllner², J. Schröder¹, L. Kong¹, M. Essig³, and L.R. Schad²

¹Section of Geriatric Psychiatry and Institute of Gerontology, Department of Psychiatry, Heidelberg University, Heidelberg, Germany

²Computer Assisted Clinical Medicine, Medical Faculty Mannheim/Heidelberg University, Mannheim, Germany

³German Cancer Research Center, Heidelberg, Germany

This study evaluates the reliability of frequently used segmentation programs (SPM, FreeSurfer, FSL) using a realistic digital brain phantom and MRI brain acquisitions from patients with manifest Alzheimer's disease (AD, n = 34), mild cognitive impairment (MCI, n = 60), and healthy subjects (n = 32) matched for age and sex. The analysis of the brain phantom dataset demonstrated that both, the SPM and the FreeSurfer package underestimate gray matter and overestimate white matter with increasing noise. The FSL package calculated overall smaller brain volumes with increasing noise. In contrast, image inhomogeneity had only minor, nonsignificant effects on the results obtained with SPM or FreeSurfer 5.1 but on those of FSL (increased white matter volumes with decreased gray matter volumes). Analyses of the patient data returned decreasing volumes of gray and white matter with progression of brain atrophy independent of the segmentation programs used. The analysis of patient data demonstrated that FSL and SPM calculated more white than gray matter. Best results can be obtained with good image quality. With poor image quality, especially image noise, SPM provides the best segmentation results. Both, FSL and SPM, have difficulties with the classification of gray and white matter voxels of elderly people, due to white matter and gray matter contrast effect. An optimized template for segmentation had no significant effect on segmentation results. The best segmentation results in elderly people can be obtained with FreeSurfer.

P125. Successful Recording of Visual Evoked Potentials in a 9.4-T Static Magnetic Field

J. Arrubla¹, I. Neuner^{1,2,3}, D. Hahn^{1,2}, F. Boers¹, and N. Jon. Shah^{1,3,4}

¹Institute of Neuroscience and Medicine—4, Forschungszentrum Jülich GmbH, Jülich, Germany

²Department of Psychiatry, Psychotherapy and Psychosomatics, RWTH Aachen University, Aachen, Germany

³JARA—BRAIN-Translational Medicine, RWTH Aachen University, Aachen, Germany

⁴Department of Neurology, RWTH Aachen University, Aachen, Germany

Introduction. Simultaneous recording of electroencephalography and functional magnetic resonance imaging has shown a number of advantages that make this multimodal technique superior to fMRI alone. Recording these multiple measures is advantageous for many aspects of cognitive neuroscience, pharmacological studies, sleep studies or evoked potential studies. Here, we explore the possibility of recording visual evoked potential (VEP) in a 9.4-T static magnetic field. **Methods.** EEG data were recorded from 15 healthy volunteers (10 male, 5 female), mean age of 34.5 (SD 12.6) years. EEG data were recorded from each subject outside of the scanner (0 T) and inside a Siemens 9.4-T human whole-body scanner (Siemens Medical Systems, Erlangen, Germany). Visual stimuli were presented separately and recorded at 9.4 T and 0 T. The stimuli consisted of 200 flashes of white light with an intensity of 12 cd/m², duration of 500 ms and ISI between 2 and 4 seconds. EEG data were first down-sampled to a rate of 250 Hz, filtered at 0.16 to 20 Hz and re-referenced to Fz. The data recorded at 9.4 T were corrected for ballistocardiogram (BCG) artefact by the means of independent component analysis (ICA), where the components were visually inspected and those activities which were related to heartbeat events were excluded. Data were then segmented around the event markers, 50 ms before and 250 ms after the stimulus. The segmented data were later subjected to extended infomax ICA using the Runica algorithm. The presence of VEPs was evaluated at Oz channel. The resulting independent components were inspected for topography, ERP signal, and consistency across single trials to determine event related potential components. **Results.** Independent components representing clear VEPs were found in all 15 subjects at 0T. However in the 9.4T scanner, data from 10 subjects yielded clear VEPs. Paired *t* test showed no significant difference in the latencies of the visual P100 recorded at 0-T and at 9.4-T static magnetic fields; $t(14) = -0.546$, $P = .594$. There was no significant difference in the amplitude of the visual P100 recorded at 0-T and at 9.4-T static magnetic fields; $t(14) = -2.12$, $P = .052$. **Discussion.** The results of this study confirm the feasibility of recording evoked potentials at 9.4 T. ICA proved to be effective in removal of the BCG artefacts and also for identifying the event related potentials. Our results show that the latencies of the ERPs do not differ when the stimulation was performed at 0-T or 9.4-T static magnetic fields. This finding supports the assumption that the speed of primary sensory perceptions is not

altered by the 9.4-T static magnetic field.

P126. Successful Recording of Auditory P300 in a 9.4-T Static Magnetic Field

I. Neuner^{1,2,3}, J. Arrubla¹, D. Hahn^{1,2}, F. Boers¹, and N. Jon. Shah^{1,3,4}

¹Institute of Neuroscience and Medicine – 4, Forschungszentrum Jülich GmbH, Jülich, Germany

²Department of Psychiatry, Psychotherapy and Psychosomatics, RWTH Aachen University, Aachen, Germany

³JARA—BRAIN-Translational Medicine, RWTH Aachen University, Aachen, Germany

⁴Department of Neurology, RWTH Aachen University, Aachen, Germany

Introduction. One of the advantages of ultra-high field MRI is the possibility of imaging at increased spatial resolution with EEG during rest and different tasks. Simultaneous measurements lay the foundations for an EEG-informed, single-trial analysis approach to the fMRI data. Here we explore the feasibility of recording evoked potentials which resemble very early stages of cognitive processing such as the P300 in a 9.4-T static magnetic field. **Methods.** EEG data were recorded from 15 healthy volunteers (10 male, 5 female), mean age of 34.5 (SD 12.6) years. EEG data were recorded from each subject outside of the scanner (0 T) and inside a Siemens 9.4-T human whole-body scanner (Siemens Medical Systems, Erlangen, Germany). An auditory oddball paradigm was presented and delivered via headphones. Subjects were presented with a series of high (1000 Hz) “task relevant” target tones and lower (500 Hz) “task irrelevant” tones of 50-ms duration, 85 dB, and interstimulus interval between 2 and 14 seconds. Target probability was 20%. EEG data were first down-sampled to a rate of 250 Hz, filtered at 0.16 to 20 Hz and re-referenced to average. The data recorded at 9.4 T were corrected for ballistocardiogram (BCG) artefact by the means of independent component analysis (ICA), where the components were visually inspected and those activities which were related to heartbeat events were excluded. Data were then segmented around the event markers, 50 ms before and 450 ms after the stimulus. The segmented data were later subjected to extended infomax ICA using the Runica algorithm. The presence of VEPs was evaluated at Pz channel. The resulting independent components were inspected for topography, ERP signal, and consistency across single trials to determine event related potential components. **Results.** Independent components representing clear P300 peaks were found in all 15 subjects at 0 T. However, in the 9.4-T scanner data from 12 subjects yielded clear ERPs. Paired *t*-test showed no significant difference in the latencies of the auditory P300 recorded at 0-T and at 9.4-T static magnetic fields; $t(14) = 1.474$, $P = .163$. There was no significant difference in the amplitude of the auditory P300 recorded at 0-T and at 9.4-T static magnetic fields; $t(14) = -2.084$, $P = .056$. **Discussion.** The results of this study confirm the feasibility of recording the P300 at 9.4-T static magnetic fields. Our results show that the latencies of the evoked potentials do not differ significantly between 0-T

or 9.4-T static magnetic fields. This finding supports the assumption that the speed of very early cognitive processing is not altered by the 9.4-T static magnetic field.

PI27. Neural Correlates of Memory Load During Search Period in Visuo-Spatial Working Memory Task

M. Suriya Prakash¹ and R. Sharma¹

¹Stress and Cognitive Electro-Imaging Laboratory, Department of Physiology, All India Institute of Medical Sciences, New Delhi, India

Objective. Neural mechanisms underlying visuo-spatial working memory (WM) and its modulation by memory load are not well understood. The objective of this study is to investigate the neural correlates of WM during search period in a visuo-spatial WM task involving simultaneous encoding, retention, retrieval and its modulation by memory load using quantitative EEG. **Participants and methods.** Healthy male volunteers (n = 26) performed a visuo-spatial WM task with three memory loads (3, 6, and 8 pairs of identical abstract pictures). In each memory load, an array of pairs of identical abstract pictures (each unit of a pair in different spatial locations in the array) was presented for 10 seconds during which the spatial location of the pictures had to be encoded. After encoding, the pictures were hidden in the array. All pairs of pictures had to be matched correctly to complete the load. The time interval of 2 seconds (search period) which starts from opening a picture and searching for its matching pair was taken for further analysis. 128-channel Geodesic Sensor Net system (Electrical Geodesics Inc., Eugene, OR, USA) was used for EEG acquisition. Standardized low-resolution electromagnetic tomography (sLORETA) was used to determine the activity of the brain regions involved during search period of visuo-spatial WM task. **Results.** ANOVA measures were performed to examine the effect of memory load on various neural correlates of WM during search period. *P* value of less than .05 was considered statistically significant. During search period we observed significant load-related increase in the activity of left medial frontal gyrus, left lingual gyrus and right parahippocampal gyrus while the activity of right paracentral lobule decreased. **Conclusions.** With increasing visuo-spatial WM load, there is increase in the activity of neural substrates of visuo-spatial attention system and decrease in the activity of the motor system during initial time interval (0-750 ms) of search period while there is sustained increase in the activity of medial frontal gyrus of visuo-spatial WM system. This emphasizes the key role of medial frontal gyrus in determining the temporal activity pattern of other neural substrates to execute navigation in visuo-spatial WM task.

PI31. An Ocular Artifacts Removal Method and Its Validation Based on Information Loss of EEGs

H. Kawaguchi^{1,2} and T. Kobayashi¹

¹Graduate School of Engineering, Kyoto University, Kyoto-shi, Kyoto, Japan

²Japan Society for the Promotion of Science, Tokyo, Japan

Removal of electroencephalogram (EEG) ocular artifacts, such as eye-blinks and eye-movements, is important to reduce measurement time and increase signal-to-noise ratio of event-related potentials and event-related synchronizations/desynchronizations. For this reason, a variety of methods has been reported for the removal of ocular artifacts from measured EEGs as a preprocessing analysis.^{1,2} One of the most popular methods used to remove ocular artifacts is based on independent component analysis (ICA), which is a blind source separation method, and assumes that several independent components (ICs) reflect ocular artifacts. The previous studies using ICA were mainly intended to identify ICs reflecting ocular artifacts.^{3,4}

Almost all the previous methods focused mainly on the extent to which the ocular artifacts are removed. However, a few of the original EEGs may be concurrently removed as well. Although there are several methods for reducing the original EEG, there are few quantitative assessment methods for validation because there is no access to the ideal EEGs in experimental data. Therefore, there is no quantitative criterion against which the performance of a removal method^{5,6} can be based. In addition, with an increase in the number and type of ocular artifacts in a single trial, the number of ICs representing those ocular artifacts that may be extracted by the previous methods based on ICA also increases,⁷ and some of the true EEGs may also be concurrently removed. Nevertheless, little attention has been given to this issue.

In this study, we focused mainly on the extent to which the true EEGs are retained and proposed a localized removal method for ocular artifacts. The proposed method is based on a combination of empirical mode decomposition (EMD) with ICA and the Kalman filter. EMD is a data-driven method that analyzes nonlinear and nonstationary data for multiscale decomposition and time-frequency analysis. To validate the performance of the proposed method, we made pseudo-EEGs consisting of the ideal artifacts-free EEGs and 5 types of simulated ocular artifacts (1 eye-blink and 4 eye-movements: up, down, left, and right) and compared results with previously reported 2 ICA-based removal methods that employed only ICA⁴ and ICA + EMD.⁶ As quantitative criterions, we employed not only the correlation coefficient but also the root mean square error. To validate the performance of the proposed method, we assessed information loss using pseudo-EEG data containing ocular artifacts and confirmed that the proposed method successfully removed the ocular artifacts and reduced information loss of true EEGs.

Acknowledgments

Ministry of Education, Culture, Sports, Scientist and Technology, Japan.

References

1. Croft RJ, Barry RJ. *Clin Neurophysiol.* 2000;30:5-19.
2. Jung TP, Makeig S, Humphries C, et al. *Psychophysiology.* 2000;37:163-178.
3. Joyce CA, Gorodnitsky IF, Kutas M. *Psychophysiology.* 2004; 41:313-325.

4. Okada Y, Jung J, Kobayashi T. *Physiol Meas*. 2007;28:1523-1532.
5. Croft RJ, Chandler JS, Barry RJ, Cooper NR, Clarke AR. *Psychophysiology*. 2005;42:16-24.
6. Lindsen JP, Bhattacharya J. *Psychophysiology*. 2010;47:955-960.
7. Junshui M, Sevinc B, Peining T, Vladimir S. *J Neurosci Methods*. 2011;196:131-140.

PI32. Dry-Contact Multichannel EEG Using Novel Multipin Electrodes

P. Fiedler¹, S. Griebel², S. Biller¹, C. Fonseca^{3,4}, F. Vaz⁵, L. Zentner², F. Zanow⁶, and J. Haueisen^{1,7}

¹Institute of Biomedical Engineering and Informatics, Ilmenau University of Technology, Ilmenau, Germany

²Department of Mechanism Technology, Ilmenau University of Technology, Ilmenau, Germany

³Universidade do Porto, Faculdade de Engenharia, DEMM, Porto, Portugal

⁴SEG-CEMUC-DME, University of Coimbra, Coimbra, Portugal

⁵Centro de Física, Universidade do Minho, Campus de Azurém, Guimarães, Portugal

⁶eemagine Medical Imaging Solutions GmbH, Berlin, Germany

⁷Biomagnetic Center, Department of Neurology, University Clinic Jena, Jena, Germany

Introduction. New fields of application for brain function analysis include brain-computer interfaces, intelligent prosthesis and ambient assisted living. In this context, electroencephalography (EEG) is the most commonly used technique for mobile, ubiquitous signal acquisition. Thus, besides reproducible and reliable signal quality, electrode technologies for rapid, unobtrusive EEG acquisition are required. Hence, conventional Ag/AgCl electrodes are inapplicable due to technologically inherent application limitations and necessary preparation procedures. We present a novel type of electrode cap enabling dry-contact multichannel EEG. **Materials and methods.** The distinct shape of each electrode incorporates 24 thin pins on a single baseplate. While the pin design enables hair layer interfusion, the common baseplate electrically interconnects the single pins, thus resulting in increased contact surface. A flexible polymer substrate for each electrode ensures adaption to the local head curvature, hence maintaining not only contact reliability and signal quality but also comfort. 97 electrically conducting coated polymer electrodes were integrated into a textile-based cap using a quasi-equidistant electrode layout. Using the novel cap in conjunction with a commercial EEG amplifier, we recorded EEG signals on 5 volunteers with normal hair length. Furthermore, we repeated the signal acquisition using a conventional electrolyte gel based cap, enabling a direct comparison between both electrode technologies. **Results.** After application of the dry cap system, for all volunteers more than 70% of the electrodes provided sufficient signal quality. Comparison to the subsequently recorded EEG signals using conventional electrodes revealed similar signal characteristics in a frequency range between 1 and 40 Hz for

spontaneous EEG, alpha activity and a visual evoked potential. The spectra of the dry EEG showed slightly increased drift for frequencies below 1 Hz. During the whole measurement procedure no extensive adduction was necessary and the subjects reported comfortable, unobtrusive fit of the cap. **Conclusions.** The dry application scenario eliminates the need for preparation procedures, thus enabling rapid application and immediate as well as long-term recordings. For 5 subjects we demonstrated signal quality of the majority of the electrodes to be comparable to conventional gel-based cap systems. Furthermore, we proved compatibility of the cap system with conventional, commercial EEG amplifiers. The proposed novel cap system enables preparation-free, dry multichannel EEG, thus promoting new fields of application for EEG analysis.

Acknowledgments

This work was supported by German Ministry of Science (3IPT605A) and Thuringia Ministry of Science (2012FG 0014, TNA X-1/2012).

PI33. The Bihemispheric Cooperation in Early Word Detection Revealed in EEG and TMS Experiments Using Bilateral Lexical Decision

V. Rochas¹, T. Rihs¹, G. Thut³, N. Rosenberg¹, Th. Landis¹, and Ch. Michel^{1,2}

¹Functional Brain Mapping Laboratory, Department of Fundamental Neurosciences, University of Geneva, Geneva, Switzerland

²Biomedical Imaging Center (CIBM), Geneva, Switzerland

³Centre for Cognitive Neuroimaging, Institute of Neuroscience and Psychology, College of Medical, Veterinary and Life Sciences, University of Glasgow, Glasgow, Scotland

Despite the dominance of the left hemisphere in language function, the right hemisphere also processes language in certain circumstances. Here we investigated the cooperation between the two hemispheres using a lexical decision task with presentation of pair of letter strings being neutral or emotional words and pseudo-words. Participants had to detect real words. Two independent studies were performed: a high-density EEG study ($n = 13$) and an event-related TMS study ($n = 10$). Results showed that, starting at 50ms, the visual cortices and bilateral superior temporal and parietal areas were implied very early in the treatment of written words according to the side of presentation and the emotionality of the word. The detection of emotional words presented in the left hemifield was particularly associated with participation of the right hemisphere, mainly around the temporoparietal junction. Based on the present findings, an adaptive bilateral network model involving the superior temporal and parietal areas was proposed for early written word detection processing.

A third experiment combining theta burst stimulation with EEG is also in place to challenge the short-term plasticity of the brain and its ability to recover from a unbalanced stimulation of one of the two homologous areas in the word detection task.

PI 34. Transcranial Direct Current Stimulation Over the Primary Motor Cortex in Children and Adolescents: TMS/EEG Study

V. Moliadze¹, T. Schmanke¹, E. Lyzhko², S. Bassüner¹, Ch. Freitag¹ and M. Siniatchkin¹

¹Department of Child and Adolescent Psychiatry, Psychosomatics and Psychotherapy Goethe-University of Frankfurt am Main, Frankfurt am Main, Germany

²Institute of Mathematical Problems of Biology, Pushchino, Moscow Region, Russia

Introduction. Transcranial direct current stimulation (tDCS) is a non-invasive technique for brain stimulation that has been used to study fundamental mechanisms of neuronal plasticity. Successful application of this technique as a therapeutic tool for adult neurological and psychiatric diseases such as stroke, migraine, epilepsy, Parkinson's disease and major depression, may prompt us to use tDCS in pediatric studies. Since the developing brain shows a greater capacity of brain plasticity, noninvasive brain stimulation might induce greater benefits in children than in adults. Thus, tDCS can provide insight into normal and aberrant developmental neurology and neurophysiology in children. So far, applications of tDCS in the pediatric studies are not well developed. Recent study about the safety of the use of tDCS in children suggests that there is a minimal risk associated with this technique. Further studies regarding effective use of tDCS in children/adolescents are needed. To detect changes in cortical excitability we analysed motor evoked potentials (MEPs) and TMS evoked potentials (N100) before and after tDCS over the primary motor cortex. **Methods.** Anodal, cathodal or sham tDCS (1 mA) was applied for 10 min on the left M1_{HAND} in 19 healthy participants, aged between 11 and 16 years. tDCS was delivered by a battery driven stimulator (NeuroConn GmbH, Ilmenau, Germany) through conductive-rubber electrodes (5 × 7 cm). The minimum period between sessions for a single subject was 7 days, and sessions were applied in randomized order. MEPs and TMS-evoked N100 were measured by TMS-electromyograph (EMG) and 64-channel EEG pre and immediately after stimulation as well as every 10 minutes after tDCS up to 60 minutes. **Results.** In all subjects the tDCS was well tolerated. An important finding of this study is that 1 mA anodal as well as cathodal tDCS resulted in a significant increase of MEP amplitudes. Sham tDCS did not induce significant MEP alterations. Interestingly, 1-mA cathodal stimulation suppressed significantly the N100 amplitude of TMS-evoked potentials compared with baseline and sham stimulation. In contrast to that effect, the anodal tDCS did not modify the N100 amplitudes significantly when compared with sham stimulation. **Conclusion.** Our results suggest that the tDCS stimulation effects differ between children and adults. This should be taken into account for applications of the stimulation technique in treatment neurological and psychiatric disorders in children.

PI 35. Network Correlates of the Spacing Effect

R. Thézé¹, A.G. Guggisberg¹, L. Nahum², and A. Schnider¹

¹Division of Neurorehabilitation, University Hospital Geneva, Geneva, Switzerland

²Institution de Lavigny, Hôpital neurologique, Lavigny, Switzerland

Improved retention of items repeated apart in time is a robust phenomenon known as the "Spacing Effect" (SE). Although multiple hypotheses have been proposed, very little is known about its neural mechanisms. Recent studies^{1,2} have demonstrated that immediate repetition induced a specific electrical activity in the left medial temporal lobe (MTL) that was absent during spaced repetition. In this study, we obtained high-density EEG recordings from 14 healthy subjects during a continuous recognition task in which pictures were either repeated immediately or after 9 intervening items. Task-induced changes in coherence between brain regions were quantified and localized. Immediate repetition induced a specific coherence increase in the theta band between the orbito-parahippocampal region and the inferior parietal region, between 200 and 400 ms after picture presentation. This increase was absent during spaced repetition. The magnitude of theta-band synchronization in individual subjects correlated significantly with their delayed recognition of the presented pictures. These findings suggest that immediate repetition required a specific but vulnerable consolidation process associated with theta-band synchronization between limbic and parietal areas. The Spacing Effect arises in subjects in whom this theta-band synchronization is less efficient. Hence, the Spacing Effect seems to result from a lack of large-scale synchronization of theta oscillations which in turn leads to deficient encoding during immediate repetition of trained items.

References

1. James C, et al. *Hippocampus*. 2009;19:371-378.
2. Nahum L, et al. *Hippocampus*. 2011;21:689-693.

PI 36. The Disgusted Brain: Olfactory Stimulation in Functional MR Imaging

L. Meier¹, H. Friedrich², K. Jann^{1,3}, B. Landis², R. Wiest⁴, A. Federspiel¹, W. Strik⁵, and T. Dierks¹

¹Department of Psychiatric Neurophysiology, University Hospital of Psychiatry, University of Bern, Bern, Switzerland

²Department of ORL, Head and Neck Surgery, Inselspital, University of Bern, Bern, Switzerland

³Department of Neurology, University of California Los Angeles, Los Angeles, CA, USA

⁴Institute of Diagnostic and Interventional Neuroradiology, Inselspital, University of Bern, Bern, Switzerland

⁵University Hospital of Psychiatry, University of Bern, Bern, Switzerland

Disgust is one of the most basic and universal human emotions. A wide variety of stimuli can evoke disgust, but when it comes to avoiding environmental hazards, disgust elicited via olfactory input plays an essential role. The aim of this basic research study is to shed light on neuronal and behavioural basics of olfactory disgust processing. Twenty healthy subjects underwent functional MR imaging. All subjects were right-handed and had normal olfaction. Two odour stimuli (1 disgusting, 1 pleasant) were presented to the subjects inside the scanner in a pseudo-randomized event related paradigm. Odours were presented bi-rhinally with a computer-controlled airflow olfactometer. Every olfactory stimulation was followed by fresh airflow. Subjects rated both odours for pleasantness and intensity inside the scanner. The contrast of cortical BOLD activation between the conditions "pleasant odor" and "disgusting odor" were calculated based on a random-effects general linear model in order to find specific neuronal correlates of disgust sensation. The analysis of odor rating data showed that the pleasant odor was clearly rated as pleasant, while the negative odor was rated as disgusting. Intensity ratings of the 2 odors did not differ significantly from each other. The results of the disgusting versus pleasant odor contrast revealed brain activations in the insula (bilaterally), ACC and frontal and parietal areas. These results are in line with studies investigating neuronal correlates of disgust elicited via other sensory input channels (visual, tactile). In particular the strong activation of the bilateral anterior insula indicates that this area plays a significant role in olfactory disgust processing.

PI37. Effects of Continued Neurofeedback Training Using Sensorimotor Rhythm

M. Witte¹, S.E. Kober¹, C. Neuper^{1,2}, and G. Wood¹

¹Department of Psychology, Karl-Franzens-University of Graz, Graz, Austria

²Laboratory of Brain-Computer Interfaces, Institute for Knowledge Discovery, University of Technology Graz, Graz, Austria

The sensorimotor rhythm (SMR, 12-15 Hz) has been often used in brain-computer interface and neurofeedback studies.^{1,2} This component predominates over central cortical areas during periods of relaxed but attentive wakefulness and is thought to reflect reduced sensory and motor excitability.^{3,4} One theoretical model of SMR function proposed that a thalamo-cortical loop generates inhibitory SMR oscillations allowing for improved cognitive performance without interfering inputs.^{5,6}

However, a direct proof that SMR neurofeedback enhances processing capabilities of the brain is difficult to obtain and past studies mainly focused on single parameters. Another issue to consider is the role of psychological factors like mood, motivation, intelligence, and personal traits that may influence the performance of neurofeedback users. Furthermore, reports on sustained effects of SMR training over longer time periods are rarely found in the literature. Here, we applied EEG recordings

to systematically unravel the impact of SMR neurofeedback on psychological and electrophysiological parameters. Our results support the view that SMR neurofeedback influences the way the brain processes stimuli-related sensory information and ultimately affects higher order cognitive functions.

Acknowledgments

European STREP Program—Collaborative Project No. FP7-287320—CONTRAST.

References

1. Pfurtscheller G, et al. *Neuroimage*. 2006;31:153-159.
2. Vernon D, et al. *Int J Psychophysiol*. 2003;47:75-85.
3. Gruzelier J, et al. *Prog Brain Res*. 2006;159:421-431.
4. Serruya MD, Kahana MJ. *Behav Brain Res*. 2008;192:149-165.
5. Sterman MB. *Biofeedback Self Regul*. 1996;21:3-33.
6. Sterman MB. *Clin EEG*. 2000;31:45-55.

PI38. The Relevance of Homo- and Heteroscedasticity for the Averaging of Auditory-Evoked MEG and EEG Responses

R. König¹, A. Matysiak¹, W. Kordecki², C. Sielużycki¹, N. Zacharias¹, and P. Heil³

¹Special Lab Non-invasive Brain Imaging, Leibniz Institute for Neurobiology, Magdeburg, Germany

²Department of Management, University of Business in Wrocław, Wrocław, Poland

³Department of Auditory Learning and Speech, Leibniz Institute for Neurobiology, Magdeburg, Germany

In MEG and EEG data analyses, it is common practice to arithmetically average event-related magnetic fields (ERFs) or electric potentials (ERPs) across single trials and subsequently across subjects to obtain the so-called grand mean. Comparisons of grand means of peak amplitudes of evoked components like the auditory M100 or N100 or of time-varying signals (waveforms), for example between conditions, are then often performed by subtraction. These operations, and their statistical evaluation by parametric tests like ANOVA, tacitly rely on the assumption that the data follow the *additive model*, have a normal distribution, and a homogeneous variance. This may be true for single trials following the signal-plus-noise model, but these conditions are rarely met when ERFs or ERPs between subjects are compared, meaning that the additive model is seldom the correct model for computing grand mean waveforms. As a consequence, such comparisons can be problematic and can lead to wrong conclusions.

We show, using auditory-evoked MEG and EEG responses from different experimental paradigms, that the non-normal distributions and the heterogeneity of variance observed instead result because ERFs and ERPs follow the *mixed model* with additive and multiplicative components. For peak amplitudes, like the M100 and N100, the multiplicative component dominates. The application of a particular transform,

the asinh-transform, to data following the mixed model transforms them into the requested additive model with its normal distribution and homogeneous variance. Furthermore, the asinh-transform does not only stabilize the variance across time, but, as required for, for example, ANOVA, it also equalizes the variance across conditions. Our findings question the common practice of simply subtracting arithmetic means of auditory-evoked ERFs or ERPs without proper transformation of the data. Since the nature of the neural sources generating ERFs and ERPs are similar, and the principles involved in the measuring techniques are identical for all sensory modalities studied by MEG and EEG, there is good reason to assume that our findings are also applicable to other than auditory waveforms. They should thus have widespread implications.

Acknowledgments

This study was supported by the Deutsche Forschungsgemeinschaft (SFB-TRR 31 A6; KO1713/10-1).

PI39. Loudness Dependence of the Auditory-Evoked N1m/P2m Component: A Magnetoencephalography Study

C. Wyss^{1,2}, F. Boers², J. Arrubla², J. Dammers², W. Kawohl¹, I. Neuner^{2,3}, and N.J. Shah^{2,4}

¹Department of Psychiatry, Psychotherapy and Psychosomatics, Zurich University Hospital for Psychiatry, Zurich, Switzerland

²Institute of Neuroscience and Medicine—INM 4, Forschungszentrum Jülich, Jülich, Germany

³Department of Psychiatry, Psychotherapy and Psychosomatics, RWTH Aachen University, Aachen, Germany

⁴Department of Neurology, Faculty of Medicine, JARA, RWTH Aachen University, Aachen, Germany

Introduction. Loudness dependence of auditory-evoked potentials (LDAEP) has been suggested by a number of studies as an indicator of the central serotonergic system.¹⁻³ The most common strategies used to determine the LDAEP by means of EEG are single-electrode estimation and dipole source analysis. A recent study found a significant difference between scores obtained with these 2 methods.⁴ Confounding activation of a frontal source in the single-electrode method may cause this difference. Several authors suggest a frontal protective mechanism being activated during presentation of high tone intensities.^{5,6} Therefore, a detailed investigation of the LDAEP generators and their temporal dynamics is needed. **Methods.** In the present study, we investigated 19 healthy volunteers (male, mean age 26.1 ± 3.9) by means of magnetoencephalography (MEG). Evoked responses to brief sinusoidal tones of 6 intensities (10-60 dB SL) were recorded using a whole-head 248 magnetometer system. Volunteers were instructed to not pay attention to the tones while watching a silent movie for distraction. After artifact rejection applying independent component analysis,⁷ the MEG data were averaged and magnetic field tomography (MFT)^{8,9} was applied. MFT provides full 3D reconstruction across time

to analyse the N1m and P2m components. Voxelwise MFT RMS values were calculated for each subject in time windows of 50 ms between 0 and 400 ms. The group analysis was performed using the generalized linear model. One-sample permutation *t* test was performed for each tone intensity in order to identify the activation of the group. A voxel based whole brain analysis with statistical thresholds set at $P = .05$ and family-wise error correction for multiple comparisons was performed. **Results.** We found significant activation in the time window of the N1m wave (75-125 ms, according to the global field power maps calculated in MEG sensor space) for the highest tone (60 dB SL) in inferior, medial and superior temporal gyri, operculum, pre- and postcentral gyri and superior parietal gyri. In the time window of the P2m wave (175-225 ms), there were additionally activated regions mainly in the right superior occipital gyrus, right inferior and middle frontal gyrus, right insular gyrus and left posterior cingulate gyrus. **Conclusion.** Preliminary results show that activations after presentation of auditory stimuli became more widespread comprising multimodal areas in the time window of the P2m compared to that of the N1m. The current findings provide insight into the neurophysiological mechanisms of LDAEP and will therefore have a direct impact on the methodology used to analyse data recorded during LDAEP.

Acknowledgments

Swiss National Science Foundation (SNSF), EMDO Stiftung, Zurich, C. Wyss, W. Kawohl.

References

1. Hegerl U, Juckel G. Intensity dependence of auditory evoked potentials as an indicator of central serotonergic neurotransmission: a new hypothesis. *Biol Psychiatry*. 1993;33(3):173-187.
2. Lee IH, et al. Loudness dependence of auditory evoked potentials (LDAEP) correlates with the availability of dopamine transporters and serotonin transporters in healthy volunteers—a two isotopes SPECT study. *Psychopharmacology*. 2011;214(3):617-624.
3. O'Neill BV, Croft RJ, Nathan PJ. The loudness dependence of the auditory evoked potential (LDAEP) as an in vivo biomarker of central serotonergic function in humans: rationale, evaluation and review of findings. *Hum Psychopharmacol*. 2008;23(5):355-370.
4. Hagenmuller F, et al. Determination of the loudness dependence of auditory evoked potentials: single-electrode estimation versus dipole source analysis. *Hum Psychopharmacol*. 2011;26(2):147-154.
5. Giard MH, et al. Dissociation of temporal and frontal components in the human auditory N1 wave: a scalp current density and dipole model analysis. *Electroencephalogr Clin Neurophysiol*. 1994;92(3):238-252.
6. Picton TW, et al. Intracerebral sources of human auditory-evoked potentials. *Audiol Neurotol*. 1999;4(2):64-79.
7. Dammers JR, et al. Integration of amplitude and phase statistics for complete artifact removal in independent components of neuromagnetic recordings. *IEEE Trans Biomed Eng*. 2008;55(10):2353-2362.
8. Ioannides A, Bolton J, Clarke C. Continuous probabilistic solutions to the biomagnetic inverse problem. *Inverse Probl*. 1990;6(4):523.
9. Dammers J, Ioannides A. Neuromagnetic localization of CMV generators using incomplete and full-head biomagnetometer. *Neuroimage*. 2000;11(3):167-178.

PI40. Increased Gamma Brainwave Amplitude in Different Meditation Traditions

C. Braboszcz^{1,2}, R.B. Cahn³, J. Levy⁴, M. Fernandez^{5,6}, and A. Delorme^{1,2,7}

¹Université de Toulouse, UPS, Centre de Recherche Cerveau et Cognition, Toulouse, France

²CNRS UMR5549, Toulouse, France

³Department of Psychiatry, University of California, Irvine, CA, USA

⁴Université de Toulouse, UPS, Toulouse, France

⁵Meditation Research Institute, Swami Rama Sadhaka Grama, Rishikesh, India

⁶Mahamudra–Tradición Yoga Himalayo, Santiago, Chile

⁷Swartz Center for Computational Neuroscience, University of California, San Diego, CA, USA

Meditation is a mental practice that has been shown to have positive effects on both mental and physical health and that is now integrated into many clinical protocols. However its mechanisms of action are still unknown and despite decades of electroencephalography (EEG) research on meditators, the basic effects of meditation on EEG are still being defined. In this study, we addressed the hypothesis that different types of meditation may lead to some similar and other different neural correlates as state and trait effects. We compared subjects proficient in 3 different types of meditative practices with a group of control participants. Meditation practices included a well-known open awareness meditation (Vipassana), breath-/mantra-focused meditation (Himalayan Yoga), and a passive “nothingness meditation” (Shoonya practice within the Isha Yoga tradition). Each group had 16 gender-matched participants of similar age ranges. Participants were asked to practice 20 minutes of meditation followed or preceded by 20 minutes of instructed mind wandering (IMW). Meditators of all traditions tended to show significantly higher 60- to 110-Hz gamma activity than control subjects during the meditation period. We observed a trend in the same direction when comparing the meditators with the control in the IMW tasks. This gamma activity was independent of muscle activity and eye-movement activity as isolated using independent component analysis techniques. In addition, we observed higher 7- to 11-Hz alpha activity in the Vipassana group during meditation compared to all other groups. We did not observe systematic differences when comparing the meditation with the IMW tasks. We have shown that regular meditation practice evokes changes in the higher frequency gamma range of the EEG that may be a common denominator across a wide variety of meditation practices as well as demonstrating that Vipassana practice seems to correspond with greater alpha power relative to the other 2 assayed meditative practices. Our results emphasize the value of including control participants and groups of different meditation traditions following the same experimental protocol for studies aiming at characterizing the neural correlates of meditative states.

PI42. Age-Related Reorganization of Local Connections Between Visual Cortical Areas

L. Rosas-Martinez¹, E. Milne¹, and Y. Zheng¹

¹Sheffield Autism Research Lab, Department of Psychology, University of Sheffield, Sheffield, UK

Changes in stimulus specificity such as luminance or colour alter neuronal activity and modulate cortical circuits. At the local scale, developmental change in the functional specificity of connections has not been completely determined. We aim to identify the developmental features of local connections in response to stimulus specificity, during early visual processing. EEG recordings of typically developing participants (12 adults, and 35 children aged 7-17 years) were used to assess functional segregation elicited by achromatic and chromatic steady-state visual-evoked potential. We performed spectral analysis on artefacts-free epochs of all 128 electrodes for all subjects. Results revealed both sustained and transient activity of cortical networks, and differences were found between children and adults. Specifically, the chromatic response was dominated by the fundamental component in adults but not in children, and children showed reduced spectral energy in the second harmonic generated by the achromatic stimulus. These findings indicate reduced transient response in children associated with achromatic processing, and reduced sustained response associated with chromatic processing. Our results suggest that children and adults might process visual information using different cortical networks. This work might provide insights on EEG assessment of potentially disrupted functional networks underlying atypical development.

PI43. Gamma-Activity in the Frontal Lobe Represents Self-Consciousness and Sustained Attention of Musicians and Traumatic Brain Injured Patients

Y. Urakami¹, K. Kawamura^{2,3}, Y. Washizawa^{3,4}, K. Hiroyoshi^{3,5}, A. Cichocki³

¹Hospital and Research Institute, National Rehabilitation Center for Persons with Disabilities, Tokorozawa, Japan

²Department of Anatomy, Medical School, Keio University, Tokyo, Japan

³RIKEN Brain Science Institute, Laboratory for Advanced Brain Signal Processing, Wako-shi, Japan

⁴Department of Communication Engineering and Informatics, The University of Electro-Communications, Tokyo, Japan

⁵Department of Functional Brain Imaging, Human Brain Research Center, Graduate School of Medicine, Kyoto University, Kyoto, Japan

Objective. Music perception involves acoustic and auditory scene analysis, processing of interval relations, of musical syntax and

semantics, and activation of premotor representations of actions. We have shown that gamma-activity during music perception especially in the prefrontal cortex reflect the processing of music in an integrated attention consciousness level. Traumatic brain injured patients (TBI) frequently fail to maintain consistent goal-directed behavior due to their impairments of sustained attention. This study aimed to clarify the role of gamma activity in normal subjects (including musicians) and in TBI during music perception. *Methods.* Participants were 10 normal subjects; 5 musicians (age: 21-25 years) and 5 age-matched nonmusicians and 10 patients with TBI (diffuse axonal injury and frontal contusion). Participants listened to the music from ear-phone with eyes-closed sitting in a dark experimental room. Music 1 was Anton Dvorak "From the New World Symphony" and Music 2 was Mozart Requiem K. 626. We collected spontaneous brain activity in 3 conditions; resting state with eyes-closed (for 1 minute), music-listening and imaging the music without stimulation, examinations were performed by recording with a 60-channel EEG. Using Morlet wavelet time-frequency analysis, root mean square (RMS) was calculated in each frequency band. *Results.* During music listening, compared with resting state, RMS of gamma activity was significantly decreased, especially in the prefrontal cortex both in musicians and nonmusicians. During imaging the music, the musicians' gamma activity was significantly decreased in almost the entire parts, whereas the nonmusicians' gamma activity increased in the frontal lobe. Gamma-activity of TBI tended to decrease in whole brain during music listening compared with resting-state, the RMS ratio of resting-state and music listening significantly decreased in normal subjects compared with TBI in right frontal area in Music 1, in frontal area in Music 2. *Discussion.* TBI often results in diffuse axonal injury, which produces cognitive impairment with disconnecting nodes in distributed brain networks. Nonsignificant decrease of gamma-activity in frontal area during music perception in TBI compared with normal subjects suggests that they failed to integrate the music due to sustained attention impairments which are associated with an increase within the default mode network (DMN). Significant decrease of gamma-activity in the frontal lobe during music-listening suggests the changes in connectivity within DMN function of highly integrated self-consciousness and sustained attention.

PI44. Don't Let Time Outrun You: Assessing the Influence of Age on Processing of Temporal Information in Speech

N. Giroud¹, V. Dellwo², and M. Meyer^{1,3}

¹Research Unit for Neuroplasticity and Learning in the Healthy Aging Brain, University of Zurich, Zurich, Switzerland

²Phonetics Lab, University of Zurich, Zurich, Switzerland

³Center for Integrative Human Physiology, University of Zurich, Zurich, Switzerland

A body of recent studies has shown that normal aging is accompanied by cognitive decline in several domains and by

structural as well as functional neuroplastic changes. However, remarkably little is known about the relationship between normal aging and speech processing, although unlike many other cognitive functions, language is relatively well preserved until old age. While recent research has investigated to what extent elderly are able to use spectral information during speech perception, this planned project aims at understanding how elderly make use of temporal information to decode spoken language. Due to the high temporal resolution of the EEG method we are able to study neural activity during language processing unfolding in time. It is planned to conduct a series of cross-sectional EEG studies in combination with a comprehensive screening of hearing performances and cognitive skills. By presenting temporally manipulated auditory speech signals, we will focus on neural decoding differences during the processing of low-frequency temporal information on the one hand and fine-structure information on the other, as a function of age. It is planned to investigate this issue by (a) using a preattentive mismatch negativity (MMN) paradigm in combination with an inverse solution approach (LORETA) and (b) by applying a time-frequency analysis (wavelet approach) of non-phase-locked changes in brain oscillations and coherence analysis. The goal is to investigate neural discrimination abilities of temporal aspects of speech stimuli as well as age-related differences in lateralization of brain circuits. On the background of a steadily increase of citizens in the senior age cohort we are convinced that this project makes an important contribution. It will help to understand how language functions may be better preserved in the healthy aging brain, thus guaranteeing successful conversation. Undoubtedly, this significantly contributes to their quality of life.

PI45. Don't Get Lost in Details: The Relevance of Global Information in Auditory Language Processing

K.S. Rufener^{1,2}, F. Liem¹, V. Dellwo³, and M. Meyer²

¹International Normal Aging and Plasticity Imaging Center (INAPIC), Zurich, Switzerland

²Department of Neuropsychology, University of Zurich, Zurich, Switzerland

³Department of Phonetics and Phonology, University of Zurich, Zurich, Switzerland

Speech can be described as a transient acoustic signal, consisting of information on mainly 2 different timescales: segmental information, representing phoneme features and suprasegmental information, corresponding to the syllabic structure and intonation contour. Segmental information modulates in a time range of about 25 ms, whereas suprasegmental information takes place in a time range of about 250 ms. However, it is still matter of debate which of these 2 temporal integration windows is crucial for successful speech processing. Moreover, it remains an open question how age-related hearing loss

and cognitive impairment influence this elementary auditory integration processes.

This cross-sectional EEG study examines 3 samples of healthy adults with age-appropriate hearing performance. By presenting specifically degraded speech stimuli, manipulated either in temporal fine structure or spectral envelope, we measure age specific behavioral performance and neural activation patterns. Using high-density EEG, we analyze the temporal dynamics within stimulus-specific neural oscillation patterns. Furthermore, we examine the underlying neural sources.

Preliminary behavioral data show a main effect manipulation: sentences degraded on their temporal fine structure were processed significantly less successful over all age samples, than sentences degraded on their spectral envelope. Furthermore, we find a main of effect age in processing spectrally degraded sentences exclusively; older adults show significantly worse performance in processing these stimuli compared to young adults. As for the EEG data, we find a similar activity pattern between the performance in processing envelope-degraded sentences and the power within the theta band (3-6 Hz). In contrast, a negative relationship between lower gamma-band power (40-48 Hz) and task performance can be observed for both manipulations.

Our results argue for a general relevance of local information in speech processing. In addition, it can be assumed that successful speech processing in older adulthood relies more on global than local characteristics, irrespective of the subjects' hearing performance. Our data support the notion of a crucial role of slow neural oscillations in processing the syllabic structure that the speech signal is made up of. The negative relationship between gamma band and task performance is assumed to represent a neural correlate of efficient speech perception. Planned source localization will shed more light on the topography of the measured oscillation patterns.

PI 46. Putting a Low-Cost, Mobile EEG System Through Its Paces With a Walking Auditory Oddball Task

J.D. Jones-Rounds¹ and R. Raizada^{2,3}

¹Human Electroencephalography and Psychophysiology Laboratory, Department of Human Development, Cornell University, Ithaca, NY, USA

²Department of Psychology, Cornell University, Ithaca, NY, USA

³Department of Brain & Cognitive Sciences, University of Rochester, Rochester, NY, USA

As the field of brain imaging continues to move out into the “real” world, the potential applications in clinical and non-clinical settings abound. However, many practical questions regarding the implementation of mobile sensors and acquisition devices remain unanswered. Specifically, how well do inexpensive multi-sensor commercial EEG systems perform in a laboratory setting? And what can they do out in the “real” world? Can typical event-related potentials (eg, P300) be captured and classified accurately? Which headset mounting position achieves the highest

signal-to-noise ratio? Here we demonstrate, using both a simple regressive classifier and a basic threshold classifier, the utility of the data collected from 14 healthy young adults who participated in a 2-stimulus auditory oddball task, while wearing a low-cost Emotiv EEG headset in 1 of 2 mounting positions, while in both a standard, electromagnetically-attenuated laboratory setting and an ambulatory, out-of-lab setting. We also present the event-related potential (ERP) data, focusing on the P300 waveform, collected from these participants within each of the 4 scenarios/interactions: Forward headset position while walking (Forward Walking); Forward Sitting; Reverse Walking; Reverse Sitting. In summary, we found that Emotiv headsets in both the forward and reverse mounting positions can capture a P300 ERP (defined here as the difference wave [between standard and target trials] mean amplitude within a 300-500 ms poststimulus window) from several midline parietal and frontal electrodes, during the Sitting condition. However, we found that the polarity of the oddball/target ERP can appear inverted at frontal electrode sites, in the Sitting condition, regardless of off-line referencing scheme. In the Walking condition, the high-amplitude noise caused by electrode movement obscures the ERP signal. But importantly, regardless of the P300-like waveform's polarity at a given electrode or the experimental condition, both of the simple classifier schemes we tested performed above chance. These results demonstrate that although significant limitations exist when using low-cost EEG systems in real-world scenarios, these devices can successfully capture usable information. Ongoing work to bring these devices into long-term clinical monitoring situations, and nonclinical situations such as classrooms, will need to address movement-related artifacts both algorithmically and mechanically.

PI 47. EEG Beamforming to Extract Better Features of Motor Imagery in a Two-Class Real-Time BCI

W. Staljanssens¹, G. Strobbe¹, P. van Mierlo¹, R. Van Holen¹, and S. Vandenberghe¹

¹Department of Electronics and Informations Systems, Ghent University, Ghent, Belgium

A general problem in the design of an EEG-BCI system is the poor quality and low robustness of the extracted features, affecting overall performance. However, BCI systems that are applicable in real-time and outside clinical settings require high performance. Therefore, we have to improve the current methods for feature extraction.

In this work, we investigated EEG source reconstruction techniques to enhance the extracted features based on a linearly constrained minimum variance (LCMV) beamformer.¹ Beamformers allow for easy incorporation of anatomical data and are applicable in real time. A 32-channel EEG-BCI system was designed for a 2-class motor imagery (MI) paradigm. We optimized a synchronous system for 2 untrained subjects and investigated 2 aspects. First, we investigated the effect of using beamformers calculated on the basis of 3 different head models: a template 3-layered boundary element method (BEM)

head model, a 3-layered personalized BEM head model and a personalized 5-layered finite difference method (FDM)² head model including white and gray matter, CSF, scalp, and skull tissue. Second, we investigated the influence of how the regions of interest, areas of expected MI activity, were constructed. On the one hand, they were chosen around electrodes C3 and C4, as hand MI activity theoretically is expected here. On the other hand, they were constructed based on the actual activated regions identified by an fMRI scan. Subsequently, an asynchronous system was derived for one of the subjects and an optimal balance between speed and accuracy was found. Lastly, a real-time application was made. These systems were evaluated by their accuracy, defined as the percentage of correct left and right classifications. From the real-time application, the information transfer rate³ (ITR) was also determined.

An accuracy of $86.60\% \pm 4.40\%$ was achieved for subject 1 and $78.71\% \pm 0.73\%$ for subject 2. This gives an average accuracy of $82.66\% \pm 2.57\%$. We found that the use of a personalized FDM model improved the accuracy of the system, on average 24.22% with respect to the template BEM model and on average 5.15% with respect to the personalized BEM model. Including fMRI spatial priors did not improve accuracy. Personal fine-tuning largely resolved the robustness problems arising due to the differences in head geometry and neurophysiology between subjects. A real-time average accuracy of 64.26% was reached and the maximum ITR was 6.71 bits/min.

We conclude that beamformers calculated with a personalized FDM model have great potential to ameliorate feature extraction and, as a consequence, to improve the performance of real-time BCI systems.

References

1. Van Veen B, et al. *IEEE Trans Biomed Eng.* 1997;44(9):867-880.
2. Vanrumste B, et al. *Brain Topogr.* 2001;14(2):83-92.
3. Shannon CE, Weaver W. *The Mathematical Theory of Information.* Urbana, IL: University of Illinois Press; 1949.

PI48. Induced and Evoked EEG Signatures of Noise-Vocoded Word Processing: The Graded Impact of Acoustic Degradation

M. Pefkou¹, R. Becker², C. Michel¹, and A. Hervais-Adelman³

¹Auditory Language Group, Geneva, Switzerland

²Functional Brain Mapping Lab I, Geneva, Switzerland

³Brain & Language Lab, Geneva, Switzerland

The electroencephalographic (EEG) correlates of degraded speech perception have been explored in a number of studies that examine speech recognition in adverse conditions. However, such investigations are frequently inconclusive as to whether the observed differences in brain responses between conditions are the result of the different acoustic properties of stimuli that have been degraded to be more or less intelligible or whether they relate to cognitive processes implicated in comprehending challenging stimuli.

In this study, we used noise vocoding (with 4, 8, and 16 channels) to manipulate the intelligibility of monosyllabic words. In order to produce a spectrally matched, but always incomprehensible control condition, we spectrally rotated the stimuli. We recorded EEG from 14 participants who listened to a series of noise vocoded (NV) and noise-vocoded spectrally-rotated (NVro) words, while they carried out a detection task (targets were animal words, appearing pseudorandomly at a mean frequency of 1 in 9). We specifically sought brain responses that were modulated by intelligibility of the NV stimuli (a corollary of the number of channels, or spectral complexity), after subtraction of NVro-related responses. This should reflect those aspects of the brain electrical response that are related to the intelligibility of acoustically degraded monosyllabic words, while controlling for spectral complexity.

Analyses of event-related potentials (ERPs) showed 2 post-stimulus time windows in which this effect was apparent. From 295 to 425 ms, ERP amplitude at several central and occipital electrodes shows a monotonic relationship with intelligibility. 600 to 635 ms poststimulus onset, ERP amplitude in left frontal and central electrodes displays an inverted-U shaped relationship with intelligibility. The early response appears to be linked directly to the intelligibility of the stimuli, while the latter may be a reflection of the cognitive processes associated with effortful reconstruction of the degraded stimuli.

Time-frequency decomposition of the EEG signal revealed an interaction between spectral complexity and rotation, manifest as a monotonic increase in event-related desynchronization (ERD) in the alpha band at a left temporo-central electrode cluster from 440 ms to 620 ms reflecting a direct relationship between the strength of alpha-band ERD and intelligibility. This confirms previously reported findings of intelligibility-related alpha ERD effects, which, however, were not contrasted with spectrally matched stimuli.

By carefully matching degraded words with their spectrally matched incomprehensible homologues, we reveal the complex spatiotemporal pattern of evoked and induced processes involved in degraded speech perception, largely uncontaminated by purely acoustic effects.

PI49. Face Processing in Preschool Aged Children: An MEG Neuroimaging Study

W. He¹, J. Brock¹, and B. Johnson¹

¹Macquarie Centre for Cognitive Science, Level 3, Australian Hearing Hub, Macquarie University, Macquarie Park, New South Wales, Australia

Introduction. It is unclear whether the underlying mechanisms of face perception mature early or late in development. One prominent way to exam this question is to study the well-known face sensitive brain response, termed N170 or its magnetic equivalent M170, which discriminates faces from other non-face objects based on a larger amplitude to face stimuli around 170 ms from stimulus onset in adults.¹ The current study

measured the M170 from preschoolers using a unique child-sized magnetoencephalography (MEG) system.² Furthermore, we evaluated the effective connectivity of cortical networks underlying the M170 using dynamic causal modeling (DCM); and compared the connectivity patterns in children with those of adults. **Methods.** Fifteen children (aged 4.46 ± 0.93 years) and 15 adults (aged 27.6 ± 6.46 years) viewed pictures of faces, cars, as well as their phase-scrambled counterparts.³ Brain responses of children and adults were measured using a child-sized 64 channel MEG system and a conventional 160 channel adult MEG system respectively. Surface waveforms were analyzed by averaging the strongest response across occipital and temporal sensors separately on each hemisphere based on the time window determined by visual checking on individual data. DCM analyses assumed that the M170 was mediated by sources in the occipital face area (OFA), fusiform face area (FFA), and superior temporal sulcus (STS). Using Bayesian model selection, we evaluated 3 models of the interconnections between these regions based on previous studies using DCM.⁴⁻⁶ **Results.** Analyses of surface waveforms showed that face-sensitive M170 responses were obtained from both groups, and there were no significant differences in M170 amplitude or latency between adults and children found specific to faces. In the DCM analysis, the first and simplest model with only forward intrahemispheric connections from OFA to FFA and STS had the largest model evidence in adults, while in children, the second model with extra interhemispheric connections between OFA and contralateral FFA showed the largest model evidence. **Conclusions.** High-level face encoding mechanisms indexed by the M170 are present in children as young as 4 years; and the core face network underlying the M170 has a similar organization in children and adults. However, the functional organisation of the face network undergoes further development and fine-tuning before it reaches adult capacities.

Acknowledgments

Australian Research Council Centre of Excellence in Cognition and its Disorders (CE110001021) <http://www.ccd.edu.au>.

References

1. Rossion B, Jacques C. The N170: understanding the time course of face perception in the human brain. In: Luck SJ, Kappenman ES, eds. *The Oxford Handbook of Event-Related Potential Components*. New York, NY: Oxford University Press; 2011:115-142.
2. Johnson BW, et al. *Clin Neurophysiol*. 2010;121:340-349.
3. Kuefner D, et al. *Front Hum Neurosci*. 2010;3:1-22.
4. David O, et al. *Neuroimage*. 2006;30:1255-1272.
5. Fairhall SL, Ishai A. *Cereb Cortex*. 2007;17:2400-2406.
6. Chen CC, et al. *Neuroimage*. 2009;45:453-462.

PI50. Cortical Processing of Different Tastes in Humans: A Matter of Time?

K. Ohla¹

¹German Institute of Human Nutrition Potsdam-Rehbrücke, Nuthetal, Germany

In spite of decades of research, we know very little about the time course of cortical activations during gustatory perception in humans. Only a marginal number of event-related potentials (ERP) and magnetic fields studies have been conducted on taste so far owing to difficulties in stimulus control; the existing results suggest, however, differences in response latencies for different tastants and/or taste qualities. The aim of the study was to characterize the gustatory ERP and its cortical processing to different tastes and to investigate the nature of differences in response latency. We recorded EEG while participants received salty, sweet, bitter, and sour solutions. Participants were to respond as quickly as possible to the tastes and to rate taste intensity and pleasantness. Electrical neuroimaging analyses were performed to characterize the time course of the ERP and to localize the gustatory response patterns in the brain. The ERP yielded amplitude differences between tastes that can, in part, be attributed to differences in perceived intensity. Furthermore, we found that behavioral and neuronal (ERP) response latencies were strongly correlated; responses to salty and sour were faster than responses to sweet and bitter. When accounting for the difference in response latencies, source analyses revealed similar cortical activation patterns for all tastes. The results suggest that different tastes share a common cortical network that is activated at different times. Taste-specific differences in response latencies indicate that different tastes reach awareness at different instants.

PI52. Examination of the Effect of Acute Levodopa Administration on the Loudness Dependence of Auditory-Evoked Potentials (LDAEP) in Humans

K. Hitz¹, K. Heekeren¹, C. Obermann¹, T. Huber¹, G. Juckel², and W. Kawohl¹

¹Department of Psychiatry, Psychotherapy and Psychosomatics, Zurich University Hospital for Psychiatry, Zurich, Switzerland

²Department of Psychiatry, Ruhr-University Bochum, Bochum, German

The loudness dependence of the auditory-evoked potential (LDAEP) is considered a noninvasive in vivo marker of central serotonergic functioning in humans. Nevertheless, results of genetic association studies point toward a modulation of this biomarker by dopaminergic neurotransmission. We examined the effect of dopaminergic modulation on the LDAEP using L-3,4-dihydroxyphenylalanine (levodopa)/benserazide (Madopar) as a challenge agent in healthy volunteers. A double-blind placebo-controlled challenge design was chosen. Forty-two healthy participants (21 females and 21 males) underwent 2 LDAEP measurements, following a baseline LDAEP measurement either placebo or levodopa (levodopa 200 mg/benserazide 50 mg) were given orally. Changes in the amplitude and dipole source activity of the N1/P2 intensities (60, 70, 80, 90, and 100 dB) were analyzed.

The participants of neither the levodopa nor the placebo group showed any significant LDAEP alterations compared to the baseline measurement. The test-retest reliability

(Cronbach's alpha) between baseline and intervention was 0.966 in the verum group and 0.759 in the placebo group, respectively. The administration of levodopa showed no effect on the LDAEP. These findings are in line with other trials using dopamine receptor agonists.

References

1. Gallinat J, Bottlender R, et al. *Psychopharmacology (Berl)*. 2000;148(4):404-411.
2. Hegerl U. *Pharmacopsychiatry*. 1994;27(2):47-48.
3. Hegerl U, Gallinat J, et al. *J Affect Disord*. 2001;62(1-2):93-100.
4. Hegerl U, Gallinat J, et al. *Int J Psychophysiol*. 1994;17(1):1-13.
5. Kawohl W, Giegling I, et al. *Int J Neuropsychopharmacol*. 2008;11(4):477-483.
6. O'Neill BV, Croft RJ, et al. *Psychopharmacology (Berl)*. 2006;188(1):92-99.
7. O'Neill BV, Croft RJ, et al. *Hum Psychopharmacol*. 2008;23(5):355-370.
8. O'Neill BV, Guille V, et al. *Hum Psychopharmacol*. 2008;23(4):301-312.
9. Volkow ND, Wang G, et al. *J Neurosci*. 2001;21(2):RC121.

PI53. EEG- and fMRI-Based Communication Tools in Disorders of Consciousness: Which Is the Most Reliable Method?

D. Gabriel¹, A. Comte^{1,2,3}, J. Henriques⁴, E. Magnin^{3,5}, L. Grigoryeva⁴, J.-P. Ortega^{4,6}, E. Haffen^{1,2,7}, T. Moulin^{1,2,3,5}, L. Pazart¹, and R. Aubry^{1,8,9}

¹Centre d'investigation Clinique-Innovation Technologique, Inserm 808, CHU de Besançon, France

²Laboratoire de Neurosciences de Besançon, Université de Franche-Comté, Besançon, France

³Département de recherche en imagerie fonctionnelle, CHU de Besançon, France

⁴Laboratoire de Mathématiques de Besançon, Université de Franche-Comté, Besançon, France

⁵Service de neurologie, CHU de Besançon, Besançon, France

⁶Centre National de la Recherche Scientifique, Besançon, France

⁷Service de psychiatrie de l'adulte, CHU de Besançon, France

⁸Espace Ethique Bourgogne/Franche-Comté, CHU de Besançon/CHU de Dijon, France

⁹Département douleur soins palliatifs, CHU de Besançon, France

The assessment of cognition in patients presenting disorders of consciousness (vegetative state or minimally conscious state) is often challenging. Although awake, these patients may be unable to exhibit reliable motor responses and thus remain unresponsive to behavioral investigations. New neuroimaging methods have been used to detect the presence of volition and awareness through mental imagery tasks. An inspiring study conducted by Monti et al. (2010) showed that these tasks combined with fMRI could even be used as a communication tool in patients presumptively diagnosed as unresponsive. However, difficulties related to cost, availability, and the necessity to transfer the patient to the machine prevents the use of fMRI in a routine basis. Electroencephalography (EEG) may overcome

these problems since it is far less expensive and can easily be transported to the patient's bedside. However, although EEG and mental imagery have recently been combined to assess vegetative state patients' awareness (Cruse et al., 2011), no EEG-based communication has been established yet. The aim of the present work is to replicate the same mental imagery paradigms presented in the literature in order to compare the reliability of fMRI- and EEG-based communication tools on the same group of healthy subjects.

Sixteen healthy participants performed 2 mental imagery sessions. In the first session, fMRI was used in a protocol similar to the one in Monti et al. (2010) where the subjects had to answer 3 autobiographical yes/no questions by imagining either playing tennis or moving from room to room in their house. The second session was performed a few weeks later with a 64-electrode EEG and replicated the mental imagery tasks proposed in Cruse et al. (2011) consisting in answering 3 autobiographical yes/no questions by imagining squeezing their right hand or wiggling the toes of their feet.

Data analyses first replicated the methodology used in the original articles, but new procedures were also developed. In the fMRI context, 5 automatic methods were used to classify communication scans' responses. As to EEG, several signal extraction methods were implemented, some of them based on parametric time series models regularly encountered in the treatment of financial signals. Patterns of cerebral activity are explored individually in each participant and compared to the expected answers. The comparison of both neuroimaging-based communication tools are presented and discussed.

PI54. Postmovement Event-Related Potentials Recorded in Remote Brain Loci Are Preceded by an Increase of EEG Phase Synchronization

M. Kukleta¹, B. Baris Turak², and J. Louvel¹

¹Central European Institute of Technology (CEITEC), Masaryk University, Brno, Czech Republic

²Service de Neurochirurgie Stéréotaxique, Hôpital Ste Anne, Paris, France

The current study focused on the network engaged in the generation of post-movement evoked potentials (late movement potentials [LMPs]) obtained during voluntary movements with the aim to analyze temporospatial characteristics of these potentials and associations with operations which took place in this period of the task. Intracerebral EEG records obtained from 42 epilepsy surgery candidates (28 men, 14 women, age range 18-49 years) during repeated self-paced hand movements were used in the study; the averaged records with solitary evoked responses starting after the peak of rectified EMG were analyzed. Such LMPs were found in 13 subjects in the following anatomically delineated brain regions: the left gyrus cinguli anterior, the right gyrus frontalis superior, the right gyrus frontalis medialis, the right and left gyrus frontalis medius, the left gyrus frontalis inferior, the right gyrus precentralis, the left gyrus postcentralis, the right lobulus parietalis inferior, the left

gyrus cinguli posterior, the left precuneus, the left cuneus, the left gyrus lingualis, the left gyrus parahippocampalis, the right gyrus temporalis medialis. The records from remote brain sites exhibited closely before the LMP onset a significant increase of phase synchronization. The mean r -value was 0.17 ± 0.23 in the “baseline” period from 4.0 to 0.8 seconds prior to the movement and 0.84 ± 0.13 (-0.72 ± 0.04 in 3 negative correlations) in the 300-ms period preceding closely the LMP onset (difference significant in all cases; $P < .001$, Mann–Whitney U test). The postmovement location of LMPs and the simplicity of the task, which practically excluded the implication of error detection or the implication of any other additional operation, suggested an association between the LMPs and comparison of the predicted and the actual result of the action, which is known to take place in this epoch. As the accordance between an intention and its result has a crucial role for the creation of agentive experience, the attempted description of large-scale network generating the LMPs could be considered as a step toward structural delineation of this significant component of human consciousness.

Acknowledgments

Supported by the project “CEITEC–Central European Institute of Technology” (CZ.1.05/1.1.00/02.0068) from European Regional Development Fund.

P155. Brain Oscillations Reveal Neural Mechanisms of Associative Memory in Aging

M. Crespo-Garcia^{1,2}, J.L. Cantero¹, and M. Atienza¹

¹University Pablo de Olavide, Sevilla, Spain

²University of Konstanz, Konstanz, Germany

Episodic memory, particularly those mechanisms that allow the association of contextual details are impaired in aging. Evidence indicates that semantic congruence may reduce this memory deficit. Here, we investigate the neural mechanisms that mediate this benefit. For this, 30 young and 28 older adults were presented with biographical cues and famous faces at a particular spatial location. For each trial, subjects indicated whether or not there was a matching between the face and the preceding cue. Memory for facelocation associations was later evaluated in a surprise recognition test. EEG oscillatory activity of successfully learned associations during encoding was first analyzed at the sensor level, and next at the source level with beamformers. For this, we extracted information about amplitude and consistency of phase across trials. We additionally computed cross-frequency coupling (CFC) between sources that were modulated by semantic congruence and other frequency bands. Results indicated that semantic congruence during encoding was able to enhance associative recognition in the two groups but was unable to eliminate the age-related memory deficit. All subjects showed stronger theta power for congruent than for incongruent faces in the left prefrontal

cortex. But only the theta power increase in the left inferior frontal gyrus (IFG) was correlated with memory gains. The sensor analysis also revealed a late (860 ms, 4 Hz) effect of congruence in older adults that was localized in the left parahippocampal gyrus (PHG). The IFG and PHG theta sources also showed an enhanced CFC with alpha (10 Hz) and beta (18 Hz) bands during encoding; but only theta-beta coupling between frontal and mediotemporal regions was modulated by age. Particularly, we found that CFC was stronger in older adults, and was negatively correlated with associative memory. Two main conclusions can be derived from this study. First, our results have confirmed prior results from fMRI studies, and suggest that theta oscillations mediate semantic processes that are beneficial for episodic memory in both young and older adults. Second, although semantic elaboration was not affected by normal aging, results from correlations with performance and from CFC analyses suggest that such benefit may involve different neural mechanisms in young and older adults. The former depend more on control mechanisms in the prefrontal cortex, whereas the latter rely more on associative mechanisms in regions of the medial temporal lobe.

P157. ERP Components as Indicators of Cognitive Change Across Healthy Mid-Aged Adults, Healthy Older-Adults, and AD Patients

S. Connell¹ and K. Kilborn¹

¹School of Psychology, University of Glasgow, Glasgow, Scotland

Changes in cognitive ability that occur with increasing age may be difficult to distinguish from initially mild deficits caused by Alzheimer’s disease (AD). We examined a set of cognitive event-related potentials in healthy older individuals aged 50–85 years, and in individuals aged 65 years and over diagnosed with mild probable AD. Participants engaged in an associative memory task comprising spoken word and visual image associates presented simultaneously. Subjects decided by button press whether each pair was “new” or “old,” where old items were repetitions of new items after either a short (5–13) or long (17–39) item interval. 128-channel EEG was recorded continuously during the task. **Participants.** Mid-adults (50–65 years, $n = 49$), older-adults (66–85 years, $n = 39$), and AD patients (65+ years, $n = 62$). **Results.** N2: Pair-wise group comparisons showed that the N2 amplitude was greater for mid-adults and older-adults than patients ($P = .007$ and $P = .001$). Mid-adults and older-adults did not differ from each other. FN400: ANOVA on amplitude revealed main effects of memory ($P = .000$) and group ($P = .000$). Amplitude of old items greater than new (short $P = .000$ and long $P = .000$). Amplitudes were lower overall in AD group than the 2 healthy groups ($P = .000$ and $P = .000$). N400: Anova on amplitude revealed an interaction ($P = .047$). Amplitude in mid-adults was greater in the long condition compared to the new ($P = .001$), but not for older-adults or AD patients. Parietal Old/New Effect: Main effects of memory ($P = .001$) and group ($P = .047$). Amplitude was

lower in AD patients across all conditions than the mid-adults ($P = .037$). Mid-adults did not differ from older-adults, older-adults did not differ from AD patients. All 3 groups showed greater amplitude for the short condition than new (mid-adults $P = .000$, older-adults $P = .035$, patients $P = .004$;) and the long compared to the new (mid-adults $P = .000$, older-adults $P = .029$, and patients $P = .038$). P6: Amplitudes for the mid-adults were greater than both the older-adults ($P = .050$) and patients ($P = .000$) and greater for the older-adults compared to the patients ($P = .009$). Mid-adults and older-adults had higher P6 amplitudes for the short ($P = .000$, $P = .006$) and long ($P = .002$, $P = .011$) conditions compared to the new. Patients showed no difference in amplitude across the conditions. *Conclusions.* The present study shows the N2, FN400, and the Parietal old/new effect differentiate between presence and absence of AD while the N400 differentiates across age, regardless of AD presence. Interestingly, more in-depth analysis of the 500- to 700-ms window, specifically the P6 component, was the one component which differentiated between all 3 groups.

PI58. Postmovement ERPs Elicited During Target Variant of Visual Oddball Task

A. Damborská^{1,2}, M. Brázdil^{1,3}, I. Rektor^{1,3}, and M. Kukleta¹

¹CEITEC—Central European Institute of Technology, Masaryk University, Brno, Czech Republic

²Department of Physiology, Faculty of Medicine, Masaryk University, Brno, Czech Republic

³First Department of Neurology, St. Anne's Faculty Hospital, Masaryk University, Brno, Czech Republic

Remote brain regions within cognitive networks are known to cooperate during sensorimotor coupling, that is, during cognitive operations associated with the processing of a sensory signal up to the processes linked to a given motor action. It is also known that several frontal and parietal brain regions are activated after movement execution, when resulting action is compared with intention of the task. The aim of present study was to identify nodes of neural network engaged in the postmovement epoch. We searched for postmovement event-related potentials (ERPs) recorded intracerebrally in 17 epileptic patients during target variant of the visual oddball task. Each patient had 2 to 10 electrodes examining frontal, temporal, and parietal lobes of either or both hemispheres. ERPs were elicited by target stimuli in all subjects. Regions generating isolated ERP components in the postmovement period were found in 11 subjects in frontal, temporal, and parietal lobes. In individual subjects with more than one generator of postmovement ERP, their onsets regarding to movement execution were either identical or different.

These results confirm that during target variant of the visual oddball task, the postmovement ERPs are generated in large-scale neural network. This network includes frontal, temporal, and parietal regions. Observed differences in latency of postmovement ERP components suggest heterogeneity of underlying processes.

Acknowledgments

Supported by the project “CEITEC—Central European Institute of Technology” (CZ.1.05/1.1.00/02.0068) from the European Regional Development Fund.

PI65. QEEG/LORETA Electrical Imaging and Z-Score LORETA Neurofeedback: New Paradigm to Neuropsychiatric Diagnosis and Treatment

J.L. Koberda^{1,2,3}, A. Bienkiewicz¹, I. Koberda^{1,2}, P. Koberda^{1,2}, and A. Moses^{1,2}

¹Tallahassee Neuro-Balance, Tallahassee, FL, USA

²Florida State University, Tallahassee, FL, USA

³Carrick Institute for Graduate Studies, Cape Canaveral, FL, USA

Introduction of QEEG/LORETA brain imaging has improved our diagnostic ability in neuropsychiatric practice by identification of dysregulated cortical areas implicated in patient's symptoms.¹⁻³ Additional use of LORETA Z-score neurofeedback (NFB) enables us to directly target this area of dysregulation in order to improve associated with them symptoms.⁴⁻⁶ Based on approximately 200 patients treated in our clinic with Z-score LORETA NFB, a detailed analysis of selected cases will be presented. Cases will include depression/anxiety, chronic pain, epilepsy and cognitive dysfunction. Specific areas of dysregulation attributed to particular condition identified by LORETA will be presented: anterior cingulate and insular cortex in pain syndromes⁶; as well as specific Brodmann's areas in other cases. Follow-up findings of QEEG/LORETA electrical imaging after NFB and computerized cognitive testing will be discussed. In addition, cases of Z-score LORETA NFB mediated cognitive enhancement will be shown. This presentation encompasses examples of the application of functional neurology in neuropsychiatry.

References

1. Koberda JL, Moses A, Koberda P, Koberda L. Clinical advantages of quantitative electroencephalogram (QEEG)—electrical neuroimaging application in general neurology practice [published online March 26, 2013]. *Clin EEG Neurosci*. doi:10.1177/1550059412475291.
2. Koberda JL. Clinical advantages of quantitative electroencephalogram (QEEG) application in general neurology practice. Presented during the Society of Applied Neuroscience Meeting. *Neurosci Lett*. 2011; 500(suppl 1):32.
3. Koberda JL. Application of quantitative EEG and LORETA in general neurology practice for detection and localization in epilepsy. Presented during the American Academy of Neurology (AAN) meeting (April 23, 2012) *Neurology* suppl.
4. Koberda JL, Moses A, Koberda P. Cognitive enhancement using 19-electrode Z-score neurofeedback. *J Neurother*. 2012;3.
5. Koberda JL. Autistic spectrum disorder (ASD) as a potential target of Z-score LORETA neurofeedback. *The Neuroconnection: Winter 2012 Edition (ISNR)*.
6. Koberda JL, Koberda P, Bienkiewicz A, Moses A, Koberda L. Pain management using 19-electrode Z-score LORETA neurofeedback. *J Neurother*. In press.

PI66. Deviant EEG Resting States Associated With Psychotic Symptoms in Adolescents Affected by the 22q11.2 Deletion Syndrome

M. Tomescu¹, T. Rihs¹, J. Britz¹, A. Custo¹, F. Grouiller^{1,2}, M. Schneider³, M. Debbané^{3,4}, S. Eliez³, Ch. Michel¹

¹Functional Brain Mapping Laboratory, Department of Fundamental Neuroscience, University Medical Center, CMU, Geneva, Switzerland

²Center for Biomedical Imaging (CIBM), Department of Radiology and Medical Informatics, University of Geneva, Geneva, Switzerland

³Office Médico-Pédagogique Research Unit, Department of Psychiatry, University of Geneva School of Medicine, Geneva, Switzerland

⁴Adolescent Clinical Psychology Research Unit, Faculty of Psychology, University of Geneva, Geneva, Switzerland

Individuals with 22q11.2 deletion syndrome (22q11DS) have a 30-fold increased risk to develop schizophrenia in adulthood compared with healthy controls. EEG microstates at rest have been shown to deviate in adults with schizophrenia and are thus potential candidates as early biomarkers for schizophrenia in 22q11DS. EEG microstates are stable, short periods (~100 ms) of scalp potentials with consistent topographies across subjects and recordings. We used high-density EEG to investigate the microstates in 13 adolescents with 22q11DS and 14 age-matched controls. Dominant EEG microstates in 5 minutes of eyes-closed EEG were identified using k-means cluster analysis and by fitting these microstates back to the data we explored between-group differences in terms of EEG microstate duration, global presence, and their within-group correlation with clinical symptoms. In the 22q11DS patients the microstate class A, previously shown to be related to the auditory resting state network, had decreased global presence and the microstate class C, previously shown to be related to the salience resting state network, had increased duration with respect to controls. In patients the mean duration of class A microstates was negatively correlated with positive symptoms while a positive correlation was found between the mean duration of microstate C and disorganization symptoms of schizotypy. Moreover, by median-splitting into low versus high schizotypy patients, we show significant differences of these microstate classes within the 22q11DS group, which could be indexing the increased risk of the high schizotypy patients group to develop schizophrenia if confirmed by longitudinal studies.

PI68. Differences in Auditory Target Processing: Comparisons of Methadone-Substituted Patients, Active Opiate Users, and Non-Drug Users

G.Y. Wang^{1,2}, R. Kydd^{2,3}, T.A. Woudes³, M. Jensen¹, B.R. Russell^{1,2}

¹School of Pharmacy, The University of Auckland, Auckland, New Zealand

²Centre for Brain Research, The University of Auckland, Auckland, New Zealand

³Department of Psychological Medicine, Faculty of Medical and Health Sciences, The University of Auckland, Auckland, New Zealand

Methadone maintenance treatment (MMT) has been used as a treatment for opiate dependence since the mid 1960s. Despite its clinical utility, concern has been raised about possible effects of MMT on cognitive function. While studies utilising neuropsychological testing suggest that opiate addiction impairs cognitive performance, results from studies on MMT are conflicting. Studies using other measures of cognitive function such as event-related potentials (ERPs) are few. Our study aimed to investigate differences in electrophysiological activity between patients undergoing MMT ($n = 32$), active opiate users ($n = 17$), and non-drug users ($n = 25$), during an auditory oddball task. This approach was to help differentiate the effects of MMT from other opiate use, and to control for the confounding effects of co-morbid drug use. It contrasts with most previous studies that have used opiate abstainers as controls. Neuroscan 4.3 was used to acquire ERP from the cephalic sites using 10-20 international system. Participants were presented with 60 target tones (1000 Hz) dispersed quasi-randomly (2 targets never appeared together) among a series of 280 background tones (500 Hz) (intensity = 75 dB; duration = 50 ms; ISI = 1 second; $r/f = 5$ ms). Participants were asked to respond to target tones not to background tones with a button press. Speed and accuracy were stressed equally. The midline sites Fz, Cz, and Pz were selected for analysis. The P300 amplitude at Fz was significantly higher in the MMT group ($M = 7.8$, 95% CI = 5.6-9.9) than in the opiate users ($M = 2.1$, 95% CI = -1.6 to 5.7); however, both groups were not significantly different from the non-drug users ($M = 3.7$, 95% CI = 0.6-6.7). There was no group difference in the P300 latency. The opiate users also exhibited smaller N200 amplitude than the MMT at Fz and non-drug user groups at Cz, whereas the MMT group was not different from the non-drug users in either the amplitude or latency of the N200. Task performance by the MMT group was comparable to that of non-drug users, but the opiate users had a greater number of task-related errors than the non-drug users. Decreased N200 amplitude in opiate users suggests an impaired ability to selectively attend to the task at hand and discriminate between stimuli. Our findings suggest cognitive impairment associated with opiate use may be reduced following MMT. Cognitive impairment of patients undertaking MMT observed in some studies may be related to their history of recreational drug use. The findings are limited by small sample sizes and other unmeasured factors including level of drowsiness, nutritional status and methadone plasma concentration.

Acknowledgments

The University of Auckland, New Zealand, The New Zealand Pharmacy Education Research Fund.

Reference

1. Attou A, Figiel C, Timsit-Berthier M. Opioid addiction: P300 assessment in treatment by methadone substitution [in French]. *Neurophysiol Clin.* 2001;31(3):171-180.

2. Kouri E, Lukas S, Mendelson J. P300 assessment of opiate and cocaine users: effects of detoxification and buprenorphine treatment. *Biol Psychiatry*. 1996;40:617-628.
3. Muller BW, Specka M, Steinchen N, et al. Auditory target processing in methadone substituted opiate addicts: the effect of nicotine in controls. *BMC Psychiatry*. 2007;7:1-9.

PI 69. Emotional Processing in Parkinson's Disease and Anxiety: An EEG Study of Visual Affective Word Processing

N. Dissanayaka^{1,2}, T. Au², A. Angwin³, J. O'Sullivan^{1,2}, G. Byrne^{4,5}, P. Silburn^{1,2}, R. Marsh⁵, G. Mellic^{2,6}, and D. Copland^{1,3}

¹UQ Centre for Clinical Research, University of Queensland, Brisbane, Queensland, Australia

²Neurology Research Centre, Royal Brisbane & Women's Hospital, Brisbane, Queensland, Australia

³School of Health & Rehabilitation Sciences, University of Queensland, Brisbane, Queensland, Australia

⁴School of Medicine, University of Queensland, Brisbane, Queensland, Australia

⁵Department of Psychiatry, Royal Brisbane & Women's Hospital, Brisbane, Queensland, Australia

⁶Eskitis Institute for Cell & Molecular Therapies, Griffith University, Brisbane, Queensland, Australia

Background. Abnormal processing of emotions, including blunted arousal and startle reflex when responding to threatening negative stimuli have been reported in Parkinson's disease (PD). Moreover, 25% of PD patients experience DSM-IV anxiety disorders and these affective disturbances add to the complexity of this disease. This study examined emotional processing in PD using EEG. **Methods.** Nineteen (19) nondemented PD patients, including 6 with anxiety disorders and 13 without anxiety disorders, and 19 healthy controls completed a visual word affective priming task while ERPs were simultaneously recorded using a 128-channel EGI sensor net. The affective priming paradigm consecutively presented negatively or neutrally valenced 2 words in a short stimulus onset asynchrony of 150 ms. Participants evaluated the valence of the second word (target word). Amplitudes of ERPs were examined at 200 to 350 ms, 400 to 600 ms, and 600 to 800 ms time windows corresponding to P3a, P3b, and LPP, respectively. Repeated measures ANOVA were computed to examine congruency and target valence effects on the ERP amplitudes for within and between groups. **Results.** In controls, larger P3a ($F = 8.7$, $P < .01$) and LPP ($F = 15.3$, $P < .01$) amplitudes for *negative compared to neutral* stimuli were observed at frontal (Fz) and right parietal (P4) regions, respectively. These effects were lost in PD patients without affective disturbances ($F_{Fz} \text{ P3a: } F = 0.002$, $P = 0.97$; $F_{P4} \text{ LPP: } F = 3.84$, $P = .07$). A *larger LPP amplitude for congruent negative compared to neutral target stimuli* in the midline parietal region (Pz) was observed in these PD patients ($F = 5.4$, $P = .04$). Interestingly, anxiety moderated this Pz-LPP amplitude in an opposite direction ($F = 4.3$, $P < .05$).

In comparison to PD without anxiety, PD with anxiety showed a larger LPP amplitude for *neutral compared to negative* stimuli. **Discussion.** These ERP variations can be generated by structural and functional impairment in the amygdala previously reported in PD. Degeneration of the mesolimbic and mesocortical dopaminergic pathways in PD also account for these changes. Future research using EEG source localisation and fMRI in PD will allow determining underlying structural and functional connections.

PI 70. How Theta Amplitude Is Related to fMRI Resting State Networks During Working Memory in Patients With Schizophrenia

A. Bänninger¹, M. Kottlow^{1,2}, L. Díaz Hernández¹, and T. Koenig¹

¹Department of Psychiatric Neurophysiology, University Hospital of Psychiatry, University of Bern, Bern, Switzerland

²Institute of Pharmacology and Toxicology, University of Zurich, Zurich, Switzerland

Deficits in working memory processes are a core feature of schizophrenia. While in healthy subjects, the fMRI-BOLD signal is usually decreased in regions of the so called default mode network (DMN) during tasks, patients seem to both fail to deactivate these task-negative regions as well as to activate task positive regions. Furthermore, working memory load induces an increase in frontal EEG theta (5-8 Hz) power in healthy subjects, while reduced activity has been found in this patient group.

The simultaneous measurement of EEG and fMRI has become an established technique in order to obtain spatially well-defined indices of metabolic activity from the fMRI as well as EEG based information about the fast dynamics of stimulus processing. With the so-called covariance mapping, the fluctuations of fMRI resting state networks (RSN) are temporally correlated with the dynamics of EEG spectral amplitudes. As a result, the spatial distributions of frequency domain EEG fluctuations that were significantly associated with the dynamics of the RSNs are obtained.

We computed covariance maps of EEG theta amplitude from the retention period of a verbal Sternberg working memory task and the dynamics of the DMN and a frontoparietal control network (FPCN) in a preliminary single-trial analysis on schizophrenia patients and healthy controls.

An inverse relation between the DMN and theta amplitude was found in healthy controls, meaning that when the DMN was up-regulated, theta amplitude was down-regulated. In patients, this effect was not visible. For the FPCN in contrast, an inverse correlation with theta amplitudes was found in patients, whereas no significant association with theta oscillations resulted in healthy controls.

These results support the notion that patients with schizophrenia may express aberrant patterns of up- or down-regulation

of task-positive and -negative networks respectively in relation to theta amplitude. This may lead to the known deficits in working memory performance.

Acknowledgments

Supported by SNF Sinergia Grant No. 136249.

PI 71. Feasibility of Neurofeedback Training to Modify Brain States Relevant for Mental Health

L. Díaz Hernández¹, A. Bänninger¹, and T. Koenig¹

¹Department of Psychiatric Neurophysiology, University Hospital of Psychiatry, University of Bern, Bern, Switzerland

Spontaneous EEG signal can be parsed into sub-second time epochs with quasi-stable EEG scalp field topographies separated by rapid configuration changes. These epochs are called microstates and manifest different brain functional states exerting different effects on information processing. Resting-state EEG microstates in patients with schizophrenia show concise and well-replicable peculiarities: In several independent samples, a specific class of microstate with a frontocentral distribution has been found to be consistently shorter in schizophrenic patients when compared to healthy controls, the so-called microstate class D. This shortening has been correlated to positive psychotic symptoms. Therefore, it is reasonable to think that if patients can learn to normalize microstate class D; this might help reducing psychotic symptoms. A useful method for learning to self-regulate brain states is EEG based neurofeedback. This method is effective, inexpensive and has been used for research and treatment like in epilepsy, ADHD, stroke and others. The present study aims to explore if healthy subjects are able to regulate the presence of class D microstates by means of neurofeedback training. We present the technical setup and the training protocol, which includes baseline assessments, training of up- and down-regulation and transfer trials.

Acknowledgments

Supported by SNF Sinergia Grant No. 136249.

PI 72. Impaired Decision Making and Reward Learning in Adolescents With Attention Deficit/Hyperactivity Disorder (ADHD): A Simultaneous EEG–fMRI Study

T.U. Hauser^{1,2}, R. Iannaccone^{1,3}, C. Mathys⁴, J. Ball¹, R. Drechsler¹, D. Brandeis^{1,5,6}, S. Walitza^{1,5}, and S. Brem¹

¹University Clinics for Child and Adolescent Psychiatry (UCCAP), University of Zurich, Zurich, Switzerland

²Neuroscience Center Zurich, University of Zurich and ETH Zurich, Zurich, Switzerland.

³PhD Program in Integrative Molecular Medicine, University of Zurich, Zurich, Switzerland

⁴Wellcome Trust Centre for Neuroimaging, University College London, London, UK

⁵Zurich Center for Integrative Human Physiology, University of Zurich, Zurich, Switzerland

⁶Department of Child and Adolescent Psychiatry and Psychotherapy, Central Institute of Mental Health, Medical Faculty Mannheim/Heidelberg University, Mannheim, Germany

Adaptive decision making is an essential skill for survival. Maladaptive decision making processes have been found in several psychiatric disorders, for example in attention deficit/hyperactivity disorder (ADHD). However, the precise mechanisms of these deficits in ADHD remain largely unknown. Computational approaches in psychiatry help to determine the mechanisms of learning impairments in psychiatric patients and to relate them to neurophysiological changes. ADHD is characterized by inattentiveness, impulsivity and hyperactivity. It has been associated with impairments in the mesencephalic dopamine system, which projects to the ventral striatum and the medial prefrontal cortex.

In this simultaneous electroencephalogram (EEG) and functional magnetic resonance imaging (fMRI) study, we investigated the behavioral and neural impairments in juvenile ADHD patients in a probabilistic reversal learning task. We used a Bayesian hierarchical Gaussian filter model to infer the decision processes of the subjects. We found that ADHD patients had a less steep decision function. This means that ADHD patients act less deterministically than healthy controls. We further found that ADHD patients show impairments in the medial prefrontal cortex during reward evaluation and anticipation. In the ventral striatum, ADHD patients showed similar responses during reward anticipation, but failed to respond during outcome evaluation. Our EEG data confirm our fMRI findings.

This study provides crucial insights into the impaired decision making processes in ADHD and thus furthers the understanding of this highly prevalent disorder.

PI 73. EEG Levels of Ketamine-Induced Cortical Disinhibition Are Positively Associated With Changes in Pupil Size, and Not Oculomotricity

P.H. Boeijinga¹

¹Biomedical Research Expertise, former FORENAP/AstraZeneca CNS Consulting, Strasbourg, France

Ketamine, a NMDA noncompetitive antagonist, has been used as a model of psychosis. Eyes-closed EEG, in particular high-frequency GAMMA activity seems to possess relevance for applications in psychiatry but the putative neuronal bio-marker is ill localized. Moreover, there is a risk for extracerebral contamination related to eye movements. For future drug interaction studies, attempts to find the true central origins are of high value; pupil size was considered as a second, potentially useful, pharmacodynamic since in a translational perspective several other NMDA antagonists are known to produce mydriasis in mice.

Data were obtained from 2 randomized, double-blind, placebo-controlled design ketamine (0.5 mg/kg intravenous) versus saline-dummy on 2 test days in healthy subjects ($n = 14$, $n = 5$). Quantified EEG (qEEG) in eyes closed and eyes opened conditions (3 minutes for each condition) was recorded with 28 scalp electrodes. sLORETA has been applied on the decomposed activity from 33–48 Hz. Static measurements of pupil size was measured on both eyes at the same time with a computerized infrared pupillometer after 10-minutes adaptation to the light condition. Eye movements were scored in a separate run.

Ketamine produced psychotic-like positive symptoms, and significantly increased resting gamma EEG pronounced under eyes closed conditions. Maximal effects were in temporal cortex domains. Pupil size correlated with absolute GAMMA magnitude but spontaneous nystagmus did not.

It is concluded that the high-frequency EEG response to ketamine was related to a direct cortical effect. Face validity of EEG spectra following ketamine with clinical observations of patients remain to be improved.

PI 74. Differences in Neural Mechanisms Underlying Speech Production in Autism Spectrum Disorders as Tracked by Magnetoencephalography (MEG)

E.W. Pang^{1,2}, T. Valica^{1,2}, M.J. MacDonald¹, A. Oh¹, J.P. Lerch^{1,2}, and E. Anagnostou^{2,3}

¹Hospital for Sick Children, Toronto, Ontario, Canada

²University of Toronto, Toronto, Ontario, Canada

³Holland Bloorview Kids Rehabilitation Hospital, Toronto, Ontario, Canada

Children with autism spectrum disorders (ASD) have a variety of speech and language difficulties. It is not known whether a consistent neurobiological deficit underlies these impairments. Magnetoencephalography (MEG) is a neuroimaging modality with high temporal resolution and has been used to examine neurobiological deficits seen in autism. We tested children with ASD and matched controls in the MEG using 2 simple tasks, phoneme production and open-and-close-mouth, to compare the neural substrates of basic speech production and oromotor control. **Methods.** A total of 21 children with ASD and 21 age- and sex-matched controls (mean: 11.4 years; range: 5–18 years; 4:1 male:female) were tested in a 151-channel whole-head MEG. Children were visually cued to speak /pa/ aloud in one condition or simply open and close their mouths in another condition. MEG data were submitted to source localization using beamforming algorithms to identify key regions. Time courses (virtual sensors) were reconstructed at nodes in each of these regions for each individual and then grand-averaged. Peak latencies were identified from the grand average and the amplitudes (magnetic field strength) peak-picked for each individual. **Results.** Twenty-two virtual sensors were reconstructed with coverage over the whole head. For the mouth-open-and-close condition, significant amplitude differences were seen between ASD and controls at left and right precentral gyrus

(BA4). For the /pa/ production condition, significant amplitude differences were seen between ASD and controls in left inferior gyrus (L BA 47). **Discussion.** Bilateral primary motor areas (L/R BA4) are known to play important roles in motor function and control. Left inferior frontal gyrus (L BA47) is known to be a key region involved in language, especially word, production. Our findings of abnormal activations with such simple tasks suggest that we are tapping neural substrates that underlie basic oromotor control and phoneme production. Our findings of significant differences in these regions between ASD and controls raise the possibility that abnormalities in these regions could contribute to higher order speech and language production deficits.

Acknowledgments

This research was funded by CIHR (MOP-89961) and the Ontario Brain Institute (IDS-11-01).

PI 75. The Neurobiological Basis of Eye Movement Desensitization and Reprocessing Efficacy: An EEG Monitoring Study

G. Di Lorenzo¹, M. Pagani², L. Monaco¹, A. Daverio¹, A.R. Verardo³, I. Giannoudas¹, P. La Porta³, C. Niolu¹, I. Fernandez³, and A. Siracusano²

¹Department of Systems Medicine, University of Rome "Tor Vergata", Rome, Italy

²Institute of Cognitive Sciences and Technologies, CNR, Rome, Italy

³EMDR Italy Association, Bovisio Masciago (MB), Italy

Background. A neurobiological basis for Eye Movement Desensitization and Reprocessing (EMDR) has been recently demonstrated. The aim of this study was to compare before and after EMDR therapy the electric signals deriving from the electroencephalographic (EEG) monitoring during bilateral ocular stimulation (BS). **Methods.** A 37-channel EEG was used to record neuronal activation during whole EMDR sessions. Twenty-eight victims of psychological traumas were investigated at the first EMDR session (T0) and at the last one performed after processing the index trauma (T1). Comparisons between the EEG signals during the BS period at T0 and T1 were performed. Electrical source images were analyzed for each EEG band by eLORETA using nonparametric statistics. Between-group differences were evaluated by the exceedence proportion test at $P < .01$, F value over 2 z -score, and a cluster extent major than 27 voxels. **Results.** As compared to T0, EEG during bilateral ocular stimulation at T1 showed a significantly decreased neuronal activity in the visual cortex in all bands with the exception of gamma band in which the electric signal in left prefrontal and bilateral superior parietal cortex was significantly diminished. The opposite comparison showed increased activity post-EMDR in right dorsolateral frontal cortex and fusiform gyrus (delta band), right dorsolateral frontal cortex (theta band) and left temporal lobe, fusiform gyrus, and right temporofrontal cortex (gamma band). **Conclusions.** The implemented

methodology made possible to monitor the specific activations associated with bilateral ocular stimulation during EMDR therapy. In the largest group of victims of psychological traumas investigated hitherto by EEG, the analyses demonstrated following EMDR a shift of the maximal electric activity from visual cortex to frontal and temporo-parietal regions. These findings suggest that processing of the traumatic event moves from areas elaborating the pathological images of the index trauma to regions with an established cognitive and associative role. Furthermore, the activation post-EMDR of dorso-lateral frontal cortex speaks in favor of a restored function of such area in inhibiting pathological amygdalar function, responsible of the cortical hyperactivation state in trauma-related disorders, as PTSD. Processing the traumatic events following successful EMDR therapy resulted in distinct neurobiological patterns of brain activations during bilateral ocular stimulation associated with a significant relieve from negative emotional experiences.

Acknowledgments

EMDR International Association (EMDRIA), EMDR Europe.

PI76. Relationship Between the Brain Structure and Social Functioning in the Patients With Schizophrenia

T. Shimada¹, Y. Matsuda^{1,2}, A. Monkawa¹, T. Monkawa¹, R. Hashimoto¹, K. Watanabe¹, and Y. Kawasaki¹

¹Department of Neuropsychiatry, Kanazawa Medical University, Ishikawa, Japan

²Division of Innovative Research, Kanazawa Medical University, Ishikawa, Japan

Objective. Previous studies have revealed that the patients with schizophrenia have decreased social functioning.¹ In addition, studies using magnetic resonance imaging (MRI) reveal that links pathophysiological changes in the superior temporal gyrus volume with the development of hallucinations and thought disorder in patients with schizophrenia.² On the other hand, there are few studies examined between the superior temporal gyrus volume and social functioning in the patients with schizophrenia. In this study, we examined relationship between the brain structure and social functioning in the patients with schizophrenia using MRI and social functioning scale³–Japanese version (SFS-J).⁴ **Methods.** The sample consisted of 20 (14 women, 6 men) patients with schizophrenia who met DSM-IV criteria. We measured the brain structure using 3T-MRI (Siemens), and social functioning using SFS-J.⁴ SFS-J had 7 factors, which were withdrawal, interpersonal, prosocial, recreation, independence-competence, independence-performance, employment occupation. We analyzed brain images using voxel-based morphometry toolbox (VBM8) for statistical parametric mapping (SPM8). **Results.** A multiple regression model, with SFS factors and whole brain volume used as confounding covariates. It showed 6 significant positive correlations

($P < .0001$, uncorrected). Those were (a) correlation between withdrawal and left superior temporal gyrus volume, (b) correlation between withdrawal and right medial temporal gyrus volume, (c) correlation between interpersonal and left superior temporal gyrus volume, (d) correlation between recreation and left dorsolateral prefrontal cortex volume, (e) correlation between recreation and right inferior temporal gyrus volume, and (f) correlation between independence-competence and left superior temporal gyrus volume. **Conclusions.** These results suggested that the deficits of the brain structure may underlie the decreased social functioning in the patients with schizophrenia. It was suggested that the decrease in left superior temporal gyrus and dorsolateral prefrontal cortex volume became easy to cause poorness of withdrawal, interpersonal, and recreation.

References

1. Hill K, Startup M. *Psychiatry Res.* 2013;206:151-157.
2. Sun J, Maller JJ, Guo L, Fitzgerald PB. *Brain Res Rev.* 2009;61:14-32.
3. Birchwood M, Smith J, Cochrane R, Wetton S, Copestake S. *Br J Psychiatry.* 1990;157:853-859.
4. Nemoto T, Fujii C, Miura Y, et al. *Jpn Bull Soc Psychiatry.* 2008;17:188-195.

PI77. Curvature of the Temporal Pole in Patients With Schizophrenia: Statistical Characteristics and Its Visualization

Y. Matsuda^{1,2}, T. Shimada², T. Monkawa², A. Monkawa², K. Watanabe², and Y. Kawasaki²

¹Division of Innovative Research, Kanazawa Medical University, Ishikawa, Japan

²Department of Neuropsychiatry, Kanazawa Medical University, Ishikawa, Japan

Objectives. Previous researches have shown morphometrical changes in the superior temporal gyrus volume in patients with schizophrenia.¹ There are several anatomical structures in the superior temporal gyrus, thus details of morphometrical abnormality in the superior temporal gyrus remain unclear. In this study, we divided the superior temporal gyrus into 6 regions, and examined abnormality in cortical structure in detail. We focused on the curvature, which represents structural folding of gyrus and sulcus, of the superior temporal gyrus. **Methods.** The sample consisted of 31 (6 women, 25 men) healthy controls and 17 (10 women, 7 men) patients with schizophrenia. The magnetic resonance imaging were collected using a Siemens 3-T imaging system. We obtained mean curvature using FreeSurfer package (<https://surfer.nmr.mgh.harvard.edu/>).² In the analysis, we conducted region of interest (ROI) analysis. ROIs were defined by the anatomical parcellation of Destrieux atlas.³ We selected 6 ROIs, which were the anterior transverse temporal gyrus (of Heschl), the lateral aspect of the superior temporal gyrus, the planum polare of the superior temporal gyrus, the planum temporale of the superior temporal gyrus, the temporal pole, and the transverse temporal sulcus at each hemisphere. Mean curvature values of each ROI were obtained. To

test the differences between groups (controls vs patients) of mean curvature, 3-way analyses of variance (ANOVAs) were conducted. The first factor was group (2 groups), the second factor was ROI (6 ROIs), and the third factor was hemisphere (2 hemispheres). **Results.** The main effects of ROI was significant, $F(5, 230) = 222.07$, $P < .00001$. The interaction between group and ROI was also significant, $F(5, 230) = 2.98$, $P < .05$. Simple main effect for mean curvature of the temporal pole was significant, $F(1, 276) = 4.17$, $P < .05$. **Conclusions.** We found the simple main effect for mean curvature of the temporal pole. It indicated that the temporal pole structure of patients with schizophrenia was less elevation of gyrus and sulcus at least statistical level. We reconstructed MRI image into 3-D images, and presented 3-D reconstructed structure of the temporal plane.

References

1. Sun J, Maller JJ, Guo L, Fitzgerald PB. *Brain Res Rev.* 2009;61:14-32.
2. Fischl B. *Neuroimage.* 2012;62:774-781.
3. Destrieux C, Fischl B, Dale A, Halgren E. *Neuroimage.* 2010;53:1-15.

PI 78. Ventral Striatum Gray Matter Density Reduction in Schizophrenia Patients With Psychotic Emotional Dysregulation

K. Stegmayer¹, H. Horn¹, A. Federspiel¹, N. Razavi¹, T. Bracht¹, K. Laimböck¹, W. Strik¹, T. Dierks¹, R. Wiest², T.J. Müller¹, and S. Walther¹

¹University Hospital of Psychiatry, Bern, Switzerland

²Institute of Interventional and Diagnostic Neuroradiology, Inselspital, University of Bern, Bern, Switzerland

Introduction. Substantial heterogeneity remains across studies investigating changes in gray matter in schizophrenia. Differences in methodology and variance in schizophrenia symptom patterns may contribute to inconsistent findings. To address this problem, we recently proposed to group patients in symptom domains, which were mapped on three candidate brain circuitries namely the language, the limbic and the motor system. The aim of the present study was to investigate whether patients with prevalent symptoms of emotional dysregulation would present structural neuronal abnormalities in the limbic system. **Method.** Forty-three right-handed medicated patients with schizophrenia were assessed with the Bern Psychopathology Scale (BPS). The patients and a control group of 34 healthy individuals underwent structural imaging at a 3-T MRI scanner. Whole brain voxel-based morphometry (VBM) was compared between patient subgroups with different severity of emotional dysregulation. **Results.** Patients with severe emotional dysregulation showed significantly decreased gray matter volume in the right ventral striatum compared to patients without emotional dysregulation. Comparing patients with severe emotional dysregulation and healthy controls, several clusters of significant decreased gray matter density were

detected in patients, for example, the right ventral striatum, bilateral thalamus, and the ventral prefrontal cortex. No significant effect in the ventral striatum was found comparing all patients with all controls. **Discussion.** Decreased gray matter density in the right ventral striatum was associated with severe symptoms of emotional dysregulation in schizophrenia patients. The ventral striatum is a key region of the limbic system, indicated to be involved in the generation of incentive salience and psychotic symptoms. The present results support the hypothesis that grouping patients according to specific clinical symptoms allows identifying patient subgroups with specific structural alterations.

PI 79. Neurophysiological Markers of Obsessive Compulsive Disorder

L.J. Koorenhof¹, S.J. Swithenby¹, and A. Martins-Mourao¹

¹Open University, Milton Keynes, UK

Quantitative electroencephalography (QEEG) enables useful categorisations of individual profiles of brain activity and their relation with clinical symptoms. This study investigates QEEG and event related potentials differences between people with obsessive compulsive disorder (OCD) and control subjects, together with the correlations between neuro-physiological and behavioural measures in the OCD group. The aim was to find neurophysiological markers that inform understanding of the brain mechanisms underlying OCD.

The study included 36 people with OCD (22 females; mean age 45 years, range 18-66 years), and 33 comparison subjects without a mental health disorder (20 females; mean age 39 years, range 18-64 years), matched for years of full-time education. QEEG was recorded (19 channel, linked ears, common average, and digitised at 250 Hz) for 5 minutes with eyes closed and with eyes open. A Visual Continuous Performance Task (VCPT) was administered, and analysis focussed on the p300 wave. Artifacts were rejected and the data was post filtered (0.3 Hz to 50 Hz, 45-55 Hz notch). Spectral power was individually normalised. The Minnesota Multiphasic Personality Inventory-II-RF was administered to all subjects and the Yale Brown Obsessive Compulsive Scale (Y-BOCS) to OCD subjects.

During eyes closed the OCD group showed significantly ($P < .05$) increased beta2 power in midline and anterior regions. During eyes open there were widespread significant ($P < .05$) increases in theta and beta2 power and decreases in alpha power. Mann-Whitney rank statistics showed midline and posterior differences in alpha and beta2 power between people with below and above median Y-BOCS scores. Applying a 2-parameter linear model (obsession and compulsion score) suggested that the beta2 dependence is driven primarily by the obsession component. The event related potentials showed no peak or latency differences in P3a, but P3b was increased in amplitude and delayed in latency in the OCD group compared to controls ($P < .000$).

The data are interpreted using Saxena's model¹ of an aberrant positive feedback loop in the fronto-striatal network, which predicts hyperactivity in the orbito-frontal and anterior cingulate cortices in people with OCD. A decrease in alpha might be a sign of hyperactivity and the observed increases in beta activity could reflect a heightened state of alertness when experiencing obsessive thoughts in people with OCD. The preliminary ERP data are consistent with the described model. More detailed data from evoked response experiments and their correlation to behavioural data will be presented.

Reference

1. Saxena S. Neuroimaging and the pathophysiology of obsessive compulsive disorder. In Fu SC, Cho Y, Russell TA, Weinberger, D, Murray R, eds. *Neuroimaging in Psychiatry*. London, UK: Martin Dunitz; 2003:191-224.

P180. Alterations of Auditory and Visual Processing in Velo-Cardio-Facial (22q11.2 deletion) Syndrome: A Group at High Genetic Risk for Schizophrenia

T.A. Rihs¹, M. Tomescu¹, K.W. Song¹, A. Custo¹, J.F. Knebel², M. Murray², S. Eliez³, C.M. Michel¹

¹Functional Brain Mapping Laboratory, Department of Fundamental Neurosciences, University of Geneva, Geneva, Switzerland

²Neuropsychology and Neurorehabilitation Service, Department of Clinical Neurosciences, University Hospital Center and University of Lausanne, Lausanne, Switzerland

³Office Médico-Pédagogique Research Unit, Department of Psychiatry, University of Geneva School of Medicine, Geneva, Switzerland

We aim to identify EEG biomarkers of auditory and visual perception in participants that have an identified genetic risk for schizophrenia. We tested participants born with a microdeletion on chromosome 22 and diagnosed with 22q11.2 deletion syndrome. It is characterized by a high percentage of early-onset psychosis and a 30% risk to develop schizophrenia. We compare participants with 22q11DS and age matched controls with high density EEG source imaging during an auditory gating paradigm with simple click sounds as well as a paradigm investigating visual contour perception with Kanizsa shapes. When comparing 22q11DS participants with controls in the auditory paradigm, we find increased map strength at the central N1 component that is related to increased anterior cingulate and medio dorsal frontal cortex activations in 22q11, while decreased amplitudes of the lateral N1 and the P2 correspond to significantly reduced activation in left auditory cortex in 22q11 DS (Rihs, 2012). For the perception of visual contour stimuli, differences emerged again at later stages of processing during a time related to contour perception (320-370 ms) with reduced activation over areas of ventral visual stream processing followed by an increased activation of the middle frontal gyrus in 22q11DS. The increased activation seen over anterior

cingulate and medio-dorsal cortex in the auditory paradigm and of middle frontal gyrus in the visual paradigm could result from structural differences observed in young adults with 22q11DS. At later stages of both auditory and visual processing, we find significantly reduced activity over auditory cortex and ventral visual cortex, which would correspond to deficits in higher order auditory and visual processing. Further research and results from our longitudinal studies will show if these reduced activations of sensory cortices could be candidate markers for the development of schizophrenia.

P181. Electrophysiological Indices of Reward Anticipation in Subjects With Deficit and Nondeficit Schizophrenia

U. Volpe¹, E. Merlotti¹, A. Vignapiano¹, V. Montefusco¹, G.M. Plescia¹, O. Gallo¹, P. Romano¹, A. Mucci¹, and S. Galderisi¹

¹Department of Psychiatry, University of Naples SUN, Naples, Italy

The present report is part of a larger study investigating brain imaging, electrophysiological, and neurocognitive correlates of reward anticipation in schizophrenia. The electrophysiological protocol was designed to verify an impairment of reward anticipation in patients with schizophrenia and its association with primary negative symptoms. To this aim, For the present event-related potentials (ERPs) were assessed in 11 patients with deficit schizophrenia (DS), characterized by the presence of primary and enduring negative symptoms, 23 patients with nondeficit schizophrenia (NDS) and 23 healthy controls (HC).

Event-related potentials were recorded during the anticipation of five different outcomes, small (SR) or large (LR) reward, small (SP) or large (LP) punishment or no-outcome (NO). ERP topography was analyzed using RAGU¹ and ERP tomography by means of sLORETA.² Our ERP results revealed that only DS patients showed topographic abnormalities in early processing stages (<200 ms) and a reduced activity of the ERP generators in a distributed circuit, including bilateral occipito-temporal regions, posterior cingulate, as well as left frontal and parietal areas, during the anticipation of reward. In the late processing stages (400-500 ms) only NDS subjects showed topographic abnormalities. In the same time interval, sLORETA showed for DS patients a reduced current source density in the bilateral inferior parietal, left precentral regions, and right insula; for NDS patients a reduced current source density in the bilateral precentral, postcentral, and inferior parietal areas, left middle frontal and right inferior temporal areas.

Our findings showed different pattern of abnormalities depending on the patient subgroup, on the anticipated outcome and on the examined time frame. In particular, DS patients were impaired in early processing stages for cues anticipating reward, while both DS and NDS subjects were impaired in the late stages. According to source imaging findings, the 2 patients subgroups partially share the impairment of left fronto-parietal circuits in late processing stages, when integration of

task relevance is carried out; only DS patients showed abnormalities in the early stages during reward anticipation, when a fine modulation of sensory processing is carried out. These data are in line with other findings from our group showing an impairment of the attentional enhancement of the auditory N100 only in DS patients.³

Acknowledgments

Funded by Compagnia San Paolo di Torino–Neuroscience Call.

References

1. Koenig T, et al. *Comput Intell Neurosci*. 2011;2011:1-14.
2. Pascual-Marqui RD. *Methods Find Exp Clin Pharmacol*. 2002; 24(suppl C):91-95.
3. Mucci A, et al. *Schizophr Res*. 2007;92:252-261.

PI85. Functional Connectivity of Broca's Region: Symptom-Specific Changes in Formal Thought Disorder (FTD) in Schizophrenia

K. Laimboeck¹, K. Jann¹, S. Walther¹, A. Federspiel¹, R. Wiest² W. Strik¹, and H. Horn¹

¹University Hospital of Psychiatry Bern, Bern, Switzerland

²Institute of Diagnostic and Interventional Neuroradiology, University Hospital Bern (Inselspital), Bern, Switzerland

Introduction. Decreased connectivity in functional networks has been described in schizophrenia. Our group recently demonstrated specific changes within the left language network in formal thought disorder (FTD). In the present study, we further investigate the symptom-specific changes in

functional connectivity of the frontal component of this network. We hypothesized that functional connectivity would be decreased in FTD and expected this changes to be more pronounced for BA 45 than for BA 44. **Methods.** A total of 17 schizophrenic patients and 18 matched healthy controls (all right-handed) absolved a silent reading task during BOLD fMRI. Patients were categorized according their scores in the scale for the assessment of thought, language, and communication (TLC) as FTD or non-FTD. The frontal component of the language system in schizophrenic patients was determined in our previous work by independent component analysis (ICA). We separated this region in BA44 and BA45 according to the Broadmann Atlas implemented in BVQX. We used the signal time courses of these seed regions as independent predictors in a general linear model. The resulting functional networks in FTD and nFTD patients were compared using unpaired *t* tests ($P < .05$; 2-sided, cluster size corrected). Signal time courses of seeds and remaining clusters were correlated with each other in both patient groups and HC using an in-house MATLAB script. Symptom-relatedness of altered connectivity was further evaluated by the calculation of Spearman's rank correlation of ROI-to-ROI-connectivity and TLC-scores. **Results.** Contrary to our hypothesis, functional connectivity of the frontal components of the language system in schizophrenic patients was increased in FTD patients compared to schizophrenic patients without FTD and healthy controls. These changes were more pronounced for BA 45 than for BA 44. Increased connectivity of BA45 and posterior language regions correlated with symptom severity in FTD patients. Correlations with symptom severity were also apparent for the precuneus, the caudate nucleus and the ACC.